DEVELOPMENT AND EVALUATION OF PASSIVE SAMPLING DEVICES TO CHARACTERIZE THE SOURCES, OCCURRENCE, AND FATE OF POLAR ORGANIC CONTAMINANTS IN AQUATIC SYSTEMS

Jonathan Karl Challis

A Thesis Submitted to the Faculty of Graduate Studies in
Partial Fulfillment of the Requirements for the Degree of

DOCTOR OF PHILOSOPHY

Department of Chemistry
University of Manitoba
Winnipeg, MB, Canada

ABSTRACT

The primary goal of this dissertation was to develop and evaluate an improved aquatic passive sampling device (PSD) for measurement of polar organic contaminants. Chemical uptake of current polar-PSDs (e.g., POCIS – polar organic chemical integrative sampler) is dependent on the specific environmental conditions in which the sampler is deployed (flow-rate, temperature), leading to large uncertainties when applying laboratory-derived sampling rates *in-situ*. A novel configuration of the diffusive gradients in thin-films (DGT) passive sampler was developed to overcome these challenges.

The organic-DGT (o-DGT) configuration comprised a hydrophilic-lipophilic balance® sorbent binding phase and an outer agarose diffusive gel (thickness = 0.5–1.5 mm), notably excluding a polyethersulfone protective membrane which is used with all other polar-PSDs. Sampler calibration exhibited linear uptake and sufficient capacity for 34 pharmaceuticals and pesticides over typical environmental deployment times, with measured sampling rates ranging from 9–16 mL/d. Measured and modelled diffusion coefficients (D) through the outer agarose gel provided temperature-specific estimates of o-DGT sampling rates within 20% (measured-D) and 30% (modelled-D) compared to rates determined through full-sampler calibration. Boundary layer experiments in lab and field demonstrated that inclusion of the agarose diffusive gel negated boundary layer effects, suggesting that o-DGT uptake is largely insensitive to hydrodynamic conditions.

The utility of o-DGT was evaluated under a variety of field conditions and performance was assessed in comparison to POCIS and grab samples. o-DGT was effective at measuring pharmaceuticals and pesticides in raw wastewater effluents, small creeks, large fast-flowing rivers, open-water lakes, and under ice at near-zero water

temperatures. Concentrations measured by o-DGT were more accurate than POCIS when compared to grab samples, likely resulting from the influence *in-situ* conditions have on POCIS. Modelled sampling rates were successfully used to estimate semi-quantitative water concentrations of suspect wastewater contaminants using high-resolution mass spectrometry, demonstrating the unique utility of this o-DGT technique.

This dissertation establishes o-DGT as a more accurate, user-friendly, and widely applicable passive sampler compared to current-use polar-PSDs. The o-DGT tool will help facilitate more accurate and efficient monitoring efforts and ultimately lead to more appropriate exposure data and environmental risk assessment.

ACKNOWLEDGEMENTS

Thank you to my fellow graduate and undergraduate students, lab managers, technicians, and post-docs I encountered during my research. Thank you to Mimi, Al, Luis, Kevin, Shira, Angelique, Marie-Claire, Trisha, Chelsea, Dana, Adam, and many others! Be it banging our heads on the LC-MS/MS, long days sampling the Red River (rain or shine), mesocosm experiments, extracting samples, venting about our often frustrating research, conferencing, group lunches… the list goes on. Thank you all!

To my family and friends, thank you for your support! You are all amazing and I love you! Aaron, my whole life you've always been great at forcing me away from my work when I couldn't seem to do it myself. Thank you for that. To my good friend Paul. Thank you for all the late night chats over a glass (or two…) of Jameson's. You always helped take my mind off my research. To all my friends, whether you knew it or not, you helped keep me balanced and sane throughout this journey. Thank you!

To Mom and Dad, thank you for your incredible encouragement, love, and support in everything I do, it is truly motivating and inspiring. I would not be here without the opportunities and support you have provided me in my life and throughout my PhD. I am so grateful and privileged to have such amazing parents. I love you.

Lisha, I dedicate this thesis to you. I owe you the most! Thank you for being my best friend and love of my life throughout this journey. Thank you for inspiring and supporting me every single day, no matter what. Especially in these final months. I'm sorry if I haven't been my normal self and for my above-normal forgetfulness lately… I blame my thesis brain. Yet, through everything, you always stuck by me and found a way to put a smile on my face. Thank you for your patience, understanding, and love!

TABLE OF CONTENTS

LIST OF TABLES

LIST OF FIGURES

LIST OF EQUATIONS

$$R = (1/4\sqrt{N})\left(\frac{\alpha - 1}{\alpha}\right)\left(\frac{k}{1 + k}\right)$$

$$H = A + B/u + Cu$$

$$C_s(t) = C_w \frac{k_1}{k_2}(1 - e^{-k_2 t})$$

$$C_s = C_w \frac{k_1}{k_2} = C_w K_{sw}$$

$$k = \frac{k_o A}{K_{sw} V_s} = \frac{R_s}{K_{sw} V_s}$$

$$C_w = \frac{M_s}{K_{sw} V_s[1 - exp(-R_s t/K_{sw} V_s)]}$$

$$C_w \approx \frac{M_s}{R_s t}$$

$$\frac{1}{k_o} = \frac{\delta_w}{D_w} + \frac{\delta_m}{D_m K_{mw}} + \frac{\delta_b}{D_b K_{bw}}$$

$$\frac{1}{k_o} \approx \frac{\delta_w}{D_w}$$

$$C_{TWA} = \frac{M_{POCIS}}{R_s t}$$

$$C_{DGT} = \frac{M_{DGT}\Delta g}{DAt}$$

$$C_{DGT} = \frac{M_{DGT}(\Delta g + \delta)}{DAt}$$

$$D = \frac{k\Delta g}{C_s A}$$

$$\frac{1}{M_{DGT}} = \frac{\Delta g}{DC_{DGT}At} + \frac{\delta}{DC_{DGT}At}$$

$$LogD_T = \frac{1.37023(T-25) + 0.000836(T-25)^2}{109 + T} + Log\frac{D_{298K}(273+T)}{298}$$

$$D_w(cm^2/s) \approx \frac{1.326 \times 10^{-4}}{\eta^{1.14}V^{0.589}}$$

$$D_w(cm^2/s) \approx \frac{3.3 \times 10^{-5}\varepsilon^m}{\sqrt[3]{M}}$$

$$M_{DGT} = R_s C_w t$$

$$R_s = \frac{DA}{\Delta g}$$

LIST OF ABBREVIATIONS

2,4-D – 2,4-dichlorophenoxy acetic acid

A – exposed surface area of sampler

ANOVA – analysis of variance

ARG – antibiotic resistance gene

CCME – Canadian Council of Ministers of the Environment

C_{DGT} – time-weighted average concentration measured by DGT

CE – collision energy

CID – collision induced dissociation

C_s – concentration in sampler

C_{TWA} – time-weighted average water concentration

C_w – concentration in water

D – diffusion coefficient in water (D_w), membrane (D_m), biofilm (D_b)

DBL – diffusive boundary layer

DDA – data dependent acquisition

DDT – dichlorodiphenyltrichloroethane

DGT – diffusive gradients in thin-films

DIA – data independent acquisition

DOC – dissolved organic carbon

DOM – dissolved organic matter

D_T – diffusion coefficient at temperature

EC_{50} – effect concentration causing 50% of the population to exhibit the observed end-point

ESI – electrospray ionization

HLB – hydrophilic-lipophilic balance

HRMS – high resolution mass spectrometry

R – chromatographic resolution

N – theoretical plate count (efficiency)

H – theoretical plate height

α – chromatographic selectivity

k – chromatographic retention/capacity

u – mobile phase flow-rate

A – eddy diffusion

B – longitudinal diffusion

C – mass transfer

k – uptake rate constant

k_1 – sorption rate constant

k_2 – desorption rate constant

K_{bw} – biofilm-water partition coefficient

K_d – solid-water partition coefficient

k_{direct} – direct photolysis rate constant

K_{mw} – membrane-water partition coefficient

k_o – overall mass transfer coefficient

K_{oc} – organic carbon partition coefficient

K_{ow} – octanol-water partition coefficient

K_{sw} – sampler-water partition coefficient

LC – liquid chromatography

LC_{50} – lethal concentration required to kill 50% of the population

LC-MS/MS – liquid chromatography tandem mass spectrometry

LDPE – low-density polyethylene

LOD – limit of detection

LOQ – limit of quantification

m – Archie's Law exponent

M – molecular weight

M_{DGT} – mass analyte on DGT sampler

MRM – multiple reaction monitoring

M_s – mass analyte on sampler

MS/MS – tandem mass spectrometry

NHCN – Norway House Cree Nation

o-DGT – organic-DGT

PAH – polyaromatic hydrocarbon

PBT – persistent, bioaccumulative, and toxic

PCB – polychlorinated biphenyls

PE – polyethylene

PES – polyethersulfone

PFAS – per- and polyfluoroalkyl substance

PFDA – perfluorodecanoic acid

PFHpA – perfluoroheptanoic acid

PFHxA – perfluorohexanoic acid

PFHxS – perfluorohexanesulfonic acid

PFNA – perfluorononanoic acid

PFOA – perfluorooctanoic acid

PFOS – perfluorooctanesulfonic acid

PFPeA – perfluoropentanoic acid

PFUnDA – perfluoroundecanoic acid

pK_a – acid dissociation constant

POC – polar organic contaminant

POCIS – polar organic chemical integrative sampler

POP – persistent organic pollutant

PPCP – pharmaceuticals and personal care product

PRC – performance reference compound

PSD – passive sampling device

QQQ – triple quadrupole tandem mass spectrometry

QTOF – quadrupole time-of-flight mass spectrometry

R_s – sampling rate

SD – standard deviation

SPE – solid phase extraction

SPMD – semi-permeable membrane device

t – time

TWA – time-weighted average

V – molar volume

V_s – sampler/sorbent volume

WQG – water quality guideline

WWTP – wastewater treatment plant

δ – phase thickness

δ_b – biofilm layer thickness

Δg = diffusive gel thickness

δ_m – membrane layer thickness

δ_w – water boundary layer thickness

ε – porosity

η – water viscosity

$\Phi_{\lambda,direct}$ - direct photolysis quantum yield

CHAPTER 1

1. **INTRODUCTION TO POLAR ORGANIC CONTAMINANTS AND PASSIVE SAMPLING IN AQUATIC SYSTEMS**

Jonathan K. Challis

This dissertation focuses on the development and applications of passive sampling techniques to understand the occurrence, sources, transport, and fate of anthropogenic contaminants in surface waters. This chapter summarizes many of the fundamental topics underpinning the research in this dissertation, including context around the specific contaminants of interest, instrumental analysis, a summary of aquatic sampling techniques, basic theory behind passive sampling, and the impetus for developing an improved polar passive sampling device. Lastly, the objectives and hypotheses of this thesis will be outlined, followed by a brief summary of each research chapter.

1.1 Polar Organic Contaminants in Aquatic Systems
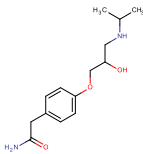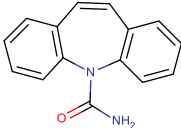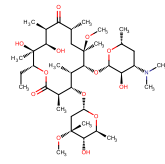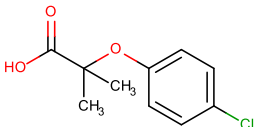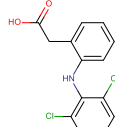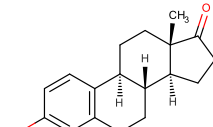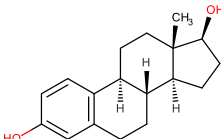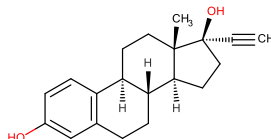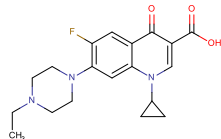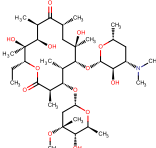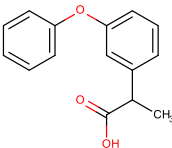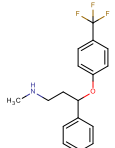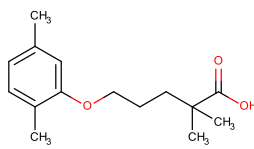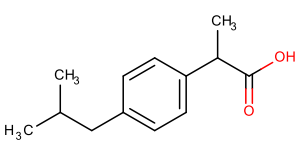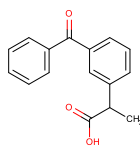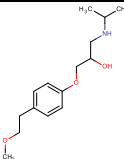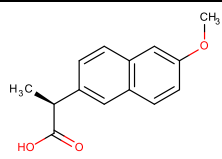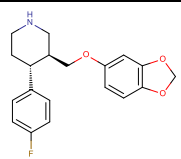
The study of anthropogenic organic contaminants in the environment has been an area of great interest for decades. Initially, much of this research focused on persistent organic pollutants (POPs), generally characterized by the three properties commonly known as PBT: persistent, bio-accumulative, and toxic. The study of these chemicals trace back to the pioneering work of Rachel Carson's 1962 book *Silent Spring*, in which dichlorodiphenyltrichloroethane (DDT) was found accumulating in the food chain and threatening exposed organisms, such as birds of prey (Carson, 1962). Shortly after, Jensen et al. (1969) identified similar phenomena occurring with polychlorinated biphenyls (PCBs). Over the 30 years that followed, the study of PBT chemicals in the environment formed the foundation for much of the research occurring in the fields of environmental chemistry and ecotoxicology. This collective work culminated in successful chemical regulation, most notably through the Stockholm Convention on POPs and the 2001 signing of the international environmental treaty to eliminate or restrict production and use of twelve chemicals, famously known as the 'Dirty Dozen'
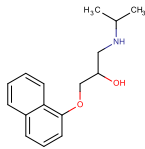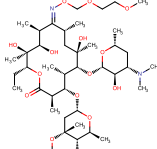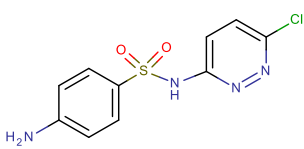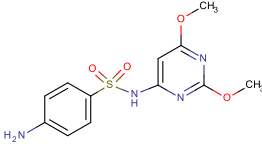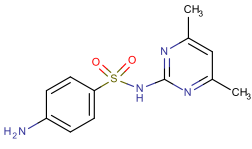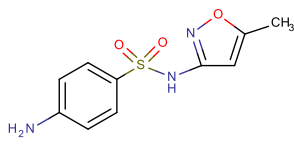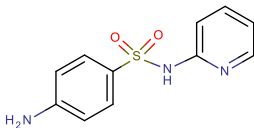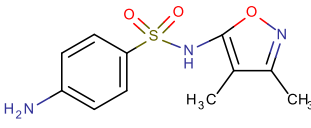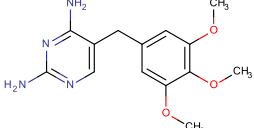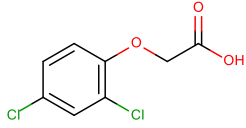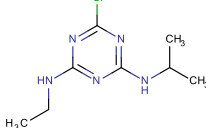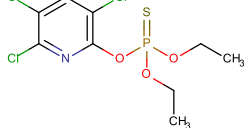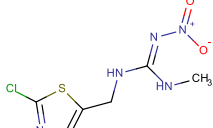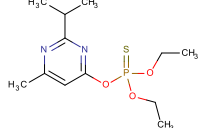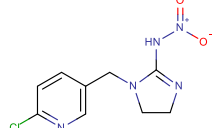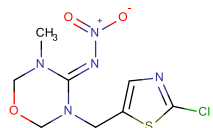
(Karlaganis et al., 2001), and mechanisms by which to add additional chemicals to the treaty, as has been done for perfluorooctanoic acid (http://chm.pops.int/). Most of these PBT chemicals are, by definition, non-polar and lipophilic, as the tendency to bio-accumulate in biota requires partitioning into non-polar compartments within an organism (e.g., fatty tissues) (Schwarzenbach et al., 2005a). While both legacy and emerging POPs remain a major area of research, the spectrum of organic contaminants being studied in the environment has broadened significantly, including major contaminant classes not characterized by this typical PBT criteria.

Of particular interest to this dissertation are polar organic contaminants (POCs). This family of contaminants is not as clearly defined as POPs, however generally encompasses polar, water soluble chemicals that are amenable to analysis by liquid chromatography (LC) and have log octanol-water partition coefficients (logK$_{ow}$) values less than ≈5 (Reemtsma et al., 2016). These POCs tend to persist in the water column making them highly mobile in aquatic systems and thus potential stressors on water quality. Throughout the literature, numerous classes of chemicals have been labelled under the umbrella of POCs, including pharmaceuticals and personal care products (Daughton and Ternes, 1999; Fent et al., 2006; Heberer, 2002; Kümmerer, 2009a; Loos et al., 2013), hormones and endocrine disrupting compounds (Arditsoglou and Voutsa, 2008; Yu et al., 2011) pesticides (Moschet et al., 2014; Novic et al., 2017), certain per- and polyfluoroalkyl substances (PFASs) (Kaserzon et al., 2012; Loos et al., 2013; Wang et al., 2017), and many others, including metabolites and transformation products (Reemtsma et al., 2006). Pharmaceuticals and pesticides are the major contaminants of interest in this thesis (Table 1.1), discussed in detail below.

Table 1.1: Pharmaceuticals and pesticides studied in this thesis. Pharmaceuticals (27 in total) are listed first in alphabetical order, followed by pesticides (7 in total). Physical-chemical properties of each target chemical are given. References for the $LogK_{ow}$ and pK_a values provided at end of table.

ATENOLOL		CARBAMAZEPINE		CLARITHROMYCIN	
$C_{14}H_{22}N_2O_3$	266.3 g/mol	$C_{15}H_{12}N_2O$	236.3 g/mol	$C_{38}H_{69}NO_{13}$	748.0 g/mol
$LogK_{ow} = 0.16^b$	$pK_a = 9.6^b$	$LogK_{ow} = 2.45^a$	$pK_a = 13.9^a$	$LogK_{ow} = 3.1^c$	$pK_a = 9.0^c$

CLOFIBRIC ACID		DICLOFENAC		ESTRONE	
$C_{10}H_{11}ClO_3$	214.6 g/mol	$C_{14}H_{11}Cl_2NO_2$	296.1 g/mol	$C_{18}H_{22}O_2$	270.4 g/mol
$LogK_{ow} = 2.6^h$	$pK_a = 3.2^h$	$LogK_{ow} = 0.70^a$	$pK_a = 4.2^a$	$LogK_{ow} = 3.1^a$	$pK_a = 10.5^a$

17β-ESTRADIOL		17α-ETHYNYLESTRADIOL		ENROFLOXACIN	
$C_{18}H_{24}O_2$	272.4 g/mol	$C_{20}H_{24}O_2$	296.4 g/mol	$C_{19}H_{22}FN_3O_3$	359.4 g/mol
$LogK_{ow} = 4.0^a$	$pK_a = 10.4^a$	$LogK_{ow} = 3.7^a$	$pK_a = 10.5^a$	$LogK_{ow} = 0.28^g$	$pK_a = 6.1^g$

ERYTHROMYCIN		FENOPROFEN		FLUOXETINE	
$C_{37}H_{67}NO_{13}$	733.9 g/mol	$C_{15}H_{14}O_3$	242.3 g/mol	$C_{17}H_{18}F_3NO$	309.3 g/mol
$LogK_{ow} = 3.1^a$	$pK_a = 8.8^a$	$LogK_{ow} = 3.9^h$	$pK_a = 4.2^h$	$LogK_{ow} = 3.8^a$	$pK_a = 10.1^h$

GEMFIBROZIL		IBUPROFEN		KETOPROFEN	
$C_{15}H_{22}O_3$	250.3 g/mol	$C_{13}H_{18}O_2$	206.3 g/mol	$C_{16}H_{14}O_3$	254.3 g/mol
$LogK_{ow} = 4.8^a$	$pK_a = 4.7^a$	$LogK_{ow} = 4.0^a$	$pK_a = 4.9^a$	$LogK_{ow} = 3.1^b$	$pK_a = 4.5^b$

METOPROLOL		NAPROXEN		PAROXETINE	
$C_{15}H_{25}NO_3$	267.4 g/mol	$C_{14}H_{14}O_3$	230.3 g/mol	$C_{19}H_{20}FNO_3$	329.4 g/mol
$LogK_{ow} = 1.7^b$	$pK_a = 9.7^b$	$LogK_{ow} = 3.2^a$	$pK_a = 4.2^a$	$LogK_{ow} = 4.0^g$	$pK_a = 10.3^h$

Table 1.1 continued.

PROPRANOLOL		ROXITHROMYCIN		SULFACHLORPYRIDAZINE	
$C_{16}H_{21}NO_2$	259.3 g/mol	$C_{41}H_{76}N_2O_{15}$	837.0 g/mol	$C_{10}H_9ClN_4O_2S$	284.7 g/mol
$LogK_{ow} = 3.5^g$	$pK_a = 9.4^g$	$LogK_{ow} = 2.8^c$	$pK_a = 9.2^c$	$LogK_{ow} = 0.89^h$	$pK_a = 2.0, 5.9^f$

SULFADIMETHOXINE		SULFAMETHAZINE		SULFAMETHOXAZOLE	
$C_{12}H_{14}N_4O_4S$	310.3 g/mol	$C_{12}H_{14}N_4O_2S$	278.3 g/mol	$C_{10}H_{11}N_3O_3S$	253.3 g/mol
$LogK_{ow} = 1.5^c$	$pK_a = 1.9, 5.9^c$	$LogK_{ow} = 0.80^c$	$pK_a = 2.3, 7.4^c$	$LogK_{ow} = 0.89^a$	$pK_a = 2.1, 5.7^a$

SULFAPYRIDINE		SULFISOXAZOLE		TRIMETHOPRIM	
$C_{11}H_{11}N_3O_2S$	249.3 g/mol	$C_{11}H_{13}N_3O_3S$	267.3 g/mol	$C_{14}H_{18}N_4O_3$	290.3 g/mol
$LogK_{ow} = 0.35^h$	$pK_a = 2.2, 8.6^d$	$LogK_{ow} = 0.05^c$	$pK_a = 1.5, 5.0^e$	$LogK_{ow} = 0.91^a$	$pK_a = 4.0, 7.1^a$

2,4-DICHLOROPHENOXY ACETIC ACID (2,4-D)		ATRAZINE		CHLORPYRIFOS	
$C_8H_6Cl_2O_3$	221.0 g/mol	$C_8H_{14}ClN_5$	215.7 g/mol	$C_9H_{11}Cl_3NO_3PS$	350.6 g/mol
$LogK_{ow} = 2.8^j$	$pK_a = 2.74^j$	$LogK_{ow} = 2.61^a$	$pK_a = 1.6^a$	$LogK_{ow} = 4.7^i$	$pK_a = N/A^j$

CLOTHIANIDIN		DIAZINON		IMIDACLOPRID	
$C_6H_8ClN_5O_2S$	249.7 g/mol	$C_{12}H_{21}N_2O_3PS$	304.3 g/mol	$C_9H_{10}ClN_5O_2$	255.7 g/mol
$LogK_{ow} = 0.64^i$	$pK_a = 11.1^k$	$LogK_{ow} = 3.9^i$	$pK_a < 2.5^j$	$LogK_{ow} = -0.41$	$pK_a = N/A^k$

THIAMETHOXAM	
$C_8H_{10}ClN_5O_3S$	291.7 g/mol
$LogK_{ow} = 0.80^i$	$pK_a = N/A^k$

The following literature sources were used to obtain the reported LogK_{ow} and pK_a values (not all references represent original sources):

a. Westerhoff et al., 2005; b. Vieno et al., 2007;
c. Le-Minh et al., 2010; d. Challis et al., 2013;
e. Boreen et al., 2004; f. Boreen et al., 2005;
g. Monteiro and Boxall, 2010; h. Macleod et al., 2007;
i. Bade et al., 2015; j. Mackay et al., 1997; k. Lu et al., 2015

1.1.1 *Pharmaceuticals*

Measurements of pharmaceuticals in the environment date back to the mid-1980's (Halling-Sorensen et al., 1998), however it was not until the early 2000's, following two influential reviews (Daughton and Ternes, 1999; Halling-Sorensen et al., 1998) and a nationwide reconnaissance of U.S. surface waters (Kolpin et al., 2002) that pharmaceuticals, as environmental contaminants, entered the public and scientific consciousness. The rationale for this focus on pharmaceuticals related to concerns regarding their bioactivity and continuous release into the environment (Brooks et al., 2009). Additionally, the diversity in chemical structure and function across many pharmaceutical classes makes the study of these contaminants complex and multifaceted (Brooks et al., 2009; Daughton and Ternes, 1999). The 27 pharmaceuticals studied in this dissertation, detailed in Table 1.1 along with pertinent physiochemical properties, represent the following classes: antibiotics (clarithromycin, enrofloxacin, erythromycin, roxithromycin, sulfachlorpyridazine, sulfadimethoxine, sulfamethazine, sulfamethoxazole, sulfapyridine, sulfisoxazole, trimethoprim), β-blockers/anti-hypertensives (atenolol, metoprolol, propranolol), non-steroidal anti-inflammatory drugs (diclofenac, fenoprofen, ibuprofen, ketoprofen, naproxen), cholesterol-lowering drugs (clofibric acid, gemfibrozil), hormones (estrone, 17β-estradiol, 17α-ethynylestradiol), anti-seizure drugs (carbamazepine), and anti-depressants (fluoxetine, paroxetine). This specific list of pharmaceuticals was chosen largely based on reported occurrence in surface waters globally (Beek et al., 2016; Hughes et al., 2013) and in some cases the potential for adverse toxicological impacts in non-target organisms (Arnold et al., 2014; Backhaus, 2014; Kuster and Adler, 2014; Pal et al., 2010).

1.1.1.1 Sources and Occurrence

The major route of pharmaceuticals to the aquatic environment is via human-use and excretion, resulting in a mixture of both parent pharmaceuticals and their metabolites entering municipal wastewater treatment plants (WWTP). Lack of complete removal results in many of these bioactive compounds and their metabolites being released into surface waters (Monteiro and Boxall, 2010). Although most human-use pharmaceuticals are not persistent relative to POPs, they are typically being released continuously from WWTPs, leading to pseudo-persistence in downstream aquatic systems (Daughton and Ternes, 1999). Animal husbandry represents a second significant source of pharmaceuticals to the environment, often as runoff from fields containing animal manure (Sarmah et al., 2006) or more direct secondary inputs through use in aquaculture (Kümmerer, 2009b). Improper household disposal, hospital use, and manufacturing emissions of pharmaceuticals can contribute to localized inputs, however represent minor sources overall (Monteiro and Boxall, 2010).

The benefits that pharmacology provides to all facets of our societies far outweigh the potential threats they pose as environmental contaminants. As such, wastewater treatment represents the primary line of defence capable of limiting, or in ideal cases stopping the release of these contaminants into aquatic environments (Le-Minh et al., 2010; Miège et al., 2009; Yang et al., 2011). However, the degree of treatment efficacy depends upon many factors, including the physical-chemical properties (e.g., polarity, solubility, persistence) of the chemical itself and the type of wastewater treatment (Miège et al., 2009; Yang et al., 2011). Conventional wastewater treatment techniques such as activated sludge treatment and subsequent clarification

(Yang et al., 2011), aerated lagoon treatment (Li et al., 2013; Matamoros et al., 2009), or even constructed wetland polishing (Matamoros et al., 2009) are typically not effective at complete removal of most pharmaceuticals from wastewater. Advanced treatment processes, including ozonation, UV-irradiation, activated carbon adsorption, and membrane separation have proven more effective, however for most pharmaceuticals complete removal is still rarely achieved (Le-Minh et al., 2010; Yang et al., 2011), leading to the observed pseudo-persistence in the environment.

To date, concerns around pharmaceuticals in surface waters are largely isolated to effluent-dominated ecosystems, where downstream dilution of the wastewater plume is limited (Beek et al., 2016; Du et al., 2014; Pal et al., 2010). Concentrations of pharmaceuticals in most surface waters receiving wastewater inputs are in the ng/L range (Beek et al., 2016; Hughes et al., 2013). Beek et al. (2016) provide a comprehensive global survey of pharmaceutical concentrations in surface waters. Of the 16 pharmaceuticals most frequently detected across five global geographical regions, 10 of them were part of the 27 pharmaceutical suite studied in this work.

Table 1.2 summarizes the global average and maximum concentrations of these ten common analytes. Average concentrations range from 3 ng/L (estradiol) to 187 ng/L (carbamazepine), with maximum observed concentrations reaching µg/L levels and detection frequencies of 23-50% (Beek et al., 2016). Concentrations in WWTPs are typically an order of magnitude greater than levels in impacted surface waters (Monteiro and Boxall, 2010), however observed downstream concentrations depends largely on the extent of dilution occurring in the receiving water body (Petrie et al., 2014).

Table 1.2: Global average and maximum concentrations for 10-of-the-16 most commonly measured pharmaceuticals in surface waters across the five geographical regions defined by the United Nations regional groups (Africa, Asia-Pacific, Eastern Europe, Latin American and Caribbean States, Western Europe and Others Group - includes North America, Australia, and New Zealand), according to the global survey conducted by Beek et al. (2016).

Compound	Average (ng/L)	Max (µg/L)	Sample number (n)	Detection frequency
Carbamazepine	187	8.1	25115	48%
Clofibric acid	22	7.9	2947	23%
Diclofenac	32	18.7	7017	50%
Estrone	16	5.0	2228	35%
Estradiol	3	0.012	297	34%
Ethynylestradiol	43	5.9	1530	31%
Ibuprofen	108	303	6950	47%
Naproxen	50	32.0	3229	45%
Sulfamethoxazole	95	29.0	8599	47%
Trimethoprim	37	13.6	3060	29%

In addition to aqueous concentrations, which are important to characterize exposure and toxicity to non-target aquatic organisms, pharmaceutical mass loadings are necessary to understand the source and extent of contributions to downstream waters (Novic et al., 2017), which typically scale with population (MacLeod and Wong, 2010; O'Brien et al., 2017). This thesis will, in part, demonstrate the utility of water concentrations for exposure assessment (Chapter 2), mass loadings for source apportionment (Chapter 2 and 4), and the importance of downstream dilution on observed concentrations in receiving waters (Chapter 4).

1.1.1.2 Environmental Fate

A common adage in the chemical and biological sciences is 'structure dictates function'. This is no less true when it comes to characterizing the fate and behaviour of pharmaceuticals in aquatic systems. The diversity of structures observed across pharmaceutical classes dictate complex fate processes responsible for the behaviour of these contaminants in the environment. Much of the initial assessment of pharmaceutical fate was based upon models and frameworks developed to understand

the behaviour of POPs in the environment, including properties dictating transfer of chemical between phases (air-water and particle-water partitioning) and transformation of chemicals, both biotic (metabolism, conjugation, and microbial degradation) and abiotic (oxidation, reduction, hydrolysis, and photolysis) (Fent et al., 2006; Heberer, 2002). Given the low vapour pressures and rates of hydrolysis for most pharmaceuticals, volatilization and hydrolysis are typically very minor transport and transformation mechanisms in the environment (Daughton and Ternes, 1999; Tixier et al., 2003). Generally speaking, photolysis, sorption, and biotransformation represent the three most important mechanisms dictating the fate of pharmaceuticals in aquatic systems (Challis et al., 2014; Fent et al., 2006; Fono et al., 2006; Kümmerer, 2009b; Le-Minh et al., 2010; Löffler et al., 2005; Monteiro and Boxall, 2010; Petrie et al., 2014; Tixier et al., 2003; Tolls, 2001).

Photolysis. The presence of aromatic rings and conjugated-π systems, functional groups, and heteroatoms common across nearly all pharmaceuticals results in appreciable absorbance in the UV-C wavelength range, often with tailing absorbance past 290 nm and in some cases into the UV-A range (>315 nm) (Boreen et al., 2003). These contaminants will undergo direct photolysis when exposed to natural sunlight (Challis et al., 2014). However, many pharmaceuticals with minimal absorbance overlap with natural sunlight (>290 nm) may still undergo significant photo-degradation via indirect photolysis. Through interaction with other light-absorbing species known as photosensitizers (e.g., organic matter, carbonate, nitrate, iron), transfer of energy from photo-excited species to the pharmaceutical can cause a chemical transformation (Leifer, 1988). These indirect photolysis mechanisms are inherently more complex as

chemicals can interact through multiple pathways with photo-generated transient species, including triplet excited dissolved organic matter (^{3}DOM), singlet oxygen (^{1}O$_2$), hydroxyl radicals ($^\bullet$OH), and others (Bodhipaksha et al., 2015; Challis et al., 2014; McNeill and Canonica, 2016). Additionally, DOM can act through competing mechanisms, including scavenging of reactive oxygen species (Bodhipaksha et al., 2015; Wenk et al., 2013, 2011) and light screening (Guerard et al., 2009; Lu et al., 2015; Miller and Chin, 2005), further complicating the characterization of photolytic mechanisms in natural waters.

The extent of direct photolysis for a given compound is generally reported as a pseudo first-order direct photolysis rate constant (k_{direct}). Similarly, a direct photolysis quantum yield ($\Phi_{\lambda,direct}$), which describes the efficiency in which a chemical reacts/transforms upon absorption of photons over a specific wavelength range (Leifer, 1988), can be determined using chemical actinometry (Dulin and Mill, 1982; Laszakovits et al., 2017). Photolysis rate constants are directly dependent upon the incident light intensity at the time of measurement, and thus have limited predictive utility under differing light conditions. Conversely, the $\Phi_{\lambda,direct}$ is a powerful characteristic property of a chemical that allows k_{direct} to be predicted in principle under any light conditions (Challis et al., 2014; Leifer, 1988).

The pharmaceuticals studied in this thesis (Table 1.1) all undergo direct or indirect photolysis to some extent and for many represent the major attenuation mechanism in natural surface waters. For example, the class of sulfonamide antibiotics have been studied extensively in the environmental photochemistry literature (Challis et al., 2014). Despite the structural similarities characteristic of the sulfonamide class, k_{direct}

and $\Phi_{\lambda,direct}$ varies significantly compound to compound, and kinetics can be highly

dependent on solution pH (Boreen et al., 2005, 2004; Challis et al., 2013). Generally

speaking, sulfonamides can be characterized as photo-labile, undergoing relatively

rapid photo-degradation with half-lives of <1 day under natural sunlight (Boreen et al.,

2005, 2004; Challis et al., 2013). In contrast, direct photo-degradation of carbamazepine

is limited, with indirect photolysis mechanisms typically varying with type and

concentration of water constituents (e.g., DOM) (Jasper and Sedlak, 2013). Reported

half-lives range from ≈10 days in an outdoor mesocosm experiments (Cardinal et al.,

2014; Lam et al., 2004) to ≈100 days in summer and ≈450 days in fall at 50° N latitude,

calculated based on a measured $\Phi_{\lambda,direct}$ (Andreozzi et al., 2003).

Sorption. Traditional approaches describing organic contaminant partitioning to

soils and sediments mostly involve hydrophobic type interactions and have often proven

inadequate for pharmaceuticals (Brooks et al., 2009; Sassman and Lee, 2005; Tolls,

2001), as many drug classes are weak acids, bases, or zwitterions. As a result

hydrophobic-driven interactions can be less important and tend to underestimate

sorption (Ternes et al., 2004) compared to other binding processes such as ion

exchange and ion bridging, surface complexation, and hydrogen-bonding (Sassman

and Lee, 2005; Tolls, 2001). Pharmaceuticals with large solid-water partition coefficients

(K_d) have a tendency to sorb solid suspended particles or activated sludge during

primary or secondary wastewater treatment stages, ending up in the sewage sludge

during settling (Le-Minh et al., 2010). For example, tetracycline and quinolone

antibiotics and anti-depressants like fluoxetine have been found at elevated levels in

suspended particulate matter and sludge of WWTP influents (Petrie et al., 2014), with

sludge K_d values as large as 8000 L/kg (tetracycline) (Le-Minh et al., 2010). These compounds can have implications down the line where wastewater irrigation and/or biosolid amendment practices are used for agriculture (Prosser and Sibley, 2015), as these compounds have the potential to be re-mobilized through runoff from agricultural fields (Drillia et al., 2005; Sassman and Lee, 2005; Tolls, 2001). Additionally, veterinary pharmaceuticals, namely antibiotics, are common as growth-promoters in livestock, and thus can enter agricultural soils more directly via excretion (Prosser and Sibley, 2015; Sarmah et al., 2006; Tolls, 2001).

Once in receiving waters, sorption can become less prevalent since concentrations of suspended particles in most surface waters is far less than those in wastewater influent (Zhou and Broodbank, 2013). Additionally, large water-particle ratios have the potential to shift equilibrium in chemical-particle interactions, thereby releasing pharmaceuticals back to the dissolved aqueous phase (Hajj-Mohamad et al., 2017). The extent of these sorption processes for individual pharmaceuticals will vary from system to system as specific sedimentation parameters like particle concentration in the water column, particle composition (e.g., fraction organic carbon), and settling velocity can have significant impacts on the extent of sorption (Tixier et al., 2003).

Biodegradation. Bacteria and fungi are the two organisms most relevant to biodegradation of pharmaceuticals, with the former typically playing the most significant role in aquatic systems (Caracciolo et al., 2015; Ghattas et al., 2017; Greskowiak et al., 2017; Kümmerer, 2009a). Biodegradation plays a very important role in the attenuation of pharmaceuticals in WWTPs (Yamamoto et al., 2009; Yang et al., 2011) and while microbial activity is typically reduced significantly in natural surface waters due to lower

bacterial density and diversity compared to undiluted wastewaters (Kümmerer, 2009a), it remains an important natural attenuation mechanism (Fono et al., 2006). Yamamoto et al. (2009) reported biodegradation half-lives in laboratory activated sludge experiments ranging from 5 days for propranolol to 125 days for carbamazepine, corresponding to relative removal rates of 60% and <0.1%, respectively. Conversely, Fono et al. (2006) studied the attenuation rates of pharmaceuticals in an effluent-dominated river and found that biotransformation was the major removal mechanism for most compounds, even over photolysis, with half-lives ranging from 17 days for naproxen and ibuprofen to 53 days for metoprolol in microcosm incubations with river water (Fono et al., 2006).

Biofilms can also play important roles in the degradation and fate of pharmaceuticals in WWTPs (Casas et al., 2015) and receiving waters (Huerta et al., 2016; Writer et al., 2011). In fact, designed biofilm reactors have proven effective treatment techniques for pharmaceuticals in wastewaters (Casas et al., 2015). Additionally, in-stream biofilms, generally forming layers on streambed sediments in wastewater influenced systems can be important compartments for accumulation of pharmaceuticals (Huerta et al., 2016) and even degradation of certain classes of compounds (e.g., endocrine disrupting chemicals) (Writer et al., 2011).

While the weight-of-evidence suggests that microbial degradation is an important mechanism for pharmaceuticals (Caracciolo et al., 2015), it remains that biodegradation rates can be highly dependent upon the specific and sometimes unique conditions of an individual experiment or field site, varying by as much as three orders of magnitude, depending on microbial and environmental conditions (Greskowiak et al.,

2017), making compound specific generalization, comparisons, and applications across different systems challenging.

1.1.1.3 Ecotoxicology

Pharmaceuticals are biologically active compounds designed to elicit a biological response in the target organism (human or animal) at therapeutic doses. As such, concerns regarding interactions with non-target organisms has led to significant research to characterize the ecotoxicology of these contaminants (Santos et al., 2010). Since most pharmaceuticals illicit effects via specific modes of action, and many physiological pathways are conserved across taxa, standard toxicity test methods are often not sufficient for measurement of certain endpoints (Boxall et al., 2012). For most pharmaceutical compounds, concentrations in surface waters (Table 1.2) are many orders of magnitude below therapeutic doses and typically at least one order of magnitude below concentrations at which adverse effects have been reported in non-target organisms (Arnold et al., 2014; Corcoran et al., 2010; Santos et al., 2010). This is demonstrated in Figure 1.1, with standard acute and chronic endpoints generally ranging from ≈ 0.01 to 100 mg/L, whereas environmental concentrations of these contaminants are typically in the ng/L to low µg/L levels (Table 1.2).

Of course, there are exceptions. A widely studied physiological response in exposed organisms is vitellogenin induction, an egg-yolk protein essential for reproduction in females. Feminization of male fish due to vitellogenin induction has been observed upon exposure to low concentrations (1-5 ng/L) of the potent birth control hormone 17α-ethynylestradiol (Caldwell et al., 2012; Kidd et al., 2007). The antidepressant fluoxetine and other lipophilic pharmaceuticals, including

diphenhydramine, sertraline, and carbamazepine, have been measured in fish tissues

from effluent-dominated systems (Brooks et al., 2005; Du et al., 2014), with evidence

suggesting that these pharmaceuticals can bioconcentrate and bioaccumulate in

aquatic food chains (Du et al., 2014) and lead to behavioural effects, for example

modified aggression and reproductive behaviours in predatory fish (Brodin et al., 2014).
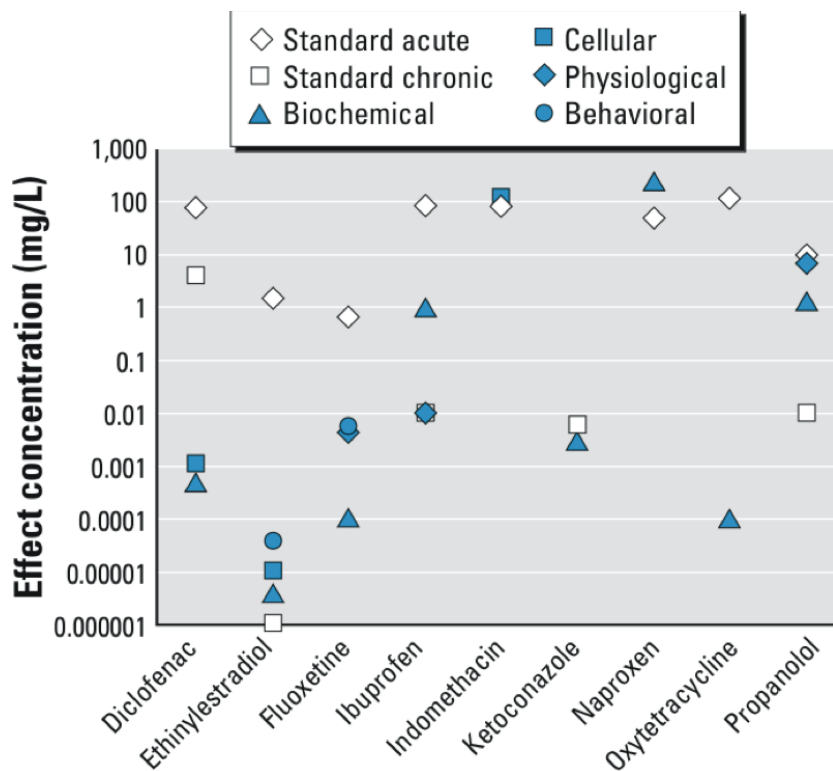
Figure 1.1: Effect concentrations for standardized acute and chronic fish studies (recommended for use in current regulatory risk assessments) (white points) and reported non-standard toxicity endpoints in fish and invertebrates (blue points). Figure is public domain reproduced from Environmental Health Perspectives. Image and modified caption from Boxall et al. (2012) (DOI 10.1289/ehp.1104477)

While characterization of effects for a wide range of organisms exposed to

individual pharmaceuticals has been relatively well studied (Arnold et al., 2014), a

number of challenges and gaps regarding the ecotoxicology remain (Boxall et al., 2012).

For example, because pharmaceuticals are always being released from WWTP as

complex mixtures containing multiple bioactive compounds, the question of chronic

mixture toxicity remains an area of significant interest (Backhaus, 2014; Boxall et al.,

2012). Another area of pressing concern to researchers relates to the ubiquitous nature

of antibiotics in our environment, which pose a very different, but potentially serious

ecotoxicological challenge compared to other classes of pharmaceuticals. Namely, the

selection and dissemination of anti-microbial resistant microorganisms (Boxall et al.,

2012; Kümmerer, 2009c; Pepper et al., 2018). Although the presence of antibiotic

resistance genes (ARGs) in most environments with wastewater influences is now well

established (Anderson et al., 2015b, 2013; Chaves-Barquero et al., 2016; Huijbers et

al., 2015; Pei et al., 2006) their relative importance as a vector and route of exposure to

the human population remains to be seen (Huijbers et al., 2015). Measurement of ARGs

in a wastewater-influenced river system is demonstrated in Chapter 2 of this thesis.

1.1.2 Pesticides

Modern pest control practices in agriculture began in the 1940's and 50's with the

discovery of highly effective synthetic chemical pesticides. The enormous benefits

synthetic pesticides provided to the agricultural industry led to steady increases in both

the amount and number of new pesticides used worldwide over the 20 year period

between approximately 1960 and 1980 (Stephenson and Solomon, 2007). At the time,

both environmental regulations relating to pesticide use and the fields of environmental

chemistry and ecotoxicology were in their infancy. This lack of regulation and

understanding led to a number of highly PBT pesticides entering the environment with

resulting ecotoxicological implications. In fact, eight of the infamous 'dirty dozen' POPs

banned or restricted by the Stockholm Convention in 2001 were pesticides used during

this era: aldrin, chlordane, DDT, dieldrin, endrin, heptachlor, mirex, and toxaphene

(Karlaganis et al., 2001). Today, the manufacture, registration, and use of pesticides is

highly regulated, requiring the development of comprehensive environmental fate and

toxicological profiles of new and current pesticides prior to (re)registration (Stephenson

and Solomon, 2007). Nonetheless, even though best practices regarding use and

regulation are significantly stricter than past practice, pesticides remain a highly

contentious and fiercely debated topic amongst scientists, politicians, and the public.

The seven pesticides studied, detailed in Table 1.1 along with pertinent selected

physiochemical properties, represent the following classes: neonicotinoids (imidacloprid,

thiamethoxam, and clothianidin); organophosphates (chlorpyrifos and diazinon);

triazines (atrazine); and 2,4-dichlorophenoxyacetic acid (2,4-D).

1.1.2.1 Sources and Occurrence

Neonicotinoids were developed in the 1980's and released to market in the

early 1990's (imidacloprid). They are common insecticides use to control pests on

mustard, oilseed rape, canola, and corn crops, as well as a number of fruit and

vegetable crops (Anderson et al., 2015). They are used extensively throughout the

Prairie Provinces, primarily as seed-treatments (Main et al., 2014), and represent 24%

of the global market share for insecticides (Anderson et al., 2015). Neonicotinoids were

considered potential replacements for organophosphate and carbamate pesticides but

have come under significant fire due to their toxicity to pollinators and specifically their

proposed link to major bee die-offs globally (Stokstad, 2013). The European Union have

taken the most drastic steps in response to this increased pressure by significantly

restricting their use in 2013 and recently voting to ban all outdoor uses (Erickson, 2018).

Atrazine, registered for commercial use in the U.S. in 1959, is a herbicide used for selective control of broadleaf and grassy weeds, primarily on corn crops (Solomon et al., 1996). In 2006 atrazine was applied across approximately 1.1 million hectares of planted land throughout Ontario and parts of Quebec, accounting for 94% of Canada's corn production (Lazorko-Connon and Achari, 2009). This usage rate is relatively small, as corn is not a major crop in Canada, especially when compared to the United States. In 1993 an estimated 500 tonnes of atrazine were applied in Ontario compared to ≈5000 tonnes in Illinois, a major corn growing state in the Midwestern U.S. Corn Belt (Solomon et al., 1996). This difference in usage patterns across the Canadian-U.S. border is a major theme in Chapter 2 of this dissertation.

Introduced in the 1940's, 2,4-D is an effective broad-spectrum herbicide for weed control and remains one of the oldest and most commonly used pesticides on the market. It is used around the globe, with major markets in the U.S., South America, Europe, and Russia (Islam et al., 2017). Annual usage in the U.S. is around 20,000 tonnes, with 66% of that in agriculture, 23% pasture/rangeland, and 11% residential, including extensive use on golf courses (Islam et al., 2017).

Organophosphates were introduced as replacements of organochlorine pesticides in the 1970's and 1980's (Galloway and Handy, 2003). Chlorpyrifos and diazinon, at times in their registration history, have been two of the most widely used insecticides globally for both agricultural and residential purposes (Galloway and Handy, 2003; Wang et al., 2017). While still used today, concerns around there presence and toxicity in the environment have led to residential bans in many jurisdictions and

countries and significant restrictions on use in agricultural, resulting in declining use over the last 20 years (Johnson et al., 2011; Solomon et al., 2014).

Water bodies in proximity of agricultural areas are at risk of pesticide contamination through overland or subsurface runoff, drainage of applied pesticide, or spray-drift during application. Many factors can influence the extent of pesticide runoff, including application method (e.g., foliar-spray versus seed coating), crop type, catchment size, soil type and retention capacity, and seasonal precipitation dynamics, especially in relation to timing of applications (Szöcs et al., 2017). Additionally, the chemical properties of the pesticide itself can be important in dictating the mobility of the chemical once applied (e.g., K_d). Small volume aquatic systems, including streams and wetlands, in close proximity to agricultural land represent high risk systems, as pesticide inputs from edge-of-field are likely to be intense and dilution potential low, leading to elevated pesticide concentrations (Main et al., 2015, 2014; Szöcs et al., 2017). Larger river systems receiving inputs from these small agricultural streams will generally represent comparatively minor exposure scenarios, but remain important to understand transport and mass loadings through a watershed (Novic et al., 2017; Szöcs et al., 2017). Pesticides residues in aquatic environments generally range from ng/L to low µg/L levels, depending on the proximity to the source and degree of dilution in the receiving water (Fenner et al., 2013). Specific pesticide occurrence data in the environment will be discussed in more detail in the body of the thesis. Specifically, Chapters 2 and 4 explore the occurrence and transport of pesticides through a large watershed, including in streams, large rivers, and lakes.

1.1.2.2 Environmental Fate

As with pharmaceuticals, the chemical structure of pesticides, and thus their physiochemical properties will dictate their fate and behaviour in the environment, making it difficult to generalize fate processes across pesticide classes. While, the major processes governing the fate and behaviour of pesticides in aquatic environments are much the same to those described for pharmaceuticals, namely photolysis, sorption, and biodegradation, volatilization and hydrolysis can also be more important for certain pesticides (Fenner et al., 2013). Overall, current-use pesticides have much improved environmental profiles compared to legacy pesticides. For example, DDT has an estimated environmental half-life of 3 to 20 years, with both biotic and abiotic degradation mechanisms following dehydrochlorination, leading to the primary metabolite DDE, also highly persistent and toxic in the environment (Lintelmann et al., 2003). The following section will summarize some of the specific mechanisms controlling the fate of pesticides relevant to this thesis (Table 1.1)

For the neonicotinoids, only 1.6-28% of applied parent compound is taken up by the target crop (depending on type of application), leaving a large amount of active ingredient with potential to enter soil and water compartments (Anderson et al., 2015a). Soil half-lives of thiamethoxam, imidacloprid, and clothianidin are variable in the available literature, ranging from 6-3001 days, 9-1250 days, and 17-6931 days, respectively (Anderson et al., 2015a). Neonicotinoids are water soluble and thus expected to be mobile in soils during precipitation events and end up in surface waters. Lu et al. (2015) reported direct photolysis quantum yields of 0.019 (thiamethoxam), 0.013 (clothianidin), and 0.0092 (imidacloprid) which corresponded to estimated direct

photolysis half-lives under summer sunlight (50°N latitude) of <12 hours. However, these estimations represent near surface processes only, as the authors reported a 98% reduction in degradation rates at a depth of ≈18 cm in shallow wetland mesocosms (Lu et al., 2015). Overall, neonicotinoid pesticides are labile in aquatic environments.

In contrast, atrazine is more persistent. The reported aquatic half-life of atrazine ranges depending on the experimental conditions, but is typically >100 days and in some cases more than 1 year (Lazorko-Connon and Achari, 2009). A major factor dictating this range in reported persistence is hydrolysis rates, which under certain conditions can be important in limiting the persistence of atrazine. For example, the presence and concentration of humic acids and the pH can result in hydrolysis half-lives ranging from 35 to 742 days (Solomon et al., 1996). Although volatilization is minor given the low vapour pressure and Henry's law constant, there have been reports of atrazine in rain water (Goolsby et al., 1997; Miller et al., 2000). Atrazine will undergo photolysis to varying extents, with indirect mechanisms typically dominating based on the specific water conditions (Fenner et al., 2013; Torrents et al., 1997). The formation of multiple photo-degradation products have been observed (Torrents et al., 1997). Atrazine is relatively recalcitrant towards microbial degradation due to the presence of the *s*-triazine ring (Solomon et al., 1996).

The herbicide 2,4-D is very water soluble, has a low vapour pressure and Henry's law constant, and a small K_d, suggesting likely transport and occurrence in aquatic systems. Estimated half-lives in water and soil are 30 and 10 days respectively (Messing et al., 2011). 2,4-D is known to undergo microbial transformation through oxidative de-alkylation and ring cleavage, however to what extent is very much

dependent upon specific microbial conditions (Fenner et al., 2013). Organophosphates can volatilize into the atmosphere quite readily immediately post-application, adsorb quite strongly to soils under specific soil conditions (e.g., chlorpyrifos $K_d \approx$ 50-2000 and K_{oc} = 1000-31,000 mL/g), and/or undergo abiotic hydrolysis and microbial degradation in waters and soils (Solomon et al., 2014). Chlorpyrifos has a hydrolysis half-life of 16 days at pH 9 and ≈70 days at pH 5-7, an aqueous photolysis half-life of 30 days, and microbial degradation half-lives in soil and water ranging from approximately 10 days to <300 days (Solomon et al., 2014)

1.1.2.3 Ecotoxicology

While pharmaceuticals and pesticides are both considered to be bioactive chemicals, as noted earlier the ecotoxicology of pharmaceuticals is highly nuanced given the intended sub-lethal mechanisms in target organisms, and thus similar effects in non-target organisms (e.g., behavioral changes) (Figure 1.1). This is in contrast to pesticides, which are designed to be lethal to target pests at concentrations applied to crops. Therefore, the toxicology of pesticides to non-target organisms can represent more serious exposure scenarios and possible adverse effects. It is therefore not surprising that a crucial aspect of pesticide registration is the study of un-intended effects on non-target organisms. As a result, a relatively large body of acute and chronic toxicology data exist for potential non-target organisms. As a summary, acute and chronic aquatic life benchmark values in freshwater for fish, invertebrates, and non-vascular and vascular plants, are provided in Table 1.3. These values are taken from the U.S. Environmental Protection Agency's Office of Pesticides Program (https://www.epa.gov/pesticide-science-and-assessing-pesticide-risks/aquatic-life-

benchmarks-and-ecological-risk). Acute toxicity is calculated based on LC_{50} or EC_{50} - values and chronic toxicity is determined using the no-observed-adverse-effect-concentration. These toxicological values along with water quality guidelines for protection of aquatic life from the Canadian Council of Ministers of the Environment are used in Chapter 2 to assess risk posed to aquatic organisms based on exposure distributions developed from measured concentrations of these pesticides.

Table 1.3: Acute and chronic aquatic life benchmarks for fish, invertebrates, and non-vascular and vascular plants in freshwater for the pesticides studied in this thesis. All values are in µg/L.

Class: mechanism[a]	Compound	Fish		Invertebrates		Nonvascular plants	Vascular plants
		Acute	Chronic	Acute	Chronic	Acute	Acute
Triazine herbicide: inhibition of photosystem II	Atrazine	2650	5	360	60	1	4.6
Neonicotinoid insecticides: bind acetylcholine receptors	Thiamethoxam	50,000	20,000	17.5	N/A	97,000	90,000
	Clothianidin	50,750	9700	11	1.1	64,000	121,000
	Imidacloprid	114,500	9000	0.385	0.01	10,000	N/A
Synthetic auxin herbicide: phtyo-hormonal disruption	2,4-D	40,800	23,600	12,500	16,050	3880	300
Organophosphate insecticides: acetylcholine-esterase inhibitor	Chlorpyrifos	0.9	0.57	0.05	0.04	140	N/A
	Diazinon	45	0.55	0.11	0.17	3700	N/A

[a](Stephenson and Solomon, 2007). N/A – benchmark not provided by USEPA OPP.

1.1.3 Analysis of Polar Organic Contaminants

Liquid chromatography triple quadrupole tandem mass spectrometry (LC-MS/MS) has become the gold standard for quantitative analysis of polar organic contaminants in environmental media (Petrović et al., 2005; Sarkar et al., 2009; Ternes, 2001; Vanderford and Snyder, 2006). Most of these methods employ electrospray ionization (ESI) due its relative simplicity, broad applicability to a wide range of polar chemicals, and its compatibility with LC (Oss et al., 2010; Petrović et al., 2005). These multi-residue LC-MS/MS methods provide sufficient separation between target analytes

and from highly polar aqueous interferences, good sensitivity, and excellent selectivity, crucial for avoiding isobaric interferences in complex environmental matrices. Additionally, triple quadrupole instruments have excellent linear dynamic ranges (5-6 orders of magnitude) making them ideal for targeted environmental measurements. These methods are typically conducted with isotope dilution to account for analyte loss incurred during extraction and ion signal modification resulting from matrix effects during ionization. A fully quantitative LC-MS/MS isotope dilution method is used throughout this dissertation for the multi-residue analysis of 34 target pharmaceuticals and pesticides shown in Table 1.1.

More recently, advancements in high-resolution mass spectrometry (HRMS) techniques, including quadrupole time-of-flight (QTOF) and Orbitrap instruments, has led to the emergence of powerful suspect and non-target screening methods useful for contaminant discovery and identification of suspect contaminants without an *a priori* list of target chemicals (Hug et al., 2014; Li et al., 2017; Schymanski et al., 2014b; Wode et al., 2015). However, the 'unknown' nature of the contaminants identified through these HRMS screening approaches means that measurement by isotope dilution is often impossible, leading to limitations regarding analyte quantification with these methods (Pieke et al., 2017). Chapter 5 of this dissertation demonstrates the utility of suspect screening of polar organic contaminants using HRMS LC-QTOF. The following sections will briefly describe the governing theory behind the two aforementioned analytical instruments utilized in this work; high-performance liquid chromatography (HPLC) and mass spectrometry (MS).

1.1.3.1 High-Performance Liquid Chromatography

Liquid chromatography is a separation technique that uses a liquid mobile phase to transport and separate sample components as they migrate through a packed stationary phase. Reverse-phase HPLC, used throughout this dissertation for its applicability to small molecule analysis (<2000 Da) of polar and non-polar compounds, employs a high performance solvent pump and chromatographic column with polar mobile phase (solvent) and non-polar stationary phase (column). Analyte separation by HPLC is dictated by differential interactions of the target analytes with the mobile and stationary phases, governed largely by analyte polarity, as the sample mixture flows through the chromatographic column. These differences in analyte interactions result in varying mobility through the analytical column, thereby separating components into distinct bands or zones that can be subsequently analyzed. In order to achieve consistent and quantitative chromatography a number of fundamental HPLC parameters can be adjusted.

These parameters are optimized during method development with the goal of achieving the required chromatographic resolution in the shortest possible time. Resolution (R), a measure of how well two eluting peaks can be differentiated in a chromatographic separation, is affected by three fundamental parameters: efficiency (N), selectivity (α), and retention/capacity (k) described in *Equation 1.1* (Skoog et al., 2007):

$$R = \left(1/4\sqrt{N}\right)\left(\frac{\alpha - 1}{\alpha}\right)\left(\frac{k}{1 + k}\right)$$

Equation 1.1

The selectivity (α), or separation factor, is the ability of a chromatographic system to distinguish between two components based on their relative rates of

migration. Selectivity can be altered by changing the solvent strength, pH, stationary

phase or column temperature. The retention or capacity factor (k) measures the degree

of retention of a given analyte on the chromatographic column and can be adjusted by

altering the mobile phase composition. Column efficiency is a measure of the analyte

dispersion as it travels through the HPLC system and is dictated by a theoretical plate

count (N) which describes the number of equilibrium stages occurring as a solute

migrates through the analytical column.

The term plate height (H) describes the length of a column needed to produce

one equilibration stage (i.e., one theoretical plate) and is a better measure for

comparing column performance. For a given analytical column of fixed length, a larger

N means a smaller H, resulting in greater efficiency and thus sharper peaks. The van

Deemter equation (*Equation 1.2*) describes the effect mobile phase flow-rate (u) has on

H, with terms *A, B*, and *C* describing factors contributing to band broadening (i.e.,

chromatographic efficiency) (Skoog et al., 2007).

$$H = A + B/u + Cu$$

Equation 1.2

Eddy diffusion (*A*) describes the differential pathways molecules will take through a

particle packed column. This leads to distribution of analytes from the sharp pulse

introduced at the front of the column to the broad peak detected at the end of the

column. Band broadening due to eddy diffusion can be minimized by using uniform size

and homogenous packing of stationary phase particles. Longitudinal diffusion (*B*) occurs

along the length of the analytical column arising from axial diffusion of analyte

molecules from the concentrated pulse to more dilute regions. Effects of longitudinal

diffusion can be reduced by decreasing the column temperature (less kinetic energy)

and/or increasing the flow-rate. Finally, the mass transfer kinetics (*C*) controlling the sorption and de-sorption of analytes from the stationary phase can differ amongst molecules in the analyte band as they move through the column, leading to peak broadening. The effects of slow mass-transfer can be minimized by reducing the extent of non-equilibrium in a number of ways: thin-film coatings on stationary phase particles to decrease the diffusional distance during sorption/de-sorption, increasing column temperature to increase diffusion coefficients, and decreasing mobile phase flow rate to provide more time for mass transfer and thus equilibration.

These fundamental parameters can be optimized during method development by varying specific chromatographic conditions, including organic solvents (e.g., methanol, acetonitrile), mobile phase composition during gradient elution (% aqueous: organic), solvent pH, flow-rate, column temperature, column chemistry (e.g., C_{18}, C_8, phenyl, cyano, amino), column dimensions (length, internal diameter, particle size and packing), and injection volume. Specific details of the optimized chromatography for the analytes studied here are provided throughout this dissertation.

1.1.3.2 Mass Spectrometry

There are several popular types of mass analyzers that differ in the fundamental way in which they separate species on a mass-to-charge (*m/z*) basis. In all cases, production of negatively or positively charged gas phase ions is required for separation and manipulation by the MS. With LC-MS this process is achieved by introducing the solvated sample into an ionization source where the samples is aerosolized and subsequently vaporized in the heated chamber. Common LC-MS compatible ionization

sources include electrospray ionization (ESI), atmospheric pressure chemical ionization (APCI), and atmospheric pressure photoionization (APPI).

ESI is a soft ionization technique compatible with moderate to highly polar molecules and used exclusively in this dissertation. Successful ESI involves the following four stages (Trufelli et al., 2011):

- Addition of charge to the aerosolized liquid phase analyte during introduction into the ionization chamber via the nebulizer needle;

- Production of charged droplets at the tip of the nebulizing needle through Taylor Cone formation;

- Evolution of the charged droplets by solvent evaporation (gas flow and heat) and droplet fission;

- Formation of charged gas phase ions.

Positive and negative mode ESI typically involves the formation of $[M+H]^+$ (basic species) and $[M-H]^-$ ions (acidic species), respectively, which can be optimized by adjusting the solution/eluent pH according to an analytes pK_a. These charged gas phase ions electrophoretically migrate towards the capillary (inlet to the mass analyzer) as a result of opposite charges applied between the nebulizer needle and capillary, where an electric field across the capillary accelerate the ions into the mass analyzer (Skoog et al., 2007).

Ionization efficiency is dependent on the chemical properties of the analyte, which will dictate sensitivity via LC-MS analysis. However, the ionization process is often subject to interfering species present in the sample matrix and mobile phase solvents that can serve to modify ionization efficiencies, resulting in ion suppression or,

less commonly, ion enhancement. This is especially relevant when dealing with environmental samples with complex matrices. Liquid phase processes are thought to be the major contributor to signal suppression in ESI, a result of four primary mechanisms (Trufelli et al., 2011):

- Competition for available charges and access to droplet surface from matrix components;

- Interfering compounds increasing the viscosity and surface tension of charged droplets, thereby altering their formation and evaporation efficiency;

- Non-volatile additives (e.g., buffers) suppressing droplet formation through inclusion of solid particles;

- Mobile phase additives and interfering species forming ion-pairs with pre-formed analyte ions.

Characterizing ion suppression in LC-MS analysis remains a highly complex problem of primary importance to achieve quantitative measurements, and is thus a major goal of sample preparation and method optimization. The quantitative data presented throughout this dissertation utilizes isotope dilution to account for ion suppression. Chapter 5 is especially relevant to this discussion, as it explores a semi-quantitative approach to dealing with LC-MS matrix effects when isotope dilution is not applicable.

The following will briefly highlight the operating principles of the two mass analyzers utilized in this dissertation, quadrupole (Q) and time-of-flight (TOF) MS. Quadrupole mass analyzers use electric fields to separate ions according to their *m/z* ratio as they pass through the central axis of four parallel poles (circular or hyperbolic shaped rods) that have DC and RF voltages applied to them (Skoog et al., 2007). By

optimizing the magnitude of these voltages only ions of specific *m/z* ratios will travel the length of the quadrupole and into the detector, while other non-targeted ions will have unstable trajectories through the poles causing them to crash out of the analyzing device. The ability to isolate detection to individual ions makes quadrupole mass analyzer highly sensitive and selective.

The most common type of quadrupole mass analyzer and the primary instrument uses in this work is the triple quadrupole (QQQ) MS. The combination of three quadrupoles in tandem facilitates various MS scan modes and experiments to be conducted in order to ensure reliable and quantitative identification, and specifically to differentiate between co-eluting isobaric interferences. The most common application of a QQQ MS for quantitative multi-residue measurements is a dynamic multiple reaction monitoring (MRM) method. MRM methods use the first quadruple (Q1) to screen for specific *m/z* ratios during specific time windows corresponding to the elution of chromatographic peaks. This initial ion scan is known as the pre-cursor ion. Q2, also known as the collision cell, is typically an octopole or hexapole containing an inert collision gas (N_2) where collision induced dissociation (CID) of the parent ion occurs. The parent ion fragments in Q2 forming characteristic product ions that are selected for transmission through the third quadrupole (Q3) and into the detector. In many cases pre-cursor ions will fragment into more than one characteristic product ion, often deemed quantifier and qualifier ions, which are used as supporting evidence to differentiate target analytes from co-eluting isobaric interferences. While QQQ mass analyzers remain the work-horses for quantitative multi-residue analyses due to their low cost, reproducibility, sensitivity, selectivity, and large linear dynamic range, their unit

resolution and poor mass accuracy make them inadequate for HRMS applications like suspect and non-target screening.

Time-of-flight (TOF) mass analyzers are considered a HRMS instrument, which are often defined as mass analyzers with resolution > 10,000 (Gross, 2004). The basic principle of TOF MS employs a field-free flight tube in which ions of different m/z ratios will travel through the flight tube at different speeds, separating and detecting individual ions through correlation with their flight times. Increasing the flight path increases the resolving power of the instrument which is the specific focus of many TOF designs. For example, the orthogonal reflectron is a retarding electric field located after the flight tube that slows all incoming ions to zero kinetic energy and then re-ejects them into the flight tube, thus increasing the total flight distance and focusing the spatial distribution of ion packets as a result of the initial flight, ultimately increasing resolving power of the instrument (Gross, 2004). Combining quadrupole and TOF mass analyzers is especially advantageous to provide the selectivity and MS^2 capabilities of the QQQ with the high resolution and mass accuracy afforded by the TOF MS. Current QTOF instruments have a resolving power and mass accuracy of ≈30,000 and 2-5 ppm, respectively, facilitating exact mass and molecular formula determination of suspect or unknown compounds, as demonstrated in Chapter 5 using an LC-QTOF instrument.

1.2 Environmental Sampling

Sampling is the first and most important step in almost all analytical procedures. Acquiring representative samples will often define a successful monitoring program or sampling campaign. Environmental sampling can be particularly challenging, as levels

of contaminants can fluctuate significantly in the receiving environment (Beek et al., 2016). In aquatic systems, sampling is typically achieved using any of the following four techniques, individually or in concert: grab sampling, active sampling, passive sampling, or biomonitoring. Each technique is defined below and summarized in Table 1.4.

- **Grab sampling**, also known as discrete or spot sampling, uses a sealable bottle (usually plastic or glass) to take a specific volume of water from a discrete location in a body of water, typically at a set depth below the surface.

- **Active sampling** is essentially an automated grab sample with a programmable pump to fill pre-loaded bottles at specific time- or flow-proportional intervals.

- **Passive sampling** is a simple, non-mechanical device that relies on molecular diffusion of aqueous analytes from the sampled medium (water) to a collecting medium (sampler), as a result of a chemical potential gradient between the two compartments (Górecki and Namienik, 2002). Passive sampling devices (PSDs) are often deployed in systems and left for days to months until retrieval and extraction in the laboratory. PSDs are comprised of a material, typically a polymeric powder, membrane, or film that sorbs the analytes of interest. The rest of the sampler comprises the housing materials used to hold the sorbent in place.

- **Biomonitoring** is a type of passive sampling that uses a living organism (plant or animal) as the collecting medium to measure contamination in the environment. Common biomonitors for various environmental compartments include lichen and pine needles (air contamination), vegetables (soil contamination), and fish and mussels (water contamination) (Górecki and Namienik, 2002).

Table 1.4: Comparing the four primary aquatic sampling techniques.

Advantages	Disadvantages
GRAB SAMPLING	
- Very simple to do - Requires very little training - Low cost and minimal equipment - Almost any lab will have the basic infrastructure to take and process grab samples - Can provide highly resolved concentration data if enough samples are taken - Widely accepted as the standard water sampling protocol - Data interpretation is simple	- Only provides a single snap-shot in time of the system - In systems with multiple stochastic inputs it is very easy to miss contamination events - Can quickly incur large number and volume of samples in a large monitoring program - Unless large volumes are sampled detection limits can be an issue - Depending on volume and type of sample filtering (0.45 µm) can be very time consuming - Samples need to be processed quickly as analyte stability during storage can be labile
ACTIVE SAMPLING	
- Automated and programmable to take grab samples without a person present - Can provide highly resolved concentration data - Takes integrative samplers, usually over 24 hour periods (time-proportional sample) - Also provides options to acquire flow-proportional samples, useful for scenarios where flow-rate may be variable - More likely to capture input events that may cause changes in contaminant concentration	- Requires a power source, electronics, moving parts - Systems are large, bulky, difficult to transport, and obvious (potential target for vandalism) - Represent challenges for remote field work - Systems are very expensive - Can quickly incur large number and volume of samples in a large monitoring program - Unless large volumes are sampled detection limits can be an issue - Depending on volume and type of sample filtering (0.45 µm) can be very time consuming - Samples need to be processed quickly as analyte stability during storage can be labile
PASSIVE SAMPLING	
- Simple to use and relatively cheap - Simple transport and storage, even in large quantities - Provides continuous *in-situ* monitoring - Deployments can range from days to months depending on application - Improved detection limits, especially during longer deployments (e.g., weeks) - Sampling only the truly dissolved chemical fraction - Time-weighted average (TWA) concentrations are generally more representative of levels that organisms are exposed to - Long term storage and sample archiving is possible - Sample matrices are often cleaner - Sample extraction requires fewer steps	- Most passive samplers cannot provide short-term, highly resolved concentration data - Requires some training and expertise to use properly - Upfront costs necessary to conduct passive sampling (deployment cages and cables, sampler materials) - Calculation of quantitative TWA concentrations require compound-specific sampling rates - Most samplers require laboratory calibration experiments to determine sampling rates - Sampling rates can be highly dependent upon environmental conditions therefore large uncertainties associated with applying lab-based sampling rates under field conditions - Data calculation/interpretation can be complicated
BIOMONITORING	
- Provides the true level of chemical contamination in organism of interest - No deployments required as organism (in most cases) are naturally present in the system - Contaminants that bioaccumulate in organism will have improved detection limits	- Organisms can be difficult to find and collect - Need to ensure organisms are representative of the environment (e.g., resident or migratory species) - Dealing with live organisms is challenging - Need animal use protocols and animal ethics approval - Extractions can be more challenging - Must have an understanding of species biology

1.3 Aquatic Passive Sampling

Most PSDs provide a time-weighted average (TWA) concentration, integrating contaminant fluxes over a defined deployment period. This is fundamentally different from the information obtained from individual grab samples, as demonstrated graphically in Figure 1.2. In the context of exposure and risk assessments, sometimes maximum environmental concentrations are desired for use in preliminary assessment of acute toxicity (e.g., hazard quotients) (Carlson et al., 2013a), in which case grab sampling can be preferred. Otherwise, passive sampling data is beneficial in many respects (Table 1.4)

TWA concentrations provide a more representative and realistic estimate of exposures over an organism's lifetime (Booij et al., 2016), more appropriate for understanding chronic toxicity. Additionally, for extended monitoring campaigns passive sampling is simply the most efficient, low-cost, and simple approach to acquiring reliable concentration data (Booij et al., 2016; Górecki and Namienik, 2002).
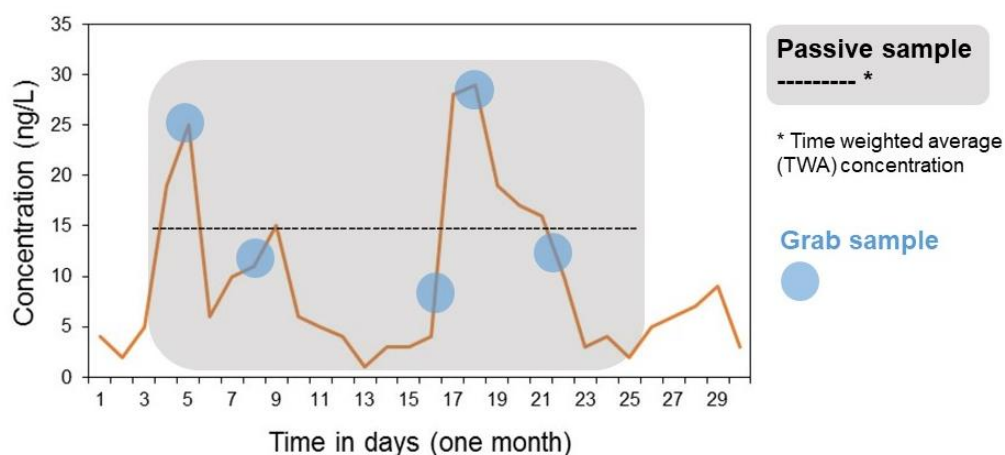
Figure 1.2: A hypothetical concentration profile (orange line) of a chemical in an aquatic system over a one month period. Blue circles represent grab sampling events and the gray box represents a three week deployment of a passive sampler. The dashed line provides a theoretical TWA concentration that passive sampling data can provide. Qualitatively, the average of all five grab sample concentrations (≈ 25, 12, 8, 28, 13 ng/L) gives an average water concentration (≈ 17 ng/L) close to that of the passive sampler TWA concentration (≈ 15 ng/L).

1.3.1 Passive Sampling theory

Chemical accumulation in aquatic PSDs can be described by two distinct uptake regimes; linear uptake and equilibrium uptake (Figure 1.3), defining the two major classes of aquatic PSDs. The exchange kinetics between water and sampler shown in Figure 1.3 can be described by a first-order, one compartment model (*Equation 1.3*), where $C_s(t)$ is the concentration of analyte in sampler at exposure time t, C_w is the analyte concentration in the water column, and k_1 and k_2 are the sorption and desorption rate constants, respectively.

$$C_s(t) = C_w \frac{k_1}{k_2}(1 - e^{-k_2 t})$$

Equation 1.3
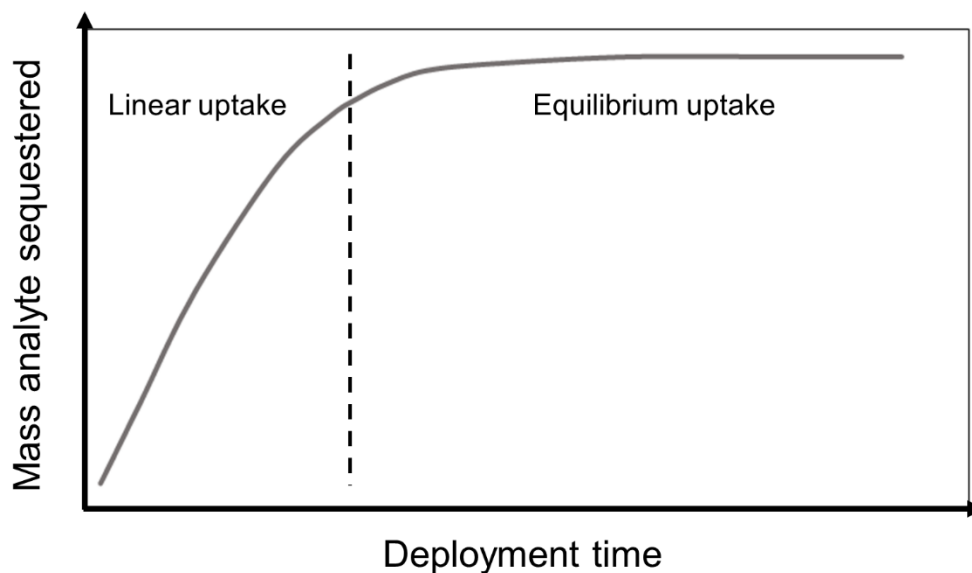
Figure 1.3: Theoretical profile (gray line) of chemical accumulation in passive sampler over time. PSDs operate in two uptake regimes (linear/kinetic and equilibrium) described by Equation 1.3.

During equilibrium uptake the deployed sampler reaches thermodynamic equilibrium with the water phase, and *Equation 1.3* can be simplified to *Equation 1.4*, where K_{sw} is the sampler-water partition coefficient.

36

$$C_s = C_w \frac{k_1}{k_2} = C_w K_{sw}$$

Equation 1.4

Equilibrium passive samplers typically describe the measurement of hydrophobic-type organic contaminants in water and have been studied extensively in the literature (Booij et al., 2016; Mayer et al., 2003; Vrana et al., 2005). Equilibrium PSDs were developed in the early 1990's for measurement of hydrophobic organic contaminants such as PCBs, PAHs, and legacy pesticides (Vrana et al., 2005). The two common types of equilibrium PSDs are the semi-permeable membrane device (SPMD) and polyethylene (PE) sheet (Allan et al., 2009; Petty et al., 2000), both of which use low-density polyethylene tubes or sheets as membranes and rely on hydrophobic-type interactions (often described using K_{ow}) to concentrate analytes. Comprehensive discussions of equilibrium PSDs can be found elsewhere (Allan et al., 2009; Booij et al., 2007; Petty et al., 2000). The remainder of this introduction will be dedicated to describing kinetic PSDs and their applications for measuring POCs.

Linear uptake into a PSD requires that the rate of mass transfer into the receiving phase is linearly proportional to the chemical potential gradient between water and sampler during the exposure time (Figure 1.3). A relationship approximating this linear uptake can be derived using the uptake rate constant (k), defined in *Equation 1.5*, where k_o is the overall mass transfer coefficient, V_s is the sampler/sorbent volume, and R_s is the sampling rate (Booij et al., 2007). Plugging *Equation 1.5* into *Equation 1.3* and re-arranging to solve for water concentration (C_w) we can obtain *Equation 1.6*, which, over short exposure times is approximated by the linear relationship in *Equation 1.7*.

$$k = \frac{k_o A}{K_{sw} V_s} = \frac{R_s}{K_{sw} V_s}$$

<div align="right">*Equation 1.5*</div>

$$C_w = \frac{M_s}{K_{sw} V_s [1 - exp(-R_s t / K_{sw} V_s)]}$$

<div align="right">*Equation 1.6*</div>

$$C_w \approx \frac{M_s}{R_s t}$$

<div align="right">*Equation 1.7*</div>

The TWA water concentration (C_w) in *Equation 1.7* can now be calculated with only the mass of analyte accumulated on sampler (M_s), exposure time (t), and sampling rate (R_s). The sampling rate, analogous to K_{sw} for equilibrium PSDs, is generally described in L/day and can be interpreted as the analyte volume in water clearing the exposed sampler as a function of time. The sampling rate parameter links the mass of analyte sequestered onto the PSD to the TWA concentration in the water column over a given deployment period. The derivation of the sampling rate is related to the overall mass transfer coefficient (k_o) and exposed surface area of the PSD (A), as in *Equation 1.5*. The term k_o is best described as the total resistance to mass transfer, made up of the sum of resistances posed by each phase as the analyte diffuses from the bulk water phase into the sampler receiving phase (Booij et al., 2007), as described in *Equation 1.8*: δ is the phase thickness of the water boundary layer (δ_w), passive sampler membrane (δ_m), and biofilm (δ_b) that can form on the surface a deployed PSD, D is the analyte diffusion coefficient through those same layers, and K_{mw}, K_{bw} are the membrane-water and biofilm-water partition coefficients, respectively.

$$\frac{1}{k_o} = \frac{\delta_w}{D_w} + \frac{\delta_m}{D_m K_{mw}} + \frac{\delta_b}{D_b K_{bw}}$$

<div align="right">*Equation 1.8*</div>

The water boundary layer, also known and referred to here as the diffusive boundary layer (DBL) is described in Figure 1.4.

The mass transfer relationship (*Equation 1.8*) describes some of the confounding factors affecting analyte uptake into a PSD and helps to understand some of the challenges and uncertainties associated with appropriately determining sampling rates in the laboratory that can be accurately applied under field conditions. For most passive sampling applications the DBL represents the largest source of uncertainty (Figure 1.4). Furthermore, for polar-PSD applications it is typical to assume that *Equation 1.8* reduces to (Alvarez et al., 2004):

$$\frac{1}{k_o} \approx \frac{\delta_w}{D_w}$$

Equation 1.9
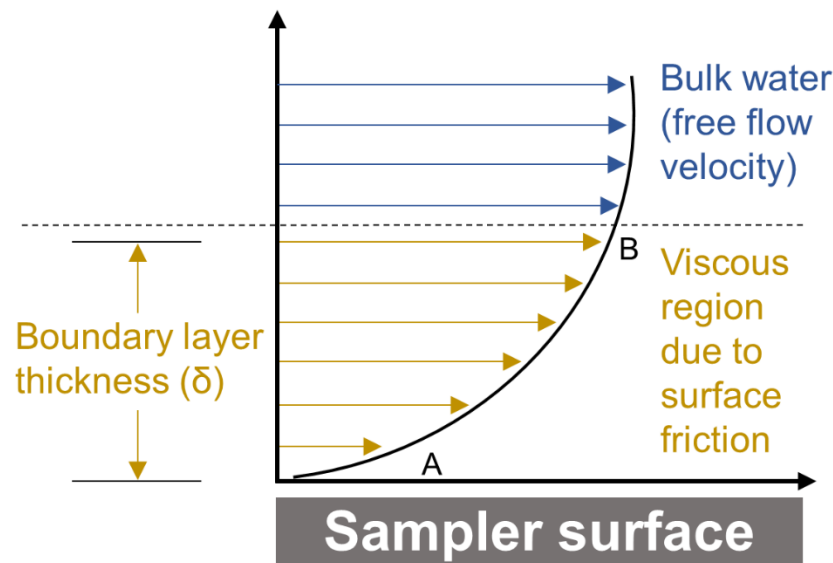
Figure 1.4: Water flowing (blue arrows) over a bounding surface (e.g., passive sampler) experiences surface friction and effects of viscosity, leading to reduced flow velocity at the immediate vicinity of the bounding surface (yellow arrows). The water boundary layer thickness (δ_w) is estimated as the distance from the bound surface (A, flow velocity approaches 0) to where the influence of surface friction first becomes important, i.e., where a reduction in flow-velocity compared to the bulk flow is detected (B). This figure describes one example of a boundary layer. It is important to note however, that the flow velocity profile of a boundary layer does not necessarily have to fit a quadratic function as depicted here.

For equilibrium PSDs, analyte transport in the membrane (e.g., K_{mw}) is well characterized (Allan et al., 2009; Booij et al., 2007), thus the simplification to *Equation 1.9* is generally not required. Membrane transport in polar-PSDs, however, is poorly understood (Fauvelle et al., 2017; Vermeirssen et al., 2012) and thus membrane resistance is often ignored out of necessity. Even with the simplified relationship of *Equation 1.9,* large uncertainties associated with the DBL ($δ_w$) can still remain. To a large extent flow-rate controls the DBL thickness, thus, applying sampling rates or partition coefficients determined under one set of flow conditions is non-ideal considering that typical surface waters can experience highly variable water flow over a given deployment period.

Other environmental conditions including water pH and temperature can also have an influence on *in-situ* sampler uptake (Harman et al., 2012; Huckins et al., 2002). For equilibrium PSDs, performance reference compounds (PRCs) have become the 'gold-standard' approach to account for confounding environmental factors impacting laboratory-derived and *in-situ* sampling rates (Booij et al., 2007; Huckins et al., 2002). The PRC approach works by enriching the PSD with isotopically labelled target analytes at a known amount (e.g., deuterated PAHs) prior to deployment. During exposure, the rate at which PRCs desorb from the sampler can be determined and used to correct laboratory derived uptake rates *in-situ*, assuming that the target analyte and PRC exhibit isotropic exchange rates (Huckins et al., 2002).

The PRC approach for kinetic polar-PSDs has been met with limited success, as polar analytes often fail to produce isotropic exchange and/or result in negligible desorption, two fundamental criteria of the PRC approach (Fauvelle et al., 2017;

40

Harman et al., 2011; Morin et al., 2012; Shaw et al., 2009). This is a result of the fundamental differences between sampler accumulation mechanisms describing uptake of polar versus non-polar analytes in kinetic- and equilibrium-PSDs, respectively. In contrast to equilibrium samplers, governed by hydrophobic partitioning processes often described using an analytes $logK_{ow}$, the analyte-sorbent interactions controlling uptake in polar-PSDs are primarily based on adsorption phenomena, which, under most environmental conditions can be effectively irreversible (Bäuerlein et al., 2012; Dias and Poole, 2002), hence the challenge of using PRCs for polar analytes. These sampling rate issues are a point of discussion in the following section as it relates to polar PSDs and a common theme throughout this dissertation, addressed in detail in Chapter 4.

1.3.2 Polar Passive samplers

The POCIS® (polar organic chemical integrative sampler) (Alvarez et al., 2004) is the most popular tool for measuring POCs ($logK_{ow} < 5$) in water and has been calibrated for well over 300 target compounds (Harman et al., 2012; Morin et al., 2012). To a lesser extent Chemcatcher® is another PSD that has been applied to aquatic passive sampling of polar analytes (Novic et al., 2017; Shaw et al., 2009; Shaw and Mueller, 2009). POCIS comprises two thin polyethersulfone (PES) membranes (typically ≈0.1 mm thick and ≈0.1 μm pore size) sandwiching a lose powdered sorbent and sealed around the edges of the membranes using two stainless steel discs, leaving a total exposed membrane surface area of ≈41 cm^2 on both sides of the sampler (Figure 1.5). The standard sorbent used with POCIS is Waters Oasis® HLB (hydrophilic-lipophilic balance) which contains apolar (benzyl groups, aliphatic chains) and polar moieties (pyrrolidone) and is advertised and widely used as an all-purpose solid-phase extraction

(SPE) product suitable for a wide range of polar to moderately non-polar analytes (Bäuerlein et al., 2012). This standard HLB POCIS configuration is sometimes referred to as the 'pharmaceutical-POCIS', as there is a second variant that contains a triphasic sorbent mixture of hydroxylated polystyrene-divinylbenzene resin (Isolute ENVþ) and a carbonaceous sorbent (Ambersorb 1500), dispersed on S-X3 bio- beads (Harman et al., 2012). The latter, known as the 'pesticide-POCIS', has been shown to be more effective for certain classes of polar pesticides, however is much less common in the literature than the pharmaceutical-POCIS (Harman et al., 2012). Going forward, any discussion throughout this dissertation regarding POCIS will exclusively relate to the pharmaceutical-POCIS configuration.

Although POCIS has become a widely accepted and indispensable PSD for a variety of applications over the last 15 years, significant challenges have led end-users to question its value as a quantitative measurement tool (Harman et al., 2011; Poulier et al., 2014). These uncertainties are related to many of the issues discussed in the previous section, namely that environmental conditions can have large impacts on sampler uptake. Without an accepted *in-situ* approach to reconcile laboratory-derived and field sampling rates (i.e., PRCs) there remains a degree of unknown uncertainty related to POCIS measurements, deeming the PSD semi-quantitative at best (Harman et al., 2011). Additionally, POCIS and current polar-PSDs lack a widely applicable and fundamental uptake model making accurate sampling rate estimations difficult (Harman et al., 2012; Miller et al., 2016). While part of this issue can be attributed to the fundamental mechanisms governing uptake and sorption in kinetic polar-PSDs, which

mostly explain the challenges with PRCs and POCIS, many of the issues are simply

related to the sampler design (Figure 1.5).

POCIS uptake is generally considered to be boundary layer controlled (Harman

et al., 2012) as the PES membrane (≈0.1 mm) is much thinner than water boundary

layers typically encountered in aquatic systems, which can range from 0.23-0.25 mm in

flowing water (Chen et al., 2013; Scally et al., 2003; Uher et al., 2013; Warnken et al.,

2006) up to 0.44-1.5 mm under quiescent conditions (Uher et al., 2013; Warnken et al.,

2006). A confounding factor related to PES is the apparent interaction certain analytes

have with the membrane (Silvani et al., 2017; Vermeirssen et al., 2012), further

complicating mass-transfer into the sampler and hindering the development of a robust

uptake model for current polar-PSDs. Temperature (Dalton et al., 2014; Li et al., 2010a;

Togola and Budzinski, 2007) and pH (Li et al., 2011) can also impact sampler uptake

significantly, but are rarely considered during laboratory calibration or field applications

of sampling rates. Overall, variation as a result of any individual parameter discussed

above (flow-rate, temperature, pH) is typically on the order of a factor-of-two and taken

together can lead to uncertainties >100% (Poulier et al., 2014). The need for an

improved polar-PSD with a simplified mechanism controlling uptake and an ability to

account for site-specific conditions affecting *in-situ* sampling rates is apparent, and

highlights the major impetus behind this thesis.

1.3.3 *Diffusive Gradients in Thin Films (DGT)*

The technique of diffusive gradients in thin films (DGT) (Davison and Zhang,

1994; Zhang and Davison, 1995) is a hugely successful and widely popular passive

sampler for inorganic species (e.g., trace metals), with applications to both aquatic and

sediment pore-water systems (Davison and Zhang, 2012). The beneficial aspects of DGT are rooted in its design (Figure 1.5). Specifically, a relatively thick diffusive hydrogel, serving to control analyte uptake, is layered on top of the binding gel which contains the sorbent responsible for sequestering analytes of interest. With DGT samplers, boundary layer and flow rate effects are greatly minimized *in-situ* through inclusion of the thick diffusive gel, making uptake into DGT sampler layer-controlled as opposed to boundary layer-controlled, as in POCIS. As a result, mass-transfer into DGT is governed by molecular diffusion, a chemical property that is well understood, simple to measure (Zhang and Davison, 1999), and in many cases amenable to modelling (Schwarzenbach et al., 2005b). In addition, temperature variation can be accounted for *in-situ* by using measured or modelled temperature-specific diffusion coefficients (Li et al., 2009). The governing DGT equations, which are derived from the fundamental relationships in Chapter 1 (*Equation 1.7* and 1.9), are provided in Chapter 3.

These many benefits of the DGT sampler have been well demonstrated and widely accepted for measurements with inorganic species (Davison and Zhang, 2012). More recently the DGT technique has been adapted for POCs with notable successes (Chen et al., 2015; 2013; 2012). Dubbed the organic-DGT or simply o-DGT, Chen et al. first developed the o-DGT for the single antibiotic sulfamethoxazole (Chen et al., 2012) and then extended the testing to 40 antibiotics in wastewaters (Chen et al., 2015; 2013). While these studies present a promising new polar-PSD that improve upon many of the challenges inherent with POCIS, much more work is needed to validate the utility and applicability of this technique for measurement of POCs.
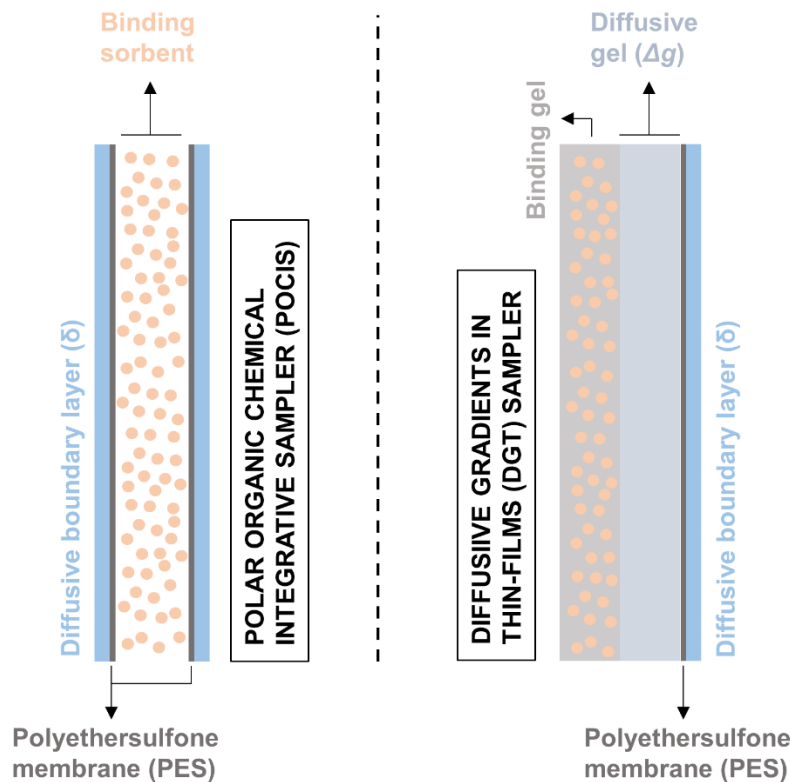
Figure 1.5: Schematic diagrams of POCIS (left) and DGT (right) passive samplers. The PES, diffusive gel, and boundary layers are to relative scale. Membrane thicknesses depicted are 10x larger than actual (PES ≈ 0.1 mm, δ ≈ 0.25 mm, Δg ≈ 1 mm). This figure depicts a typical DGT sampler, however the o-DGT configuration developed in this work has no PES membrane.

1.4 Objectives and Hypotheses

Objectives. The overall aim of this dissertation was to assess and improve upon current passive sampling tools for measurement of polar organic contaminants in aquatic systems. Specifically, two major objectives were the drivers behind much of the research presented in this dissertation:

1. To develop an improved o-DGT technique designed specifically to overcome key issues associated with current polar-PSDs; impacts of flow-rate and boundary layer on mass-transfer, challenges associated with analyte transport in, and affinity to PES membrane, and temperature effects on analyte uptake.

2. To evaluate the utility of o-DGT as an accurate polar-PSD for characterizing the occurrence, transport, and fate of POCs under challenging field conditions.

The expected outcomes of this work will contribute significantly to the field of passive sampling. Although boundary layer issues are inherently addressed based on the fundamental design of DGT (e.g., thick diffusive gel), as demonstrated extensively in the metals literature and the early development of o-DGT, this work aims to further the characterization of boundary layer effects and associated uncertainties with o-DGT as a function of flow-rate and field conditions. Furthermore, the unique contributions expected from this work relate to; the development of an o-DGT configuration that negates the issues related to PES, the feasibility of predicting sampling rates and accounting for temperature effects *in-situ*, and comprehensive field evaluations.

Hypotheses. The developed o-DGT passive sampler is hypothesized to be insensitive to water flow-rate, account for temperature effects, and demonstrate a simplified uptake model. The specific hypotheses are four-fold:

1. An o-DGT configuration without a PES outer membrane will facilitate simplified mass-transfer governed strictly by molecular diffusion through the diffusive gel.

2. Sampling rates for o-DGT will be accurately predicted based on analyte- and temperature-specific diffusion coefficients through the outer diffusive hydrogels.

3. Taken together with the expectation that o-DGT will be largely insensitive to the flow-rate of the study system, diffusion-based R_s are hypothesized to negate the need for in-situ calibrations across different systems and field conditions.

4. Finally, this o-DGT configuration will provide more accurate water concentrations compared to POCIS.

1.5 Dissertation Outline

The research projects contained within this dissertation are divided into five, standalone manuscripts (Chapters 2-6) as below.

- ❖ ***CHAPTER 2: Inputs, source apportionment, and transboundary transport of pesticides and other polar organic contaminants along the lower Red River, Manitoba, Canada.***

  - ➢ A two-year (2014-15) field study demonstrating the utility of passive sampling (POCIS) as a tool for understanding levels, sources, and transport of contaminants in an impacted river system.

  Challis, J.K., Cuscito, L.D., Joudan, S., Luong, K.H., Knapp, C.W., Hanson, M.L., Wong, C.S., **2018**. Inputs, source apportionment, and transboundary transport of pesticides and other polar organic contaminants along the lower Red River, Manitoba, Canada. *Science of the Total Environment.* 635, 803–816.

- ❖ ***CHAPTER 3: Development and calibration of an organic-diffusive gradients in thin films aquatic passive sampler for a diverse suite of polar organic contaminants.***

  - ➢ The development and calibration of an o-DGT configuration without a PES membrane. DBL experiments, sampling rates, and temperature-specific diffusion coefficients were measured and the validity and accuracy of diffusion-calculated sampling rates was tested. A brief field evaluation in a WWTP was conducted with comparisons to POCIS and grab sampling.

  Challis, J.K., Hanson, M.L., Wong, C.S., **2016**. Development and Calibration of an Organic-Diffusive Gradients in Thin Films Aquatic Passive Sampler for a Diverse Suite of Polar Organic Contaminants. *Analytical Chemistry.* 88, 10583–10591.

❖ *CHAPTER 4: Field Evaluation and In-Situ Stress-Testing of the Organic-Diffusive Gradients in Thin-Films Passive Sampler*

➢ Full scale field evaluation of o-DGT in multiple aquatic systems under challenging sampling conditions. The durability and accuracy of o-DGT was tested in fast and slow moving rivers and creeks, large open water lakes, and under ice in extreme temperatures. This work demonstrating the utility of o-DGT as an effective tool for understanding contaminant distribution, transport, and fate, across a large watershed.

Challis, J.K., Stroski, K.M., Luong, K.H., Hanson, M.L., Wong, C.S., **2018.** Field Evaluation and In-Situ Stress-Testing of the Organic-Diffusive Gradients in Thin-Films Passive Sampler. *Submitted to Environmental Science & Technology.*

❖ *CHAPTER 5: A Novel Suspect Screening Approach for Semi-Quantification of Polar Organic Contaminants in Wastewaters using the Organic Diffusive Gradients in Thin-Films Passive Sampler*

➢ A unique applications of o-DGT, utilizing the ability to calculate sampling rates based on modelled diffusion coefficients. This study uses o-DGT as a tool to conduct suspect screening of wastewater contaminants via high resolution mass spectrometry.

Challis, J.K., Almirall, X.O., Helm, P.A., Wong, C.S., **2018.** A Novel Suspect Screening Approach for Semi-Quantification of Polar Organic Contaminants in Wastewaters using the Organic Diffusive Gradients in Thin-Films Passive Sampler. *Submitted to Environmental Science & Technology.*

❖ *CHAPTER 6: Pharmaceuticals and pesticides archived on polar passive sampling devices can be stable for up to six years.*

➢ A simple study demonstrating the viability of long term freezer storage of environmental samples acquired using PSDs and the utility of polar-PSDs as environmental archival tools, ideal for long term monitoring efforts.

Challis, J.K., Hanson, M.L., Wong, C.S., **2018**. Pharmaceuticals and pesticides archived on polar passive sampling devices can be stable for up to 6 years. *Environmental Toxicology and Chemistry.* 37, 762–767.

❖ *CHAPTER 7: Overall synthesis*

➢ Summarizes the major findings and implications of the five research chapters and discusses research limitations and future recommendations.

CHAPTER 2

2. INPUTS, SOURCE APPORTIONMENT, AND TRANSBOUNDARY TRANSPORT OF PESTICIDES AND OTHER POLAR ORGANIC CONTAMINANTS ALONG THE LOWER RED RIVER, MANITOBA, CANADA

Colleague and co-author Charles W. Knapp (University of Strathclyde) conducted all of the sample processing, analysis, and interpretation of the antibiotic resistance gene (ARG) data in this chapter.

2.1 ABSTRACT

The Red River originates in the U.S., drains into Lake Winnipeg, and is a significant pathway for nutrients. We investigate its role as a source for pesticides, pharmaceuticals, per- and polyfluoroalkyl substances (PFASs) substances (PFASs), and microbes bearing antibiotic resistance genes (ARGs). We delineate agricultural, urban, and rural land-use for organic contaminants to determine the extent of chemical transboundary riverine fluxes from the U.S. to Canada, and characterize levels and trends of organic contaminants and ARGs between spring and fall 2014 and 2015. The herbicide atrazine peaked at over 500 ng/L (14-day time weighted average) near the border, indicating that the U.S. represents the major source into Canada from the Red River. Neonicotinoid insecticides had relatively constant concentrations, suggesting more widespread agricultural use in both countries. Pesticide concentrations were greatest post-application in June and July. Mass loadings of pesticides over the sampling periods, from the river to Lake Winnipeg, ranged from approximately 800 kg of atrazine, to 120 kg of thiamethoxam and clothianidin, to 40 kg of imidacloprid. Exposure distributions for atrazine exceeded benchmark water quality guidelines for protection of aquatic life (0.2% probability of exceeding chronic benchmark) with no exceedances for neonicotinoids. Seven pharmaceuticals were detected, mostly at low ng/L levels downstream of the City of Winnipeg wastewater treatment plant. Carbamazepine, the only pharmaceutical detected consistently at all sites, contributed on average 20 kg each year into Lake Winnipeg. While minor inputs were observed all along the river, city inputs represented the greatest source of pharmaceuticals to the river. Both PFASs and ARGs were observed consistently and ubiquitously, indicative of an anthropogenically-

influenced system with no indications of any single point-source signature. While

transboundary flux from the U.S. was an important source of pesticides to the Red

River, especially for atrazine, observed concentrations of all measured contaminants

suggest that known aquatic toxicological risk is minimal.

2.2 INTRODUCTION

Lake Winnipeg is the tenth largest freshwater lake in the world, and the third largest in Canada by surface area (24,000 km^2), with a watershed spanning nearly one million square kilometers over four Canadian provinces and four American states (Environment Canada, 2011). The Red River is the 3rd largest riverine input into Lake Winnipeg by volume, at approximately 16% of total inflow, and is the largest source of nutrients (Environment Canada, 2011). From 1994-2001 the Red River contributed 46% of total nitrogen and 73% of total phosphorous to the Lake (Bourne et al., 2002), largely a result of the intensive agricultural land use and high propensity for flooding in the Red River Valley (McCullough et al., 2012). With nutrient run-off, pesticides typically co-occur as the processes that drive their movement into surface waters can be shared, such as rain events (Yu et al., 2008). Furthermore, precipitation has increased significantly along the lower Red River valley and northeastern Winnipeg River watersheds over the last 20 years, increasing the potential for pesticide inputs via overland runoff. For example, in the 12 monitored tributaries of the Red River, from 1996-2005 runoff was 52–194% greater than the 1946–1995 mean (McCullough et al., 2012). These increases have not been observed throughout the entire Lake Winnipeg watershed, as small to negative changes in precipitation have been documented in the Saskatchewan River watershed and the southeastern half of the Winnipeg River watershed over this same timeframe (McCullough et al., 2012).

Wastewater represents the other major input possibly impacting water quality and contributing to contamination in the Red River. Winnipeg, the major urban centre along the lower Red River Valley, releases its treated wastewater into the Red River

either directly (North and South End treatment plants) or indirectly (West End treatment plant) to a major tributary (Assiniboine River). Furthermore, many smaller tributaries in this watershed receive sewage lagoon inputs from rural communities throughout Manitoba (Anderson et al., 2015b, 2013; Carlson et al., 2013a). The increase in livestock production, use of synthetic fertilizer, and the frequency and intensity of spring flooding specifically for the Red River Valley, have all been major contributing factors to the rapid eutrophication observed in Lake Winnipeg over the last 20 years (Schindler et al., 2012). Given the concerns around water quality and health in Lake Winnipeg, nutrient loading in the lake's major tributaries has been well characterized (Environment Canada, 2011; McCullough et al., 2012; Yates et al., 2012), but pesticides and other contaminants remain relatively uncharacterized in this system.

One unique and important aspect of this system is the fact that close to 70% of the contributing land area to the Red River watershed lies in the U.S., making source apportionment and land-use management issues highly complex and important to understand. It was for these reasons that the International Joint Commission was formed and the Great Lakes Water Quality Agreement was negotiated between Canada and the U.S. (Gilbertson et al., 1998). As a result, many of the pressing transboundary contaminant issues facing the Great Lakes were prioritized (Nisbet, 1998). Analogous transboundary and jurisdictional water security issues exist within the Red River-Lake Winnipeg system, yet much less work has been done to characterize and understand these problems. To date, there remains a paucity of data regarding the sources, loadings, and fate of organic contaminants in this watershed. Given known inputs and land-use patterns along the Red River Valley, the presence of pesticides (Rawn et al.,

1999; Szöcs et al., 2017), pharmaceuticals (Carlson et al., 2013a; Kolpin et al., 2002), and per- and polyfluoroalkyl substances (PFASs) (Hu et al., 2016; Scott et al., 2009) is highly likely based on previous observations here and elsewhere. Pesticides and pharmaceuticals represent the two major inputs (agricultural and municipal waste) into the Red River. Alternatively, PFASs, known to be highly persistent in the environment, are used in a wide variety of industrial and consumer-use products (e.g., cosmetics, firefighting foams, stain-repellent textiles) and thus have potentially varied inputs, including wastewaters, landfill leachate, and industrial waste (Wang et al., 2017), making their spatial occurrence throughout the Red River less predictable. Studying their major sources, levels, and temporal trends will help estimate risk (if any) posed to aquatic organisms in the Red River and characterize loadings to Lake Winnipeg. Furthermore, this work will help delineate contaminant sources on both sides of the border, and provide important context around contaminant use and land-management in this watershed. In addition to these chemical contaminants, the presence of antibiotic resistance genes (ARGs), a form of bio-pollution, has become a concern due to the widespread occurrence of human and veterinary antibacterial products in natural waters (Kümmerer, 2009c, 2009b). As a result, genes encoding for resistance to a variety of antibiotics have become ubiquitous in aquatic environments impacted by human activity (Anderson et al., 2013; Kümmerer, 2009c) and could act as a vector by which resistance is spread throughout the population, leading to public human health concerns (Huijbers et al., 2015).

Levels of organic contaminants in impacted waters are heavily influenced by the stochastic and often unknown nature of their inputs, which include precipitation and run-

55

off events, wastewater release, and pesticide applications (Carlson et al., 2013a). As a

result, accurate characterization through time and space can be challenging. To capture

these types of inputs in a natural system high frequency sampling must be conducted

either manually (grab sampling) or through automation (auto-sampling), both of which

have significant drawbacks and limitations (Vrana et al., 2005). Passive sampling is an

alternative method that allows for the continuous *in-situ* monitoring of contaminants

without the need of a power source (Miège et al., 2015). The polar organic chemical

integrative sampler (POCIS), used here, is the most widely used passive sampling tool

for measuring pesticides, pharmaceuticals, and other polar organics in water (Harman

et al., 2012; Morin et al., 2012).

This study had three primary objectives. First, to characterize the concentrations

and fluxes of pesticides, pharmaceuticals, and PFASs and levels of ARGs in the Red

River. Second, to determine contributions of these contaminants from the United

States, southern Manitoba, and the City of Winnipeg. Finally, to estimate possible risks

to aquatic organisms in this system resulting from exposure to these contaminants. Our

hypotheses are twofold. First, the presence of pharmaceuticals, PFASs, and ARGs will

be indicative of a river system influenced by municipal inputs, with elevated levels

observed downstream of the City of Winnipeg. Second, pesticide detections will be a

function of both application intensity (e.g., usage) and runoff events (e.g., timing and

intensity of precipitation) in the drainage basin. Specifically, in terms of usage, loadings

of atrazine from the Red River will be greater than observed in the Assiniboine River

given the intensity of corn cropping and atrazine application in the U.S. Likewise, in

terms of runoff, neonicotinoid insecticides, in the Red River will be greater than

observed in the Assiniboine River given the more intense and frequent precipitation events (e.g., runoff) characteristic of the lower Red River valley.

This work represents the only published data to date describing many of these organic contaminants and ARGs in the Red River to our knowledge, and serves as a baseline for estimating risks and informing management and monitoring around these contaminants in the Lake Winnipeg watershed.

2.3 METHODS AND MATERIALS

2.3.1 Sampling sites

Sampling was performed continuously between April and October of 2014 and 2015. With the exception of two extended deployments discussed later, sampling times generally ranged between 14 and 21 days, largely chosen opportunistically based on availability of field personnel and to avoid inclement weather. A major focus of this work is pesticide inputs, which, from November to March are expected to be insignificant compared to that of the growing season. Samplers were not deployed during spring ice melt, as ice and debris in the river at that time can destroy samplers. A total of six sites were sampled: five along the Red River and one on the Assiniboine River (Figure 2.1). Emerson is a border town and therefore integrates all net inputs coming directly from the United States. The St. Norbert site is south of the city perimeter, upstream of the South End sewage treatment plant and immediately downstream to the St. Norbert floodway diversion. The North End site is downstream of the North End Wastewater Treatment plant (WWTP) and processes approximately 70% of Winnipeg's wastewater. Downstream from the small town of Selkirk and upstream of Lake Winnipeg, both Selkirk and Breezy Point sites respectively, are more removed from known point and

non-point sources of pollution and should represent near-final inputs into Lake Winnipeg from the Red River. The Assiniboine River is the largest tributary to the Red River and integrates inputs at Headingley from western Manitoba and eastern Saskatchewan. Small changes to site selection over the two-year study were necessary due to flooding, vandalism, or other logistical factors; however, sites remained in the same general vicinity. Both the Red and Assiniboine Rivers represent watersheds in agricultural intensive regions within Manitoba and for the former, into the U.S. Specific land usage patterns are discussed in a later section.

Samplers were deployed in triplicate on stainless steel spindles inside stainless steel protective cages (30 cm high × 16 cm wide) (Environmental Sampling Technologies, St. Joseph, MO) as done elsewhere (Carlson et al., 2013a). Cages were secured to riverbanks using 3/16-inch stainless steel aircraft cable looped around trees. Cages were deployed on the east bank at Emerson, St. Norbert, and Selkirk, the west bank at North End and Breezy Point, and the south bank at Headingley. Major flooding in 2014 compromised or destroyed some samplers, as detailed in Appendix A. Eight out of 66 total deployed POCIS sets were destroyed in 2014, with 11 out of 138 POCIS lost over the entire two-year study. We do not expect this missing data to have any significant effect on calculated mass loadings or interpretation of contaminant sources or trends given the large data set taken over the two-year period.
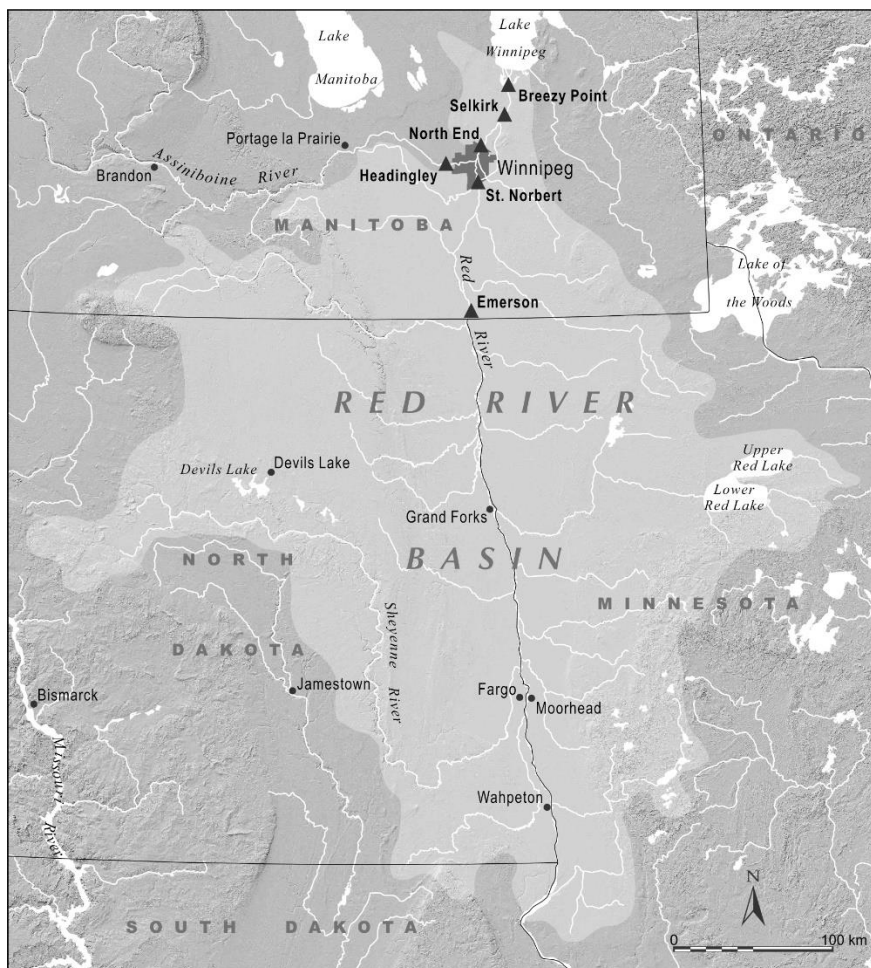
Figure 2.1: Sampling sites (black triangles) from south to north on the Red River: Emerson (N 49.008442°, W 97.215310°), St. Norbert (N 49.754725°, W 97.137746°), North End (N 49.951508°, W 97.097491°), Selkirk (N 50.142747°, W 96.864826°), and Breezy Point (N 50.278267°, W 96.851626°). The site Headingley is located on the Assiniboine River (N 49.868906°, W 97.409807°), a tributary to the Red River. Source material for this map includes information licensed under the Open Government Licence – Canada, the U.S. Geological Survey, and NASA/JPL-Caltech.

2.3.2   Target chemicals

A total of 32 contaminants were analyzed by liquid chromatography tandem mass spectrometry (LC-MS/MS): 6 pesticides, 17 pharmaceuticals, and 9 PFASs. The pesticides were: 3 neonicotinoids (imidacloprid, thiamethoxam, and clothianidin); 2 organophosphates (chlorpyrifos and diazinon); and 1 triazine (atrazine). The

59

pharmaceuticals were: 6 sulfonamide antibiotics (sulfapyridine, sulfamethoxazole, sulfisoxazole, sulfamethazine, sulfachloropyridazine, and sulfadimethoxine); 3 macrolide antibiotics (erythromycin, clarithromycin, and roxithromycin); 1 fluoroquinolone antibiotic (enrofloxacin); the antibiotic trimethoprim; 3 beta-blockers (atenolol, metoprolol, and propranolol); 2 selective serotonin reuptake inhibitors (paroxetine and fluoxetine); and 1 sodium channel blocker (carbamazepine). These compounds were measured in both study years. PFASs were measured in 2014 only and included perfluoropentanoic acid (PFPeA), perfluorohexanoic acid (PFHxA), perfluoroheptanoic acid (PFHpA), perfluorooctanoic acid (PFOA), perfluorononanoic acid (PFNA), perfluorodecanoic acid (PFDA), perfluoroundecanoic acid (PFUnDA), perfluorohexanesulfonic acid (PFHxS) and perfluorooctanesulfonic acid (PFOS). Isotopically labelled internal standard mixture used for the two classes of chemicals studied here are detailed in Appendix A.

2.3.3 Passive samplers

2.3.3.1 Polar organic chemical integrative sampler

POCIS were constructed using 200 mg of Waters OASIS™ HLB (hydrophilic-lipophilic balance) material between polyethersulfone (PES) membranes (0.1 μm pore size) (Environmental Sampling Technologies, St. Joseph, MO). Samplers were secured with two stainless steel rings to allow an exposed total membrane surface area of 41 cm^2. POCIS were stored at -20°C in ashed aluminum foil until use. Twenty-four hours prior to deployment, samplers were soaked in Milli-Q water (18 MΩ cm, Millipore Corporation, Billerica, MA) and stored at 4°C in prewashed plastic sandwich containers until deployment.

Pharmaceuticals and pesticides were extracted from organic POCIS according to (Carlson et al., 2013b). Upon retrieval, POCIS were rinsed with Milli-Q water, wrapped in ashed aluminum foil, and stored at -20°C until extraction. Extraction was generally performed within two weeks of retrieving the POCIS, during which time loss of compound was deemed insignificant (see Chapter 6 and Carlson et al., 2013b). Before extracting, POCIS were soaked in Milli-Q water for 10 minutes. Sorbent was rinsed into a 60 mL glass clean-up column containing 3-5 g anhydrous sodium sulphate (Fisher Scientific, Ottawa, ON) using 30-40 mL of methanol. In this rinsing process, the PES membranes were simultaneously extracted into the column. Internal standard mixture (details in Appendix A) (50 ng) was spiked directly onto the column along with the sorbent from each POCIS sample. The extract was gravity filtered through the column, collected in a 100 mL round bottom flask, rotary evaporated to ~2 mL at 40°C, and then fully evaporated to dryness under nitrogen gas at 40°C. Extracts were reconstituted with 1mL of 50:50 methanol: Milli-Q water and syringe filtered through 0.22 μm polytetrafluoroethylene filters (Chromatographic Specialties, Brockville, ON). Extracts were stored in glass auto-sample vials at 4°C until analysis using liquid chromatography coupled with tandem mass spectrometry (LC-MS/MS). POCIS extraction efficiencies were determined previously (Carlson et al., 2013b).

2.3.3.2 PFAS POCIS

Adapted POCIS samplers for PFAS were prepared using methods developed by (Kaserzon et al., 2012). PES membranes with 0.45 μm pore size (Pall Corporation, Ann Arbor, MI) were preconditioned by submerging them in HPLC grade methanol (Fisher Scientific, Ottawa, ON) for 20 minutes, followed by Milli-Q water for 10 minutes,

according to procedures outlined in Kaserzon et al. (2012). To maintain a 0.0375 g sorbent/cm^2 exposed surface area ratio with 41 cm^2 POCIS, 1.5375g of Sepra ZT-WAX sorbent (Phenomenex, Torrance, CA) was used. Maintaining a constant sorbent-to-surface area ratio allowed the use of previously determined sampling rates (Kaserzon et al., 2012). Samplers were secured using stainless steel disks and stored at -20°C in ashed aluminum foil until 24 hours prior to deployment, when they were conditioned for ten minutes in each of 0.1% ammonia in methanol (Fisher Scientific, Ottawa, ON), methanol, and Milli-Q water. POCIS were stored in prewashed Teflon-free containers containing Milli-Q water until deployment.

PFAS were extracted from POCIS using a method adapted from Kaserzon et al. (2012). After retrieval, PFAS POCIS were rinsed with Milli-Q water, wrapped in ashed aluminum foil, and stored at -20°C until extraction. Prior to extraction, POCIS were soaked in Milli-Q water for 10 minutes. A 70 mL plastic pre-cleaned SPE cartridge (Chromatographic Specialties, Brockville, ON), containing ~2 g anhydrous sodium sulphate and a Grade 413 filter paper (VWR, Mississauga, ON), was pre-rinsed with 15 mL methanol. Sorbent was rinsed from the membranes into the SPE cartridge using 15 mL of 0.1% ammonia in methanol, followed by 15mL methanol. The PFAS internal standard mix (Appendix A) was spiked into each sample along with the sorbent. Extracts were collected in a 50 mL round bottom flask and reduced to ~2 mL using rotary evaporation at 40°C. After evaporation to dryness under a stream of nitrogen gas at 40°C, extracts were reconstituted to 1 mL with 50:50 methanol:Milli-Q water, and syringe filtered through 0.20 μm nylon filters (Chromatographic Specialties, Brockville, ON). Extracts were stored in polypropylene auto-sample vials at 4°C until analysis.

2.3.4 Antibiotic resistance genes

Protocols for sampling of antibiotic resistance genes (ARGs) followed Anderson et al. (2013). Briefly, 500 mL sterilized polypropylene bottles (Chromatographic Specialties Inc., Brockville, ON) were used for ARG grab samples, collected in 2014 only. Each ARG water sample was filtered using a sterile, disposable Nalgene cup with a pre-installed 0.2 µm filter (Thermo Fisher Scientific Inc., Waltham, MA). The filter was removed using flame-sterilized forceps, folded, and placed into a 1.5 mL sterile polypropylene centrifuge tube. The centrifuge tube was stored frozen and shipped on ice to the University of Strathclyde (Glasgow, UK), where they were immediately stored at -80°C until further processing. Filters were sterilely quartered and transferred to screw-top centrifuge tubes; DNA were extracted were extracted via MoBio PowerSoil DNA extraction kits (Qiagen, Inc.) according to manufacturer's instructions. Eluted DNA were diluted 1:100 to minimise the presence of PCR inhibitors.

Community DNA were analyzed for the presence of 13 tetracycline and 3 sulfonamide resistance determinants via qPCR (iCycler5, BioRad). Tetracycline multiplex assays were based on primers by Ng et al. (2001) and targeted genes associated with efflux pumps (*tet*-A, -B, -C, -D, -E, -G, -K, and –L) and ribosome protection proteins (*tet*-M, -O, -Q and –S) and enzyme deactivation (*tet*X). A high-resolution temperature melt curve (Fan et al., 2007) discerned individual responses for each gene; peak areas were compared to standards (10^1 to 10^6 copies per μL; McCluskey and Knapp, 2017; Peak et al., 2007) for quantification. Sulfonamide resistance genes (*sul*1, *sul*2, and *sul*3; Chen et al., 2015; Pei et al., 2006) and 16S-rRNA (Caporaso et al., 2011), which represent a surrogate measure of total bacteria,

were similarly quantified, but as individual assays. Details around PCR methodology can be found in Appendix A.

2.3.5 Instrumental Analysis

2.3.5.1 Analysis of Pharmaceuticals and Pesticides

Pharmaceutical and pesticide concentrations were determined using an Agilent 6410B LC-MS/MS system (Agilent Technologies, Mississauga, ON). LC mobile phases were 95:5 H_2O:methanol (solvent A) and methanol (solvent B), each containing 0.05% formic acid (Fisher Scientific, Ottawa, ON). Chromatographic separations were achieved using an Agilent Eclipse Plus C18 column (2.1 $\times$ 50mm $\times$ 1.8μm particle size) (Agilent Technologies, Mississauga, ON) with a Phenomenex HPLC SecurityGuard C18 Guard Cartridge (4 $\times$ 3mm) (Phenomenex, Torrance, CA) at 42$°$C and a flow rate of 0.45 mL/min. Further details of the analytical method, including the LC gradient elution method, source parameters, MRM transitions, and limits of detection are in Appendix A.

2.3.5.2 Analysis of PFASs

Concentrations of 9 PFAS were determined using LC-MS/MS. LC mobile phases contained 95:5 H_2O:methanol (solvent A) and 90:10 acetonitrile:H_2O (solvent B), each containing 2 mM ammonium acetate (Sigma-Aldrich, St. Louis, MO). The guard and analytical column setup was the same one used for the pharmaceutical and pesticide method with a temperature and flow-rate of 40$°$C and 0.5 mL/min, respectively. An Agilent Eclipse Plus C18 column (4.6 $\times$ 30mm $\times$ 3.5μm particle size) (Agilent Technologies, Mississauga, ON) was attached at the outflow from the aqueous pump head (solvent A) and used as a PFAS trap. Further details of the analytical

method, including the LC gradient elution method, source parameters, MRM transitions, and limits of detection are in Appendix A.

2.3.6 Data Analysis

2.3.6.1 Instrumental analysis

Agilent MassHunter Workstation Software Quantitative Analysis (Version B.04.01) was used to analyze all LC-MS/MS data. Calibration curve linearity was >0.98 for all analytes and a tolerance ±20% was deemed acceptable for accuracy of individual calibration standards and quantifier:qualifier MRM transition ratios.

2.3.6.2 Passive sampling data

Time-weighted average (TWA) concentrations were calculated using POCIS sampling rates specific to each analyte (Table A3). Tables A4a-e, A5, and A6a-h in Appendix A provide the raw data for the target analytes detected in this study, and report the mass of analyte on POCIS for individual samples (M_{POCIS}, mass in ng). The reported TWA concentration (C_{TWA}, ng/L) represents the mean of triplicate POCIS deployed over time (t), calculated using *Equation 2.1*, where R_S (L/d) is the compound specific POCIS sampling rate:

$$C_{TWA} = \frac{M_{POCIS}}{R_s t}$$

Equation 2.1

Given that POCIS sampling rates are sensitive to water flow (Harman et al., 2012), it is important to acknowledge the inherent uncertainties (Poulier et al., 2014) associated with POCIS in dynamic and variable flowing system as the Red River. Chemical fluxes (kg/d) were calculated at sites that had Environment Canada gauging

stations (Emerson, St. Norbert, Selkirk, Headingley). Daily discharge volumes were obtained from Environment Canada Water Level and Flow website (https://wateroffice.ec.gc.ca/). The calculation of flux data assumed homogenous concentrations at the cross-sectional area of the river where the gauging stations/POCIS samplers were located. Prism v. 5.01 (GraphPad Software, LaJolla, CA) was used for statistical analysis. Specific tests are stated with the specific data set to which they were applied. Significant differences were defined as $p < 0.05$. Errors are presented as standard deviations of the mean, unless otherwise stated.

2.3.6.3 Exposure distributions

Exposure distributions were constructed for the four pesticides detected consistently across sampling sites and times, over the two years (raw data in Table A4a-e). Atrazine, thiamethoxam, clothianidin, and imidacloprid concentrations in the Red River at all sites and in the Assiniboine River at Headingley were used to generate exposure distributions for each River. Data were plotted on a logarithmic-probability scale using the Weibull ranking equation (Solomon et al., 2000).

2.3.6.4 ARG data

Abundances of genes are presented as log-transformed values; differences between sites was tested using a Kruskal-Wallis test by ranks ($p < 0.05$).

2.3.6.5 Quality Assurance/Quality Control (QA/QC)

POCIS lab and field blanks were extracted and analyzed alongside each set of environmental samples. Field blanks were taken to each sampling site and left open to the atmosphere while retrieval and deployment of the POCIS took place. For all

analytes reported in this study, levels observed in lab and field blanks were negligible with the exception of PFUnDA, which was detected at elevated levels in all samples, and thus was not considered in this study.

2.4 RESULTS AND DISCUSSION

The following sections will describe the major findings and implications of this work, organized by contaminant class: pesticides, pharmaceuticals, PFASs, and ARGs, in order. The initial section below summarizes the hydrology and land-use descriptors of the Red River valley, information that is drawn upon in the proceeding discussions to help contextualize the observed levels, fluxes, and sources of each contaminant.

2.4.1 Watershed and Land Use Descriptors

Runoff from treated agricultural fields likely represents the major input of the four pesticides detected in this study. Soil type, topography, and seasonal climate conditions to a large extent control the movement of these pesticides into the Red River (Rawn et al., 1999). The Red River has an effective drainage area just shy of 150,000 km^2, 74% of which is farmed (65% cropland, 9% pasture) (McCullough et al., 2012; Yates et al., 2012). Much of this farmland is concentrated along a stretch of low relief terrain characterized by underlying sediments with very low permeability (McCullough et al., 2012). Precipitation and melt events often exceed soil infiltration capacity, leading to a high frequency of seasonal overland flooding and runoff events within the Red River watershed, resulting in significant losses of field applied pesticides (Rawn et al., 1999). Our study sites in Manitoba spanned approximately 250 km from the U.S./Canada border at Emerson to Breezy Point, near the mouth at Lake Winnipeg. On the U.S. side,

our sampling at Emerson integrates over 600 km of largely agricultural inputs along the river, from the head waters of the Red River on the North Dakota – Minnesota border at the northern edge of the Midwestern Corn Belt, to the Canadian border, allowing net inputs from the U.S. to be characterized. The Emerson sampling site on the east bank of the Red River is downstream of two small sewage lagoon releases (on the opposite west bank) from both the U.S. (Pembina) and Canadian (Emerson) border towns, both with combined populations of approximately 1,000. The Assiniboine River originates in Eastern Saskatchewan and flows into the Red River at The Forks in downtown Winnipeg, Manitoba. The Assiniboine River has a drainage basin of approximately 60,000 km^2, which is also predominately agricultural-use (Rawn et al., 1999).

Canada does not have a readily available inventory of regional pesticide-use data, making estimations of annual application volumes difficult to ascertain. Crops in southern Manitoba are primarily grains and cereals. Canola is also a major crop, and corn is grown but in a very limited capacity (Manitoba agriculture statistics, 2016). Atrazine use in Manitoba in the late 1990s was estimated to be around 12,000 kg annually (Rawn et al., 1999). In 2006 an estimated 25,000 kg of atrazine was applied across 17,000 hectares (Wilson, 2012). In contrast, approximately 135,000 kg of atrazine was applied annually in the late 1990s within the U.S. area of the Red River watershed alone (Rawn et al., 1999). Based on raw data from the USGS National Water-Quality Assessment Project (https://water.usgs.gov/nawqa/pnsp/usage/) an estimated 800,000 kg per year were applied on average in North Dakota and Minnesota from 2006-2015. While only a portion of this land area lies in the Red River drainage basin (Figure 2.1) these U.S. inputs likely represent the major source of atrazine to the

Red River. Neonicotinoids on the other hand are used extensively in southern Manitoba

to support canola, soy bean, and grain crops. Canola represented the single largest

crop by seeded area in Manitoba at over 1.2 million hectares (Manitoba agriculture

statistics, 2016). The most common application of neonicotinoids is seed coatings, and

given that 95% of canola grown in Canada is treated with a neonicotinoid active

ingredient (Main et al., 2014), we expect extensive inputs of these pesticides from

southern Manitoba. On the U.S. side of the Red River drainage basin (North Dakota,

South Dakota, and Minnesota), neonicotinoids are also extensively used. Average

annual use across all three states over the 5-year period between 2010 and 2014 was

29000 kg of imidacloprid, 28000 kg of thiamethoxam, and 79000 kg of clothianidin

(USGS National Water-Quality Assessment Project, 2018).

Table 2.1: Summary values for the Red and Assiniboine River hydrographs in 2014 and 2015. Mean, median, and total discharge values calculated from April 29 – October 28, 2014 and April 11 – October 28, 2015. Data obtained from Environment Canada Water Office (https://wateroffice.ec.gc.ca/).

Discharge (m^3/s)	Emerson		St. Norbert		Selkirk		Headingley	
	2014	2015	2014	2015	2014	2015	2014	2015
Mean	325	164	400	224	743	403	305	149
Median	259	97	321	160	746	384	307	96
Total (m^3)	5.1×10^9	2.9×10^9	6.3×10^9	3.9×10^9	1.2×10^{10}	7.0×10^9	4.8×10^9	2.6×10^9

Hydrographs shown in Figure 2.2 describe the daily discharge from the Red

River (Emerson, St. Norbert, Selkirk) and Assiniboine River (Headingley) between April

and October over the two-year study. Full ice-coverage, normally from December to

March, means that many of the hydrological gauging stations are not operational in that

time. Both rivers generally see a spike in discharge in spring (usually April)

corresponding to snow melt. However, the intensity of this spike depends upon the

amount of precipitation in the watershed over the winter, the soil saturation conditions,

and the rate of melt. An early melt in 2015 (March) explains the reduced discharge in

April and May in the Red River. A second spike in river discharge generally occurs in

June/July due to heavy precipitation events characteristic of southern Manitoba at that

time. This is observed on both rivers in 2014 and 2015. However, overall it is evident

that the Red and Assiniboine River's experienced much greater flows in 2014 compared

to 2015. Comparing the mean and total discharge values (Table 2.1) over each year,

2014 was approximately double that of 2015. In fact, on occasion high water levels in

2014 led to lost samplers or delays in retrieval (details in Appendix A).
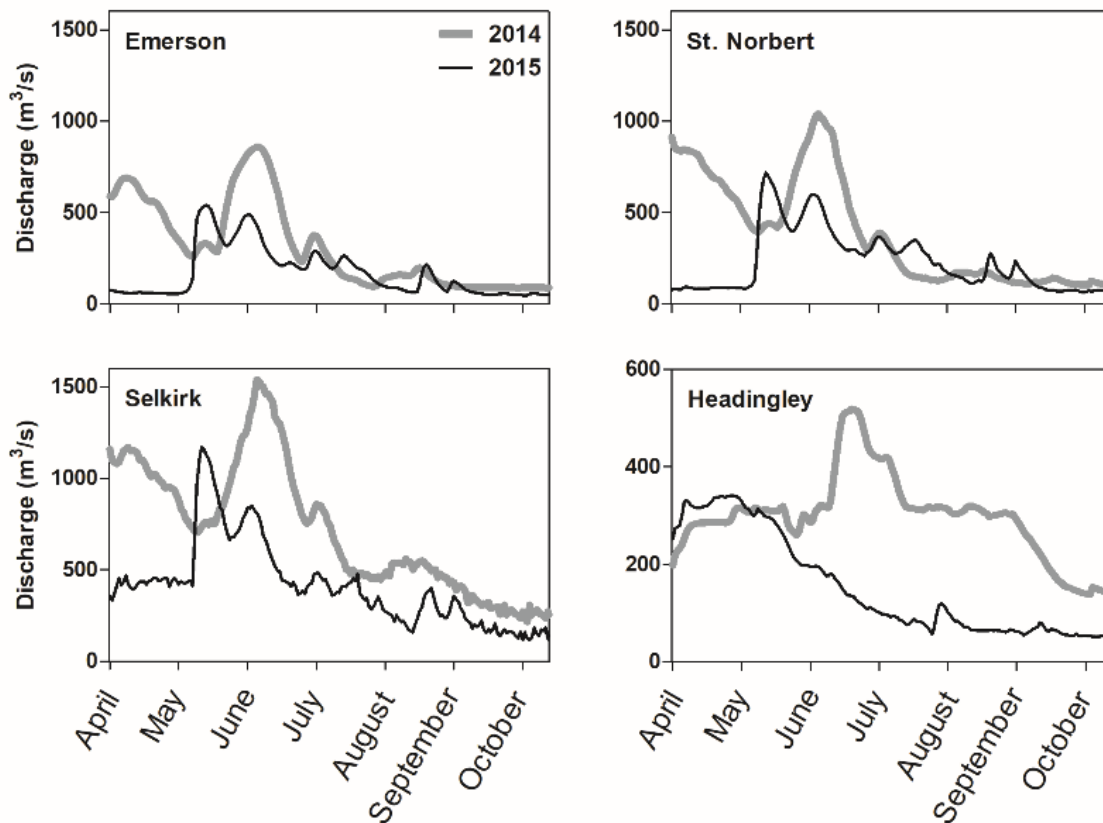
Figure 2.2: Daily flow rate over the entire study period (April to October) in 2014 and 2015 on the Red River (Emerson, St. Norbert, Selkirk) and Assiniboine River (Headingley). Data obtained from Environment Canada Water Office (https://wateroffice.ec.gc.ca/).

2.4.2 Pesticides

2.4.2.1 Pesticide concentrations and occurrence.

Of the six pesticides analyzed for in this work, four were measured at detectable levels consistently across sampling year, season, and site. Atrazine, thiamethoxam, and clothianidin were detected in 100% (n=127) of all collected samples, and imidacloprid was detected in >90% (n=116 of 127) of all samples (Figure 2.3). Chlorpyrifos and diazinon were not detected in this study by the methods employed. Table 2.2 details the mean, median, and maximum environmental concentrations of the four pesticides measured in the Red River (complete data set in Appendix A, Table A4). It is important to note that the concentrations reported here represent TWAs over a given deployment time, typically 14-21d in this study. In the case of extended deployment times caused by flooding in 2014 (42 and 59 days, Table A4), if saturation of the POCIS sorbent occurred during this time analyte concentrations may be underestimated, however this is unlikely given the large capacity and thus linear uptake range generally observed for POCIS (Harman et al., 2012). Regardless, while maximums reported here are lower than if the same concentration spikes had been captured with grab samples, TWA concentration data provides better context around longer-term, chronic exposure scenarios in these systems, a fundamental tenant of many passive samplers (Booij et al., 2016; Harman et al., 2012; Poulier et al., 2014).

Table 2.2: Summary concentration statistics for the four pesticides measured in the Red River.

Conc. (ng/L)	Thiamethoxam	Clothianidin	Imidacloprid	Atrazine
Mean	5.4	7.0	2.8	63.0
Median	3.6	5.1	2.1	24.3
Maxiumum (days)[a]	26.9 (14d)	31.7 (7d)	14.1 (7d)	520 (14d)
Site/date[b]	NB/07-2014	EM/07-2014	EM/07-2014	EM/06-2015

a – maximum environmental concentration in Red River with time (d) of POCIS deployment in brackets
b – Sampling month and year where maximum was measured (NB = St. Norbert; EM = Emerson)

71

The maximums for the three neonicotinoid insecticides thiamethoxam, clothianidin, and imidacloprid in the Red River ranged from 14.1-31.7 ng/L with mean concentrations over the two-year study <8 ng/L (Table 2.2). On the Assiniboine River at Headingley, mean concentrations of the three neonicotinoids ranged from 0.9-4.4 ng/L. In general, these average concentrations agree with other neonicotinoid occurrence data that generally falls in the low ng/L range, discussed below. However, in a Canadian context, much of the neonicotinoid measurements have been taken with grab samples in small streams, rivers, and wetlands, often representing low-dilution scenarios (Anderson et al., 2015a), making direct comparisons to this study difficult.

Main et al. (2014) measured water concentrations of thiamethoxam, clothianidin, and imidacloprid in 136 pothole wetlands adjacent to grasslands and agricultural fields in central Saskatchewan. Average detection frequencies ranged from 16-91% and mean total (sum of four active ingredients) neonicotinoid concentrations ranged from 4.0-76.8 ng/L, both varying with season, year, and crop type (Main et al., 2014). Struger et al. (Struger et al., 2017) studied fifteen streams and rivers in southern Ontario, nine of which had drainage areas <100 km^2 and were in agricultural areas (for context, the drainage area of the Red River is close to 150,000 km^2). Thiamethoxam, clothianidin, and imidacloprid exhibited detection frequencies above 90% at over half the sites sampled over the three-year study (2012-14), with mean concentrations across all 15 sites ranging from 0.21-113 ng/L. In the U.S., similar levels of neonicotinoids are observed as in Canada. Hladik and Kolpin (2015) conducted a nationwide study of 38 U.S. streams between 2012 and 2014 and reported a summed (five active ingredients, detections dominated by thiamethoxam, clothianidin, and imidacloprid) neonicotinoid

mean concentration of approximately 5 ng/L. Van Metre et al. (2017) used POCIS to monitor pesticides in 100 small streams across the U.S. Midwest and observed a maximum, mean, and median of 275 ng/L, 19.3 ng/L, and 4.0 ng/L, respectively for imidacloprid (the single neonicotinoid reported in the study). Year-round grab samples taken between 2015 and 2016 in ten major Great Lake tributaries showed median concentrations of neonicotinoids ranging from non-detect to 10 ng/L with a maximum single measurement of 230 ng/L (Hladik et al., 2018). These values are similar to mean neonicotinoid concentrations observed here in the Red River system.

The maximum, mean, and median concentration of atrazine in the Red River over the two-year study was 520, 63.0, and 24.3 ng/L (Figure 2.3, Table A4a). Concentrations in the Assiniboine River at Headingley were much lower (maximum = 10.2 ng/L; mean = 3.4 ng/L; median = 2.7 ng/L). This is unsurprising given the limited use of the pesticide in Manitoba (Rawn et al., 1999) and amount of corn grown in this part of the system, relative to the Red River proper part of the basin. Atrazine concentrations were reported by Rawn et al. (1999) in their assessment of pesticide loadings in the Red River and its tributaries over a three-year survey from 1993-1995 (Table 2.3). Concentrations of atrazine measured in the current study were greater (2-3 fold) compared to those reported in 1993-95. Aside from annual and seasonal variability in contaminant levels, fundamental differences between the data sets are expected given that Rawn et al. (1999) used grab samples taken every 2-3 weeks over the study period to characterize atrazine levels compared to our use of passive samplers which provided continuous *in-situ* time-weighted average concentrations.

Spatial-temporal trends of each pesticide can be observed in Figure 2.3. Atrazine concentrations spiked in early June corresponding with typical field-applications in May. Nowell et al. (2018) observed similar trends in their study of a suite of pesticides in 100 streams throughout the Midwestern U.S. Corn Belt. They detected atrazine at concentrations >100 ng/L at approximately 65% of agricultural impacted sites with peak concentrations observed between May and June, corresponding to major application and runoff events (Nowell et al., 2018). While the major source of atrazine is expected to be coming from use in the U.S., there is no clear pattern of spatial attenuation moving downstream along the Red River from Emerson to Breezy Point, as indicated by relatively constant mass loading in the Red River (Figure 2.4) despite small decreases in concentration with distance downstream from Emerson (Figure 2.3). This is likely due to the persistence of atrazine in aquatic systems, with half-lives ranging from 30 to >200d, depending largely on pH conditions and organic matter content of the water (Solomon et al., 1996). Given the relatively recalcitrant nature of the compound, residence times in the Red River are likely too short for degradation processes to be appreciable in the river itself (Schottler et al., 1994).

Table 2.3: Comparison of atrazine concentrations measured in the current study (2014-15) and by Rawn et al. (1999) (1993-95) in the Red River at Emerson, St. Norbert, and Selkirk sites and in the Assiniboine River at Headingley.

Conc. (ng/L)	Emerson		St. Norbert[a]		Selkirk		Headingley	
	2014-15	1993-95	2014-15	1993-95	2014-15	1993-95	2014-15	1993-95
Mean	98.8	29.4	67.8	36.0	61.3	24.7	3.4	2.1
Median	41.1	11.1	27.8	14.7	27.5	9.2	2.7	1.1
Max.	520	168	356	219	193	169	10.2	8.1

a – sampling site in Rawn et al. (1999) was approximately 25 km south of St. Norbert in Ste. Agathe.

An approximate residence time of 30 days from river source to mouth (885 km) was calculated assuming a mean annual flow of 176 m^3/s, depth of 4 m, and width of 130 m (Kimiaghalam et al., 2015). This equates to a residence time of approximately 7 days between Emerson and Selkirk (218 km). As a result, levels of atrazine in receiving waters can be highly dependent on dilution and hydraulic residence time. In fact, these factors are likely responsible for the temporal attenuation observed here for atrazine, as concentrations decreased following the spikes in June, through to the end of each sampling season in October. Background atrazine levels can be inferred from the beginning (April) and end (September-October) of each sampling year, appearing to reach a steady-state concentration in the range of 1-20 ng/L (Table A4a). Negligible levels (<5 ng/L, average) of atrazine were observed on the Assiniboine River at Headingley, suggesting that usage and thus sources from western Manitoba are minor in comparison to overall contributions to the Red River and ultimately Lake Winnipeg.

The three neonicotinoids exhibited very similar concentration profiles across sampling site and time. The spike in neonicotinoid concentrations in May/June was less pronounced than for atrazine. Concentrations between approximately May-August appear to be more consistent across space and time (especially in 2015), including on the Assiniboine River at Headingley. This is indicative of multiple diffuse sources of neonicotinoids all along the Red River Valley and from western Manitoba, which is consistent with known usage throughout the Prairie Provinces (Main et al., 2014).
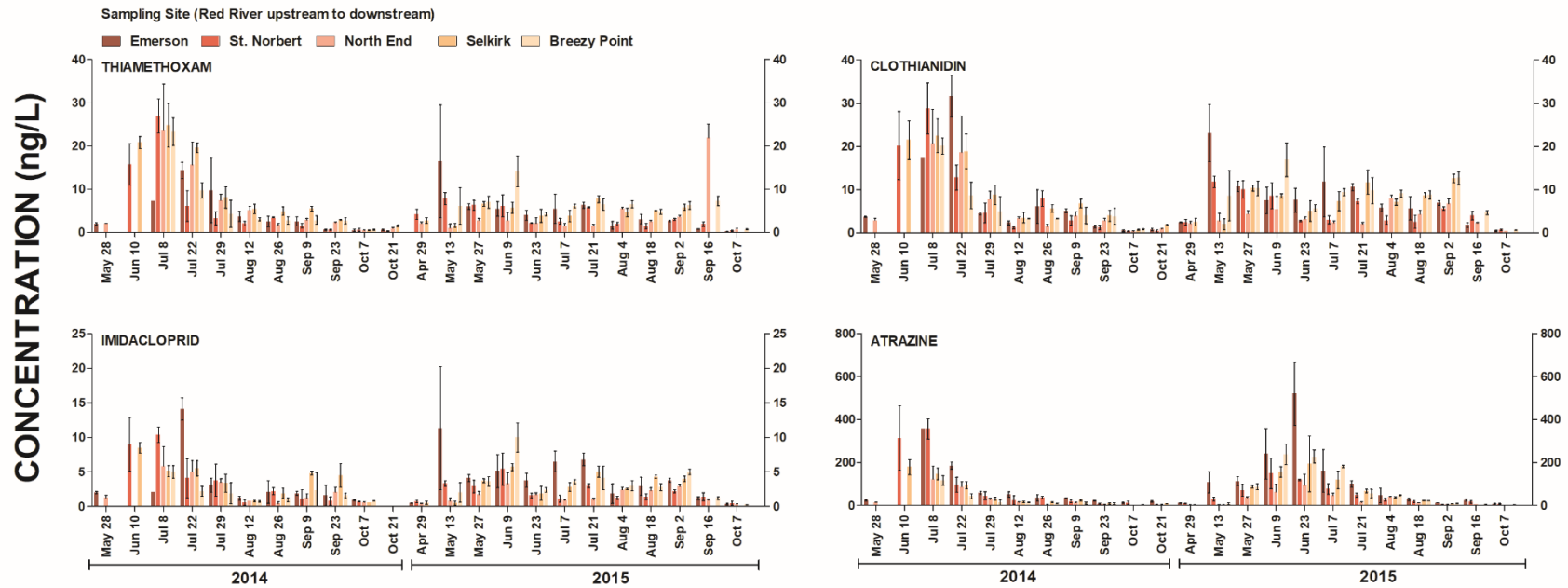
Figure 2.3: Time weighted average concentrations of thiamethoxam, clothianidin, imidacloprid, and atrazine detected over the two-year study as measured using POCIS. Bars represent the mean and standard deviation (SD) of triplicate measurements. Bar colour corresponds to sampling site in direction of flow (Emerson, St. Norbert, North End, Selkirk, Breezy Point). Headingley on the Assiniboine River is not shown.
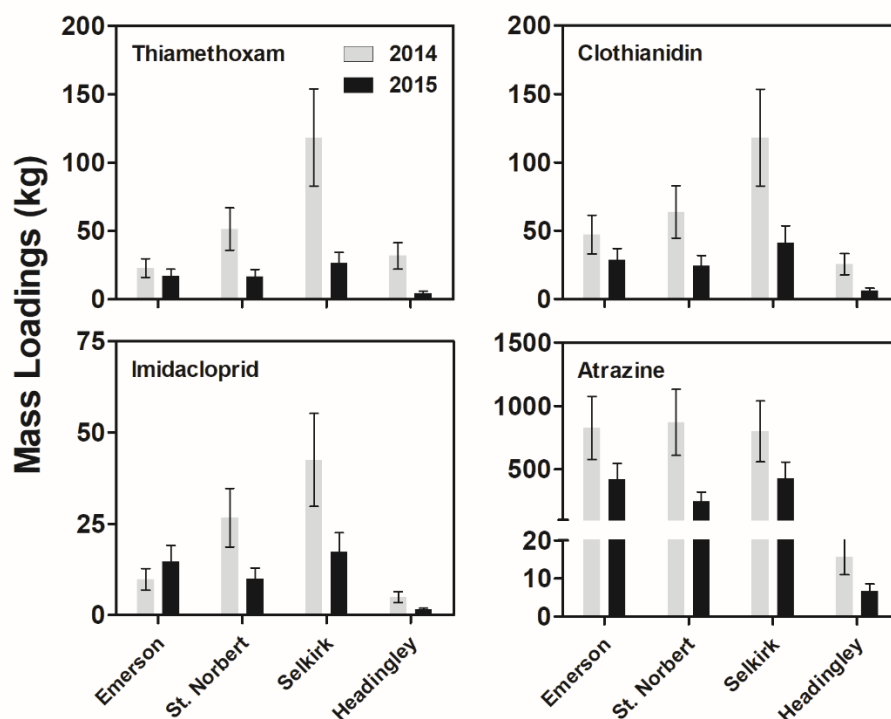
Figure 2.4: Mass loadings over the duration of each sampling season of thiamethoxam, clothianidin, imidacloprid, and atrazine along the Red River from south to north (flow direction) at Emerson, St. Norbert, and Selkirk and on the Assiniboine River at Headingley. Each bar in the plots represents 11 samples in 2014 and 12 samples in 2015. Error bars represent 30% relative standard deviation, estimated based on the uncertainty observed for replicate POCIS measurements.

2.4.2.2 Pesticide fluxes and mass loadings.

Daily fluxes (kg/d) were calculated by multiplying measured concentrations by the daily water discharge as shown in Figure 2.2. TWA water concentrations measured by POCIS (Table A4a-e) were assumed to be representative of the entire cross-sectional area of the water column at each site. The annual mass loadings presented in Figure 2.4 were calculated by summing the daily flux values over the continuous study periods in 2014 (May 28 – October 28; 154d) and 2015 (April 29 – October 28; 183d). Absolute errors in flux values are difficult to estimate given that uncertainties in

discharge data are not known. However, from the variation in replicate POCIS measurements, we can estimate the uncertainties associated with reported pesticide loadings in Figure 2.4. Using the concentration data (mean ± standard deviation) reported in Table A4a-e, the average relative standard deviation for all five compounds in all sampler over the entire study (n=627) is 29%. As an approximation, a 30% relative error was applied to the annual mass loadings. However, there is potential for a large degree of unknown uncertainty with these mass loading calculations as concentrations are measured near the banks of the river, and the extent of transverse mixing in the Red River is not well characterized. While we expect concentrations to be well-mixed, and thus, representative (given the often turbulent flows) the extent of mixing depends also upon the proximity of the POCIS sampler to the input source, which for diffuse agricultural inputs are near impossible to define.

While the data in Figure 2.4 only represent approximately half of the calendar year, contributions to mass loadings during the fall and winter months are expected to be minimal given reduced water flow, pesticide use, and pesticide inputs via processes such as runoff. Assuming the concentration and water flow remain constant from the final day of each study period (October 28th) to around March of the following year, total mass loadings of atrazine at Emerson, for example, over the remaining 211 days in 2014 and 182 days in 2015, would account for only 4% and 2% of annual loadings respectively. These likely represent conservative estimates given that flows in December, January, and February commonly drop below 30 m^3/s, compared to October and November flows that are typically closer to 60 m^3/s.

In 2014 annual atrazine mass loadings were approximately 2-to 3-fold greater than in 2015. The mass of atrazine in the Red River is largely conserved within study years from Emerson (2014 mass = 830kg, 2015 mass = 420kg) to St. Norbert (870kg, 245kg) to Selkirk (800kg, 430kg). Given that atrazine is not expected to degrade markedly in the transport time between sites, our data would suggest that inputs from southern Manitoba are minor.

Rawn et al. (1999) observed a similar spatial trend for atrazine, although their loading estimates were less, ranging from 100-150 kg annually. Reasons for the 4-8 fold difference in atrazine loadings between studies may include changes in atrazine use over the last 20 years (USGS National Water-Quality Assessment Project, 2018) where increases in regional and state usage patterns (i.e., North Dakota) have been observed, a lack of integrative, continuous sampling by Rawn et al. (1999) and stochastic variation across years and seasons. Rawn et al. (1999) also measured mass loadings of atrazine in a number of Red River tributaries, including the Assiniboine River. They estimated an annual mass of 1.7kg (1994) and 1.4kg (1995) coming from the Assiniboine River, which is smaller than the approximately 16kg (2014) and 7kg (2015) of atrazine estimated here. In seven other Red River tributaries, annual mass loadings of atrazine are much less; ranging from 0.005-0.78 kg (Carlson et al., 2013a; Rawn et al., 1999), supporting the evidence here that atrazine is largely coming from the U.S. In the Minnesota River, which is more comparable in size to the Red River, Schottler et al. (1994) reported an annual flux for atrazine of 1100kg in 1990 and 2000kg in 1991.

The annual mass loadings of neonicotinoids tell a different story than atrazine. In 2014 there appears to be a systematic increase in mass loadings of thiamethoxam,

clothianidin, and imidacloprid moving downstream from Emerson to Selkirk, indicative of multiple significant sources throughout southern Manitoba. However, in 2015 this pattern is much less pronounced (Figure 2.4), for reasons unclear at this time. It may simply be a result of variation between years related to the timing of pesticide applications and precipitation and runoff events. In 2014, a one-month period from mid-June to mid-July accounted for 55-67% of the annual mass loadings of neonicotinoids at the three Red River sites in Figure 2.4 (Emerson, St. Norbert, and Selkirk). Such periods of comparatively brief, intense inputs did not occur in 2015, potentially resulting in the more plateaued spatial pattern observed for the neonicotinoids moving downstream from Emerson. In general, mass loadings of the neonicotinoids ranged from 10-120 kg annually (Figure 2.4).

As noted, there is a 2- to 3-fold difference in loadings for the detected pesticides between 2014 and 2015. This may in part be a result of the 2-fold greater flows observed in 2014 in both rivers (Figure 2.2). We assume that the bulk of the pesticides are moved into the rivers by surface runoff, and so greater flows would result in greater movement of residual pesticides (Schottler et al., 1994). Additionally, it is estimated that 0.2–3% of applied pesticide reaches surface waters, depending largely on application type (e.g., foliar spray, seed coatings) and timing of rainfall events (Schottler et al., 1994). Assuming application techniques were similar in the Red River valley in 2014 and 2015, a major factor resulting in greater 2014 loadings could be related to the timing of rain events in relation to pesticide applications.

2.4.2.3 Risk associated with pesticide exposures

Water concentrations over the two-year study (Table A4a-e) were used to generate exposure distributions for thiamethoxam, clothianidin, imidacloprid, and atrazine (Figure 2.5). Exposure distributions can provide exceedance probabilities of specific threshold toxicity benchmarks for exposed organisms (Solomon et al., 2000). To screen for potential adverse impacts of these pesticides, water quality guidelines (WQGs) for the Protection of Aquatic Life were referenced from the Canadian Council of Ministers of the Environment (CCME) (Canadian Environmental Quality Guidelines, 2014). The CCME report long-term freshwater benchmarks of 1800 and 230 ng/L for atrazine and imidacloprid, respectively. As the CCME do not report protection of aquatic life guidelines for thiamethoxam or clothianidin, freshwater aquatic-life benchmarks from the USEPA Office of Pesticide Programs were referenced instead (U.S. Environmental Protection Agency, 2017a). Toxicity benchmarks of 17500 ng/L (invertebrate, acute) and 1100 ng/L (invertebrate, chronic) represented the most sensitive benchmark values available for thiamethoxam and clothianidin, respectively. The Office of Pesticide Programs compiles acute and/or chronic benchmarks for fish, invertebrates, and vascular and nonvascular plants (U.S. Environmental Protection Agency, 2017a). Where applicable, the chronic toxicity benchmarks were considered given that most of our exposure data represents 14-21d TWA concentrations which represent exposure durations consistent with the USEPA protocols for chronic screening-level risk assessments (Nowell et al., 2018; U.S. Environmental Protection Agency, 2017b). These threshold values for each pesticide were compared to exposure distributions (Figure 2.5) to calculate exceedance probabilities and hence assess risk.

81
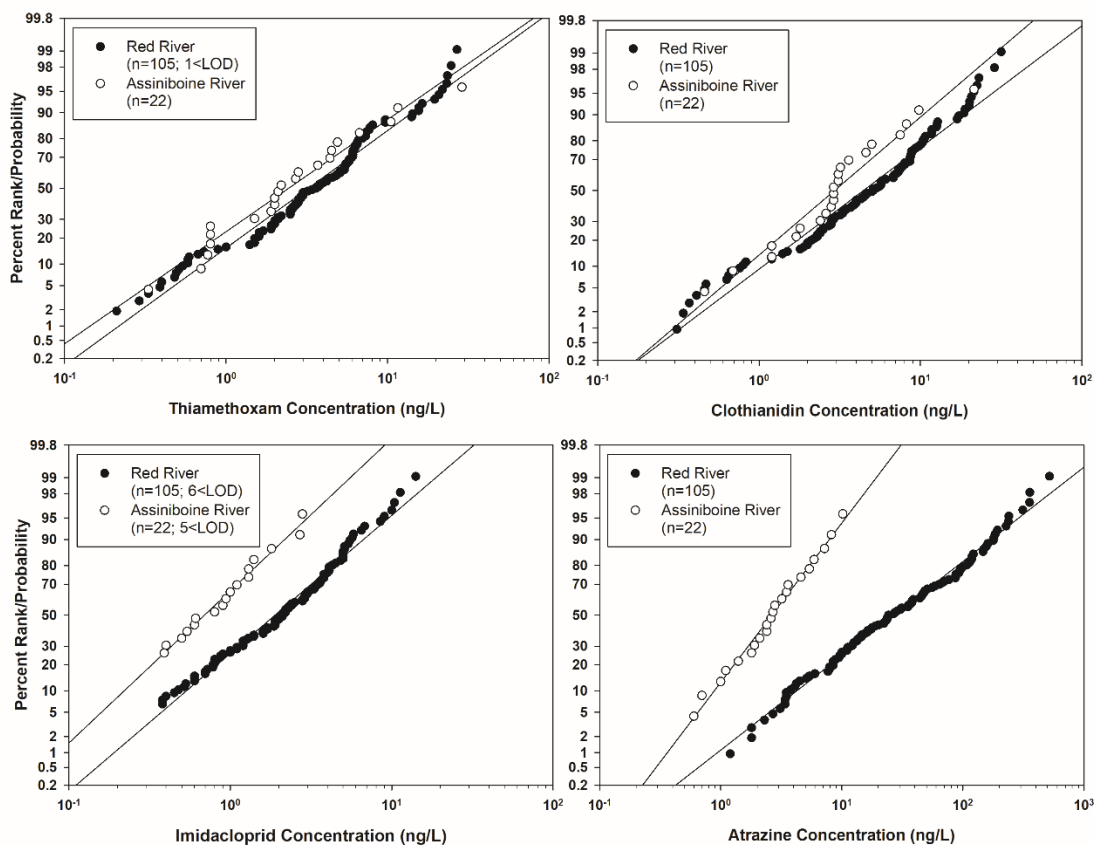
Figure 2.5: Exposure distributions for TWA concentrations of thiamethoxam, clothianidin, imidacloprid, and atrazine in the Red River (black circles) and Assiniboine River (open circles). Raw data in these plots from Table A4a-e. Data was plotted on a logarithmic-probability scale. Plotting positions on the y-axis were expressed as percentages calculated using the Weibull ranking equation = 100i/(i+1) where i is the ranked datum and n is the total number of data points in the data set. Data below the limit of detection (LOD) was included in the Weibull rankings but not plotted in the probabilistic exposure distributions. Linear regression statistics for each distribution in Table A8.

The levels of pesticides observed in this study represent no acute risk to aquatic life. Although concentrations reported here represent time-weighted averages and thus likely underestimate maximum short-term concentration spikes, acute guidelines are in most cases orders-of-magnitude larger than our observed concentrations. For a more conservative estimate of thiamethoxam risk (compared to the benchmark values above) a 35 day chronic no-observed-effect concentration of 300 ng/L was considered (Pickford et al., 2018). The probability of exceeding this chronic end-point in the Red and

Assiniboine River was determined to be <0.01%. No other individual neonicotinoid exceeded any toxicity benchmark. The other predicted exceedance was for atrazine with a 0.2% probability of exceeding the CCME long-term WQG of 1800 ng/L. Taken together, current exposures of these insecticides do not appear to pose any acute or chronic risk to non-target aquatic organisms. However, given the varied inputs and resulting suite of chemical classes present in the Red River, as demonstrated here, cumulative risks resulting from exposure to chemical mixtures is important to acknowledge. While this falls outside the scope of this study, this data can contribute to any future efforts to characterize cumulative risks in this system.

2.4.3 Pharmaceuticals

Of the 17 pharmaceuticals measured in this study, carbamazepine was the only one detected consistently at all sites (Figure A1 and Table A4e). Carbamazepine is an active pharmaceutical ingredient prescribed globally as an anti-epileptic medication (Cunningham et al., 2010). Given its widespread use and relative persistence in the environment, carbamazepine has become ubiquitous in impacted surface waters (Cunningham et al., 2010). The other six pharmaceuticals of note (antibiotics clarithromycin, sulfapyridine, sulfamethoxazole, trimethoprim and β-blockers metoprolol, propranolol) were only detected at the North End Red River site, downstream of the North End WWTP (Figure A3 and Table A5). The specific pharmaceuticals detected here are typical of effluent-impacted surface waters (Carlson et al., 2013a; Fairbairn et al., 2016). Concentrations generally ranged from 0.2-35 ng/L with notable spikes in the levels of sulfapyridine (250 ng/L) and clarithromycin (170 ng/L).

The mean carbamazepine concentration over the entire study at all sites (Red and Assiniboine, n=127, 11<LOD) was 2.8 ng/L, ranging from 0.3-13.8 ng/L. Concentrations at the North End site immediately downstream of the WWTP were elevated, with a mean of 6.8 ng/L (n=22, 1<LOD). The ten greatest concentrations observed for carbamazepine in this study were measured at the North End site. The levels of carbamazepine observed here were similar to those observed elsewhere in Manitoba and the U.S. For example, concentrations of carbamazepine in Dead Horse Creek, a small tributary to the Red River that receives sewage lagoon effluent from two small towns in southern Manitoba, ranged from non-detect to mean concentrations of 16-24 ng/L (Carlson et al., 2013a). Fairbairn et al. (2016) measured carbamazepine in the Zumbro River watershed in southeastern Minnesota and found concentrations ranging from below detection-0.83 ng/L at upstream sites to 73-150 ng/L at downstream sites. The CCME long-term freshwater WQG for carbamazepine is 10,000 ng/L which is nearly three orders of magnitude above the maximum concentration observed here. The Dutch government adopted an Average-Annual Environmental Quality Standard for carbamazepine of 500 ng/L (Moermond and Smit, 2016), a much more conservative value. Regardless, even the maximum concentration observed in this study (13.8 ng/L) remains well below these guideline values, suggesting that carbamazepine pose little known risk to organisms in the Red River, or downstream receiving waters.

Total average loadings downstream of the North End WWTP over the two years was approximately 20 kg carbamazepine, equating to 0.11 kg/d at Selkirk. Variation in annual loadings of carbamazepine were minimal (Figure A2) compared to the pesticides measured in this study (Figure 2.4), consistent with inputs being completely wastewater

derived, and therefore largely independent of variable precipitation patterns and hydrodynamic river conditions. Dead Horse Creek estimated a total load of 0.07 kg carbamazepine over the 2010 summer discharge event (Carlson et al., 2013a), consistent with a much smaller population. Mass loadings <5 kg in the Assiniboine River at Headingley were comparable to the upstream Emerson and St. Norbert sites on the Red River (Figure A2).

The City of Winnipeg is the largest settled population (≈700,000) in the Red River valley, however many smaller cities and municipalities lie along the river on both sides of the border and represent possible sources of municipal effluent. The largest of these, Fargo, ND (≈121,000); Moorhead, MN (42,000); and the Greater Grand Forks area, ND (≈98,500) contribute their municipal wastewater upstream of the Canadian border, and could explain the observed background levels of carbamazepine ranging from ≈0.5-2 ng/L at Emerson and St. Norbert. Additionally, there may be small inputs from the two small border towns of Pembina and Emerson. Given that environmental concentrations of pharmaceuticals typically scale with population (Anderson et al., 2004), based on the lagoon inputs into Dead Horse Creek from two towns totalling ≈18,000 (mentioned above, Carlson et al., 2013a), Pembina and Emerson combined (population ≈ 1000) would contribute approximately 0.004 kg of carbamazepine annually to the Red River. This estimate is crude, in that it assumes no transformation or other losses (e.g., sorption to particulate matter, sedimentation) from the water column throughout the river. Nonetheless, it is clear that upstream contributions of carbamazepine to the load of this chemical in the lower Red River are negligible compared to the inputs from the City of Winnipeg.

Per capita loadings of the pharmaceuticals downstream of the North End WWTP can be calculated based on the measured chemical concentrations (Table A4e and A5), an estimated average daily Red River discharge at the North End site (8.8×10^6 m^3/d), the WWTP average daily discharge (2.0×10^5 m^3/d), and the served population of 404,000 people. Per capita loadings for the seven pharmaceuticals measured in this study ranged from 7 – 150 µg/person/d (Table A7). These are rough estimates as they are extrapolated from downstream concentrations, and not the raw effluent. That said, our estimates are in general agreement with other Canadian studies reporting per capita loadings estimated from raw effluent (comparison in Table A7). Carlson et al. (2013a) reported loadings ranging from 24 – 203 µg/person/d coming from rural wastewater lagoons (population 18,000) and (MacLeod and Wong, 2010) observed loadings from 2 to 115 µg/person/d from two WWTPs in Alberta serving 750,000 and 250,000 people.

2.4.4 Per- and polyfluoroalkyl substances (PFASs)

Eight of nine PFASs monitored in this study were detected regularly throughout the duration of the 2014 sampling campaign. PFUnDA was not detected above the elevated background contamination observed in most samples. The raw POCIS TWA concentration data for PFDA, PFHpA, PFHxA, PFNA, PFOA, PFOS, PFHxS, and PFPeA can be found in Appendix A (Table A6a-h). Data for PFHxS and PFPeA is not presented in Figure 2.6 because experimentally measured POCIS sampling rates have not been determined for these compounds. Therefore, concentrations of those analytes are presented in Table A6g-h as mass on POCIS per day (ng/d) and represent relative levels of PFHxS and PFPeA. To estimate semi-quantitative TWA water concentrations of PFHxS and PFPeA, the mass/d can be divided by an estimated sampling rate based

on the six experimentally measured sampling rates used for PFDA, PFHpA, PFHxA, PFNA, PFOA, and PFOS (Kaserzon et al., 2012). The measured sampling rates reported by Kaserzon et al. (2012) differ maximally by approximately a factor of two, ranging from 0.16-0.36 L/d, which is expected given the structural similarities between these analytes. Given this, taking the average of the six known sampling rate values (0.26 L/d) offers one approach to estimating a reasonable sampling rate value for PFHxS and PFPeA. Of course, end users of this data should be careful with this approach and may wish to regard the resulting data as semi-qualitative.

The maximum measured concentration was 8.5 ng/L PFOS. Generally, concentrations of the six PFASs ranged from 0.5-2 ng/L (Figure 2.6). Additionally, increased concentrations downstream of the North End WWTP at the North End site were not observed, suggesting that the WWTP is not a major point-source and that multiple more diffuse inputs along the River may be responsible for these PFAS levels. The PFAS measurements here are consistent with single grab sample concentrations taken by Scott et al. (2009) at two sites on the Red River in 2005 and at a single site on the Assiniboine River close to the Saskatchewan border. Scott et al. (2009) measured 14 PFASs including seven of the compounds measured here (excluding PFPeA).
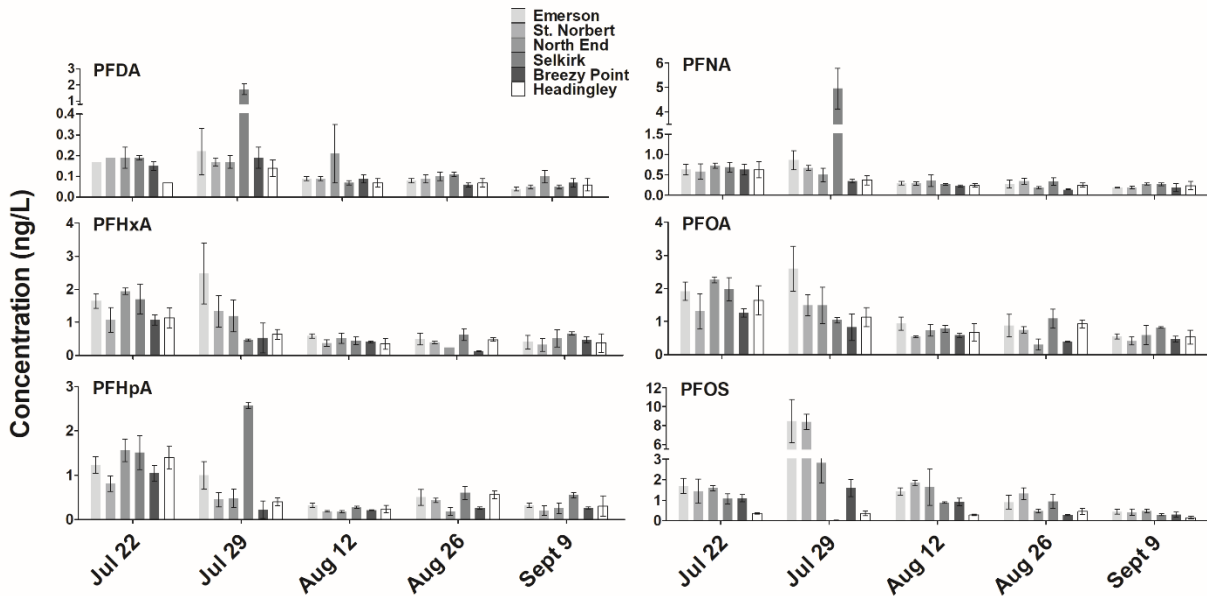
Figure 2.6: Concentrations of six PFAS in the Red River (Emerson, St. Norbert, North End, Selkirk, Breezy Point) and Assiniboine River (Headingley) as measured by the adapted PFAS-POCIS. Left to right on each plot is summer (July 22) to fall (September 9) in 2014 and within each group of bars light gray to dark gray represents direction of flow on the Red River. Headingley, on the Assiniboine River, is the white bar. Each bar represents the mean and standard deviation (error bars) of triplicate POCIS.

Concentrations of the six common PFASs measured by Scott et al. (2009) on the Red River ranged from 0.15-1.67 ng/L. Notable concentrations of PFHpA (10.5 ng/L), PFOA (6.9 ng/L), and PFHxA (5.8 ng/L) measured in the Assiniboine River by Scott et al. (2009), albeit much further west than our Headingley site, were significantly greater than concentrations observed here (Figure 2.6). While there does not seem to be obvious spatial or temporal trends in these systems as they relate to PFAS levels, concentrations of PFDA, PFNA, and PFHpA do appear to spike at the Selkirk site during the July 29th deployment. Selkirk, Manitoba is a town of approximately 10,000 that releases its municipal and industrial waste effluent into the Red River, however without further sampling and investigation, it is difficult to know what, if anything, is the cause of these concentration spikes. The Canadian federal water quality guideline for PFOS is

6800 ng/L (Environment and Climate Change Canada, 2017), nearly 1000 times larger than any concentration of PFAS observed here.

2.4.5 Antibiotic resistance genes

Total bacteria levels were not statistically different across all locations (Kruskal-Wallis, H = 7.3, p = 0.20) (Table A9). Similarly, the sums of tetracycline resistance genes were not statistically different along the river (KW, H = 2.67, p = 0.76), while the sums of sulfonamide resistance genes were different (KW, H = 9.50, p = 0.09) with lower levels at Selkirk. Patterns of "total resistance" are often inadequate to describe the patterns along a river. As such, we examined the trends of individual resistance gene-determinants (Figure A4). Patterns of "total bacteria" were also included to help visual comparisons (Figure A4, 16SrRNA plot). It should be noted that gene-determinants *tet*-E, -G, -L, -O, -Q and -X had minimal or non-detected signals, and therefore were subsequently excluded in further analyses (Table A10).

Tetracycline resistant gene-determinants *tet*-A, *tet*-B and *tet*-C are related to bacterial efflux pumps, used for detoxification and are relatively common in the samples, with uniform distributions. They are most commonly associated with Gram-negative bacteria (Chopra and Roberts, 2001). *Tet*-A were found in relatively low levels except in Emerson; while *tet*-B and *tet*-C had rather uniform concentrations along the Red River and at Headingley.

Tet-D, -E, -G, -K, -M were found in greater abundances and frequency downstream from the North End WWTP, north of Winnipeg and Headingley. *Tet*-M encodes for a ribosome-protection protein in both Gram-negative and –positive bacteria. The others represent genes related to efflux-pumps in Gram-negatives. These gene

determinants are signatures of human impacts, particularly in wastewater treatment plants and their effluent (Gatica et al., 2016).

Sulfonamide resistance genes have become rather ubiquitous in natural systems (Byrne-Bailey et al., 2009). Many bacterial isolates with the *sul*1 gene have been associated with integrase1 genetic elements in integrons (Byrne-Bailey et al., 2009), which enhances their dissemination of antibiotic resistance in areas of pollution. The presence of *sul*-genes suggest anthropogenic impact to the waters, agricultural and municipal, especially when all three determinants (*sul*1, *sul*2, *sul*3; Figure A4) are present (Pei et al., 2006).

2.5 CONCLUSIONS

This study provides a spatial and temporal assessment of pesticides, pharmaceuticals, PFASs, and ARGs in the Red River of the Lake Winnipeg watershed, measured using POCIS passive samplers in 2014 and 2015. Pesticides represented the major contaminant of interest given the intensive agriculture in the watershed, both in the United States and southern Manitoba. Mass loading estimates helped differentiate chemical sources along the River. For atrazine, inputs to the Red River were largely from the United States, consistent with usage patterns of the herbicide throughout the U.S. side of the Red River watershed compared to in southern Manitoba. As hypothesized, inputs of atrazine from western Manitoba were minor. Neonicotinoid loadings were more indicative of usage all along the Red River valley on both sides of the border, and throughout western Manitoba (Assiniboine River). Annual mass loadings of these pesticides ranged from approximately 40 kg (imidacloprid) to 800 kg (atrazine). Screening for potential toxicity of these pesticides demonstrated no

significant concern based on exposure distributions and protection of aquatic life benchmarks. Of the seven pharmaceuticals detected in the Red River, carbamazepine was the single one measured consistently through time and space, at concentrations ranging from 0.5-15 ng/L. Pharmaceutical concentrations were elevated at the North End site, downstream of the City of Winnipeg's major wastewater treatment plant. PFASs and ARGs were found at levels typical of an impacted river system, however exact sources were less clear as profiles were indicative of potentially multiple diffuse sources throughout the watershed. This work will help inform best management practices within the Lake Winnipeg watershed and aid in the efforts to understand contaminant sources and improve water quality of this lake.

While the focus of this specific chapter was the characterization of contaminants and not assessment of the sampling technique, it is important to note a crucial challenge associated with POCIS use, which is especially relevant in the context of the following chapters. For many reasons detailed in the following chapters, the variability in reported POCIS sampling rates can be quite large for individual compounds. Because this variation and uncertainty is not well characterized and understood, selecting the appropriate sampling rate for a given application can be very challenging and represents the major issue for end-users of POCIS. Here, we take the approach of averaging all reported sampling rates for a given compound in order to avoid bias from any aberrant outliers (Table A3). While we deem this approach to be most prudent for POCIS end-users, there are still considerable uncertainties associated with this practice. A PSD that avoids this issue of sampling rate variability, and other uncertainties, is developed and evaluated in the following chapters.

CHAPTER 3

3. DEVELOPMENT AND CALIBRATION OF AN ORGANIC-DIFFUSIVE GRADIENTS IN THIN FILMS AQUATIC PASSIVE SAMPLER FOR A DIVERSE SUITE OF POLAR ORGANIC CONTAMINANTS

3.1 ABSTRACT

A unique configuration of the diffusive gradients in thin films sampler for polar organics (o-DGT) without a polyethersulfone membrane was developed, calibrated, and field-evaluated. Diffusion coefficients (D) through agarose diffusive gels ranged from $(1.02–4.74)\times10^{-6}$ cm^2/s for 34 pharmaceuticals and pesticides at 5, 13, and 23°C. Analyte-specific diffusion-temperature plots produced linear ($r^2 > 0.85$) empirical relationships whereby D could be estimated at any environmentally relevant temperature (i.e., matched to *in situ* water conditions). Linear uptake for all analytes was observed in a static renewal calibration experiment over 25 days except for three macrolide antibiotics, which reached saturation at 300 ng (≈15 d). Experimental sampling rates ranged from 8.8–16.1 mL/d, and were successfully estimated with measured and modelled D within 19 and 30% average relative error, respectively. Under slow flowing (2.4 cm/s) and static conditions, the *in situ* diffusive boundary layer (DBL) thickness ranged from 0.023–0.075 cm, resulting in a maximum contribution to mass transfer of <45%. Estimated water concentrations by o-DGT at a wastewater treatment plant agreed well with grab samples and appeared to be less influenced by the boundary layer compared to that of polar organic chemical integrative samplers (POCIS) deployed simultaneously. The o-DGT sampler is a promising monitoring tool that is largely insensitive to the DBL under typical flow conditions, facilitating the application of measured/modelled diffusion-based sampling rates. This significantly reduces the need for sampler calibration, making o-DGT more widely applicable, reliable, and cost-effective compared to current polar passive samplers.

3.2 INTRODUCTION

The value of passive sampling devices (PSDs) for measuring and monitoring environmental contaminants is evidenced by thousands of research articles and numerous reviews published over the last 15 years (Davison and Zhang, 2012; Harman et al., 2012; Mayer et al., 2003; Vrana et al., 2005; Zabiegała et al., 2010). Advantages over traditional grab sampling include continuous *in-situ* monitoring, cleaner sample matrices, biomimetic applications, improved detection limits and sampling efficiencies, ease of storage, and simplified archiving.

At this time, for polar PSDs, the POCIS (polar organic chemical integrative sampler) (Alvarez et al., 2004) is the most widely used tool for measuring hydrophilic contaminants ($logK_{ow} < 5$) in water (Harman et al., 2012; Morin et al., 2012). To a lesser extent, Chemcatcher® has also been applied to aquatic passive sampling of polar analytes (Charriau et al., 2016; Lissalde et al., 2016; Mills et al., 2007; Shaw et al., 2009; Shaw and Mueller, 2009). Despite the many advantages over grab and automated sampling, polar-PSDs lack a robust, fundamental uptake model (Harman et al., 2012) and an accepted method for *in-situ* exposure corrections (Harman et al., 2012; Mazzella et al., 2010; Morin et al., 2012; Shaw et al., 2009). These two issues greatly limit their reliability as quantitative measurement tools.

Significant discrepancies between laboratory-derived POCIS sampling rates (R_s – L/d) and those observed in the field result from confounding environmental factors (e.g., flow rate, temperature, biofouling, DOC, pH etc.) affecting sampler uptake (Harman et al., 2012). The 'gold-standard' in passive sampling is the use of performance reference compounds (PRCs) to account for these factors *in situ.* Although the PRC approach has

94

been extensively developed for equilibrium PSDs and hydrophobic contaminants (Allan et al., 2009), very limited success has been reported for polar PSDs (Jacquet et al., 2012; Mazzella et al., 2010; Miège et al., 2012; Shaw et al., 2009). Furthermore, while partitioning processes typically govern analyte-sorbent interactions in equilibrium samplers, adsorption phenomena control uptake in polar PSDs (Bäuerlein et al., 2012; Dias and Poole, 2002). As a result, POCIS and Chemcatcher® often fail to produce isotropic exchange and/or have negligible desorption, two fundamental criteria of the PRC approach (Charriau et al., 2016; Harman et al., 2011; Morin et al., 2012; Shaw et al., 2009). A further confounding factor is the interaction that many polar analytes have with polyethersulfone membranes used in polar PSDs (Vermeirssen et al., 2012); the kinetics and mechanisms of which are poorly understood. For these reasons, an all-encompassing, widely applicable PRC approach to polar PSDs is highly unlikely. While *in silico* methods for predicting sampling rates for POCIS using artificial neural networks and molecular descriptors have been attempted, these remain in their infancy and are inherently complex (Miller et al., 2016).

Without an accepted approach to correct for *in-situ* sampling rates, POCIS has been deemed to be, at best, semi-quantitative (Harman et al., 2011; Poulier et al., 2014), with total uncertainties in reported concentrations estimated at >100% (Poulier et al., 2014). Water flow-rate and temperature are two site-specific conditions that effect *in situ* uptake in POCIS and contribute to these large uncertainties. The influence of flow-rate on POCIS is a result of the diffusive boundary layer (DBL), which controls analyte uptake (Alvarez et al., 2004) and thus confounds efforts to predict sampling rates. The literature suggests that increases in flow-rate typically increase POCIS R_s by a factor of

≈2 (Harman et al., 2012), but could increase by up to 4- to 9-fold (Alvarez et al., 2004). A similar two-fold increase in R_s has been observed over the temperature range 5-25°C (Li et al., 2010a; Togola and Budzinski, 2007), a factor rarely considered in both the calibration and application of POCIS. As a result of these confounding influences on sampler uptake, a robust model to predict R_s and ultimately reduce the need for laborious calibrations is unlikely for current polar PSDs. Therefore, there is need for a polar PSD that is less sensitive to site-specific conditions, and more amenable to modelling.

The diffusive gradients in thin films (DGT) (Davison and Zhang, 1994; Zhang and Davison, 1995) passive sampler is popular for inorganic species (e.g., trace metals) in both aquatic and sediment porewater systems (Davison and Zhang, 2012). The sampler is comprised of a diffusive gel controlling analyte uptake and a binding gel sequestering analytes. Of note is the fact that the diffusive gel is thicker than the typical thickness of the DBL, making DGT largely insensitive to changing hydrodynamic conditions (Uher et al., 2013; Zhang and Davison, 1995). Additionally, since measurement of temperature-specific diffusion coefficients (D) through the thick diffusive gel is well established and relatively simple to do (Chen et al., 2013), determination of sampling rates with temperature is trivial (as R_s can be calculated from D), allowing DGT to, at least in part, account for temperature differences between laboratory calibrations and field deployments. Removing uncertainties related to flow rate and temperature significantly increases the applicability of polar PSDs for routine monitoring, and has been extensively tested, validated, and applied for DGT with metals (Davison and Zhang, 2012). Recently, Chen et al (2015, 2013, 2012) extended the DGT approach to polar

organic contaminants (organic-DGT or o-DGT), first with the antibiotic sulfamethoxazole (Chen et al., 2012), then to measure forty antibiotics in wastewater (Chen et al., 2015 and 2013).

Our o-DGT configuration without the polyethersulfone outer membrane (i.e., the diffusive gel acting as the outer membrane) was used to expand the technique to a suite of 34 pharmaceuticals and pesticides to determine if o-DGT can accurately estimate water concentrations based strictly on measured or modeled diffusion coefficients (D), significantly reducing the need for laborious sampler calibration. These were measured at three temperatures to develop empirical relationships to allow accurate prediction at environmentally relevant temperatures. Additionally, D-values and corresponding sampling rates were modeled and compared to experimental measurements. We calibrated o-DGT using a static renewal system, to characterize the duration of the kinetic/linear uptake regime and the effect of the DBL on sampler uptake. Lastly, o-DGT was evaluated under field conditions at a wastewater treatment plant, and the DBL was estimated *in-situ.*

3.2.1 DGT Theory

The most common and simplest DGT equation relates the time weighted average (TWA) water concentration (C_{DGT}) to the mass of analyte on sampler (M_{DGT}), thickness of the diffusive gel layer (Δg), exposed area (A), deployment time (t), and analyte diffusion coefficient through the diffusive gel (D):

$$C_{DGT} = \frac{M_{DGT}\Delta g}{DAt}$$

Equation 3.1

The success of DGT for measurement of metals is partly due to the simplicity of *Equation 3.1*, and thereby the convenience of ignoring the DBL. With exception to quiescent waters application *Equation 3.1*, with $\Delta g \geq 0.8$ mm, is valid under most naturally flowing conditions ($\geq \approx 2$ cm/s) (Gimpel et al., 2001), with errors <10% (Davison and Zhang, 2012; Scally et al., 2006). However, several assumptions are inherent in the application of *Equation 3.1* (Davison and Zhang, 2012), including a negligible DBL (and other potential resistances to mass transfer, e.g., biofilms); and analyte diffusion through both water and diffusive gel are equivalent (Scally et al., 2006). We test the validity of *Equation 3.1* for our analytes and investigate the influence of the DBL on o-DGT uptake using the more appropriate and complete DGT equation which accounts for boundary layer thickness (δ) (*Equation 3.2*):

$$C_{DGT} = \frac{M_{DGT}(\Delta g + \delta)}{DAt}$$

Equation 3.2

3.3 METHODS AND MATERIALS

3.3.1 Chemicals and Reagents

Stock solutions of the 34 target and 28 internal standard (IS) mixtures were prepared in pure methanol at 10 ng/μL and 2 ng/μL, respectively. Further details on other reagents are found in Appendix B. The complete list of 34 target analytes, abbreviations, and the 28 matched isotopically labelled internal standards or surrogates (in brackets) are given below:

17β-estradiol[c], E2 (E2-d$_4$)[f]; 17α-ethynylestradiol[c], EE2 (EE2-d$_4$)[f]; 2,4-Dichloro-phenoxy

acetic acid[a], 2,4-D (2,4-D-^{13}C$_6$)[g]; Clofibric Acid[b], CLO (CLO-d$_4$)[f]; Diclofenac[b], DIC (DIC-

d$_4$)[f]; Estrone[c], E1 (E1-d$_4$)[g]; Fenoprofen[d], FEN (IBU-d$_3$)[f]; Gemfibrozil[a], GEM (GEM-d$_6$)[f];

Ibuprofen[a], IBU (IBU-d$_3$)[f]; Ketoprofen[d], KET (KET-d$_4$)[f]; Naproxen[b], NAP (NAP-d$_3$)[f] [MS

negative mode compounds]. Atenolol[a], ATE (ATE-d$_7$)[f]; Atrazine[b], ATR (ATR-d$_5$)[f];

Carbamazepine[b], CBZ (CBZ-d$_{10}$)[f]; Chlorpyrifos[a], CPY (CPY-d$_{10}$)[d]; Clarithromycin[a], CLA

(Josamycin)[b]; Clothianidin[h], CLT (CLT-d$_3$)[h]; Diazinon[a], DIA (DIA-d$_{10}$)[f]; Enrofloxacin[a],

ENR (ENR-d$_5$)[f]; Erythromycin[a], ERY (Josamycin)[b]; Fluoxetine[a], FLU (FLU-d$_6$)[g];

Imidacloprid[c], IMI (IMI-d$_4$)[f]; Metoprolol[a], MET (MET-d$_7$)[f]; Paroxetine[e], PAR (FLU-d$_6$)[g];

Propranolol[a], PRO (PRO-d$_7$)[f]; Roxithromycin[a], ROX (Josamycin)[b]; Sulfadimethoxine[a],

SDM (SDM-d$_6$)[d]; Sulfamethazine[a], SMZ (SMZ-^{13}C$_6$)[g]; Sulfamethoxazole[a], SMX (SMX-

d$_4$)[d]; Sulfapyridine[e], SPY (SPY-d$_4$)[e]; Sulfisoxazole[a], SXZ (SMX-d$_4$)[d];

Sulfachloropyridazine[a], SCP (SMZ-^{13}C$_6$)[g]; Thiamethoxam[h], TMX (TMX-d$_3$)[h];

Trimethoprim[a], TRI (TRI-d$_3$)[f] [MS positive mode compounds]. All target chemicals were

of >98% purity except for ERY, which was 95% pure. Stable isotope standards were all

of >99% isotopic purity. Target analytes were obtained from (a) Sigma-Aldrich (Oakville,

ON); (b) MP Biomedicals (Montreal, QC); (c) EQ Laboratories Inc. (Atlanta, GA); (d) ICN

Biomedicals (Irvine, CA); (e) Toronto Research Chemicals (Toronto, ON); (f) C/D/N

Isotopes Inc. (Pointe-Claire, QC); (g) Cambridge Isotopes (Andover, MA); (h) Syngenta

Canada Inc. (Guelph, ON).

3.3.2 Sampler details

3.3.2.1 o-DGT preparation

The standard o-DGT configuration used in this experiment, unless otherwise stated, was a 0.75 mm, 25 mg HLB binding gel (Figure B2) and a 1.0 mm diffusive gel. Diffusive and binding gels were prepared using 1.5% agarose gel (molecular biology grade, Sigma-Aldrich). Agarose was made by placing the agarose-water mixture (1.5%) in a boiling water bath until agarose was fully dissolved. Gels were cast in sheets using a Bio-Rad Laboratories (Mississauga, ON) Mini-Protean® casting system (Figure B2) employing 0.5, 0.75, 1.0, and 1.5 mm casts. Gels were cut from square casts (A=73 cm^2) into 6x2.6 cm diameter (5.3 cm^2) disks, rinsed periodically with Milli-Q water over ≈24 hours, and stored at 4ºC in 5 mM KNO$_3$ solution. Binding gels used the same 1.5% agarose, with the addition of 0.35 g OASIS™ HLB powder (Waters Corporation, Milford, MA) per casted sheet (25 mg HLB per disc, nominal). Assembled o-DGT were stored in 5 mM KNO$_3$ solution at 4ºC until use.

For making binding gels, the gel/HLB mixture (≈5 mL of gel + 0.35 g HLB per cast) was vortexed to homogenize the HLB throughout the 1.5% agarose, immediately poured, and subsequently flipped horizontal to set, allowing the bulk of the HLB to settle to one surface of the gel. This provided binding gels with 25 mg of HLB (nominal) per gel disk (binding gel disks pictured below). The 0.75 mm binding gel was placed on the standard plastic DGT base (HLB side face-up) with the diffusive gel layered on top, and sealed with the standard DGT cap (exposure A=3.1 cm^2).

3.3.2.2 o-DGT Extraction

Retrieved samplers were disassembled and diffusive gel discarded. The binding gel was placed in a 50 mL glass test tube, spiked with 50 ng of IS mixture directly onto the gel and left for ≈15 min, to allow the IS to soak into the binding gel. Given high extraction efficiencies (Table B4), this length of soaking time was sufficient. Separate 3×3 mL aliquots of methanol were added with sonication for 2 min between each addition. The aliquots were combined in a separate test tube and evaporated to dryness by nitrogen blowdown. Dried samples were reconstituted in 1 mL of 50:50 MeOH:H_2O and filtered through a 0.22 µm PTFE syringe filter (Pall Life Sciences, Mississauga, ON) into LC amber vials. Samples were stored at $4^{o}C$ for no longer than 3 days before analysis by liquid chromatography-tandem mass spectrometry (LC-MS/MS).

3.3.3 Instrumental Analysis

All sample analysis was conducted by LC-MS/MS. Separations were achieved with an Agilent 1200 Series (Agilent Technologies, Mississauga, ON) binary pump, degasser, and column heater connected to a Phenomenex (Torrance, CA) Kinetex XB-C_{18} column (50 mm × 2.1 mm × 1.7 µm particle size) and C_{18} SecurityGuard ULTRA Cartridge (2.1 mm I.D.). Detection was done using an Agilent 6410B MS equipped with an electrospray ionization source in positive and negative mode under two separate methods. Details of the gradient elution methods (Table B1), example chromatograms (Figure B1), MS source parameters (Table B2a), *m/z* transitions and optimized parameters for analyte detections (Table B2b and B2c), and instrument detection limits (Table B3) can be found in Appendix B.

3.3.4 Experimental Details

3.3.4.1 Diffusion Measurements

A two-compartment diffusion cell (Figure B4) (Zhang and Davison, 1999) was used to measure D at 5, 13, and 23°C (±0.5°C), spanning the range typically observed in the environment. The solution pH ranged from 5.5-6.5. Further details are in Appendix B. The mass of analyte in the receiving cell was plotted as a function of time (Figure B5) to obtain a line with a slope equal to the first-order diffusion rate constant, *k*. *Equation 3.3* below was then used to calculate D (cm^2/s), where Δg is the diffusive gel thickness, C_s is the initial analyte concentration in the source cell, and *A* is the area of the connecting window:

$$D = \frac{k\Delta g}{C_s A}$$

Equation 3.3

3.3.4.2 o-DGT Calibration

Laboratory-based sampler calibration was conducted to measure the uptake dependence on time, and determine the capacity of the sampler throughout its linear/kinetic uptake regime. Samplers were exposed in a 40 L glass tank containing 25 L of 5 mM KNO$_3$ (deionized water) spiked with the 34-analyte mixture (2 ng/mL nominal) and renewed every 24-48 h. Water pH was constant around 5.5 and temperature ranged from 21-25 °C over the course of the experiment. To produce a flowing system samplers were suspended from a motorized variable-speed carousel and rotated through the water at a linear velocity of ca. 2.4 cm/s (Figure B7).

Eight duplicate sets of standard samplers (0.75 mm, 25 mg HLB binding gel and a 1.0 mm diffusive gel) were deployed in the tank and sampled at 3, 6, 8, 12, 15, 18, 22,

and 25 days to produce an o-DGT uptake time-series. An additional set of o-DGT containing an outer PES membrane (0.1 µm pore size, Environmental Sampling Technologies, St. Joseph, MO) was also deployed and retrieved along with the 8 d standard o-DGT (no PES) for comparison (Figure B3). Further sets of o-DGT were deployed for boundary layer measurements (see below).

3.3.4.3 Diffusive Boundary Layer (DBL)

Samplers with different diffusive gel thicknesses (0.5, 0.75, 1.0, 1.5 mm) were exposed under flowing (≈2.4 cm/s) and static conditions. The experiment under flowing conditions was done with three duplicate sets of o-DGT (0.75, 1.0, 1.5 mm) deployed for 8 d. Under static conditions, four duplicate sets of o-DGT (0.5, 0.75, 1.0, 1.5 mm) were deployed for 10 d in glass tanks containing 4 L of 5 mM KNO_3 (Milli-Q H_2O) and spiked with the 34-analyte mixture at 2.5 ng/mL (nominal). When o-DGT are deployed simultaneously with different gel thicknesses (Δg), the DBL (δ) can be estimated *in-situ.* Manipulating *Equation 3.2* gives (Chen et al., 2013):

$$\frac{1}{M_{DGT}} = \frac{\Delta g}{D C_{DGT} A t} + \frac{\delta}{D C_{DGT} A t}$$

Equation 3.4

3.3.4.4 Field Demonstration

The calibrated o-DGT sampler was tested at a wastewater treatment plant in northern Manitoba, Canada (site details can be found in Appendix B). Both o-DGT and POCIS samplers were co-deployed for 21 d (July 3-24, 2015) in large POCIS cages (Environmental Sampling Technologies) equipped with HOBO Water Temp Pro v2 loggers (two readings per hour, ±0.2°C accuracy) (Hoskin Scientific LTD., Burlington, ON) in July 2015 at three sites: treatment plant intake/influent (tertiary lagoon),

treatment plant effluent (directly prior to leaving the plant), and at the intake to the community's drinking water treatment plant, which also served as the upstream control site. Triplicate grab samples (500 mL) at the three sites were taken twice; at deployment and retrieval of the samplers. Details of POCIS extractions are in Chapter 2 and elsewhere (Carlson et al., 2013b). Grab sampling protocols followed procedures developed in our lab (Carlson et al., 2013a). Water samples were filtered through 0.45 µm Metricel membrane filters (Pall Life Sciences) and the filtrate was spiked with 50 ng of IS mixture prior to solid phase extraction (SPE) by 3 cc/60 mg OASIS™ HLB cartridges (Waters Corporation). After pre-conditioning with methanol followed by water, samples were drawn through at ≈5 mL/min and eluted with 3 mL of methanol. The remaining extract was processed exactly as above for o-DGT samples. Extraction efficiencies by SPE have been determined in our lab previously (Carlson et al., 2013b).

3.3.5 *Statistical Analysis*

Prism v. 5.01 (GraphPad Software, La Jolla, CA) was used for statistical analysis. A one-way ANOVA with a Tukey post-hoc test was used to compare measured analyte concentrations by o-DGT, POCIS, and grab samples for the field data. Significant differences were defined as $p < 0.05$. Errors are presented as standard deviations of the mean, unless otherwise stated.

3.4 RESULTS AND DISCUSSION

3.4.1 *Polyethersulfone (PES) Membrane*

While many additional details of sampler development and optimization can be found in Appendix B, one important consequence of sampler development was the

decision to exclude the PES membrane as the outer layer of o-DGT. Given PES is used in all current polar-PSDs, a brief discussion of the issue follows.

The extent of uptake into PES varied largely between analytes, but was detected in significant quantities for most compounds (Figure B3). Generally speaking, the moderately-polar compounds, e.g., fluoxetine and diazinon (higher $LogK_{ow}$), tend to be preferentially retained on PES compared to the more highly polar analytes, e.g., many of the sulfonamide antibiotics. These data agree well with earlier findings (Vermeirssen et al., 2012). For some compounds, the mass of analyte extracted from PES was significantly more than from the HLB binding gel itself (chlorpyrifos, diazinon, fluoxetine, paroxetine, roxithromycin, estrone, 17β-estradiol, 17α-ethynylestradiol, fenoprofen, gemfibrozil), suggesting that the former is a more effective sink for these compounds (Figure B3). This poses a significant problem for o-DGT given its utility stems from the fact that the thick diffusive gel controls analyte uptake, which is predictable with the analyte's diffusion coefficient. With the inclusion of the PES membrane, this requirement is not met, complicating the uptake model, as in POCIS and Chemcatcher® (Vermeirssen et al., 2012).

3.4.2 Diffusion Coefficients (D)

3.4.2.1 Measured D

Diffusion time-series plots for all analytes at 5, 13, and 23°C can be found in Appendix B (Figure B5). Apart from recent work on antibiotics (Chen et al., 2013), measured diffusion coefficients (D) in hydrogels for polar organics are not published. All empirical D-T plots (Table B5) showed good linearity, with most compounds having r^2-values > 0.9, except clarithromycin and paroxetine (r^2-values > 0.85). The average

relative error in the slopes of all D-T plots (for compounds with 3-point regressions, n=30) was 18% (range: 0-40%). Enrofloxacin did not produce linear diffusion plots for any of the temperature experiments (not shown in Table B5), and thus a value for enrofloxacin of 2.96×10^{-6} cm^2/s measured at 25°C by Chen et al. (2013) was used. Only the 5 and 13°C D-values were used to create a two-point D-T plot for erythromycin, 17β-estradiol, and 17α-ethynylestradiol given missing data at 23°C due to poor internal standard response for that sample set. For comparison, a calculated D at 23°C of 3×10^{-6} cm^2/s (from Table B5 data) for 17β-estradiol and 17α-ethynylestradiol agrees well with the measured D of 3.6×10^{-6} cm^2/s for the structurally similar estrone. For erythromycin, a calculated D of 1.74×10^{-6} cm^2/s at 25°C (using data from Table B5) agrees with the earlier measurement (Chen et al., 2013) at that temperature (1.85×10^{-6} cm^2/s).

The sulfonamides (sulfadimethoxine, sulfamethazine, sulfamethoxazole, sulfapyridine, sulfisoxazole, sulfachlorpyridazine) in this work were also studied by Chen et al. (2013) Generally, measured D between the two studies were in agreement, differing by an average of 13% (range: 5-23%) across the six sulfonamides. With the exception of sulfachlorpyridazine (23% greater), the five D-values measured here were slightly less than those of Chen et al. (2013) likely a result of the slightly lower temperature (2°C) used in the current study. A more quantitative comparison between data sets is not possible because Chen et al. (2013) did not provide any error estimates for their D-values.

Our measured D varied maximally by 50% across all analytes at a given temperature, a range largely dictated by molecular size. For example, clarithromycin, erythromycin, and roxithromycin shared, at 4°C, the three smallest D-values ($<1.2 \times 10^{-6}$

cm^2/s), with the next closest at 1.5×10^{-6} cm^2/s, consistent with their large macrolide structures (>700 Da). Over the 18°C temperature range, D for all compounds increased consistently by an average factor of 2.2±0.2, or roughly 12% per degree. Thus, temperature-specific sampling rates, a parameter rarely considered in calibration studies, are required. Our empirical D-T relationships (Table B5) allow calculation of D at the temperature of the study system, removing uncertainty associated with fluctuating water temperatures during deployment. Therefore, we recommend deploying samplers with continuous temperature loggers to account accurately for changes in D over the deployment period.

Most studies employing DGT samplers for metals (Scally et al., 2006; Zhang and Davison, 1995) or o-DGT for polar organics (Chen et al., 2013) use *Equation 3.5* to calculate D as a function of temperature, based on a measured D at 25°C:

$$LogD_T = \frac{1.37023(T-25) + 0.000836(T-25)^2}{109 + T} + Log\frac{D_{298K}(273+T)}{298}$$

Equation 3.5

While has been used extensively for aqueous ionic species (Li and Gregory, 1974; Scally et al., 2006; Zhang and Davison, 1995), part of our impetus for measuring D at multiple temperatures was to validate this relationship for polar organic compounds. Although *Equation 3.5* requires D_{298K} to predict D_T, our measured value at 23°C was used instead, potentially biasing our calculations slightly. Predicted D_T (Table B6) at 5 and 13°C were on average within 20% of measured D (relative error), suggesting that this relationship is valid for estimating D_T.

All three diffusion experiments were conducted at pH 5.5. Consideration of pH as it relates to diffusion was not necessary with the target analytes studied here. While metals can exhibit charge effects due to Donnan potentials forming between gel and solution (Davison and Zhang, 2012), the charge density of these analytes when (de)protonated is very small compared to that of metals, and thus not expected to be an issue. Given that D is largely size-dependent, the relatively large size (>200 Da) of the target analytes should not affect D if only an acidic H atom is gained or lost. Chen et al. (2012) showed no statistically significant difference between D measured at pH 5, 7, and 9 for sulfamethoxazole, further supporting our assertion that D is not a function of pH.

3.4.2.2 Modeled D

The experimentally measured data were also compared to estimated D_w values. For unrestricted/open type hydrogels (e.g., pure agarose), D for metals is comparable between water and hydrogel (Zhang and Davison, 1999). Agarose gels have 97% (our work, data not shown) to 98% water content (Zhang and Davison, 1999), resulting in measured D in agarose for Cd and Cu within 97% of D_w (Li and Gregory, 1974; Zhang and Davison, 1999). However, modelling D for pharmaceuticals and pesticides is inherently more uncertain given their complex molecular structures, in many cases including multiple ring systems and functional groups. For example, a smaller fulvic acid structure (2400 Da) had a D in agarose of 78% that of D_w, while D of a much larger humic acid structure (16,500 Da) was 57% of D_w (Zhang and Davison, 1999). Although sizes and structural complexities of humic substances are far greater than even our

108

largest target analyte (≈800 Da), this example can provide some insight into the challenges involved with modeling molecular diffusion in agarose hydrogels.

D was modeled using both the Hayduk-Laudie model (Hayduk and Laudie, 1974) (*Equation 3.6*) and Archie's law (*Equation 3.7*), the latter of which was previously used for predictions (Chen et al., 2013):

$$D_w(cm^2/s) \approx \frac{1.326 \times 10^{-4}}{\eta^{1.14}V^{0.589}}$$

<div align="right">*Equation 3.6*</div>

where η is the water viscosity (centipoise) and V the molar volume (cm^3/mol). The latter were determined according to the diffusion volumes from Fuller et al. (1966) optimized from the LeBas method (Schwarzenbach et al., 2005b). Archie's Law relates aqueous diffusion to the effective diffusion in a medium with a characteristic porosity (ε) and Archie's Law exponent (m). If a spherical model is assumed (Zhang and Davison, 1999) then Archie's Law can be stated as (Chen et al., 2013):

$$D_w(cm^2/s) \approx \frac{3.3 \times 10^{-5}\varepsilon^m}{\sqrt[3]{M}}$$

<div align="right">*Equation 3.7*</div>

where M is the molecular weight. Values of 0.98 and 2 for ε and m, respectively, were taken from Chen *et al.* for 1.5% agarose diffusive gels (Chen et al., 2013). These values are estimates, as values for agarose hydrogels are not available. Nonetheless, given that the porosity in these gels is large, the factor by which Archie's Law adjusts D_w is small. Additionally, Zhang and Davison (1999) reported an agarose pore size > 20 nm (radius), significantly larger than the molecules studied here (<< 1 nm), suggesting that diffusing molecules should not be sterically hindered by the hydrogels.

Both models (Figure B6) generally appear to overestimate D. Archie's Law estimates D to within, on average, a relative error of 27% and a range of 4-60%, which is somewhat better than the 33% error and a 2-72% range for the Hayduk-Laudie model. A complete discussion regarding the use of modelled D for determination of o-DGT sampling rates can be found below, using estimates from Archie's law as example.

3.4.3 o-DGT Calibration

3.4.3.1 Water Concentrations

Water concentrations during the calibration study were constant for all compounds (Figure B8). For most analytes, our target concentration of ≈2 µg/L is a concentration above that expected and measured in agricultural and sewage impacted systems (Bartelt-Hunt et al., 2011; Carlson et al., 2013a; Jacquet et al., 2012). For some compounds (e.g., β-blockers in sewage effluent), 2 µg/L may reflect the 95th-centile of environmentally relevant exposures (Brown et al., 2015). Regardless, exposures at 2 µg/L tests the overall sorptive capacity of o-DGT, an important goal of this study given the much smaller size and amount of sorbent present in o-DGT compared to POCIS. In addition, exposure at such a concentration provides an idea of appropriate deployment times to ensure linear kinetic sampling.

3.4.3.2 Sampler Uptake

Unlike most hydrophobic passive samplers that can utilize *in-situ* calibration approaches (e.g., PRCs) to determine kinetic versus equilibrium uptake, o-DGT must operate in its linear uptake phase to produce quantitative TWA concentrations. Kinetic uptake in o-DGT relates directly to the capacity of the binding phase, and thus must be initially assessed through laboratory calibration to inform deployment times.
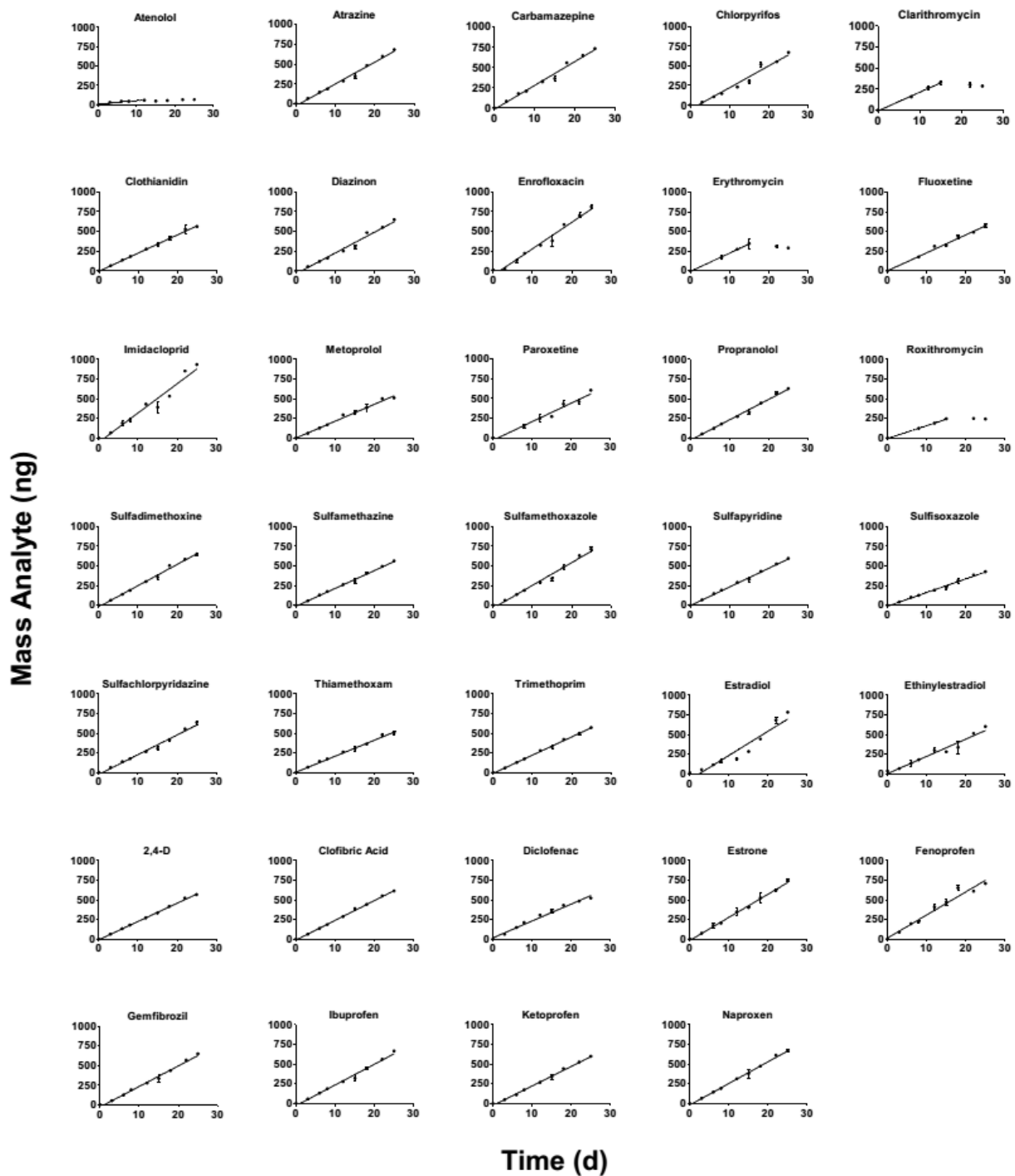
Figure 3.1: Mass accumulation of analyte into o-DGT over time. The plots shown are kinetic time-series' from the calibration experiment for all 34 analytes. Data points represent the mean of duplicate measurements ± standard deviation (error bars). Least-squares linear regressions (solid lines) of each time-series provided the slopes, which were used in determination of sampling rates. Data points for atenolol (after 12 d), clarithromycin, erythromycin, and roxithromycin (after 15 d) were excluded in the linear regressions because uptake was non-linear (saturated) beyond this point.

With the exception of four compounds (atenolol, clarithromycin, erythromycin, and roxithromycin), all analytes (Figure 3.1) displayed linear (r^2>0.9) uptake over 25 days with accumulated mass in o-DGT of 430 ng (sulfisoxazole) to 930 ng (imidacloprid), with no signs of reaching saturation or equilibrium. All three macrolide antibiotics (clarithromycin, erythromycin, and roxithromycin) displayed nearly identical uptake behaviour, reaching equilibrium at 15 d with a capacity of 250-350 ng. Taking the lowest observed sampler capacity (250 ng for roxithromycin) and a typical o-DGT R_s of 12 mL/d (Table B7), exposure under more realistic environmental concentrations (<200 ng/L) (Bartelt-Hunt et al., 2011; Carlson et al., 2013a; Jacquet et al., 2012), would require >100 d to saturate o-DGT. However, in natural waters, interfering species (e.g., DOM) will likely reduce the overall capacity of o-DGT. Thus, we suggest 2-4 weeks as an ideal deployment time to ensure kinetic uptake, even in the case of extreme field conditions that may decrease capacity further (e.g., biofouling, see Figure B9). This sampling time is typical for many applications of polar PSDs (Bartelt-Hunt et al., 2011; Carlson et al., 2013a; Jacquet et al., 2012).

3.4.3.3 *Experimental Sampling Rates*

Experimental-R_s for each analyte were determined from the slopes of the kinetic uptake plots (Figure 3.1) based on *Equation 3.8*:

$$M_{DGT} = R_s C_w t$$

Equation 3.8

The variation in R_s for o-DGT is smaller (Table B7) than for POCIS R_s, which has a general range of 50-900 mL/d (Harman et al., 2012). The smaller R_s can be largely attributed to the much smaller exposed surface area for o-DGT (3.1 cm^2) compared to

POCIS ($\approx$42 cm^2), suggesting that, if detection limits were an issue, scaling up the size of o-DGT could offer a potential solution. Experimental sampling rates were also compared to those based on D (*Equation 3.9*):

$$R_S = \frac{DA}{\Delta g}$$

Equation 3.9

Both measured- (Table B5, 23°C) and modeled-D (Figure B6) were used to determine how well D could be used to calibrate o-DGT uptake, and if it was feasible to predict R$_s$ (Figure 3.2, Table B7) based on modelled D-values to avoid experimental calibration altogether. The assumption that the DBL negligibly affects resistance to mass transfer compared to the diffusive gel (i.e., *Δg >> δ*) is fundamental to *Equation 3.1* and *3.8*; the validity of which may be tested through a comparison between sampling rates determined experimentally (E-R$_s$) and those estimated with measured (D-R$_s$) and modeled (M-R$_s$) diffusion coefficients, at consistent temperature. Good agreement is observed (at 23°C) between E-R$_s$ and D-R$_s$ (Figure 3.2, Table B7), with an average relative error of 20% across all analytes. These data strongly suggest that diffusion-based R$_s$ can be used accurately to estimate TWA water concentrations (*C$_{DGT}$*). Using D to calibrate o-DGT avoids the need for laborious sampler calibration experiments, currently a non-trivial requirement for determining sampling rates for polar PSDs (Harman et al., 2012; Shaw et al., 2009).

As discussed previously, we do not expect acid-base speciation to affect diffusion coefficients at pH values other than the one used in this study. This contrasts that of other polar PSDs, where in general, R$_s$ increased with pH for basic compounds

and decreased with pH for acidic compounds, both within 3-fold for POCIS (Li et al., 2011). While analyte affinity with HLB should change slightly due to speciation (Bäuerlein et al., 2012), some of the observed pH effects (Li et al., 2011) is likely a result of altered interaction with the PES membrane. This factor is not a concern in this study due to the elimination of PES in our o-DGT configuration. Unlike POCIS, having the diffusive gel as the rate-limiting step in o-DGT uptake should limit the effect binding affinity, as a function of pH, has on mass-transfer. This is consistent with the good agreement between D-R_s and E-R_s (Table B7), given that sorbent-analyte binding affinity has no bearing on D-R_s. That said, detailed characterization of pH effects on o-DGT uptake may be warranted as this technique further develops.

3.4.3.4 Modeled Sampling Rates

Modeled sampling rates (M-R_s) based on predicted D using Archie's Law provide good approximations of R_s, with an average relative error of 30% across all analytes (Figure 3.2, Table B7). Only six of the 34 compounds (clofibric acid, 2,4-D, diclofenac, metoprolol, paroxetine, thiamethoxam) have relative errors >50% compared to E-R_s. While these errors may be greater than desired for certain applications (e.g., exposure assessment for regulatory purposes), the small uncertainty compared to that inherent in POCIS (Poulier et al., 2014) coupled with the convenience of being able to model R_s will likely make this a powerful tool for end-users. Accordingly, o-DGT could serve as an ideal screening tool for emerging trace-level contaminants, for which chemical standards may not be commercially available, and thus lack calibrated sampling rate data with other polar PSDs (e.g., POCIS or Chemcatcher®). Modelled D-R_s for o-DGT could provide semi-quantitative concentration data for contaminants such

as pharmaceutical metabolites (Brown and Wong, 2015) or new chemicals in commerce (e.g., emerging industrial chemicals) (Howard and Muir, 2011, 2010) where detection by traditional grab sampling is insufficient or inconvenient.

Similar attempts at modelling POCIS R_s have largely focused on correlation with K_{ow}, and have been met with very limited success (Arditsoglou and Voutsa, 2008; Bartelt-Hunt et al., 2011; Morin et al., 2012), with any observed relationships applying to only small subsets of closely related analytes (e.g., antidepressants, β-blockers, hormones) (Li et al., 2010a; Macleod et al., 2007; Morin et al., 2013; Togola and Budzinski, 2007). While a very recent attempt at *in silico* predictions of POCIS sampling rates show some promise, these remain in their infancy and are not well established (Miller et al., 2016). This limits the determination of POCIS R_s to full-scale calibration experiments. Our results support the adoption of o-DGT as it offers simple calibration through measured diffusion based-R_s or modelled-R_s, drastically increasing the ease-of-use and applicability of the passive sampling technique for polar organic contaminants. That said, further work is required to better characterize and potentially improve upon our modeling efforts.
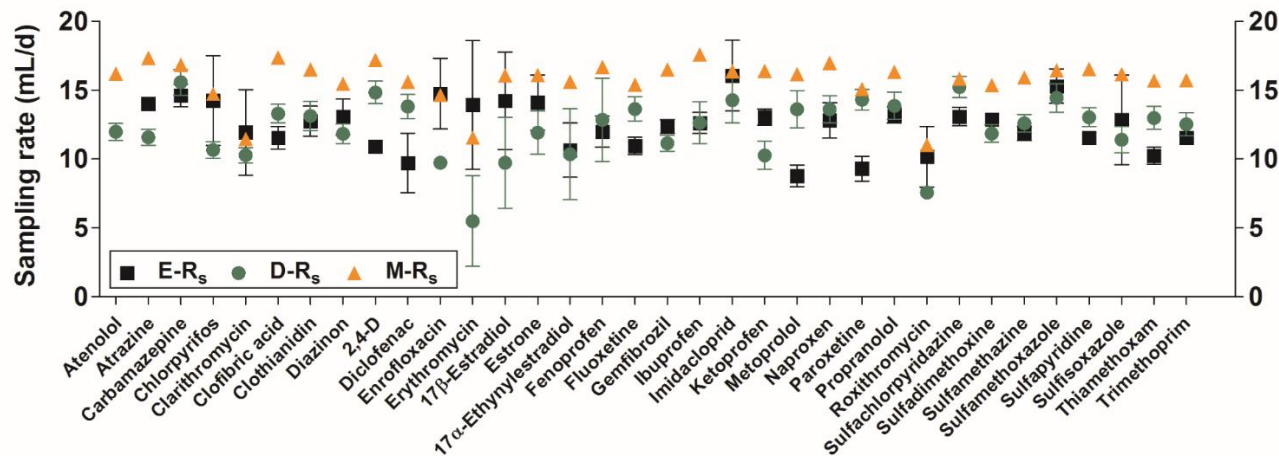
Figure 3.2: Sampling rates (R_s – mL/d) for each analyte determined experimentally (E) by sampler calibration and compared to calculated R_s based on measured diffusion (D) coefficients (23 °C) and modelled (M) D using Archie's Law (Equation 3.7). Error bars represent the propagation of uncertainties in the calibration (E-R_s) and diffusion (D-R_s) experiments.
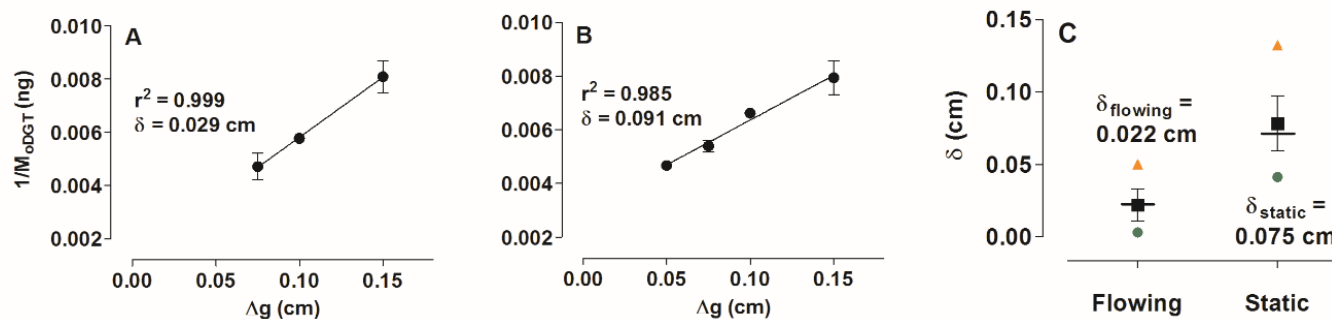
Figure 3.3: Diffusive boundary layer thickness (δ) determined using Equation 3.4, for thiamethoxam as an example, under flowing (A) and static (B) conditions. A plot of reciprocal mass (accumulated in o-DGT) as a function of diffusive gel thickness (Δg) provides the slope and y-intercept to calculate δ. Plot C shows the median δ (horizontal line) of all compounds that produced linear plots in A and B (r^2 values > 0.9 and positive y-intercepts, n=29). In plot C, the horizontal lines, black squares and errors bars represent the median, mean, and standard deviation of the estimated δ, respectively. The green circles are the measured minimum and orange triangles are the measured maximum for each δ data set (flowing and static).

3.4.4 Diffusive Boundary Layer (DBL)

Boundary layer experiments under both low-flowing (2.4 cm/s) and static conditions determined, respectively, a typical and worst-case-scenario boundary layer thickness for o-DGT applications (Figure 3.3, Table B8). This allowed for estimates of uncertainty in ignoring the DBL and using *Equation 3.1* for estimating water concentrations. Theoretically, the boundary layer thickness should decrease with increasing flow rate. However, no appreciable decrease in δ generally occurs above a linear flow velocity of $\approx$ 2 cm/s; equivalent to a slow-moving stream or river (Gimpel et al., 2001). The range in measured δ (Figure 3.3, Table B8) is not uncommon with these types of DBL experiments (Uher et al., 2013), and likely the cumulative result of experimental uncertainties (e.g., varying exposure concentrations between analytes, Figure B8) and inherent uncertainties of *Equation 3.4*. While the relative standard deviation for the flowing and static δ were within reason (50 and 25% respectively), to avoid undue bias by min and max values the median was taken as the accepted δ.

Under low-flowing conditions (2.4 cm/s in the calibration experiment) δ = 0.022±0.011 cm (average r^2 = 0.98 for linear plots of *Equation 3.4*, n = 29) agrees very well with previous measurements of δ = 0.023 cm for a suite of antibiotics in wastewater influent (Chen et al., 2013), and δ = 0.023-0.024 cm for metals in well-stirred solutions (Scally et al., 2003; Warnken et al., 2006). Additionally, δ decreased significantly for metals from static conditions to minimal stirring and remained stable as the stirring rate increased (δ = 0.025 cm at 50 and 400 rpm) (Uher et al., 2013), suggesting that a δ $\approx$ 0.022-0.024 should not change significantly under typical flow conditions.

In our static DBL experiment, δ increased significantly (unpaired two-tailed t-test, P<0.0001) from 0.022±0.011 to 0.075±0.019 cm (average r^2 = 0.96, n = 29), a value falling between previous estimates of 0.044 to 0.15 cm for metals in unstirred solutions (Uher et al., 2013; Warnken et al., 2006). While static systems may present challenges from formation of exceptionally large boundary layers, above a threshold flow rate of ≈2 cm/s, δ decreases to ≈0.023 cm (Chen et al., 2013; Scally et al., 2003; Uher et al., 2013; Warnken et al., 2006) and *Equation 3.1* can be applied without introducing significant errors into concentration estimates. For example, with a 1 mm diffusive gel (used throughout this study), ignoring the DBL (assuming δ = 0.023 cm) would underestimate concentrations by ≈20%, generally well within acceptable errors when considering environmental measurements of this type. However, including δ ≈ 0.020-0.025 cm in C_{DGT} calculations (e.g., using *Equation 3.2*) will largely eliminate this source of error in most dynamic surface waters, and is recommended. Application of a δ = 0.023 cm for o-DGT field measurements is demonstrated below in our field demonstration.

3.4.5 Field Demonstration

The o-DGT samplers were tested in a tertiary sewage lagoon (treatment plant intake – *influent*), final discharge effluent (leaving the treatment plant – *final effluent*), and at a site upstream of effluent release on Little Playgreen Lake, MB, to demonstrate the sampler's ability to estimate TWA water concentrations in comparison to POCIS and grab samples. Samplers were visually fouled after the 21d deployment, especially in the influent and final effluent sites (Figure B9). No analytes were detected in the fouled diffusive gels (data not shown), demonstrating that the biofilm formed on the diffusive

gel did not sequester analytes itself. TWA concentrations from o-DGT were determined using D-R_s at the temperature of the final effluent site (21±1°C, 21d average) based on data from Table B5 and an assumed δ = 0.023 cm (Δg + δ = 0.123 cm). Sampling rates used for POCIS are provided in Appendix B (Table B9). A total of six analytes were detected in the final effluent and influent sites by all three sampling techniques, while just o-DGT and grab samples measured a seventh analyte (naproxen) (Figure 3.4 and Figure B10). Other target analytes were measured but were below the LOQ (data not shown). The number of analytes detected here likely relates to the lower usage rates of pharmaceuticals in a small northern community of this type (population ≈7,000), and is consistent with the findings of a recent study using POCIS to measure pharmaceuticals in Cambridge Bay, Nunavut, Canada (69°N, population ≈1,500), where only 6 of 28 target analytes were detected (Chaves-Barquero et al., 2016).
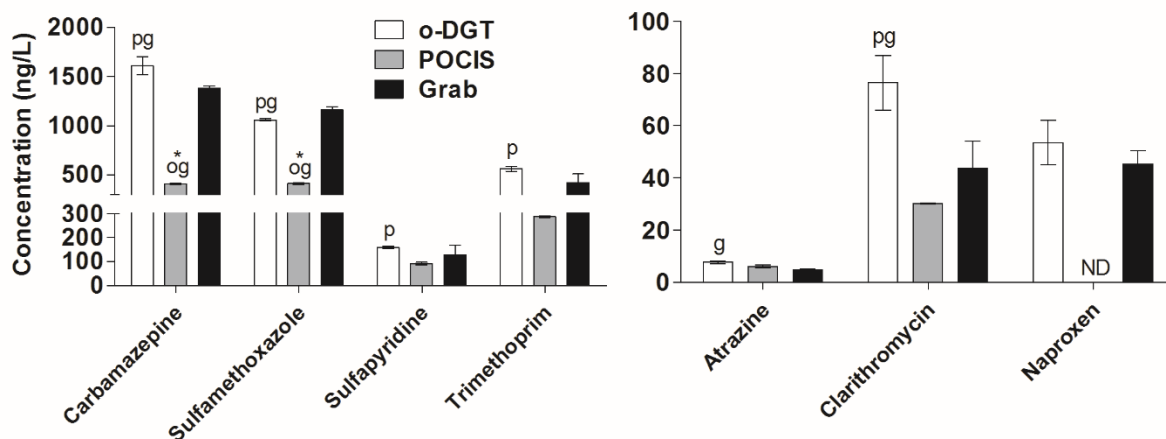
*Figure 3.4: Concentration data as measured by o-DGT, POCIS, and grab samples at the final effluent site of a wastewater treatment plant in the northern Manitoban community of Norway House Cree Nation, Canada. Plots are split by high and low concentration compounds based on y-axis scales. Bars represent the mean ± standard deviation of triplicate o-DGT samples, duplicate POCIS samples, and two sets of triplicate grab samples taken on deployment and 21 days later upon retrieval. Statistical differences between sampling techniques were tested using a one-way ANOVA with a Tukey post-hoc test at 95% confidence (α = 0.05). Letters above the bars represent statistical difference from o-DGT (o), POCIS (p), and grab (g) samples. ND = not detected. *POCIS extracts for carbamazepine and sulfamethoxazole were outside of the calibration range.*

Atrazine was the single compound detected at the upstream site, showing relatively good agreement between o-DGT, grab sample, and POCIS measurements (7.3, 6.5, and 5.3 ng/L respectively). This demonstrates that o-DGT is capable of measuring these contaminants in open surface water scenarios (despite the small o-DGT R_s), where concentrations are typically orders of magnitude lower than wastewaters or effluent-impacted downstream sites.

Although a time-series was not established over the deployment to confirm linear uptake by o-DGT, the fact that measurements agreed well with grab samples, differing on average by 25% and maximally by 55% (for clarithromycin) is a good indication of linear uptake, especially considering that some of this variation is likely a direct result of grab samples being taken only twice over the 21 d deployment period (beginning and end). However, given the small population this treatment plant serves and the fact that a large majority of the homes in the community are not piped in, we do not expect constant inputs (toilet flushing, shower use, laundry, dish washing, etc.) that are thought to be largely responsible for temporal fluctuations in levels of pharmaceuticals and personal care products in wastewater (Ort et al., 2010). This may, in part, be the reason we see such small variation between the two sets of grab samples taken 21 days apart (for all seven compounds detected: average relative standard deviation = 14%; range = 1-30%, see Figure 3.4). That said, comparisons to the grab sampling data done here should be treated as semi-quantitative, given the lack of truly time-integrative discrete sampling over the three week deployment.

Accumulated mass of detected analytes reached maximally 43% (for carbamazepine) of the minimum laboratory capacity observed in the calibration

experiment (Figure 3.1), suggesting that uptake was well within the linear uptake range of o-DGT. POCIS compared to both o-DGT and grab samples appeared systematically to underestimate concentrations (Figure 3.4 and Figure B10), and differed on average by 50% and 40%, respectively. This observation suggests that factors such as boundary layer may have affected the POCIS measurements.

A boundary layer experiment was conducted *in situ* at the final effluent site to investigate and better understand these effects on o-DGT and POCIS. Three sets of duplicate o-DGT with 0.075, 0.10, and 0.15 cm diffusive gels were deployed. All analytes detected by o-DGT except for clarithromycin (omitted due to poor linearity, $r^2 =$ 0.68) were included in the determination of the DBL (Table B10, Figure B11). The median δ = 0.043±0.039 cm (average r^2 = 0.92, n = 7) falls in between our flowing- (0.022 cm) and static- (0.075 cm) δ determined in the laboratory. The effluent discharge rate of 9 L/s, or 6.8 cm/s linear velocity based on the dimensions of the release channel where the samplers were deployed, is nearly 3-fold greater than the 2.4 cm/s used in the flowing-DBL laboratory experiment. However, the greater field-δ is not surprising, given the complex matrix and significant fouling observed on the exterior of the samplers (Figure B9).

Despite the presence of the biofilm, no evidence for degradation of the diffusive film was observed, as evident by the greater field-δ found. Our field-δ estimate includes all other external resistances to mass transfer, i.e.*,* both the DBL and biofilm. Assuming the δ = 0.043 cm applies equally to POCIS, the underestimation of TWA concentrations by POCIS can be largely explained. For example, application of a Δg = 0.045 cm to the TWA calculations for POCIS would bring the sulfamethoxazole and carbamazepine

concentrations above 1000 ng/L, much closer to those measured by o-DGT and grab samples (Figure 3.4 and Figure B10). This said, further investigation of the exact effect biofouling and DBL have on sampler uptake, for both o-DGT and POCIS, is warranted. Additionally, o-DGT should be tested in other systems to understand how biofouling may change based on the field conditions. This field evaluation demonstrates the utility of the o-DGT design in limiting the influence of boundary layer on uptake, determining temperature-specific sampling rates, estimating the DBL *in situ*, and ultimately producing accurate TWA concentration estimates.

3.5 CONCLUSIONS

This work has established the utility of o-DGT, without a PES membrane, as an effective monitoring tool offering three main advantages over current polar-PSDs: first, reduced flow rate influence on sampler uptake, second, use of temperature-specific sampling rates, and third, a predictable diffusion-based model for simple determination of sampling rates. These factors greatly increase o-DGT's applicability and ease-of-use by minimizing or eliminating the extent of calibration required for the end-user. Measured diffusion coefficients provided strong empirical D-T relationships for more accurate temperature consideration during deployment. Furthermore, modelled diffusion coefficients can predict sampling rates to within 30% (average relative error for all analytes) of measured R_s, providing the capability to use o-DGT for screening new and emerging contaminants, or for measuring compounds for which calibration has not been conducted. Deployments of three weeks in sewage influent and effluent provided accurate TWA concentration estimates, indicating that sampler capacity under typical deployment times (2-4 weeks) and conditions (impacted surface waters) should act as a

near-infinite sink (i.e., linear uptake). Use of 0.075-0.1 cm diffusive gels and application

of a 0.023 cm boundary layer is recommended for field applications to minimize/account

for flow rate and biofouling influence on o-DGT uptake. As a monitoring tool, o-DGT

provides a cost effective and widely applicable sampler that can accurately account for

the influence of important environmental factors (temperature and flow rate) affecting

the reliability of current polar PSDs.

CHAPTER 4

4. FIELD EVALUATION AND *IN-SITU* STRESS-TESTING OF THE ORGANIC-DIFFUSIVE GRADIENTS IN THIN-FILMS PASSIVE SAMPLER

A version of this chapter has been submitted as:

Challis, J.K., Stroski, K.M., Luong, K.H., Hanson, M.L., Wong, C.S., **2018.** Field Evaluation and In-Situ Stress-Testing of the Organic-Diffusive Gradients in Thin-Films Passive Sampler. *Submitted to Environmental Science & Technology.*

4.1 ABSTRACT

The organic-diffusive gradients in thin-films (o-DGT) technique has emerged as a promising aquatic passive sampler that addresses many of the challenges associated with current sampling tools used for measurement of polar organic contaminants. This study represents the first comprehensive field evaluation of the o-DGT in natural surface waters, across a wide suite of polar pharmaceuticals and pesticides. We explore the utility and limitations of o-DGT as a quantitative measurement tool compared to grab sampling and the polar organic chemical integrative sampler (POCIS) across four connected agricultural and wastewater-influenced freshwater systems spanning 600 km from the U.S. border to northern Manitoba, Canada. Overall, the suite of analytes detected with o-DGT and POCIS were similar. Concentrations in water estimated using o-DGT were greater than concentrations estimated from POCIS in 71 of 80 paired observations, and on average, the estimates from o-DGT were 2.3-fold higher than estimates from POCIS. Grab sample concentrations suggested that the systematic underestimation with POCIS were largely a result of sampling rate variation related to flow-rate and boundary-layer effects, an issue reported consistently in the POCIS literature. These comprehensive measurements in an agriculturally-influenced fast-flowing river, long-term sampling (>40 days) in a large dilute lake system, deployments in wastewaters, and under-ice at near-freezing temperatures represent effective stress-testing of o-DGT under representative and challenging conditions. Overall, its strong performance and improved accuracy over POCIS supports its use as a robust, quantitative, and sensitive measurement tool for polar organic chemicals in aquatic systems.

4.2 INTRODUCTION

Passive sampling is an integral research and regulatory tool, providing valuable

data for a variety of applications to characterize chemical presence, fluxes,

bioavailability, and partitioning across environmental compartments (Kot-Wasik et al.,

2007; Vrana et al., 2005). The polar organic chemical integrative sampler (POCIS)

represents the most common aquatic passive sampling device for polar organic

contaminants. Its wide-scale adoption in many research (Carlson et al., 2013a) and

government (Van Metre et al., 2017) laboratories can be attributed to the large body of

supporting literature, including calibration for over 300 organic contaminants (Harman et

al., 2012). Yet, significant uncertainties with POCIS have been identified (Guibal et al.,

2015a; Li et al., 2011, 2010b; Poulier et al., 2014; Vermeirssen et al., 2012) relating to

application of laboratory-derived POCIS sampling rates *in-situ* (Fauvelle et al., 2017;

Harman et al., 2011). This issue has largely been attributed to the fact that mass-

transfer into POCIS can be highly dependent on environmental conditions such as flow-

rate and temperature (Harman et al., 2012). For example, in situations where POCIS

uptake is boundary-layer controlled, *in-situ* flow-rate conditions can lead to significant

variation in sampling rates (Harman et al., 2012). These and other challenges with

POCIS have spurred the development of alternative passive sampling tools to address

these issues.

Recently, the organic-diffusive gradients in thin-films (o-DGT) passive sampler has

emerged as a promising quantitative sampling tool for polar organic contaminants in

water and sediments (Belles et al., 2017; Chen et al., 2015, 2014, 2013, 2012; Fauvelle

et al., 2015; Guibal et al., 2017; Stroski et al., 2018; Zheng et al., 2015). A large reason

for this success stems from o-DGT uptake rates being largely independent of water flow-rate as demonstrated in Chapter 3 and elsewhere (Davison and Zhang, 2012). The o-DGT configuration used here utilizes an agarose diffusive hydrogel as the outer membrane of the sampler, forgoing the thin polyethersulfone (PES) outer protective membrane used commonly with other o-DGT variants (Chen et al., 2013; Fauvelle et al., 2015; Zheng et al., 2015) and polar passive sampling devices in general (e.g., POCIS and Chemcatcher) (Harman et al., 2012; Shaw and Mueller, 2009). By avoiding the PES membrane, mass transfer in o-DGT is isolated to the diffusive gel, allowing the use of laboratory measured diffusion coefficients, at temperature, to accurately predict *in-situ* sampling rates, greatly increasing the applicability of this sampler.

To date, research into o-DGT has largely focused on laboratory development and calibration (Belles et al., 2017; Chen et al., 2013, 2012; Guibal et al., 2017), with limited field evaluations conducted mostly in raw or treated wastewaters (Chen et al., 2015; 2013). With elevated concentrations of pharmaceuticals expected in wastewaters, these studies failed to test o-DGT detection limits under natural field conditions. Given smaller exposed surface area (3.1 cm^2 versus 42 cm^2) and thicker outer membrane (i.e., the diffusive gel), o-DGT sampling rates are generally 5-20 times smaller than POCIS (Table B7; Harman et al., 2012), making detection limits in natural surface waters a critical issue yet to be addressed. Additionally, a full-scale field evaluation under a variety of challenging field conditions is greatly needed.

This work fills these gaps by characterizing the performance and utility of o-DGT in a variety of surface waters, specifically addressing durability under harsh aquatic conditions and scenarios where significant downstream dilution is relevant. A total of

four distinct, hydrologically connected systems within Lake Winnipeg and Nelson River watershed were studied with three major objectives. First, we assess the performance and durability of o-DGT through deployments in a small creek and a large fast-flowing river receiving major agricultural and municipal inputs, in a large open-water lake removed from point-source contamination representing significant contaminant dilution and subject to turbulent currents and wave-action, and under ice in extreme temperature conditions. Second, we compare o-DGT performance with that of POCIS to understand advantages and limitations of the two techniques. Finally, we use the resulting data to better understand the transport, sources, and residence of atrazine and carbamazepine throughout this large dynamic watershed as a case-study for using o-DGT to characterize fate processes of polar organic contaminants in aquatic systems.

4.3 MATERIALS AND METHODS

4.3.1 Site Details

4.3.1.1 Overview

In total, 14 sampling sites were monitored using o-DGT within the Red River, Lake Winnipeg, and Nelson River watersheds (Figure 4.1 and Figure C1-C2). Samplers were deployed in triplicate on stainless steel spindles inside stainless steel protective cages (30 cm high × 16 cm wide) (Environmental Sampling Technologies, St. Joseph, MO) equipped with HOBO Water Temp Pro v2 loggers (two readings per hour, ±0.2°C accuracy) (Hoskin Scientific LTD., Burlington, ON). Cages were secured at river/lake banks on trees (Red and Assiniboine River, Nelson River), bridges (Dead Horse Creek), buoys (Lake Winnipeg), and iced lake surfaces (Nelson River) using 3/16 inch stainless steel aircraft cable. Further site specific details are below and in Appendix C.

128

4.3.1.2 Red River

Five sites were studied along the Red River from the U.S.-Canada border to the River's mouth into Lake Winnipeg, along with two sites on tributaries: one in the Assiniboine River, and one in Dead Horse Creek (DHC) (Figure C1). These three fluvial systems receive agricultural and municipal inputs (Carlson et al., 2013a; Rawn et al., 1999). Sampling was performed continuously every 2-3 weeks between April and October, 2016 (Table C1). With the exception of DHC, this same collection of sites was used for POCIS measurements in 2014 and 2015 in Chapter 2, and thus were chosen opportunistically for comparative purposes. Temperatures across all these sites remained relatively constant over a given sampling period, ranging from 7-9°C in April, to 22-24°C in late July, to 12-14°C in October. Further information regarding hydrology and surrounding land-use patterns are in Chapter 2.

4.3.1.3 Lake Winnipeg

Lake Winnipeg (Figure 4.1) is the tenth largest freshwater lake in the world, and the third largest in Canada by surface area (24,000 km^2). Red River is the 3rd largest riverine input into Lake Winnipeg by volume, at approximately 16% of total inflow, and is the largest source of nutrients to the Lake (Environment Canada, 2011). Measurements in Lake Winnipeg were conducted at three locations (south basin, narrows, and north basin) using POCIS in 2014 and 2015 and o-DGT in 2016 (Table C2). Temperatures were only taken in 2016 for the o-DGT deployments and ranged from 18°C in the south basin and narrows to 15°C in the north basin.

Figure 4.1: Overview of the Red River, Lake Winnipeg, and Nelson River watersheds studied in this work, with selected sampling sites shown (brown triangles). Sampling sites on map are as follows: Emerson (EM) and Breezy Point (BP) on the Red River, Headingley (HD) on the Assiniboine River, and Dead Horse Creek (DHC); South basin (SB), narrows (NAR), and north basin (NB) on Lake Winnipeg; and Norway House Cree Nation (NHCN) on the Nelson River. Complete sampling site details of the Red River (south box) and Nelson River systems (north box) are provided in smaller scale maps (Figure C1 and C2). Source material for this map includes information licensed under the Open Government Licence – Canada, the U.S. Geological Survey, and NASA/JPL-Caltech.

4.3.1.4 Nelson River

The headwaters of the Nelson River drains Lake Winnipeg at the northeast edge of the north basin to form Playgreen Lake, where it splits into the east and west Nelson River channels, eventually joining again at Cross Lake. The east channel flows through the Jack River and Little Playgreen Lake, where the community of Norway

House Cree Nation (NHCN) is located, and where sampling took place. Sampling was designed to characterize inputs from the local wastewater treatment plant (WWTP) that serves ≈7000 people and releases into Little Playgreen Lake. Sampling took place in the summer of 2014 and 2015 and winter 2016 (Table C3, Figure C2). A subset of the 2015 NHCN data is presented in Chapter 3 as the field evaluation for the initial o-DGT development and calibration, and therefore will not be discussed here. Discussion will focus on the o-DGT deployments under ice on Little Playgreen Lake in 2016, where the average water temperatures were ≈0.1°C.

4.3.2 Sampling Details

4.3.2.1 Quality Assurance/Quality Control (QA/QC)

Laboratory and field blanks for o-DGT, POCIS, and grab samples were extracted and analyzed alongside each set of environmental samples. Field blanks were left open to the atmosphere during retrieval and deployment of passive samplers. For all our analytes, levels observed in lab and field blanks were negligible. Some retrieved passive samplers were stored by freezing (-20°C) for 1-3 weeks until extraction, which did not result in analyte losses based on the results in Chapter 6 and a previous study (Carlson et al., 2013b)

4.3.2.2 o-DGT

Complete details of development, optimization, assembly, and extraction of o-DGT are in Chapter 3. Briefly, o-DGT samplers were constructed using two layered gels made of 1.5% agarose (molecular biology grade, Sigma-Aldrich, Oakville, ON): A 0.75 mm, 25 mg Waters OASIS™ HLB binding gel and a 0.75 mm outer diffusive gel. Binding gels were casted on their side (horizontally) to allow the HLB sorbent to settle to one

side of the gel. The 0.75 mm binding gel was placed on the standard plastic DGT base (HLB side face-up) with the diffusive gel layered on top, and sealed with the standard DGT cap (exposed area = 3.1 cm^2). Of particular note with this configuration is the exclusion of the outer polyethersulfone (PES) membrane used in POCIS and other current o-DGT designs (Chen et al., 2015; 2013).

Using the mass of analyte on sampler (M_{DGT}), thickness of the diffusive gel layer (Δg), exposed area (A), deployment time (t), and analyte diffusion coefficient through the diffusive gel (D), o-DGT time-weighted average (TWA) water concentrations (C_{TWA}) were calculated using *Equation 3.1*. The boundary layer thickness (δ) is excluded from *Equation 3.1* because flow-rate effects on o-DGT uptake are assumed to be negligible compared to the thickness of the diffusive gels, as shown by experiment (Chapter 3). Temperature-specific diffusion coefficients were determined using the D-T empirical relationships established in Chapter 3. D was calculated based on the average *in-situ* water temperature over each deployment.

4.3.2.3 POCIS

Preparation, storage, and extraction of POCIS is described in Chapter 2 and elsewhere (Carlson et al., 2013b). POCIS were constructed using 200 mg of Waters OASIS™ HLB material between PES membranes (0.1 μm pore size) (Environmental Sampling Technologies, St. Joseph, MO). Samplers were secured with two stainless steel rings for an exposed total membrane surface area of 41 cm^2. POCIS TWA water concentrations were calculated with *Equation 2.1*, using compound-specific POCIS sampling rates (R$_s$, L/day) in Table C4.

4.3.2.4 Grab Sampling

Sampling and extraction polar organics in water are described in Chapter 3 and follow protocols developed previously in our lab (Carlson et al., 2013a). Six triplicate sets of grab samples using 500 mL ashed amber glass bottles were taken at DHC between August 9-30 for comparisons with o-DGT and POCIS. Grab samplers were extracted within one day of sampling.

4.3.3 Target Chemicals and Reagents

The 34 target analytes described in Chapter 3 were analyzed for this work. Full details of the target analytes, solutions, and reagents are in Appendix B.

4.3.4 Instrumental Analysis

Analyte concentrations were determined by liquid chromatography tandem mass spectrometry (LC-MS/MS) using an Agilent (Agilent Technologies, Mississauga, ON) 1200 Series LC pump and Agilent 6410B MS/MS in electrospray ionization positive and negative mode. Complete details of chromatographic and MS/MS methods are in Chapter 3 and Appendix B.

4.3.5 Data Analysis

Prism v. 5.01 (GraphPad Software, La Jolla, CA) was used for statistical analysis. Statistical difference ($P<0.05$) between paired o-DGT and POCIS observations at Emerson and DHC were determined by a two-way ANOVA and Bonferroni post-hoc test. Comparisons between o-DGT, POCIS, and grab samples taken at DHC were compared using a one-way ANOVA and Tukey's post-hoc test. Errors in graphs and tables are presented as standard deviations of the mean, unless otherwise stated.

4.4 RESULTS AND DISCUSSION

The following discussion is presented in two parts. The first will focus strictly on the assessment of o-DGT as a quantitative measurement tool. Performance will be assessed based on analyte detections, triplicate variability, and most importantly, comparisons with POCIS and grab samples in the Red River system and its tributaries, where the largest and most comprehensive sampling campaign using o-DGT took place. Stress-testing and sampler durability will be discussed throughout within the context of the aquatic conditions (e.g., flow, temperature) unique to each system. The second part of the discussion will demonstrate the utility of the o-DGT data to understand the distribution, fate, and sources of atrazine and carbamazepine in the Lake Winnipeg and Nelson River watershed.

4.4.1 Sampler Performance

4.4.1.1 River Deployments

Six target analytes were detected by o-DGT consistently at all sites in the Red River and the two tributaries over the 2016 sampling season (Figures C3-C5 and Tables C5-C6). Five pesticides (atrazine, thiamethoxam, clothianidin, imidacloprid, 2,4-D) and one pharmaceutical (carbamazepine) were detected in 85-100% of the samples (of 53 total sampling events), ranging from 0.3-1250 ng/L. These detection frequencies are higher than would be expected for typical grab/active samples given the concentration effect associated with analyte accumulation over extended passive sampling deployments (2-3 weeks). Diazinon and chlorpyrifos were the only two target pesticides not detected, consistent with previous observations in these systems from Chapter 2. Additionally, a suite of pharmaceuticals was detected only at the North End site,

downstream of the City of Winnipeg WWTP. Concentrations measured by o-DGT ranged from <1 to 140 ng/L with an average of 16 ng/L across all six pharmaceuticals (sulfamethoxazole, sulfapyridine, metoprolol, trimethoprim, naproxen, diclofenac). Similar concentrations of sulfamethoxazole, sulfapyridine, metoprolol and trimethoprim were observed in Chapter 2 at the same sampling site using POCIS in 2014 and 2015.

Measured concentrations across all analytes ranged from 0.4 ng/L carbamazepine to 1250 ng/L atrazine, corresponding to accumulated mass on sampler of <0.05 and >300 ng respectively. For atrazine alone, accumulated mass ranged from 0.2-330 ng. The range in concentrations observed here, nearing four orders of magnitude, is not atypical for surface waters receiving agricultural and municipal inputs (Novic et al., 2017) and highlights an important feature of an effective passive sampler, namely, sufficient sensitivity and capacity to accurately measure a suite of analytes over a wide concentration range, as demonstrated here with o-DGT. Furthermore, with the exception of a few instances (discussed later) the integrity of the outer diffusive gel was generally not compromised during the 2-3 week deployments in these river systems, suggesting that using hydrogels as the outer membrane for o-DGT (i.e., no PES membrane) is a viable and recommended approach to avoid the many complications encountered with PES (Silvani et al., 2017; Vermeirssen et al., 2012). Given the nature of the studied rivers, ranging from a slow-moving shallow creek in a densely agricultural area (DHC) to a large, heavily impacted, and fast-flowing river that is prone to flooding (Red River), these observations regarding the durability of o-DGT suggest its broad applicability to similar fresh-water systems.

4.4.1.2 Direct Sampler Comparisons

Side-by-side comparisons of o-DGT and POCIS were conducted at two sites; Red River at Emerson and Dead Horse Creek (DHC). At DHC, grab sampling was also conducted 3-4 days apart over the course of a single 21-day o-DGT and POCIS deployment (August 9-30, 2016) to inform our comparisons between the two samplers (Figure 4.2 and Figure C6). Concentrations over the deployment period in DHC were in general agreement, but differed based on the groups being compared (average across all five detected analytes: $C_{o\text{-}DGT}/C_{POCIS} \approx 1.5$, $C_{grab}/C_{o\text{-}DGT} \approx 0.90$, $C_{grab}/C_{POCIS} \approx 1.3$) and on the choice of POCIS sampling rate (R_S) used to calculate the TWA concentration (*Equation 2.1*). Of the five compounds detected in DHC over this sampling period, atrazine and carbamazepine were the two compounds with multiple literature reported POCIS R_S values. For example, laboratory measured R_S for carbamazepine vary by approximately a factor of four (0.112 to 0.397 L/d) (Li et al., 2010a; Macleod et al., 2007). These variations in POCIS R_S remain a point of contention throughout this dissertation and the literature (Fauvelle et al., 2017; Harman et al., 2012). This is demonstrated in Figure 4.2 by the large variation in calculated TWA water concentrations resulting from the choice of a single R_S value, a major issue confronting POCIS end-users (Poulier et al., 2014).

It should be noted that, unless otherwise stated, POCIS concentrations reported here applied an average R_S (shown in Figure 4.2) based on the multiple individual values reported in the literature (Table C4). This approach is meant to avoid undue bias in calculated concentrations by any single R_S value. While we believe the average-R_S approach to be prudent for POCIS end-users, especially those lacking expertise with

136

passive sampling, future efforts should validate this method through a weight-of-evidence approach (Challis et al., 2014), whereby the scientific methodology used to determine each R_S value be quantitatively evaluated based upon pre-developed and validated criteria.
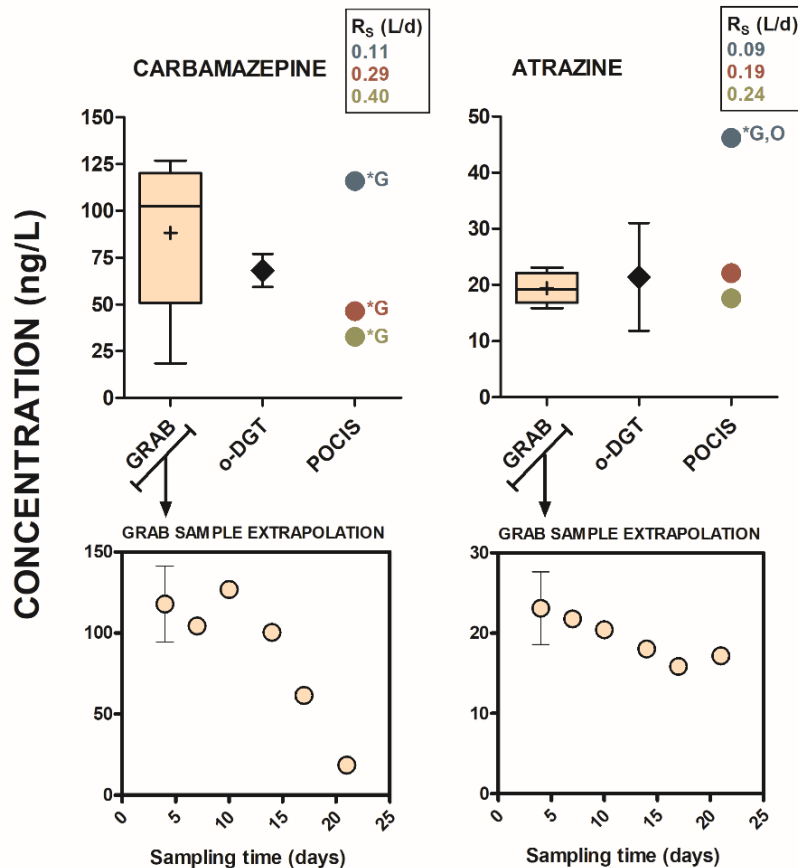
Figure 4.2: Water concentrations measured by o-DGT, POCIS, and grab sampling in DHC over 21 days from August 9-30, 2016. Six grab samples in triplicate were taken over the 21-d period. Box and whisker plots (top panel) of the six triplicate sets of grab samples represent: minimum and maximum, lower and upper quartile, median and mean (+). Extrapolation of the box and whisker plot in the bottom panel show the mean and standard deviation of each triplicate set of grab samples taken at 4, 7, 10, 14, 17, and 21 days (in most cases error bars are smaller than data point). Mean and standard deviation represent the triplicate o-DGT and POCIS data. The three POCIS data points (error bars removed for clarity) for carbamazepine and atrazine represent the TWA concentrations calculated based on the same POCIS samples but using different sampling rates (R_S – L/d). The three points correspond to the average R_S (red), largest R_S (green), and smallest R_S (blue) reported in the literature (Table C4). Thiamethoxam, clothianidin, and imidacloprid data in Figure C6. Statistical significance (P<0.05) denoted by (*) based on a one-way ANOVA and Tukey's post-hoc test. Letters beside a data point indicate that data point is statistically different from the group indicated by the letter (G=grab, O=o-DGT), e.g., *G,O indicates the POCIS concentration is statistically different from the grab sample and o-DGT mean.
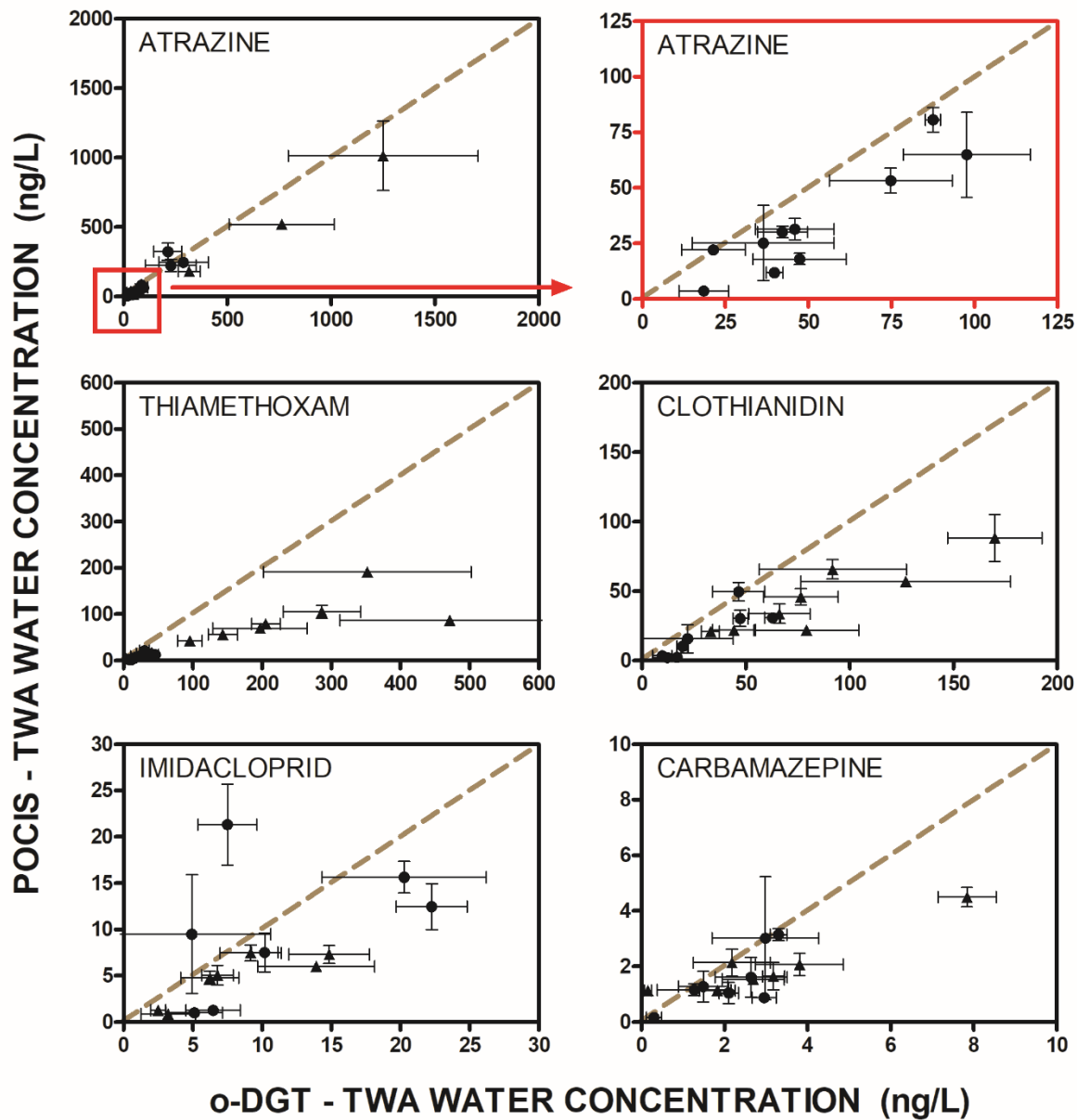
Figure 4.3: Paired o-DGT and POCIS concentrations at Emerson (circles) and DHC (triangles) (N=16) calculated using Equation 3.1 and Equation 2.1. The dashed line shows the theoretical 1:1 line of measured o-DGT and POCIS concentrations (e.g., where C_{DGT}/C_{POCIS} = 1). Each data point represents the mean ± standard deviation of triplicate o-DGT and POCIS TWA concentrations. The top panel shows atrazine over the full concentration range (left) and zoomed-in on the lower-range data points (right).

When considering all paired o-DGT and POCIS observations (Figure C7 and

Table C7) some systematic discrepancies between the two sets of samplers are

138

evident. TWA water concentrations of the five common analytes detected consistently by both samplers appear to differ systematically (Figure 4.3 and Figure C8). While only 19% (15/80) of all o-DGT measurements were statistically different from POCIS, Figure 4.3 suggests a systematic difference between the two passive samplers, with a large majority of the data points not falling along the 1:1 line. On average, o-DGT concentrations were ≈2.3-fold greater than POCIS measurements. For thiamethoxam, where the greatest discrepancy between concentrations was observed, that difference was >3-fold. The underestimation of water concentrations by POCIS has been observed in the literature, yet is seldom addressed, as discussed below.

In the initial study of o-DGT (Chapter 3) a significant underestimation (≈2-fold) by POCIS was observed when compared to paired measurements with o-DGT and grab sampling for a number of pharmaceuticals in wastewater. An *in-situ* o-DGT boundary layer thickness of ≈0.4 mm explained much of the discrepancy when applied to POCIS R_S (Chapter 3). Criquet et al. (2017) compared POCIS and 24-hour composite grab sample concentrations for a suite of pesticides and pharmaceuticals in an impacted river, and reported C_W/C_{POCIS} ratios of 2-10 for approximately 50% of their data. Less than 10% of the data had ratios ≤1 (Criquet et al., 2017). Other studies have reported similar underestimations when using POCIS (Terzopoulou and Voutsa, 2016; Van Metre et al., 2017; Zhang et al., 2008). Given this evidence, we propose that a fundamental cause of these observed discrepancies is the uncertainty in using and applying laboratory-derived POCIS R_S found in the literature (Harman et al., 2012) under field conditions, a subject of much discussion and debate in the passive sampling field (Fauvelle et al., 2017; Harman et al., 2011; Jacquet et al., 2012; Liu et al., 2013).

More specifically, the data presented here (Figure 4.3), in Chapter 3, and elsewhere (Criquet et al., 2017; Terzopoulou and Voutsa, 2016; Van Metre et al., 2017; Zhang et al., 2008) suggests this variation is specifically biased in one direction, namely, that laboratory-derived POCIS R_S are systematically greater than *in-situ* R_S, causing calculated TWA concentrations to be underestimated. This is further supported by attempts at correcting laboratory-derived R_S *in-situ* using performance reference compounds (PRCs) (Guibal et al., 2015a; Jacquet et al., 2012). For example, Guibal et al. (2015) found that TWA concentrations of pesticides calculated using PRC-corrected sampling rates increased 2- to 5-fold compared to those using laboratory-derived R_S.

4.4.1.3 Diffusive Boundary Layer

The diffusive boundary layer (DBL, δ) can be estimated *in-situ* by deploying multiple o-DGT samplers with differing diffusive gel thicknesses (*Equation 3.4*), an approach taken in Chapter 3 and elsewhere (Chen et al., 2013) and conducted here in DHC (Figure 4.4). Duplicate o-DGT samplers with 0.5, 0.75, and 1.5 mm diffusive gels were deployed in DHC for 21 days from July 19 to August 9, 2016. Using *Equation 3.4*, the data is plotted in Figure 4.4 below. An estimated median δ = 0.034 ± 0.032 cm (N=5) generally agrees well with other field-measured values for o-DGT; δ = 0.043 ± 0.039 cm (Chapter 3) and δ = 0.023 cm (Chen et al., 2013). These *in-situ* DBLs are 2-4 times thicker than POCIS membrane (PES ≈ 100 μm) (Harman et al., 2012), suggesting that in these scenarios it is likely that POCIS uptake was boundary-layer controlled while o-DGT uptake remained diffusive gel controlled. While more research is needed to delineate the exact reasons for these observed uncertainties, with the plausible mechanism described above (e.g., influence of DBL), the weight-of-evidence would

suggest that laboratory derived POCIS R_S are in fact systematically larger than *in-situ*

R_S, which would explain the observed underestimation of water concentrations here and

elsewhere (Criquet et al., 2017; Terzopoulou and Voutsa, 2016; Van Metre et al., 2017;

Zhang et al., 2008).
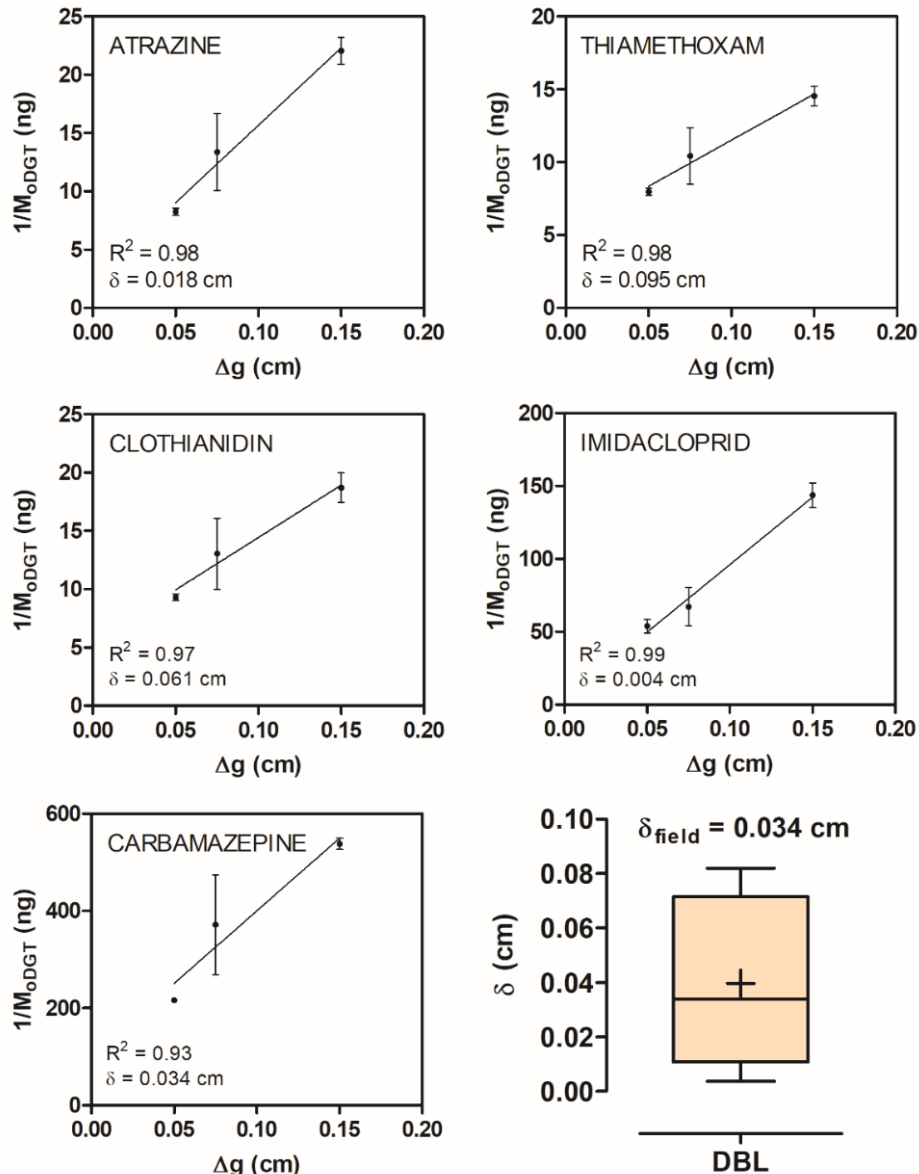
Figure 4.4: Diffusive boundary layer thickness (δ) determined using Equation 3.4 based on a plot of reciprocal mass (accumulated in o-DGT) as a function of diffusive gel thickness (Δg). The slope and y-intercept are used to calculate δ. The five detected analytes in Dead Horse Creek were used to obtain the median in-situ δ=0.034 cm (bottom right plot).

4.4.1.4 Sampler Sensitivity

Typical o-DGT sampling rates are ≈25 times less than POCIS R_S, suggesting that o-DGT sensitivity may be an issue when measuring trace level (e.g., ng/L) contaminants. However, the list of analytes detected by paired o-DGT and POCIS measurements in Red River, DHC, and Nelson River were the same. Additionally, POCIS measurements throughout Red River and Lake Winnipeg from 2014 and 2015 detected essentially the same suite of analytes as o-DGT in 2016 (e.g., Chapter 2). These observations suggest that under most surface water scenarios, o-DGT provides sufficient sensitivity to detect contaminants at single digit ng/L levels. Of course, under situations where samplers were deployed for shorter periods (e.g., <1-2 weeks) o-DGT detection limits could become an issue. Future o-DGT research is needed to characterize minimum deployment times required to provide sufficient sensitivity and accurate TWA concentrations.

One difference in analyte detections that was observed in this study between o-DGT and POCIS related to our negative mode MS analytes. Of the six o-DGT analytes detected in the Red River system at sites where both o-DGT and POCIS were deployed (Emerson, DHC), only five were measurable by POCIS. The herbicide 2,4-D was not detected using POCIS, consistent with our previous findings (Chapter 2), and caused by an apparent matrix phenomenon observed only in our POCIS samples specifically affecting our negative-mode MS method (Appendix B). In fact, all eleven negative mode analytes, many of which are known to be sampled by POCIS (Li et al., 2010a), were not quantifiable with POCIS due to the observed signal suppression, a result we attribute to the PES membrane. Given the tendency for certain analytes to bind to PES (Silvani et

al., 2017; Vermeirssen et al., 2012), extracting the membrane along with the POCIS

sorbent has been recommended to ensure optimal analyte recoveries (Silvani et al.,

2017; Vermeirssen et al., 2012). However, this practice also co-elutes unwanted

components from the PES membrane itself (e.g., polyethylene glycol compounds)

(Guibal et al., 2015a) and any environmental matrix on the PES (e.g., membrane

fouling), leading to dirtier sample extracts (Figure C9) containing known interferences

(Guibal et al., 2015a). Commercially purchased POCIS from Environmental Sampling

Technologies implement a pre-washing procedure of the PES membranes in an attempt

to remove some of these possible interferences. The POCIS used in the current study

were constructed in-house without a pre-wash of the PES membranes. This is likely the

reason that this issue is specific to our laboratory, but may be one that other

laboratories also face. Future applications of POCIS should explore potential pre-wash

strategies to alleviate this matrix issue. However, given that diffusive gels do not bind

the target analytes, demonstrated in Chapter 3, our o-DGT configuration avoids this

issue entirely by not using a PES membrane. This is evident from visually cleaner

sample matrices (Figure C9) and successful detections of negative mode analytes

(Table C9: naproxen and diclofenac). Given these and other confounding factors

(Silvani et al., 2017; Vermeirssen et al., 2012) related to the PES membrane,

implementing a pre-wash of PES or avoiding its use entirely is recommended to resolve

challenges currently associated with PES-based polar passive samplers.

4.4.1.5 Sampler Variability

      Overall, variability in triplicate measurements was greater for o-DGT compared

to POCIS, as observed in Figure 4.3 comparing the horizontal (o-DGT) and vertical

(POCIS) error bars. The average relative standard deviation (RSD) for every measured o-DGT concentration in the Red River system was 26% (N=297). For POCIS the overall average RSD was 20% (N=80). Regardless, variability with both samplers fall within expected and generally accepted thresholds for environmental measurements of this nature (Poulier et al., 2014). That said, field observations of retrieved o-DGT samplers pointed to the deployment configuration as a potential source the increased variability observed with o-DGT. All the o-DGT data presented here was acquired using the triangular POCIS spindle (Figure C10A). However, because o-DGT only has one open sampling surface, any physical impedance (e.g., the settling of particles) forming on that surface stands to impact sampler uptake greatly. On multiple occasions during sampler retrieval, a single o-DGT from a triplicate set was found fully or partially covered with particulate due to sedimentation occurring over the course of the deployment. Our repeated observations of the o-DGT housed in the triangular spindle demonstrated that the affected o-DGT surface was typically orientated away from the flow direction and thus appeared to be more susceptible to dampened flow-rate effects within the cage (Ahkola et al., 2015). This dampened water flow over the o-DGT surface allowed for greater sedimentation to occur, ultimately leading to one artificially low measurement and thus greater variability in triplicate measurements. In extreme cases, where the effected o-DGT measured zero, the value was omitted from the triplicate set (e.g., August 30, 2016 at Emerson, Table C5). In other cases, all three values were kept (e.g., June 22, 2015 at DHC, Table C5). Complete details are explained in Appendix C.

Briefly, to address this issue an improved deployment design was implemented that held all three o-DGT along the same plane, perpendicular to the long axis of the

144

cage (Figure C10E). With the samplers orientated face-down and in the same plane relative to water flow, the surfaces could remain unobstructed by settling particulate and debris. In side-by-side deployments using both configurations, average concentrations were comparable but the flat-plane orientation provided better triplicate precision (o-DGT RSD = 11% flat-plane versus 36% triangle spindle) (Table C8). Similar deployment configurations are recommended for future o-DGT applications.

Another source of variability for o-DGT resulted from possible degradation of the outer gel membrane. This occurrence was rare and site-specific in our study, however given the implications it is important to mention. On three occasions upon retrieval (twice at Breezy Point and once at North End) over the entire 2016 field season, o-DGT diffusive gels were deemed damaged (scarred surface) or in some cases completely destroyed due to aquatic insects grazing (observed upon retrieval) on the agarose gels. This prompted efforts to explore other diffusive gel materials. Stroski et al. (2018) found that polyacrylamide diffusive gels were resistant to the degradation and served as an effective alternative to agarose, especially in cases where insect grazing is expected to be a greater concern (e.g., wetlands, wastewaters). While further research is needed to determine the optimal hydrogel material for o-DGT, future applications should consider polyacrylamide as the outer diffusive gel. The observed gel degradation was independent of biofilm formation on the surface of the diffusive gels that were present on all field-deployed o-DGT. Even with extensive biofilm formation on retrieved samplers, the observed agreement between o-DGT TWA concentrations and grab sample concentrations here (Figure 4.2) and elsewhere (Chapter 3) provide indirect

evidence that biofilms have little influence on analyte uptake. However, at present a comprehensive characterization of biofilm formation on o-DGT hydrogels is lacking.

4.4.2 Lake Deployments

Samplers were deployed in Lake Winnipeg from Environment Canada weather buoys at an approximate depth of 2.5 m. Side-by-side sampler deployments were not conducted due to logistical limitations with the *MV Namao* lake surveys, making comparisons between years and among passive samplers qualitative. The purpose of these deployments was to assess the ability of o-DGT to detect chemicals under high-dilution scenarios, in an open water system far removed from point-source contamination (e.g., wastewater inputs, agricultural runoff). Additionally, it is not uncommon for high winds and weather events to produce turbulent wave action and mixing in Lake Winnipeg (Environment Canada, 2011), promoting difficult conditions for a passive sampler. This allowed for the durability of the o-DGT to be tested over extended deployment periods. The relatively harsh conditions are illustrated by the 2014 POCIS samplers in the south basin that were lost due to the membranes being blown out. Atrazine, thiamethoxam, clothianidin, and carbamazepine were the only four target analytes detected in the lake by both samplers. Concentrations measured with POCIS and o-DGT were comparable (Figure C11), within the scope of uncertainty expected when comparing these two PSDs, as highlighted earlier, and considering typical fluctuations in contaminant levels expected annually. Overall, o-DGT demonstrated sufficient durability over very long deployments (>40 days) in a large open water lake, suggesting broad applicability of this sampler to other freshwater lakes. However, it should be noted that at the single-digit ng/L levels measured in Lake Winnipeg more

typical deployment times (e.g., 3 weeks) could approach the limits of detection for o-DGT.

4.4.3 Under-Ice Deployments

Chapter 3 (Figure 3.4 and Figure B10) reported a comparison of o-DGT, POCIS, and grab samples from the Norway House Cree Nation WWTP in 2015. A portion of those results are presented again in Figure 4.5 along with 2014 and 2016 data. However, this discussion will focus on efforts to characterize wastewater inputs during the 2016 winter, including under-ice deployments of o-DGT at the upstream and downstream sites on Little Playgreen Lake to test the sampler's capability to function under near-freezing temperatures.
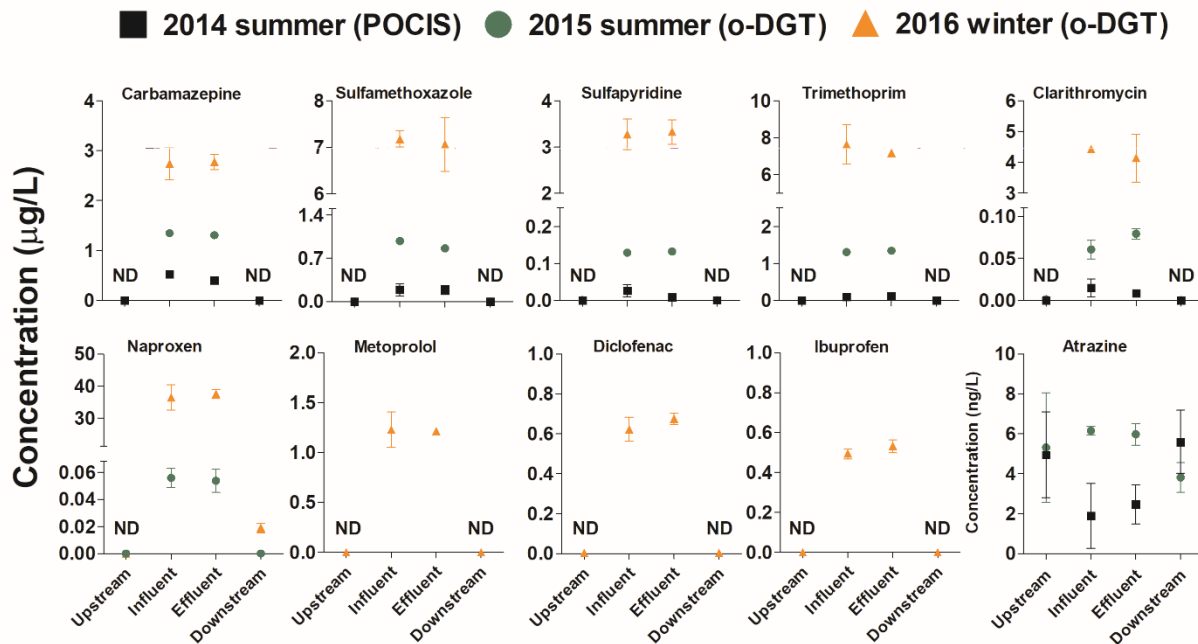
Figure 4.5: Concentrations in the NHCN WWTP and upstream and downstream of the effluent release in Little Playgreen Lake. Samplers in 2014 (POCIS) and 2015 (o-DGT) were deployed in the summer and in 2016 (o-DGT) in the winter. Note all concentrations are presented in units of µg/L except for atrazine (bottom right) in ng/L. A portion of the 2015 data set is reported in Chapter 3.

The original development of our o-DGT configuration in Chapter 3 successfully applied diffusion coefficients in the diffusive hydrogel to calculate sampling rates accurately. With this, diffusion-temperature relationships were developed for each analyte (Table B5), whereby a temperature-specific sampling rate could be calculated based on the temperature of the study system. In this way, o-DGT can account for temperature in-$situ$, removing the uncertainty associated with applying 'room temperature' (i.e., 20-25°C) sampling rates regardless of field conditions, a current issue with POCIS applications (Harman et al., 2012). Li et al. (2010a) represents one of the few studies to characterize temperature effects in POCIS calibrations fully. They found that sampling rates generally increased two-fold over a 20°C temperature change from 5 to 25°C. With no established model to adjust POCIS sampling rates for temperature (Harman et al., 2012; Li et al., 2010a), there can be significant uncertainties when considering applications to cold water systems, as appropriate POCIS sampling rates, at temperature, are not available for most compounds.

Temperatures in the lake and wastewaters ranged from 0.1-0.6 ^{o}C. Adjusted o-DGT sampling rates at these temperatures ranged from 0.9 mL/d (clarithromycin) to 4.0 mL/d (sulfapyridine). For context, the R_S at 23°C for clarithromycin is 10 mL/d and the average for all 34 analytes is ≈12 mL/d (Figure 3.2). Analyte concentrations measured by o-DGT in 2016 are presented in Figure 4.5 and Table C9 along with 2014 and 2015 data. Nine pharmaceuticals were detected at the WWTP sites in the winter, compared to six in 2014 by POCIS and seven in 2015 by o-DGT. In 2016 the only analyte detected outside of the WWTP was naproxen at the winter downstream site (20 ng/L). Atrazine was the single compound that was detected in the summer (2014 and 2015) and not the

148

winter (2016). With longer Lake Winnipeg residence in the winter (Environment Canada, 2011) the input of atrazine to the Nelson River is slowed and thus lower concentrations are expected. This, combined with the smaller sampling rates at freezing temperatures, likely explains the non-detection of atrazine (1.3 ng/L LOD, Table B3).

All other compounds were measured at elevated levels in the winter compared to the summer. Concentrations of sulfapyridine, clarithromycin, and naproxen were approximately 30-, 100-, and 1000-fold greater in the winter. Additionally, metoprolol, diclofenac, and ibuprofen, three compounds not detected in 2014 and 2015, were found at low μg/L levels at the influent and effluent sites in 2016. The NHCN WWTP utilizes three aerated outdoor lagoons for primary and secondary treatment, relying heavily on sunlight photolysis and microbial degradation to attenuate many of these contaminants prior to entering the treatment facility at the influent site. During the winter when the lagoons are near fully iced over these mechanisms are significantly reduced (e.g., microbial activity), if not entirely eliminated (e.g., photolysis). Given that many of these pharmaceuticals observed at elevated levels in the winter are known to undergo rapid photolysis (Challis et al., 2014), the reduced attenuation mechanisms occurring in the lagoons offers a plausible explanation for this observation. Additionally, elevated levels of pharmaceuticals in wastewater systems during the winter has been observed by others (Daneshvar et al., 2010b, 2010a; MacLeod and Wong, 2010).

Overall, o-DGT performed well in cold-water conditions. The ability to determine temperature-specific sampling rates accurately was crucial to obtaining accurate TWA water concentrations given that sampling rates were greatly reduced compared to 23°C values (3-10 times lower). Based on the small amount of literature detailing temperature

effects on POCIS sampling rates (Li et al., 2010a), applying room-temperature derived uptake rates to this data set would have underestimated concentrations by ≈2-3 times. This specific application of o-DGT will be of great interest to researchers studying polar contaminants in cold-water systems (e.g., arctic) (Chaves-Barquero et al., 2016).

4.4.4 Contaminant Trends

This multi-year data set in the Red River-Lake Winnipeg-Nelson River watersheds provides an opportunity to assess contaminant trends and sources as they relate to land-use patterns throughout the watershed. While this type of assessment was conducted extensively for the Red River in Chapter 2, the unique aspect of the current data set explains the movement of contaminants through these large hydrologically connected systems. Of specific interest is atrazine, which is measured from the U.S.-Canada border in the Red River, through to the south and north basins of Lake Winnipeg, and into the Nelson River system in Little Playgreen Lake. Based upon observed spatial and temporal trends along the Red River in Chapter 2 the proposed source of atrazine to the Red River and Lake Winnipeg is via transboundary transport from the U.S. Given the known wastewater inputs in these watersheds and the detection of pharmaceuticals throughout the Red River and Lake Winnipeg, carbamazepine was included in this assessment as a representative wastewater contaminant. We conducted a simple mass balance of atrazine and carbamazepine in Lake Winnipeg by assuming a single input (Red River) and output (Nelson River) to help delineate other significant sources of these chemicals to the Lake, if any. This exercise was not conducted for the neonicotinoids given the lack of data regarding their many diffuse sources throughout Manitoba and their known degradation in natural

waters (Lu et al., 2015). That said, even for atrazine and carbamazepine this is a highly simplified mass balance given the lack of fate data specific to these systems and thus should be treated as qualitative estimates.

The input of atrazine and carbamazepine into Lake Winnipeg is based on the mass loadings calculated at Selkirk in 2016 (Figure C12) and the flux data from 2014 and 2015 presented in Chapter 2 (Figure 2.4). An average annual mass loading from the Red River into Lake Winnipeg of 868 kg atrazine (Table C10) and 48 kg carbamazepine (Table C11) represent the average measured values upon which the mass balance was based. Lake Winnipeg was split into two compartments, the south basin and north basin, based on their different residence times (1.3 versus 3.5 year respectively) (Environment Canada, 2011). In addition, this mass balance assumed atrazine and carbamazepine were both conserved (no internal degradation) and at steady-state, two assumptions that facilitate a simple mass balance approximation. Schottler and Eisenreich (1997) estimated that internal transformation of atrazine in the Laurentian Great Lakes accounted for only 5-10% of total atrazine removal. Given a reported aquatic half-life >200 days (Solomon et al., 1996), assuming internal conservation of atrazine is not expected to impact the overall mass balance significantly. Other inputs and removal mechanisms such as precipitation and sedimentation are expected to be minor (<1% of total inventory) (Messing et al., 2013, 2011; Schottler and Eisenreich, 1997). Similar assumptions were made for carbamazepine given its tendency to persist in the water column, consistent with an estimated aquatic half-life >1000 days (Zou et al., 2015).

4.4.4.1 Atrazine

Modeled atrazine concentrations (as detailed in Table C10) appear to underestimate measured ones in these systems (Figure 4.6), accounting for approximately 55-60% of the total inventory. However, average measured concentrations in the lake do vary, especially in the south basin (Figure C11), where atrazine concentrations ranged from 95 ng/L in 2015 to 25 ng/L in 2016, for example. Considering this variability, our modelled predictions generally fall within the error intervals of the measured concentrations, providing reasonable estimates of mass loadings. The assumption of internal atrazine conservation makes these estimates somewhat liberal, suggesting that other sources of atrazine may be important to the overall Lake Winnipeg inventory. For example, the Winnipeg River flows into the south basin and is responsible for >40% flow into the lake (Environment Canada, 2011). Although atrazine concentrations are not expected to be high in the Winnipeg River given the lack of agriculture in the watershed, the contribution by water volume alone makes it likely that it is a secondary source of atrazine to the lake. Currently no atrazine measurements from the Winnipeg River exist, making loading estimates difficult.

4.4.4.2 Carbamazepine

Similar to our atrazine predictions above, lake-wide carbamazepine concentrations are underestimated (Figure 4.6) when assuming loadings from the Red River serve as the only substantial input of carbamazepine to Lake Winnipeg (Table C11). Our mass balance estimates accounted for ≈70% and 45% of total carbamazepine burdens in the south and north basin, respectively. The mass balance model estimates carbamazepine concentrations of around 0.1 ng/L in the Nelson River

system, helping to explain our lack of detection at upstream and downstream sites in Little Playgreen Lake over all three years of measurements, as these levels fall below our detection limits for this compound (1.7 ng/L LOD, Table B3). Our underestimation of the measured carbamazepine levels in Lake Winnipeg is not surprising given the many small communities in the area that release their wastewaters to Lake Winnipeg (Anderson et al., 2015b, 2013), and the other major volume inputs to the Lake from the Winnipeg and Saskatchewan Rivers, for which there is no contaminant data.
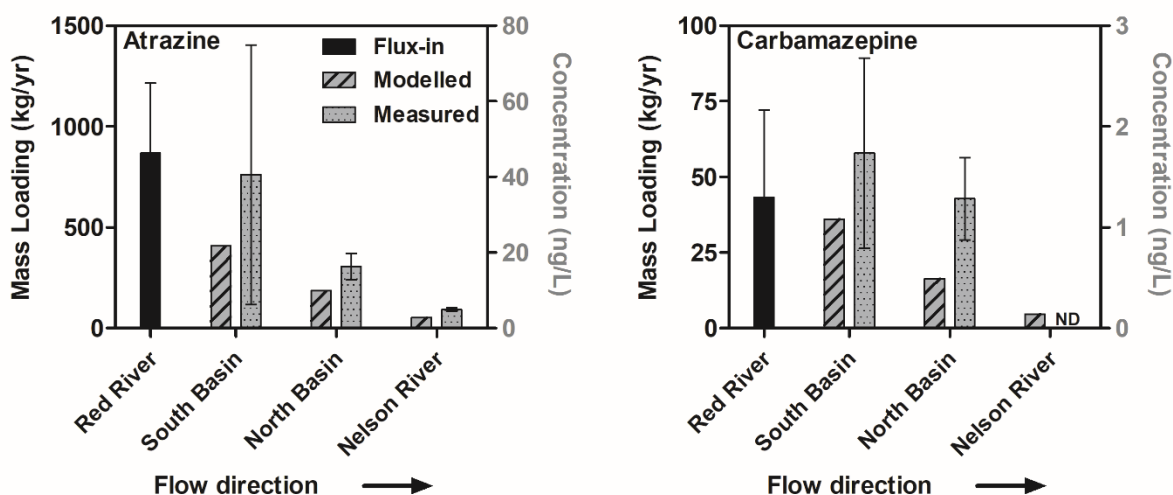
Figure 4.6: Modelled atrazine and carbamazepine concentrations in the south and north basin of Lake Winnipeg and the Nelson River estimated using the average mass loadings from the Red River at Selkirk (2014-16) as the single input to Lake Winnipeg (left y-axis, black). Average measured concentrations (2014-16) are also shown (right y-axis, grey). The south basin measured concentration represents the average between south basin and narrows.

4.5 CONCLUSIONS

The o-DGT passive sampler proved an effective measurement tool in dynamic and challenging aquatic environments. The comparisons with POCIS and grab sampling have highlighted some important advantages and challenges with o-DGT. A number of

recommendations for end-users and researchers of this technique have emerged from this work that will be important to help facilitate accurate and effective use of these passive sampling tools. From a sampler design perspective, the specific diffusive gel material used in o-DGT should be considered in future research and applications. While evidence from a recent publication by our group (Stroski et al., 2018) suggests that polyacrylamide can provide a more robust option as the diffusive gel and outer membrane compared to agarose, more research is needed. However, o-DGT configurations that avoid the use of PES membranes are still strongly encouraged in order to avoid the aforementioned (Chapter 3) challenges associated with PES. To ensure good reproducibility and precision, deployments with o-DGT should use a spindle that orientates the sampler surfaces in a flat-plane facing down so that water flows parallel across the surface of the samplers. This will ensure that sampler surfaces will remain unobstructed from settling particles during deployments. Finally, the ability to determine temperature-specific sampling rates for cold temperature applications (e.g., under-ice) provides an accurate and potentially useful tool for arctic research. Overall, the o-DGT sampler serves as a reliable and sufficiently sensitive passive sampling tool appropriate for applications in small and large rivers and lakes, wastewater treatment plants, and in cold-water environments. The accuracy of o-DGT appears to be superior to POCIS for many of these applications.

CHAPTER 5

5. A NOVEL SUSPECT SCREENING APPROACH FOR SEMI-QUANTIFICATION OF POLAR ORGANIC CONTAMINANTS IN WASTEWATERS USING THE ORGANIC DIFFUSIVE GRADIENTS IN THIN-FILMS PASSIVE SAMPLER

5.1 ABSTRACT

This study demonstrates a simple and novel approach to quantify suspect contaminants in wastewaters using the organic-diffusive gradients in thin-films (o-DGT) passive sampler. The goal of this work was to develop a method by which o-DGT could be used to determine time-weighted average water concentrations of suspect compounds semi-quantitatively, absent their isotopically labelled counterparts and measured o-DGT sampling rates. A simple quantitation strategy utilized a suite of targeted analytes as surrogate standards and estimated sampling rates in o-DGT using a previously validated diffusion model. Triplicate sets of o-DGT were deployed pre- and post-final treatment at two wastewater treatment facilities and extracts were simultaneously analyzed for a targeted suite of pharmaceuticals and pesticides and screened for non-target suspects using high-resolution quadrupole time-of-flight mass spectrometry (QTOF). Lamotrigine, venlafaxine, and des-venlafaxine were three suspect compounds identified and used as case studies to determine the feasibility and accuracy of this screening method. Surrogate standards from the suite of target analytes were used to quantify the suspect compounds, using two approaches: quantification based on 1) individual surrogate responses and 2) an averaged surrogate response. Confirmation by isotope dilution suggested that semi-quantification based on an averaged surrogate response factor was more accurate and less variable than attempting to choose individual surrogates with similar sensitivities to that of the suspect compound. The 'average' approach resulted in mean absolute differences in analyte concentrations ($C_{average}/C_{confirmed}$) of 1.3 whereas the individual 'surrogate' approach differed on average by 2.8, ranging from 0.03-30 ($C_{individual}/C_{confirmed}$). With this, time-

weighted average water concentrations were calculated using estimated sampling rates based on modelled diffusion coefficients, providing estimates of wastewater concentrations within a factor of 2. Using the o-DGT passive sampler as an environmental screening tool combined with the ability to acquire semi-quantitative water concentrations without matching analytical standards makes this a powerful approach for prioritizing polar organic contaminants for monitoring and exposure assessment.

5.2 INTRODUCTION

The advent of advanced high resolution mass spectrometry (HRMS) tools has necessitated the development of high-throughput screening approaches for efficient and accurate determination of large suites of suspect and non-target contaminants in complex environmental mixtures (Hug et al., 2014; Li et al., 2017; Schymanski et al., 2014b; Wode et al., 2015). For polar organic contaminants, much of this work utilizes electrospray ionization (ESI) HRMS due to its high sensitivity and compatibility with separation techniques like liquid chromatography (LC). However, ionization efficiencies and response factors for analytes often vary drastically among molecules in different and complex environmental matrices (e.g., wastewaters), due to ion signal modification within the ESI source (Nguyen et al., 2013; Oss et al., 2010). As contaminants identified through suspect or non-targeted screening methods are unknown at the outset by design, the lack of analytical standards required to reliably account for signal suppression or enhancement often make these approaches qualitative in nature (Li et al., 2017; Llorca et al., 2016; Moschet et al., 2017; Newton et al., 2017; Robles-Molina et al., 2014; Schymanski et al., 2014b; Wode et al., 2015). As a consequence, accurate quantification is often conducted independently using triple quadrupole tandem MS (QQQ) and isotope dilution with an *a priori* set of standards (Nguyen et al., 2013), negating much of the efficiency and screening capacity intended with these non-targeted approaches.

Methods to quantify suspects or unknowns using HRMS without isotopically labelled internal standards do exist (Caetano et al., 2005; Chalcraft et al., 2009; Golubović et al., 2016; Kruve et al., 2014; Nguyen et al., 2013; Oss et al., 2010; Pieke

et al., 2017; Raji et al., 2009), however the complexity of these methods vary, often involving modeling analyte-specific predictors of ionization efficiencies (Caetano et al., 2005; Chalcraft et al., 2009; Golubović et al., 2016; Kruve et al., 2014; Raji et al., 2009), which can be prohibitive to the non-expert end-user. For example, Chalcraft et al. (2009) developed a quantitative relationship between relative response factors and four physiochemical properties determined to be good predictors of ESI sensitivity. While successful, this approach relied on multivariate models and computational software to estimate intrinsic solute properties, tools not necessarily readily available to end-users of HRMS screening methods (Chalcraft et al., 2009). Additionally, with response factors varying strongly with analytical conditions, including with the specific instrument itself (Cech et al., 2001; Huffman et al., 2012; Pieke et al., 2017), accurate application of any single response factor model universally is highly unlikely.

A more basic approach involves the use of a known surrogate standard to quantify an analyte of interest, thereby serving the role of a matched labelled isotope. This technique is often referred to as semi-quantification (Pieke et al., 2017), and typically uses a chemical from one class to quantify a target analyte characterized by that same chemical class or family (Banerjee et al., 2012; Bu et al., 2014). Semi-quantification relies on the underlying assumption that two compounds with a high degree of structural conservation (e.g., triazine pesticides or β-blocker drugs) will behave similarly in an ESI source, and thus have similar response factors. However, given the wide range in response factors observed with ESI (Nguyen et al., 2013; Oss et al., 2010) and the complex factors impacting sensitivity (Caetano et al., 2005; Chalcraft et al., 2009; Golubović et al., 2016; Kruve et al., 2014; Raji et al., 2009), semi-quantification carries

with it inherent uncertainties. While these errors are often observed and acknowledged when applied to HRMS approaches (Banerjee et al., 2012; Bu et al., 2014), all too often semi-quantification is taken and reported as fully quantitative when applied to low-resolution QQQ MS methods (Chen et al., 2015; 2013; Xu et al., 2007; Yang et al., 2010; Zhou et al., 2012).

Nonetheless, these HRMS suspect screening methods and semi-quantification approaches are becoming indispensable tools to the environmental chemist (Moschet et al., 2017; Schymanski et al., 2014b) attempting to characterize the huge number of new, old, and emerging chemicals in commerce being released to the environment and prioritize those in need of further assessment (Howard and Muir, 2010). As these HRMS analyses and data mining methods become further streamlined and readily available, the need to integrate them into regular monitoring efforts will become more and more apparent (Hollender et al., 2017). With this improved ability to identify previously unknown or unexpected contaminants by retrospective analysis, acquiring the appropriate water samples representative of the system and inputs can be challenging, as these polar organic contaminants are often at very low and variable levels in receiving waters.

Large volume grab sampling is a common approach (Hug et al., 2014; Li et al., 2017; Wode et al., 2015), however isolated snapshots from an aquatic system are likely to miss important point and non-point source input events over an extended monitoring period. Passive sampling tools facilitate *in-situ* monitoring over extended exposure times (days to months), capturing episodic inputs and providing time-weighted average (TWA) water concentrations (Vrana et al., 2005), offering an effective alternative to grab

samples. The polar organic chemical integrative sampler (POCIS) is the most well-established passive sampling tool for measuring polar organics in aquatic systems (Harman et al., 2012). Yet, efforts to integrate POCIS into suspect and non-target screening approaches are rare, as quantitative concentration estimates require previously measured compound-specific sampling rates. POCIS lacks a fundamental uptake model (Harman et al., 2012, 2011), and thus a means by which to predict sampling rates for suspect or non-target candidates, highlighting a major obstacle to appropriately integrating these tools with HRMS techniques. Indeed, efforts to utilize POCIS for suspect and non-target screening to date have been completely qualitative (Guibal et al., 2015b; Soulier et al., 2016). The o-DGT passive sampler developed here (Chapter 3) may serve to fill this gap, as the validated diffusion-based uptake model (Figure B6) allows o-DGT sampling rates to be estimated based only on chemical structure (*Equation 3.6*).

Here, we use the o-DGT passive sampler with liquid chromatography tandem quadrupole time-of-flight mass spectrometry (LC-QTOF) to screen suspect wastewater contaminants. Uncertainties and challenges associated with semi-quantitation methods relying on single structurally related surrogates are highlighted and a simple alternative approach that takes advantage of targeted isotope dilution methods is proposed. Additionally, we establish the utility of the validated diffusion model (Chapter 3) for estimating o-DGT sampling rates, and thus determine semi-quantitative environmental concentrations of suspect contaminants based only upon chemical structure. The scheme presented here demonstrates o-DGT as a promising sampling tool and analytical quantification approach for future HRMS suspect screening efforts.

5.3 METHODS AND MATERIALS

5.3.1 Sampling Details

Wastewaters were sampled over a two-week period using o-DGT and POCIS at two wastewater treatment plants (WWTP) in the Greater Toronto Area, Ontario, Canada. Samplers were deployed side-by-side in triplicate at four sites; pre- and post-final chlorination treatment at WWTP1 and pre- and post-final UV treatment at WWTP2. Samplers were deployed on stainless steel spindles inside stainless steel protective cages (30 cm high $\times$ 16 cm wide) equipped with HOBO Water Temp Pro v2 loggers (two readings per hour, ±0.2ºC accuracy) (Hoskin Scientific LTD., Burlington, ON).

5.3.1.1 o-DGT

Complete details of development, optimization, assembly, and extraction of o-DGT are in Chapter 3 and Appendix B. Briefly, o-DGT samplers were constructed using two layered gels made of 1.5% agarose (molecular biology grade, Sigma-Aldrich, Oakville, ON); a 0.75 mm, 25 mg Waters OASIS™ HLB binding gel and a 0.75 mm outer diffusive gel. The 0.75 mm binding gel was placed on the standard plastic DGT base (HLB side face-up) with the diffusive gel layered on top, and sealed with the standard DGT cap (exposed area = 3.1 cm^2). Of particular note with this configuration is the exclusion of the outer polyethersulfone (PES) membrane used in POCIS and many other current o-DGT designs. Compound and temperature specific o-DGT sampling rates were calculated according to Table B4 for targeted analytes and *Equation 3.6* and *3.9* for the suspects.

5.3.1.2 POCIS

The standard pre-constructed POCIS samplers from Environmental Sampling Technologies (St. Joseph, MO) were used in this study. POCIS contained 200 mg of Waters OASIS™ HLB material between PES membranes (0.1 μm pore size) with an exposed total membrane surface area of 41 cm^2. Extraction protocols are described in Chapter 2 and elsewhere (Carlson et al., 2013b). POCIS sampling rates used to determine TWA water concentrations were taken from Table C4.

5.3.1.3 Active Sampling

Integrative 24 hr composite samples (~150 mL collected hourly) were taken at WWTP2 pre-treatment site in 4L glass bottles using an ISCO 6712 automated active sampler (Avensys Solutions, Toronto, ON). Samples were collected over the two week period that POCIS and o-DGT samplers were deployed in September 2016 from the 12th-13th, 14th-15th, 18th-19th, 21st-22nd, and 25th-26th. After collection, the 4L amber bottle was well-mixed and a 500 mL sub-sample was taken back to the laboratory for extraction by solid phase extraction according to protocols detailed in Chapter 3.

5.3.1.4 Quality Assurance/Quality Control (QA/QC)

Laboratory and field blanks for o-DGT, POCIS, and active samples were extracted and analyzed alongside each set of environmental samples. Field blanks were left open to the atmosphere during retrieval and deployment of passive samplers. For all our analytes, levels observed in lab and field blanks were negligible. Retrieved passive samplers were stored by freezing (-20°C) for 1-3 weeks until extraction, which is unlikely to result in analyte losses (Chapter 6).

5.3.2 Compounds

5.3.2.1 Targets

A total of 17 target native and matched isotopically labelled compounds (6 pesticides and 11 pharmaceuticals) were analyzed by liquid chromatography tandem mass spectrometry (LC-QQQ) and high-resolution quadrupole time-of-flight mass spectrometry (LC-QTOF). The pesticides were: 3 neonicotinoids (imidacloprid, thiamethoxam, and clothianidin); 2 organophosphates (chlorpyrifos and diazinon); and 1 triazine (atrazine). The pharmaceuticals were: 4 sulfonamide antibiotics (sulfapyridine, sulfamethoxazole, sulfamethazine, and sulfadimethoxine); 1 fluoroquinolone antibiotic (enrofloxacin); the antibiotic trimethoprim; 3 β-blockers (atenolol, metoprolol, and propranolol); 1 selective serotonin reuptake inhibitor (fluoxetine); and 1 sodium channel blocker (carbamazepine). A stock mixture of the isotopically labelled standards was prepared in pure methanol at 2 ng/μL for spiking environmental samples (details of labelled isotopes in Appendix B).

5.3.2.2 Suspects

Lamotrigine, venlafaxine, and des-venlafaxine (Sigma-Aldrich, Oakville, ON) were identified as suspect contaminants through our initial screening method and subsequently purchased for confirmation by LC-QQQ. Lamotrigine-($^{13}C,^{15}N_4$), venlafaxine-D_6, and (±)-o-des-methylvenlafaxine-D_6 (Sigma-Aldrich) were used as internal standards for isotope dilution.

5.3.3 *Instrumental Analysis*

5.3.3.1 *QQQ Targeted Method*

All samples (o-DGT, POCIS, and 24 hr composites) were subject to analysis with this method. The 23 target pharmaceutical and pesticide concentrations were determined quantitatively using an Agilent 6410B LC-MS/MS system (Agilent Technologies, Mississauga, ON). LC mobile phases were 95:5 H_2O:methanol (solvent A) and methanol (solvent B), each containing 0.05% formic acid (Fisher Scientific, Ottawa, ON). Chromatographic separations were achieved using an Agilent Eclipse Plus C18 column (2.1 × 50mm × 1.8µm particle size) with a Phenomenex HPLC SecurityGuard C18 Guard Cartridge (4 × 3mm) (Phenomenex, Torrance, CA) at 42°C and a flow rate of 0.45 mL/min.

Batch analyses of samples sets were conducted by running 13 calibration standards (ranging of 0.01 – 500 µg/L) along with the samples. Blanks were run between triplicate sets of samples and single calibration standards (10, 25, or 50 µg/L) were run every 15 samples as a QA/QC protocol (concentration to be within 20% of target). Linearity (R^2) of calibration standards was ≥0.98 over all analyses and all 23 analytes. Isotope dilution was conducted for o-DGT, POCIS, and 24 hr composite samples with 25 µL of the internal standard mixture spiked in each sample prior to extraction. This QQQ method was treated as fully quantitative and assumed to provide the 'true' concentration when determining the accuracy of the other quantification approaches. Further details of this analytical method, including the LC gradient elution method, source parameters, MRM transitions, and limits of detection are reported in Chapter 3 and Appendix B.

5.3.3.2 QQQ Suspect Confirmation

Suspect compounds initially identified as lamotrigine, venlafaxine, and des-venlafaxine were later confirmed by LC-QQQ. Solvents and analytical column were the same as the targeted method above. Quantifier and qualifier ions and their optimized fragmentor voltages (frag) and collision energies (CE) were as follows: Lamotrigine (frag=150): 256 → 210.9 (CE=28) and 144.9 (CE=40); Venlafaxine (frag=88): 278.2 → 121 (CE=28) and 147.1 (CE=24); Des-methylvenlafaxine (frag=85): 264.2 → 246.1 (CE=8) and 107 (CE=36). A gradient elution method started at 5%B and ramped to 80%B over 2.5 min with a preconditioning at 5% from 2.5-5 min. Standard curves were constructed with six calibration standards between 1 and 500 ng/L.

5.3.3.3 QTOF Suspect Screening Method

Only the o-DGT samples were subject to suspect screening with the QTOF HRMS method. The Waters LC – Xevo G2-XS QTOF HRMS was used to quantify the suite of 23 target pharmaceuticals and pesticides and screen for suspect contaminants. This was conducted with a full scan (m/z 100-900) positive mode ESI method (capillary voltage set at 2 kV) at a resolving power of 25,000. Data independent acquisition (DIA) and data dependent acquisition (DDA) methods were utilized to inform the mass spectral identification of potential suspects. The analytical column and gradient elution methods were the same as above. The same calibration standards as above were used for this method, however given the smaller linear dynamic range of QTOF instruments, only six standards (1-250 ng/L) were used to generate the linear calibration curves.

Suspects that were only found in the o-DGTs exposed to wastewater samples and not the blanks were tentatively screened and identified according to the scheme

proposed by Schymanski et al. (2014a). First, exact mass and molecular formula

assignment were based on isotope pattern and mass accuracy (<5 ppm). Clean MS

fragmentation data were difficult to obtain with these samples, in part, due to the

complex wastewater matrices, and thus were not used in suspect identification. Next, a

probable structure was assigned using the ChemSpider database

(http://www.chemspider.com/) and compound libraries from the literature (Wode et al.,

2015). This screening and identification process was conducted manually, without the

aid of sophisticated spectral deconvolution software packages, a large reason for the

relatively small number of identified suspects in this study. Confirmation of each

candidate suspect was confirmed with analytical standards by comparing MS, MS^2, and

retention time data using the LC-QQQ method described above.

5.3.4 Semi-Quantification and o-DGT Scheme

Figure 5.1 provides a conceptual model of the analysis and quantification

scheme evaluated in this work. Extracts of o-DGT samplers retrieved from the four

WWTP sites were spiked with 25 µL of the internal standard mixture. Of the 17

isotopically labelled standards, seven (Figure 5.1C) were reliably detected and

quantified by the QTOF full scan method in both the calibration standards and o-DGT

extracts (carbamazepine-d_{10}, atenolol-d_7, metoprolol-d_7, propranolol-d_7, atrazine-d_5,

trimethoprim-d_3, and sulfamethoxazole-d_4). These compounds represent the target

internal standards used as surrogate standards for quantifying the suspects identified in

this work (Figure 5.1D). Suspects were quantified with the response factors and the

surrogate standards in individual samples using two approaches. First, each suspect

was quantified using each of the seven target analyte response factors and surrogates

to produce seven concentrations per suspect (Figure 5.1E). This is the individual

surrogate semi-quantification method, or simply referred to here as the 'surrogate'

approach, and is common practice throughout the literature (Chen et al., 2015, 2013; Xu

et al., 2007; Yang et al., 2010; Zhou et al., 2012). Second, each suspect was quantified

using the averaged response factor of all seven target analytes (Figure 5.1F), known

here as the average surrogate semi-quantification method, or the 'average' approach. A

calibration curve for the average approach was created by taking the average response

of all seven target analytes (average response of seven natives and average response

of seven isotopes) at each concentration in the standard curve and plotting average

relative responses (native/isotope) as a function of concentration (1-250 ng/L). In

addition to the three suspects actually identified through the screening method, the

seven target analytes were also treated as suspects and thus quantified in the same

manner. This was done to increase the sample size of the test compounds for these

two quantification strategies.

These two semi-quantification approaches provided estimates of analyte mass

sequestered onto the o-DGT sampler (*Equation 1.7*). To obtain TWA water

concentrations, sampling rates had to be estimated given the lack of previously

measured values for the suspect compounds identified here. This was done using the

Hayduk-Laudie empirical diffusion model (*Equation 3.6*) (Fuller et al., 1966; Hayduk and

Laudie, 1974; Schwarzenbach et al., 2005c) and the governing o-DGT equation

(*Equation 3.9*) according to Chapter 3.
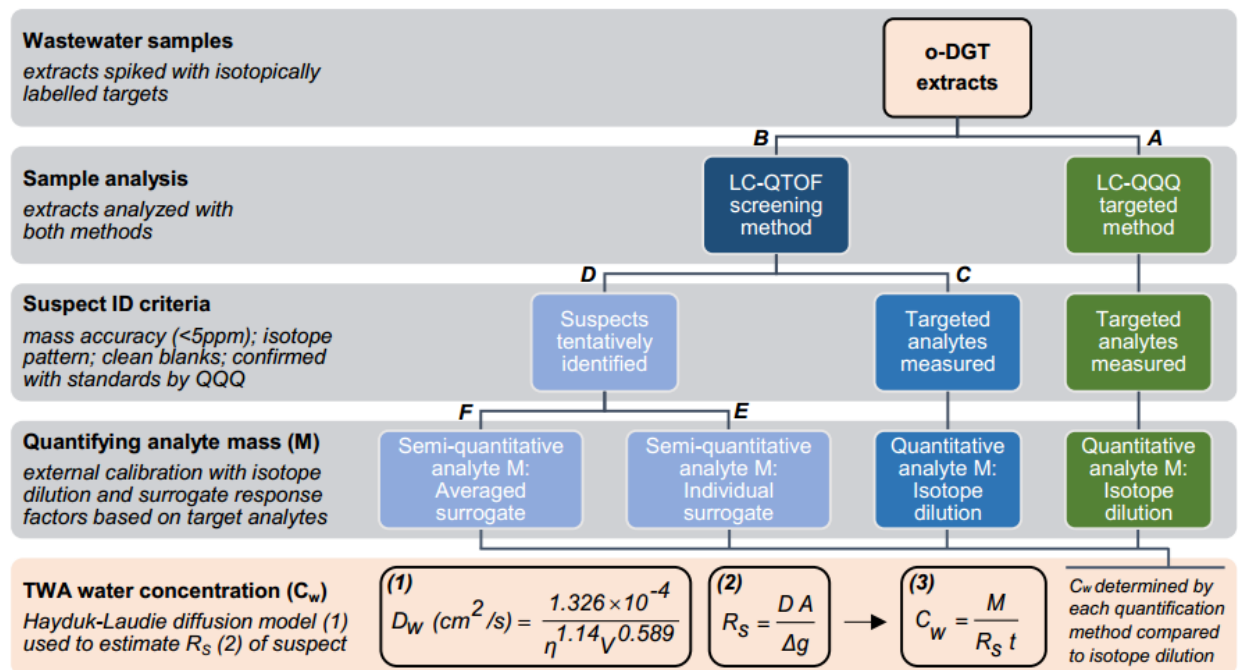
Figure 5.1: Conceptual model of the suspect screening and semi-quantification approach using o-DGT. Green boxes (A) represent confirmed concentrations with isotope dilution using triple quadrupole mass spectrometry (QQQ). Blue boxes (B) represent analysis with high resolution quadrupole time-of-flight mass spectrometry (QTOF). Using a single full-scan QTOF method the target analytes were measured and quantified by isotope dilution (C) and the suspects (D) were quantified using the individual response factors of each target analyte (E) and the average response factor of all target analytes (F). Time-weighted average (TWA) concentrations (3) were then calculated using modelled sampling rates (1 and 2) based on the structure of the suspect compound. Concentrations from semi-quantification approaches (E and F) were compared to those confirmed by isotope dilution (A and C) to determine accuracy of each approach.

5.4 RESULTS AND DISCUSSION

This discussion will describe the feasibility of our proof-of-concept approach to a simple semi-quantification strategy for suspect screening of environmental contaminants using o-DGT passive samplers. The accuracy and ease-of-use for end-users will be discussed in the context of other semi-quantification approaches used in the literature. Additionally, a fully quantitative comparison of o-DGT, POCIS, and active sampling concentrations of target analytes in wastewater will be briefly discussed.

169

5.4.1 Semi-quantification strategy

As previously mentioned, a major challenge for end-users working with HRMS suspect and non-target screening methods involves quantification without the use of analytical standards, often resulting in qualitative studies reporting the presence of suspect contaminants and their relative abundances (i.e, peak area) (Llorca et al., 2016; Wode et al., 2015). As the quantitative capabilities of HRMS technology advance (e.g., linear dynamic range or sensitivity) it is expected that more and more targeted QQQ methods will be conducted with HRMS instruments (Bijlsma et al., 2013), enabling strategies that utilize mass-labelled surrogates and target analyte response factors to quantify suspects and non-target compounds identified through screening, as demonstrated here. Figure 5.2 describes the accuracy of the average and surrogate semi-quantification approaches compared to confirmed concentrations with isotope dilution by LC-QQQ.
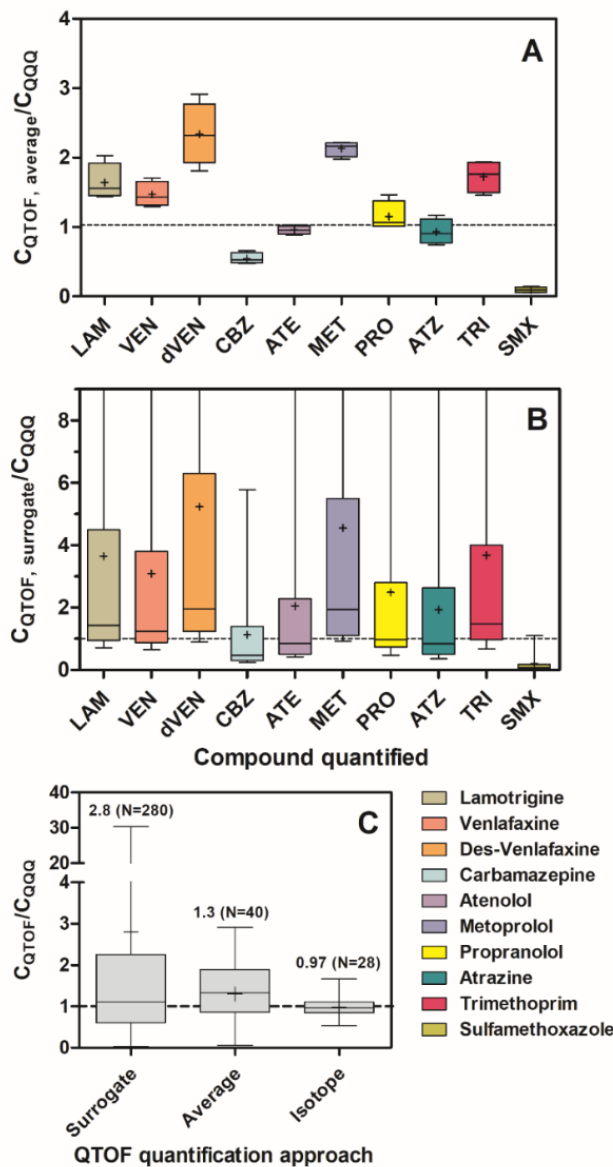
Figure 5.2: Comparison of quantification approaches. Box and whisker plots represent: minimum and maximum, lower and upper quartile, median and mean (+). C_{QTOF} indicates the concentration determined by semi-quantification using the average (A) and surrogate (B) strategies. C_{QQQ} represents the confirmed concentration by isotope dilution with LC-QQQ. The y-axis is the absolute error between the two compared concentrations (maximum cut-off in B for clarity) with the dashed line in each plot representing a ratio of 1 (i.e., zero error). The suspect compounds lamotrigine, venlafaxine, and des-venlafaxine are shown in the three most left boxes in A and B, followed by the seven target analytes used for semi-quantification (10 analytes total). Each box in panel A represents the averages of triplicate samples from each of the four wastewater sites (number of samples, N=4), determined by the averaged response factor of all seven target analytes. Boxes in panel B are the same four wastewater site samples but quantified based on each of the seven individual target analytes. Panel C (average and sample number above error bars) is a summary of both approaches in A and B and quantification with isotope dilution by QTOF and QQQ. Summary of sample numbers, in C: surrogate - 4 samples x 10 analytes x 7 surrogate responses, N=280; average - 4 samples x 10 analytes x 1 averaged response, N=40; isotope - 4 samples x 7 target analytes with paired isotope response, N=28.

Overall, semi-quantification with the averaged approach provided more accurate concentration estimates compared to selecting individual surrogates (Figure 5.2C). The average absolute error for the two semi-quantification strategies across all 10 test compounds was 1.3 (range 0.1-2.9, $C_{QTOF, average}/C_{QQQ}$) and 2.8 (range 0.03-30, $C_{QTOF, surrogate}/C_{QQQ}$). Pieke et al. (2017) took a similar approach to semi-quantification and observed similar errors. Of particular interest here is the range in absolute errors, which is much smaller for the average versus individual surrogate approach and demonstrated clearly by the box and whisker plots in Figure 5.2A and B. Given the structural variability in contaminants typical of environmental analyses, and observed across the ten analytes quantified here with these approaches, it is not surprising that a single surrogate standard would not provide accurate quantification for all analytes. Without *a priori* knowledge of response factors for suspect or non-target compounds, our data suggest that the prudent and most accurate approach to quantification is with an average surrogate response.

Not surprisingly, there are outliers with these approaches. Sulfamethoxazole was significantly underestimated by both quantification approaches, consistent with its poor sensitivity (low abundances) observed with the QTOF screening method, relative to the other target analytes. The average semi-quantification of sulfamethoxazole was underestimated by one order of magnitude ($C_{QTOF, average}/C_{QQQ} = 0.1$) while the individual surrogate semi-quantification of sulfamethoxazole was underestimated, at worst, by ≈30-fold (using trimethoprim as surrogate standard). The other nine test compounds quantified by the average approach were generally within a factor of 2. Much larger variations were observed with the individual surrogate approach (Figure 5.3).

Carbamazepine and sulfamethoxazole as individual surrogates greatly overestimated the 10 analytes by an average of ≈ 4.5 and 10 times, respectively. The other 5 individual surrogates provided more reasonable absolute errors (≈2-3, Figure 5.3 bottom panel).

Within the set of 10 test compounds, three target analytes are β-blockers and thus share a high degree of structural conservation. As such, atenolol, metoprolol, and propranolol could have similar ESI response factors, as assumed with many structurally related classes of chemicals (Caetano et al., 2005), and thus represent logical and accurate surrogate standards for each other. In fact, there are numerous examples in the literature of using a single β-blocker as a surrogate standard for a suite of β-blocker compounds (Alder et al., 2010; Gabet-Giraud et al., 2014; Maurer et al., 2007). In all cases, these LC-QQQ methods are reported as fully-quantitative. However, our data suggest there can be large inherent errors associated with inferring similar response factors for structurally related compounds. For example, semi-quantification of metoprolol with atenolol as a surrogate standard resulted in an absolute error, $C_{QTOF, surrogate}/C_{QQQ}$, of 2.2 (Figure 5.3, bottom panel), underscoring the challenge and uncertainty of predicting ESI sensitivities and response factors, especially for non-expert end-users of these HRMS screening approaches.
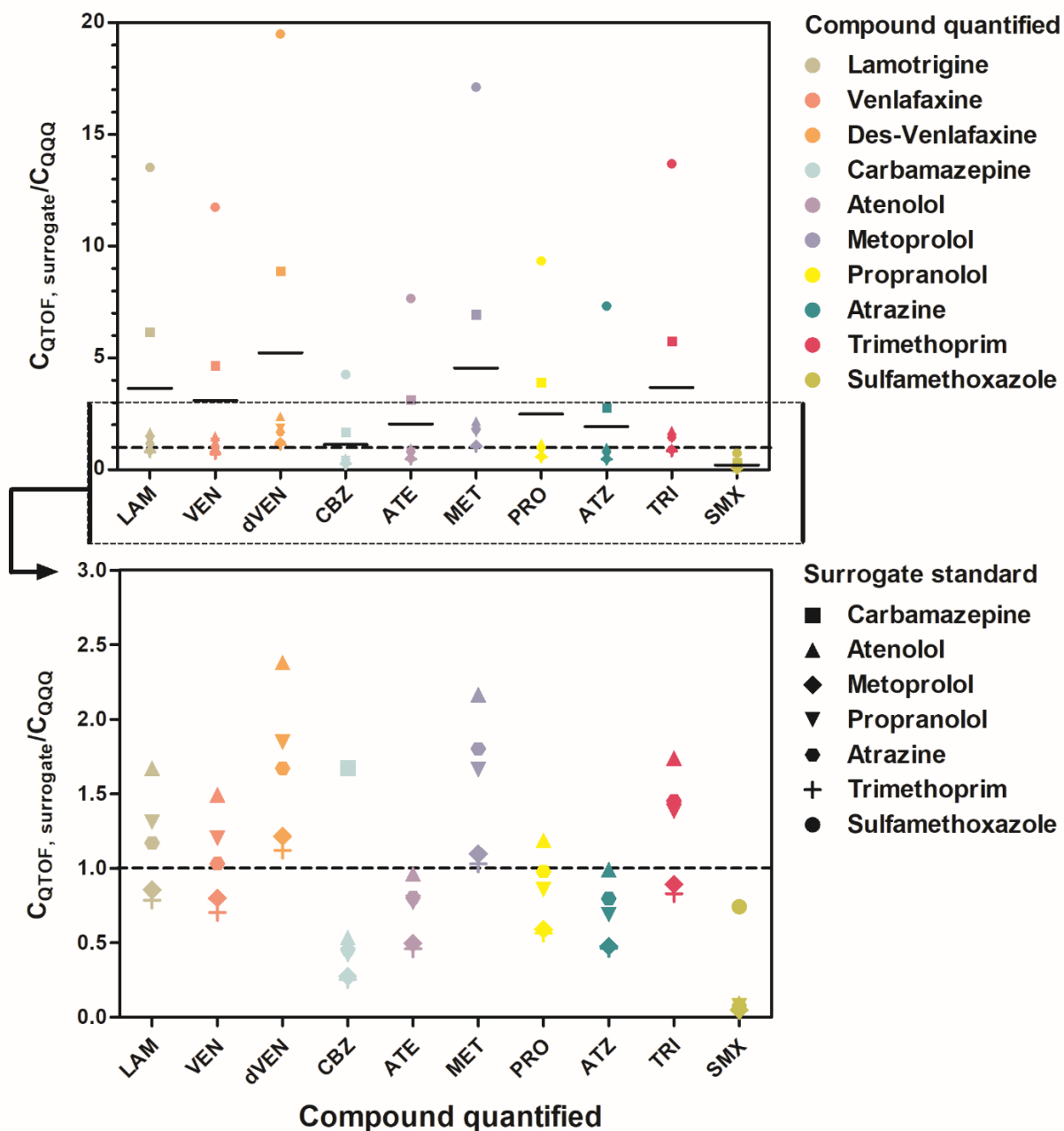
Figure 5.3: The results of the individual surrogate approach summarized in Figure 5.2B is shown in more detail here. Each data point represents the averages of triplicate samples from the four wastewater sites (N=4), quantified based on each of the seven individual target analytes, denoted by the seven shapes (black lines = average of the seven data points). The y-axis is the absolute error between the two compared concentrations with the dashed line in each plot representing a ratio of 1 (i.e., zero error). The top panel shows the entire data set and the bottom panel shows a zoomed in y-axis with data points quantified by carbamazepine (squares) and sulfamethoxazole (circles) removed.

We strongly recommend that the practice of using individual surrogate standards for semi-quantification be reported as such, namely, semi-quantitative, or in some cases even qualitative. Additionally, where applications are utilizing both targeted isotope dilution and suspect screening with a single HRMS method, an averaged response factor approach, as demonstrated here, should be used for semi-quantification of suspect and non-target compounds. Overall, this approach avoids extreme under or overestimation as a result of pairing a suspect and surrogate standard that have drastically different response factors, an issue that can present as a serious unknown uncertainty when *a priori* knowledge of compound response factors is lacking, as is the case with suspect and non-target screening methods.

5.4.2   *Estimating o-DGT sampling rates*

The ultimate goal in this suspect screening strategy was to determine TWA water concentrations of suspect compounds in wastewaters. Given o-DGT is a relatively new sampling technique, there is still only a small body of literature reporting experimentally measured sampling rates (Chen et al., 2013). As such, the utility to predict o-DGT sampling rates accurately for other compounds is apparent. Chapter 3 demonstrated this by evaluating a fundamental o-DGT uptake model based upon molecular diffusion of chemicals through the outer hydrogel membrane of the sampler. Using the Hayduk-Laudie empirical model (*Equation 3.6*), demonstrated that diffusion coefficients, and thus sampling rates (*Equation 3.9*), could be predicted based on the molecular volume of the chemical and the viscosity of water (diffusive hydrogel membranes in o-DGT are 96-98% water), with average relative uncertainties within 30%. This approach was taken

here to estimate the TWA water concentrations of the three suspect compounds

lamotrigine, venlafaxine, and des-venlafaxine (Figure 5.4).
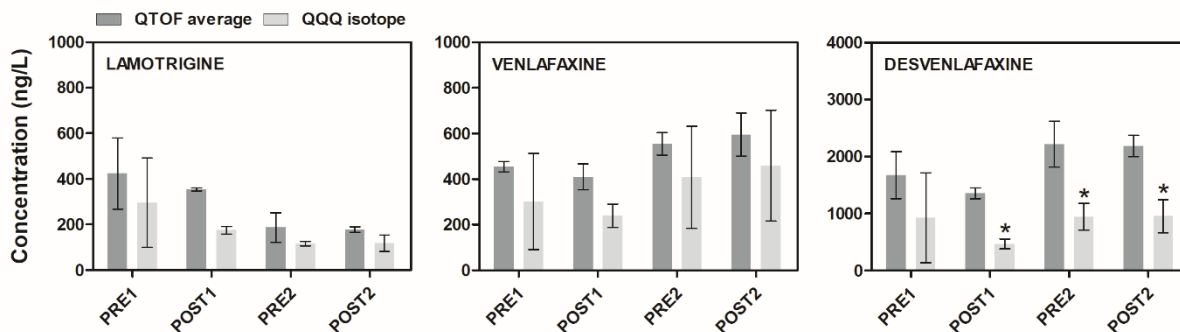
Figure 5.4: Time-weighted average (TWA) water concentrations of the three suspect compounds lamotrigine, venlafaxine, and desvenlafaxine were determined using modelled sampling rates of 16 mL/d, 12 mL/d, and 13 mL/d, respectively. Dark gray bars are the concentrations determined by the QTOF average approach. Light gray bars are confirmed concentrations by LC-QQQ isotope dilution. Bars represent the average and standard deviation (error bars) of triplicate o-DGT samples. Pre/Post 1 and 2 are the four sampling sites (pre- and post-disinfection) at the two WWTPs. Statistical difference (*) was determined by a two-way ANOVA and Bonferroni post-hoc test (p<0.05).

Average absolute errors between concentrations determined by QTOF-average

and QQQ-isotope methods were 1.6, 1.5, and 2.3 for lamotrigine, venlafaxine, and des-

venlafaxine, respectively. It should be noted that extracts initially screened with the

QTOF method had to be stored (dark fridge at 4°C) for approximately 4 months before

the isotopically labelled standards for lamotrigine, venlafaxine, and des-venlafaxine

were received in the laboratory, spiked in the extracts, and confirmed by LC-QQQ. It is

possible that during this period losses of these three suspects were incurred, thus

contributing to some of the differences observed in Figure 5.4. Additionally, given that

our o-DGT extraction procedures were not optimized for these compounds, initial losses

during extraction are possible and would impact the overall concentrations determined

by QTOF and QQQ equally. However, these extraction losses are expected to be small

given the excellent extraction efficiencies (>95%) for the diverse suite of 34

pharmaceuticals and pesticides studied here (Table B4), suggesting that the extraction

technique used here is effective for polar organic contaminants in general.

Errors associated with estimating sampling rates are expected to be in the range

of 30% (Chapter 3). This is consistent with the current data set with average errors of

25-30% when comparing concentrations of target analytes determined using modelled

and experimentally measured sampling rates (data not shown). When considering that

typical uncertainties with measurement and application of POCIS sampling rates can

often be in the range of 100-200% (Poulier et al., 2014), the errors associated with

modelling o-DGT sampling rates are reasonable, and support this sampler as a

convenient and powerful tool for HRMS suspect and non-target screening methods. Of

course, this approach could also be applied similarly to grab and active sampling

without the need to model sampling rates. However, aside from obvious benefits

afforded by passive sampling, including continuous *in-situ* monitoring, improved

detection limits, and cleaner sample matrices, o-DGT offers safe and stable sample

storage/archiving in the freezer without incurring analyte losses for at least two years

(Chapter 6), something not possible with water grab samples. This provides the

opportunity to potentially re-assess original samples with optimized extraction and

analysis protocols specific to suspect compounds that may have been identified in the

initial screening.

5.4.3 *Sampler comparisons*

Overall, concentrations measured by o-DGT, POCIS, and 24 hr composite active

samples were in good agreement (Figure 5.5). Comparing o-DGT and POCIS to active

sampling at the PRE2 WWTP site, absolute errors were 1.03 ($C_{o\text{-DGT}}/C_{active}$) and 0.90 ($C_{POCIS}/C_{active}$). Comparing o-DGT and POCIS over all four sites and nine analytes we see a larger discrepancy, with an average absolute error, $C_{o\text{-DGT}}/C_{POCIS} = 1.8$. This underestimation of POCIS concentrations compared to o-DGT is consistent with observations described in Chapter 3 and 4.

The proposed mechanism leading to this underestimation relates to the known effects flow-rate has on POCIS sampling rates (Harman et al., 2012), and the fact that laboratory-derived sampling rates appear to be larger than *in-situ* rates (Chapter 4), leading calculated TWA concentrations to bias low. This mechanism is supported by our data (Figure 5.5) when we consider the specific details of each WWTP site. Sampling site PRE1 is a very slow moving wastewater retention pond, while the other three sampling sites can be characterized by fast-flowing waters. At site PRE1, *in-situ* POCIS sampling rates are expected to be smaller than at the other sites as a result of a larger diffusive boundary-layer controlling sampler uptake. However, since POCIS lacks a robust model to account for these *in-situ* boundary layer effects, laboratory-derived sampling rates usually measured under flowing conditions are used as-is, leading to concentrations that are, in some cases, greatly underestimated, as observed at the PRE1 site for 8-of-9 target analytes (Figure 5.5). When comparing o-DGT and POCIS concentrations by site, average $C_{o\text{-DGT}}/C_{POCIS} = 3$ at the PRE1 site, while that ratio is only 1.4 averaged over the other three sites.
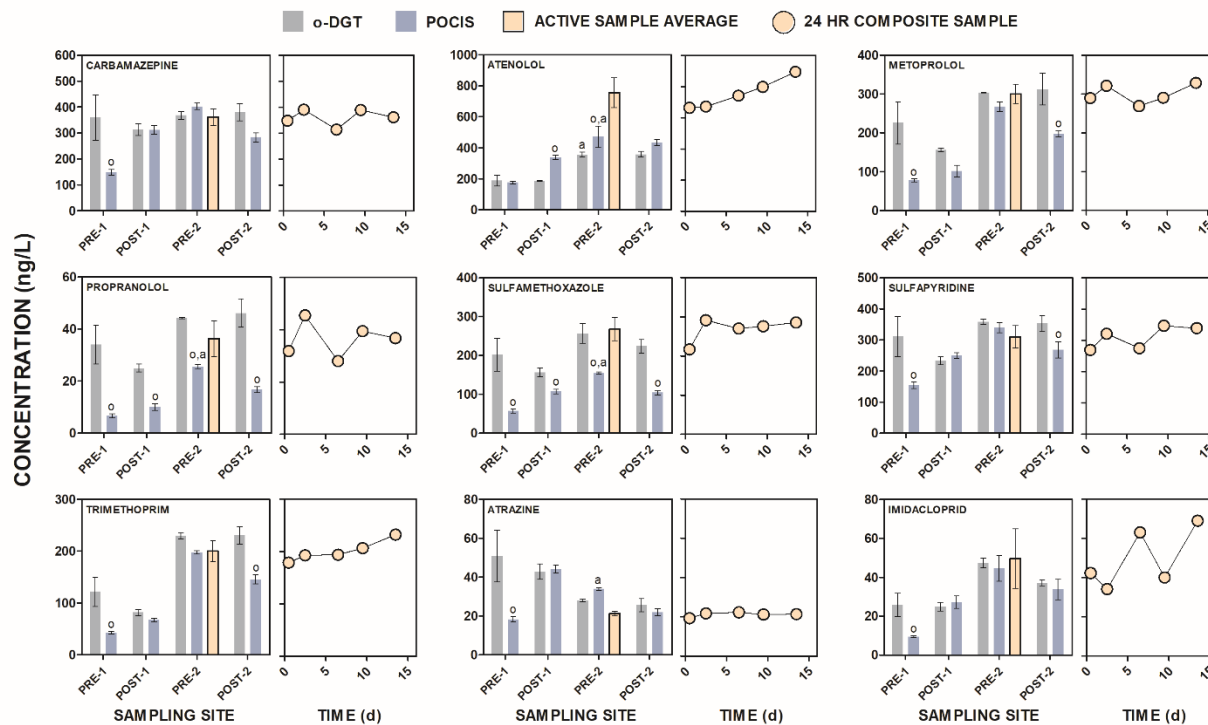
Figure 5.5: Quantitative time-weighted average (TWA) water concentrations (Equation 3.1, using measured sampling rates in Chapter 3) of the target analytes measured by the LC-QQQ isotope dilution method. Gray and blue bars represent the average and standard deviation (error bars) of triplicate o-DGT and POCIS samples. The beige bar is the average of five 24 hr composite samples over the 14 d deployment period, shown as individual sampling events (beige circles) to the right of each bar plot. Statistical difference, denoted by 'o' (o-DGT) or 'a' (active sample) was determined by a two-way ANOVA and Bonferroni post-hoc test (p<0.05). For example, atenolol PRE-2 POCIS concentration (blue bar, top middle plot) is statistically different from the o-DGT and active sample average concentration, hence 'o,a'.

5.5 CONCLUSIONS

This proof-of-concept study provides evidence in support of a semi-quantification strategy utilizing average surrogate response factors instead of individual surrogates chosen based on structural similarities to the target/suspect compound. Additionally, o-DGT served as an accurate and convenient tool for our HRMS suspect screening method, in particular for the ability to predict o-DGT sampling rates based only on chemical structure. Taken together, determining TWA water concentrations of suspect or non-target compounds using average semi-quantification and modelled sampling

179

rates will provide estimations generally within 2-fold of the 'true' concentration. By avoiding the choice of individual surrogate standards the risk of matching response factors that are drastically different for surrogate and suspect is minimized. It is recommended that HRMS target analyte lists that are used for average semi-quantification be large and structurally diverse within a target chemical class (e.g., polar organics contaminant), so as to capture a wide range of possible response factors.

CHAPTER 6

6. PHARMACEUTICALS AND PESTICIDES ARCHIVED ON POLAR PASSIVE SAMPLING DEVICES CAN BE STABLE FOR UP TO SIX YEARS

6.1 ABSTRACT

This study presents a new effort to characterize the storage stability of pharmaceuticals and pesticides on the recently developed organic-diffusive gradients in thin-films (o-DGT) passive sampler and a continuation of previously published work reporting storage on the polar organic chemical integrative sampler (POCIS). The o-DGT samplers were pre-loaded with analyte and stored in the freezer (-20 ^{o}C) to test long term storage (up to ≈ 18 months) feasibility and in the fridge (4 ^{o}C) to assess short term storage options. In addition, field exposed o-DGT from a wastewater treatment plant were stored for up to one year to test potential effects a co-extracted field matrix may have on storage stability. For the long-term laboratory storage tests, the average change in mass on o-DGT after ≈ 18 months was 9±9% across all 30 compounds. Six of these analytes showed statistically significant changes at some point during storage, compared to initial levels. The seven analytes measured in the field exposed o-DGT varied on average by 14% over the one year period compared to initial. This study also represents an addendum to our previous work with storage of spiked laboratory POCIS, which reported analyte stability up to ≈ 20 months. Here we report analyte stability after ≈ 6 years of freezer storage. Of the sixteen common analytes still used in our current analytical POCIS method, five showed statistically significant losses compared to day zero levels. Overall, the average relative change in mass on POCIS after ≈ 6 years was 14±14%. Our data suggests that analytes stored on o-DGT and POCIS are stable and appropriate for archival purposes.

6.2 INTRODUCTION

Pharmaceuticals and pesticides are contaminants frequently measured in waters using passive sampling devices (PSDs) (Carlson et al., 2013a; Novic et al., 2017; Vrana et al., 2005). Contaminant inputs can be highly stochastic (e.g., driven by runoff events) necessitating intensive monitoring efforts (Andrus et al., 2015, 2013; Carlson et al., 2013a; Novic et al., 2017; Vrana et al., 2005). Thus, the handling of large numbers of samples in the laboratory over a given field sampling season is quite common, making the storage of field-deployed PSDs a convenient and necessary element of water quality monitoring. As well, archived raw samples are inherently valuable. Retrospective analysis of existing samples, using technology unavailable at the time of the original study, can be useful for detecting new compounds (Hernández et al., 2012). However, contaminant exploration done in this way, with processed samples, is limited by the original extraction procedure. Therefore, the ability to work with raw samples (i.e., stored PSDs) to optimize extractions for new and emerging contaminants is highly valuable for contaminant discovery.

Previously, Carlson et al. (2013b) reported the results of a storage study for the polar organic chemical integrative sampler (POCIS), the most popular aquatic PSD for pharmaceuticals and pesticides (Harman et al., 2012). The authors observed stable storage with POCIS in the freezer (-20 °C) for a suite of target analytes over approximately 1.5 years (Carlson et al., 2013b). The utility of this work is evident in studies requiring storage of POCIS prior to analysis (Anderson et al., 2013; Yargeau et al., 2014). There have been studies on the stability of pharmaceutical and pesticide residues in surface waters stored refrigerated (Aboulfadl et al., 2010) and frozen in raw

wastewater samples (Fedorova et al., 2014) and in preserved or pre-treated (e.g., addition of EDTA) water samples (Llorca et al., 2014). A more detailed review of earlier works on aqueous sample storage stability can be found elsewhere (Carlson et al., 2013b). Briefly, these studies generally observe significant losses for several analytes over relatively short time periods, for instance ≤ 10 days (Aboulfadl et al., 2010), ≤ 85 days (Llorca et al., 2014), and ≤ 120 days (Fedorova et al., 2014). Clearly, sequestration of analytes onto a solid sorbent prior to freezing, be it a PSD or solid phase extraction cartridge, can represent the most effective storage and archival option.

As demonstrated throughout this dissertation, while POCIS and other similar polar PSDs (e.g., Chemcatcher) are widely used (Baz-Lomba et al., 2017; Novic et al., 2017), the limitations and uncertainties associated with their application (Harman et al., 2012; Poulier et al., 2014) are a large reason for the relatively recent efforts to develop improved polar-PSDs, as done here (Chapter 3) and elsewhere (Chen et al., 2015; 2013). Given these developments, the o-DGT technique is being adopted for monitoring (Guibal et al., 2017b) as an alternative to the current arsenal of polar PSDs.

Accordingly, a long-term storage study to quantitatively assess stability of polar organic contaminants sequestered onto o-DGT is valuable to end-users. While both POCIS and the o-DGT used here employ the same Oasis HLB sorbent as detailed in Chapters 2 and 3 (Figure 1.5), the nature of how the sorbent is configured within these two samplers differ markedly. POCIS use two polyethersulfone membranes to seal loose sorbent powder between the exposed sampling windows, while o-DGT samplers suspend the sorbent powder in agarose or polyacrylamide hydrogels. The high water content (>95%, Chapter 3) of these hydrogels raises concerns around analyte storage

stability due to potential hydrolysis and physical damage from the freeze/thaw process. Building upon knowledge acquired in our earlier study (Carlson et al., 2013b), wherein POCIS storage stability was evaluated for up to 20 months, o-DGT and POCIS devices were further examined in the present study. We report on the storage stability of 30 polar organic contaminants stored on laboratory-spiked and field-deployed o-DGT for ≈18 months and laboratory POCIS stored for over six years.

6.3 METHODS AND MATERIALS

6.3.1 Chemicals and Reagents

Stock solutions of 30 target analytes (Table 6.1) and 28 internal standard mixtures were prepared in methanol at 10 and 2 ng/µL, respectively. All chemicals were of 95% purity or higher. All stable isotope standards were of >99% isotopic purity. Complete details of standards, chemicals, and reagents in Chapter 3 and Appendix B.

6.3.2 Sampler Details

6.3.2.1 o-DGT Preparation and Extraction

The standard o-DGT configuration used in this experiment was a 0.75 mm, 25 mg OASIS™ HLB (Waters Corporation, Milford, MA) binding gel and a 1.0 mm diffusive gel. All gels were made of 1.5% agarose (molecular biology grade, Sigma-Aldrich, Oakville, ON). Binding gels were extracted using 3×3 mL aliquots of methanol (Fischer Scientific, Ottawa, ON) with sonication for 2 min between each addition. See Chapter 3 for details of o-DGT preparation and extraction.

6.3.2.2 POCIS Preparation and Extraction

POCIS samplers were assembled, spiked, and stored over six years ago as part of our initial study (Carlson et al., 2013b). Briefly, 4 grams of OASIS HLB sorbent was spiked with 600 µL of the target analyte mixture in methanol, followed by a second addition of pure methanol to ensure that the spike material was evenly mixed throughout the sorbent. The phase was dried in the dark until all the methanol had fully evaporated. From the 4 grams of spiked HLB, 18 POCIS were constructed, each containing 200 ± 2 mg of sorbent. POCIS were sealed in a clean container and stored at -20°C until extraction. Extraction of POCIS were done using glass clean-up columns as per our original protocols (Carlson et al., 2013b), described in Chapter 2.

6.3.3 Instrumental Analysis

Chemical analysis was conducted by liquid chromatography-tandem mass spectrometry. Separations were achieved with an Agilent 1200 Series (Agilent Technologies, Mississauga, ON) binary pump, degasser, and column heater connected to a Phenomenex (Torrance, CA) Kinetex XB-C_{18} column (50 mm $\times$ 2.1 mm $\times$ 1.7 µm particle size) and C_{18} SecurityGuard ULTRA Cartridge (2.1 mm I.D.). Detections were made using an Agilent 6410B triple quadrupole instrument equipped with an electrospray ionization source in positive and negative mode under two separate methods. Details of the gradient elution methods, MS source parameters, MS/MS transitions, optimized parameters for analyte detections, and instrument detection limits are provide in Chapter 3 and Appendix B.

6.3.4 Experimental details

This study was intended to mimic realistic sample storage scenarios that end-users may encounter when using PSDs for monitoring. The general study design was to store laboratory-spiked and field-deployed samplers with known analyte concentrations in either the refrigerator or freezer to assess short- and long-term stability, respectively, of analytes on PSDs.

6.3.4.1 Laboratory o-DGT Storage

Loading of o-DGT was achieved by exposing samplers to 5 mM KNO_3 spiked with the analyte mixture in gently-stirred (≈250 rpm) 5 L glass tanks. For the freezer and refrigerator storage experiments, 14 and 6 o-DGT were deployed in separate exposure experiments for 10 days (2.5 µg/L) and 3 days (25 µg/L), respectively. Duplicate o-DGT from each exposure tank were extracted and analyzed immediately to determine the initial concentrations of each analyte for the two exposures. Of the remaining o-DGT, five sets of two were placed fully assembled into individual bags and stored in the freezer at -20 °C. Duplicate sets of samplers were retrieved from storage, spiked with internal standard, extracted, and analyzed at 92, 183, 274, 366, and 563 days. One additional set was disassembled, binding gels placed into 50 mL glass test tubes, and 100 ng of the internal standard mixture was spiked directly onto the binding gels. These tubes were stored in the freezer with the other o-DGT and subsequently retrieved and analyzed after 274 days. These pre-spiked gels demonstrate an alternative approach to storage that theoretically accounts for any losses incurred during storage.

The four loaded o-DGT for the short-term refrigerator study were stored in the dark at 4 °C. Of these, two were stored fully assembled and two were stored in test

tubes as binding gels (not spiked with internal standard) for 25 days. This experiment was to evaluate storage issues with short-term delays that often take place between sampler retrieval and extraction/analysis.

6.3.4.2 Environmental o-DGT Storage

Field-deployed o-DGT were stored in the freezer for 94, 186, and 368 days to assess potential effects of environmental matrices on analyte stability. In total, three duplicate pairs of o-DGT were deployed at the final effluent site of the NHCN wastewater treatment facility described in Chapter 3 and 4. After three weeks, the o-DGT were retrieved and placed in freezer storage as-is. Samplers were visually fouled, providing a complex and realistic environmental matrix for evaluating analyte stability. Site and deployment/retrieval details are in Chapter 3 and 4.

6.3.5 Statistical analysis

Prism v. 5.01 (GraphPad Software, La Jolla, CA) was used for statistical analysis. A one-way ANOVA with a Tukey's post-hoc test was used to compare all storage time points to initial. Statistical significance defined as $p < 0.05$. Least-squares linear regression and F-tests were used to assess if slopes were significantly non-zero.

Table 6.1: Average mass (n=2, ± standard deviation) of compound on laboratory-loaded organic-Diffusive Gradients in Thin-film (o-DGT) passive samplers at each storage time (days, d) and the respective change after 563 days of storage in the freezer (-20 °C).

| Compound | Mass (ng) in o-DGT | | | | | | Δ[b] | Slope[c] |
	0 d	92 d	183 d	274 d (pre-spike)[a]	366 d	563 d		
Atenolol	86±12	88±19	96±1	96±16 (100±21)	89±6	93±14	8%	0.009
Atrazine	291±25	370±19	325±15	331±60 (351±48)	365±2	317±3	9%	0.019
Carbamazepine	321±31	389±19	316±18	343±67 (364±43)	364±6	314±1	-2%	-0.031
Chlorpyrifos	66±7	80±6	77±1	78±11 (80±8)	83±1	74±1	11%	0.009
Clofibric Acid	272±17	336±11	288±11	293±57 (314±50)	334±1	286±1	5%	0.008
Clothianidin	255±18	332±2*	295±6	321±52 (335±45)	348±1*	322±1	26%	0.097
Diazinon	222±17	283±17	248±17	251±43 (258±38)	279±1	265±4	20%	0.050
2,4-D	274±9	324±13	289±2	320±39 (321±30)	327±12	304±6	11%	0.041
Diclofenac	287±8	352±8	315±11	337±45 (345±41)	274±7	245±1	-15%	-0.124**
Enrofloxacin	216±19	286±22	251±2	263±19 (269±50)	261±32	296±30*	37%	0.092
Erythromycin	207±54	249±18	272±76	315±99 (283±21)	n/a	203±49	-2%	-0.019
17β-estradiol	258±56	315±37	304±9	363±20 (354±62)	315±87	259±11	1%	-0.009
Fenoprofen	317±34	387±7	336±21	379±82 (390±88)	354±9	357±10	13%	0.034
Fluoxetine	233±30	300±15	275±25	279±68 (284±52)	291±6	246±9	6%	-0.003
Gemfibrozil	265±10	343±9	302±16	355±58* (334±15)	336±2	305±1	15%	0.046
Ibuprofen	293±22	363±13	328±17	355±61 (373±43)	341±7	306±2	4%	-0.008
Imidacloprid	348±28	395±39	375±11	311±55 (365±82)	424±7	354±4	2%	0.005
Ketoprofen	269±18	364±8*	313±14	334±55 (347±43)	325±9	293±1	9%	-0.005
Metoprolol	267±27	329±30	290±13	286±60 (310±42)	330±11	270±8	1%	-0.009
Naproxen	302±24	380±1	330±7	351±53 (363±45)	352±17	311±2	3%	-0.018
Paroxetine	142±8	142±8	151±13	133±32 (99±19)	166±20	136±26	-4%	0.001
Propranolol	282±27	347±29	305±15	302±63 (323±49)	333±7	289±12	3%	-0.012
Sulfachlorpyridazine	273±19	359±13*	296±15	308±50 (348±24)	319±3	280±13	3%	-0.029
Sulfadimethoxine	285±19	368±10	310±19	315±62 (337±49)	342±6	290±4	2%	-0.026
Sulfamethazine	282±22	356±19	304±17	310±51 (339±37)	345±3	275±4	-3%	-0.033
Sulfamethoxazole	274±18	354±23	314±7	310±59 (350±44)	351±10	339±3	24%	0.078
Sulfapyridine	275±21	336±21	300±16	301±53 (339±41)	326±1	294±6	7%	0.009
Sulfisoxazole	72±7	89±5	84±1	79±17 (62±8)	93±2	80±1	11%	0.010
Thiamethoxam	280±20	364±21	327±10	312±63 (338±41)	335±6	266±9	-5%	-0.064
Trimethoprim	287±26	342±24	284±15	290±58 (320±45)	321±9	288±11	1%	-0.018

n/a – Significant suppression of internal standard in those samples did not allow reliable quantification
a - Mass on binding gel pre-spiked with internal standard and stored for 274 days
b - Change (Δ) in analyte mass at longest time point relative to the day zero mass
c - Linear regression of o-DGT mass as a function of time in days
* - Statistical difference from 0 d mass according to one-way ANOVA and Tukey's post-hoc test (p<0.05)
** - Slope significantly non-zero according to F-test (P value < 0.05)

6.4 RESULTS AND DISCUSSION

6.4.1 Laboratory o-DGT Storage

The average relative absolute variation in analyte mass (calculated throughout as: $\lvert (mass_i – mass_t)/mass_i \rvert \times 100\%)$ on laboratory-loaded o-DGT after 563 days (d) in the freezer was 9% (range: 1-37%) compared to initial masses (Table 6.1). These data are in good agreement with observed changes after 609 d of storage on POCIS (Carlson et al., 2013b). A large majority of target analytes exhibited small non-significant increases in mass after long-term storage. A single compound, enrofloxacin, showed a statistically significant increase (37%) in mass on sampler after 563 d. However, the slope (0.092) of the data (linear regression of the six time points) was not statistically different from zero for that same compound. Diclofenac was the single compound with a statistically non-zero slope (-0.124), however losses after 563 d were only 15%. There is little evidence for systematic, temporal changes in analyte mass during long-term freezer storage, especially when inherent variation (relative standard deviation) is considered for o-DGT duplicates due to experimental and instrument uncertainties. The average RSD for all thirty analytes across all duplicate sets in Table 6.1 (9%; 0-31%) was very similar to the summary statistics describing the overall average change in analyte mass after 563 d of storage (9%; 1-37%), suggesting that much of the observed variation during storage is a result of uncertainties in the loading, extraction, and analysis of o-DGT, and not necessarily related to storage. Furthermore, results from Chapter 3 demonstrate a 20-30% bias in sampling rate calculations when the diffusive boundary layer is ignored, suggesting that errors in this range are not unexpected.

The most convenient method for archiving is, upon sampler retrieval, to place the fully assembled o-DGT in freezer storage. This also represents the only logistically feasible method available for POCIS storage (Carlson et al., 2013b). However, because of the o-DGT design, the sorbent containing analytes is suspended in a solid hydrogel, making it safe to manipulate post-retrieval without risking sorbent/analyte losses. Therefore, the option to store the binding gel separate from the outer diffusive gel and sampler casing is available and potentially advantageous in situations where the exterior of the sampler becomes sufficiently fouled (Figure B9) or the sampler casings are needed for future deployments. Furthermore, having the binding gel safely exposed in a storage vessel (e.g., test tube) allows the end-user to enrich quantitatively the binding gel with internal standard pre-storage, theoretically accounting for any losses that may occur during the storage period. This approach is demonstrated in Table 6.1 at 274 d (pre-spike). No statistical differences were observed for all thirty analytes, comparing the pre-spiked binding gels to both the fully assembled o-DGT at 274 d and 0 d. Of course, spiking the binding gel prior to storage is only applicable to targeted analyte applications that have pre-developed analytical methods and purchased standards. For example, this storage option may be of use for analytes suspected to be particularly labile. However, for long-term archival purposes this is likely not a preferred method of storage. Furthermore, given that no significant losses are observed for the fully assembled o-DGT over the same time frame and longer, we recommend storing the retrieved sampler as-is.

Table 6.2: Average mass (n=2, ± standard deviation) of compound on laboratory-loaded o-DGT after storage in the fridge (4 °C) and the respective change after 25 d. Storage of just the binding gel was compared to storage of the fully assembled o-DGT.

Compound	0 d	Binding gel 25 d (Δ^a)	Assembled o-DGT 25 d (Δ^a)
		o-DGT mass (ng)	
Atenolol	232±12	220±10 (-5%)	224±10 (4%)
Atrazine	429±7	445±12 (4%)	426±11 (-1%)
Carbamazepine	459±8	497±1 (8%)*	483±1 (5%)*
Chlorpyrifos	206±18	226±16 (10%)	184±4 (10%)
Clofibric Acid	438±6	466±19 (6%)	466±3 (6%)
Clothianidin	455±10	473±18 (4%)	465±9 (2%)
Diazinon	352±9	371±13 (6%)	359±3 (2%)
2,4-D	472±12	471±20 (0%)	475±3 (1%)
Diclofenac	373±5	343±12 (-8%)	342±2 (-9%)*
Enrofloxacin	486±40	483±28 (-1%)	528±38 (9%)
Erythromycin	388±69	432±130 (11%)	n/a
17β-estradiol	469±125	422±136 (-10%)	338±53 (-28%)
Fenoprofen	411±10	430±72 (5%)	408±8 (-1%)
Fluoxetine	406±14	404±28 (0%)	424±6 (5%)
Gemfibrozil	407±13	413±44 (2%)	393±11 (-3%)
Ibuprofen	429±14	469±26 (9%)	455±12 (6%)
Imidacloprid	461±63	514±38 (12%)	507±10 (10%)
Ketoprofen	421±7	387±10 (-8%)*	380±2 (-10%)*
Metoprolol	420±15	411±11 (-2%)	413±3 (-2%)
Naproxen	445±17	463±34 (4%)	447±7 (0%)
Paroxetine	406±22	345±84 (-15%)	406±17 (0%)
Propranolol	418±2	439±17 (5%)	424±5 (2%)
Sulfachlorpyridazine	415±3	432±3 (4%)	442±16 (6%)
Sulfadimethoxine	436±11	431±23 (1%)	421±15 (-4%)
Sulfamethazine	436±10	455±10 (4%)	447±2 (3%)
Sulfamethoxazole	457±2	490±22 (7%)	475±4 (4%)
Sulfapyridine	483±7	493±13 (2%)	488±2 (1%)
Sulfisoxazole	417±8	420±12 (1%)	426±14 (2%)
Thiamethoxam	440±9	466±43 (6%)	467±4 (6%)
Trimethoprim	438±5	441±10 (1%)	439±11 (0%)

n/a – Significant suppression of internal standard response did not allow reliable quantification
a - Change (Δ) in analyte mass relative to the day zero mass
* - Statistical difference from 0 d mass according to one-way ANOVA and Tukey's post-hoc test ($p < 0.05$)

An analogous short-term storage (e.g., one month) experiment was conducted in the refrigerator at 4 °C to mimic potential delays that can inevitably occur during sample processing. The average variation between the two storage sets at 25 d compared to initial was 5% (Table 6.2). The maximum change observed was 15% (paroxetine) and 28% (17β-estradiol) for binding gel and fully assembled o-DGT, respectively. The latter

uncertainty is likely related to the known analytical challenges regarding our estrogen method as opposed to true observed losses. This is evident in the large RSD (25% average) associated with 17β-estradiol for the three duplicate sets in Table 6.2. Carbamazepine, diclofenac, and ketoprofen showed statistically significant changes in analyte mass after 25 d in one or both sets of o-DGT. However, these were ≤10% in all cases, and thus do not represent a significant concern regarding stability. Our results suggest that short-term storage (days to weeks) of o-DGT in the fridge, by either method, is stable however should not exceed one month. As discussed above, the addition of internal standard prior to short term fridge storage represents a safe option, especially when delays occur after the extraction process has already been initiated (i.e., binding gels placed in extraction test tubes).

6.4.2 Environmental o-DGT Storage

The o-DGT deployed in the wastewater treatment plant demonstrate analyte storage after exposure to a real environmental matrix and represents actual use of many PSDs (Anderson et al., 2013; Yargeau et al., 2014). The storage data in this case were limited to the occurrence and detection of analytes at the specific sampling site, namely, atrazine, carbamazepine, gemfibrozil, naproxen, sulfamethoxazole, sulfapyridine, and trimethoprim (Table 6.3). Average changes in analyte mass after 368 d of storage was 14%. Atrazine and gemfibrozil showed 40% and 28% increases in mass relative to initial. The only statistically significant results were observed for atrazine, which showed a mass increase after 368 d and significantly positive slope (p=0.002, n=4 for linear regression). The exact reasons for these increases is unclear, however larger errors are expected for the environmental samples (Carlson et al.,

2013b). Some of this variation may result from differences in orientation between two PSD cages and/or o-DGT samplers within the same cage (the eight o-DGT used here were deployed in two side-by-side cages). This may cause certain samplers to experience differing flow regimes (Ahkola et al., 2015) or lead to preferential fouling of certain o-DGT samplers compared to others (Chapter 4, Table C8). It should be noted that these o-DGT were severely fouled after the three-week deployment (Figure B9). Additionally, it is worth noting that the absolute change in atrazine concentration from 1.0 to 1.4 µg/L (on sampler) is still relatively small (Table 6.3), especially when considered in the context of ecological relevance. Considering these factors, our data suggest that stability after one year of storage on environmental o-DGT is viable, at least for the target analytes investigated during the present survey. Additionally, the observed variations were within reasonable range, given the uncertainties expected for such passive sampling measurements (Bartelt-Hunt et al., 2011; Jacquet et al., 2012; Poulier et al., 2014).

Table 6.3: Average mass (n=2, ± standard deviation) of compound on field deployed o-DGT at each storage time and the respective change after 368 d of storage in the freezer (-20 °C).

Compound	o-DGT mass (ng)				Δ^a	Slope[b]
	0 d	94 d	186 d	368 d		
Atrazine	1.0±0.1	1.2±0.1	1.2±0.1	1.4±0.2*	40%	0.002**
Carbamazepine	299±52	330±11	336±17	273±8	-9%	-0.089
Gemfibrozil	14±2	17±1	17±2	17±1	28%	0.009
Naproxen	7±2	11±2	10±1	8±1	6%	0.001
Sulfamethoxazole	183±25	181±3	186±4	175±6	-4%	-0.019
Sulfapyridine	27±4	26±1	27±1	26±1	-4%	-0.002
Trimethoprim	85±14	101±11	87±5	78±1	-8%	-0.034

a - Change (Δ) in analyte mass at longest time point relative to the day zero mass
b - Linear regression of o-DGT mass as a function of time in days
* - Statistical difference from 0 d mass according to one-way ANOVA and Tukey's post-hoc test (p<0.05)
** - Slope significantly non-zero according to F-test (P value < 0.05)

6.4.3 POCIS Storage

Carlson et al. (2013b) reported analyte stability data stored on POCIS up to 609 d. The aforementioned data, along with POCIS stored for over 6 years, are presented in Table 6.4. Sixteen of these analytes are common between the study of Carlson et al. (2013b) and our current analytical POCIS method. Five of the analytes that exhibited statistically significant losses after 609 d in the original storage study (atrazine, clofibric acid, gemfibrozil, sulfadimethoxine, and sulfamethoxazole) also exhibited significant losses after 6 years, compared to day zero levels. Of these, only clofibric acid showed further losses after 6 years (-31%) compared to 2 years (-17%). The average absolute change after 6 years for all sixteen analytes was 14%, compared to 12% for those same analytes after 2 years. There are a few instances (atenolol, diclofenac, sulfamethazine) where non-significant increases were observed after 6 years, compared to initial and 2 years. As mentioned previously for o-DGT, and discussed elsewhere (Carlson et al., 2013b), these non-significant fluctuations above and below initial levels are likely artefacts resulting from the uncertainties involved with spiking and extracting POCIS samples.

Table 6.4: Average mass (n=2, ± standard deviation) of analyte on laboratory spiked POCIS initially, after freezer storage for ≈ 1.5 years (data initially published in Carlson et al., 2013b), and after 6 years (present study).

Compound	POCIS mass (ng)		
	0 d	609 d (Δ^a)	2241 d (Δ^a)
Atenolol	259±7	243±11 (-6%)	290±10 (12%)
Atrazine	310±4	270±24 (-13%)*	267±9 (-14%)*
Carbamazepine	298±9	284±32 (-5%)	279±30 (-6%)
Chlorpyrifos	278±19	253±41 (-9%)	266±16 (-4%)
Clofibric Acid	335±11	277±12 (-17%)*	231±8 (-31%)*,**
Diclofenac	259±6	234±33 (-10%)	287±36 (11%)
Fluoxetine	287±17	302±20 (5%)	213±55 (-26%)**
Gemfibrozil	333±21	276±14 (-17%)*	283±20 (-15%)*
Metoprolol	313±15	283±20 (-10%)	254±33 (-19%)
Propranolol	276±21	239±21 (-13%)	276±67 (0%)
Sulfachlorpyridazine	277±11	260±43 (-6%)	243±27 (-12%)
Sulfadimethoxine	298±3	252±7 (-16%)*	258±7 (-14%)*
Sulfamethazine	281±14	249±23 (-11%)	307±35 (9%)
Sulfamethoxazole	371±31	252±39 (-32%)*	249±12 (-33%)*
Sulfapyridine	288±32	265±31 (-8%)	240±12 (-17%)
Trimethoprim	269±9	234±16 (-13%)	249±15 (-7%)

a - Change (Δ) in analyte mass at longest time point relative to the day zero mass
* - Statistical difference from 0 d mass according to one-way ANOVA and Tukey's post-hoc test ($p<0.05$)
** - Statistical difference from 609 d according to one-way ANOVA and Tukey's post-hoc test ($p<0.05$)

6.5 CONCLUSIONS

Overall, it appears that analyte stability on o-DGT is feasible for at least one year and on POCIS for at least six years. Therefore, both passive samplers serve as viable archival tools for monitoring programs interested in doing contaminant discovery on original samples at a later date. While both POCIS and o-DGT represent convenient storage tools for polar organic contaminants, there are, as demonstrated here, inherent errors and uncertainties associated with these storage processes. Immediate extraction and analysis of these environmental samples is always ideal. If and when storage is required, it is imperative that end-users do so with caution and report any associated uncertainties.

CHAPTER 7

7. OVERALL SYNTHESIS

Jonathan K. Challis

7.1 Summary and Novelty of Research Findings

Acquiring representative samples is crucial to accurately characterizing the occurrence, behaviour, and fate of chemicals in the environment. Passive sampling has become a popular tool for this purpose, the accuracy and applicability of which relies upon our understanding of how a given PSD operates (e.g., mass-transfer mechanisms, linear uptake range) and the uncertainties involved in its application. For current aquatic polar-PSDs an understanding of these fundamental uncertainties is lacking, leading to significant challenges for end-users of these techniques. The research in this dissertation describes the development, calibration, and field evaluation of the o-DGT passive sampler and the characterization of polar organic contaminants in surface waters using o-DGT and POCIS.

Chapter 2 used POCIS to characterize the occurrence and transport of pesticides and pharmaceuticals along the lower Red River valley. Atrazine, a number of neonicotinoids, and carbamazepine were measured most frequently across all sites over the two year sampling campaign. Chemical fluxes were calculated from the TWA POCIS concentrations to identify major sources of each analyte. Transboundary flux from the U.S. was identified as the major source of atrazine along the Red River and into Lake Winnipeg. Neonicotinoid sources were more diffuse, with inputs from the U.S., and south and west Manitoba. Carbamazepine was ubiquitous at low ng/L levels throughout the Red River, with spikes observed downstream of the City of Winnipeg North End WWTP where a suite of other pharmaceuticals were also detected. PFAS and ARGs were detected throughout the river, indicative of an anthropogenically-influenced system. All contaminants measured were below their individual levels of

concern when compared to short- and long-term protection of aquatic life benchmarks. Overall, POCIS served as a useful monitoring tool, however challenges with sampling rate variation were apparent and led to unknown uncertainties in our reported concentrations.

Chapters 3 and 4 focused on the development, calibration, and field evaluation of the o-DGT sampler and represent the most significant contributions from this dissertation. The following section describes a number of major findings and important implications stemming from these specific projects.

Chapter 3 summarizes the development of o-DGT:

- The o-DGT configuration developed in this work excluded the outer PES protective membrane used in all other polar-PSDs. The exclusion of PES simplified analyte uptake into o-DGT without impairing sampler functionality.

- Sampler calibration of o-DGT demonstrated sufficient capacity and linear uptake of all 34 target analytes over typical deployment times. Sampling rates were experimentally measured and ranged from 9-16 mL/day. This represented the first full calibration experiment conducted with o-DGT for a suite of analytes.

- Diffusion coefficients (D) were measured through the outer diffusive gel at three temperatures (T), facilitating the development of compound specific D-T empirical relationships whereby D could be calculated according to the temperature of the study system. A universal D-T relationship was tested against the compound-specific empirical data and demonstrated accurate D

estimations at any temperature. This is the first work to demonstrate the validity and accuracy of the D-T relationship for polar organic chemicals.

- Sampling rates calculated from D were within 20% (average relative error) of the experimentally measured R_s from the calibration study. These data suggests that R_s can be accurately estimated based on a molecules diffusion coefficient alone, greatly reducing the need for laborious full-sampler calibration studies.

- D was also modelled based on molecular volume using the empirical Hayduk-Laudie diffusivity relationship to determine the feasibility of estimating sampling rates based strictly on chemical structure. Average relative errors in modelled sampling rates were ≈30%, well within reasonable errors expected for most environmental measurements with PSDs. This effort represents the first attempts to validate an uptake model for o-DGT. The success of this model is largely attributed to the exclusion of the PES membrane.

- The diffusive boundary layer was measured under controlled flowing and static lab conditions and *in-situ* to test the hypothesis that o-DGT uptake is largely insensitive to hydrodynamic conditions. Above quiescent conditions the DBL ranged from ≈0.2 mm (lab) – 0.4 mm (field). By applying the typical DGT uptake equation that ignores the presence of a DBL, a typical 1 mm diffusive hydrogel would underestimate water concentrations by ≈20-30%.

Chapter 4 describes the comprehensive field testing of o-DGT:

- The field evaluations conducted in this chapter demonstrated that o-DGT is a viable and accurate PSD under a range of highly relevant aquatic conditions.

- The Red River was studied with o-DGT in much the same manner as in Chapter 2 with POCIS in order to compare the two techniques. In general, very similar contaminant trends were observed in 2016 with o-DGT and 2014-15 with POCIS (Chapter 2). The durability of o-DGT in a fast-flowing large river system was demonstrated. Overall, o-DGT without the PES membrane survived these conditions well over 2-3 week deployments, with the exception of a few instances where the agarose diffusive gel was grazed on and degraded by aquatic insects.

- Additionally, side-by-side deployments of o-DGT and POCIS were conducted in the Red River for direct comparisons. A systematic underestimation of TWA water concentrations was observed for POCIS compared to o-DGT. Select grab sampling over the course of passive sampler deployments in Dead Horse Creek and the NHCN WWTP (Chapter 3) and integrative active sampling in Toronto (Chapter 5) suggested that o-DGT concentrations were more accurate than POCIS, and that POCIS was underestimating the true water concentrations. This was attributed to the *in-situ* flow-rate and temperature conditions that are known to have a significant impact on POCIS sampling rates and serve to reduce uptake rates *in-situ* compared to those measured in the lab.

- Deployments in Lake Winnipeg and under ice in Little Playgreen Lake served to further test the durability of the o-DGT sampler under challenging field conditions. The o-DGT samplers proved durable during extended deployments (>40 days) in Lake Winnipeg and at near-zero water temperatures under ice.

The ability to adjust o-DGT sampling rates for near-zero temperatures was key to acquiring accurate water concentrations as uptake rates were 3-10 times lower compared to room-temperature. This work highlights the utility of o-DGT for potential applications to monitoring in extreme environments, such as the Arctic.

Chapter 5 utilizes o-DGT as a screening tool for suspect wastewater contaminants using HRMS. This work used the diffusion uptake model validated in Chapter 3 to estimate sampling rates for suspect compounds based strictly on molecular structure. Additionally, to provide a fully semi-quantitative approach we developed an average surrogate response method to quantify the suspect compounds by HRMS without matched internal standards. Overall, o-DGT TWA concentrations of suspect compounds were within 2-fold of the confirmed concentration. This study represents the first semi-quantitative approach to suspect screening using a PSD.

Chapter 6 describes the stability of analytes stored on o-DGT and POCIS samplers in the freezer for extended periods. Analytes were stable for >1.5 years on o-DGT and >6 years on POCIS, suggesting both PSDs serve as convenient and viable mechanism to archive environmental samples for retrospective monitoring and later screening of emerging and novel compounds.

Overall this research supports the use of o-DGT passive sampler as an accurate measurement tool that 1) is insensitive to hydrodynamic flow conditions, 2) can account for temperature fluctuations *in-situ*, and 3) can accurately use measured or modelled diffusion-based sampling rates. These three factors greatly improve the accuracy and applicability of o-DGT across differing aquatic conditions compared to current-use polar-

PSDs and reduces the need for laboratory or *in-situ* calibrations. Despite the much smaller sampling rates compared to POCIS, detection limits of o-DGT, even in high dilution scenarios, did not appear to be an issue. This may have, in part, been related to the much cleaner sample matrices resulting from o-DGT extraction compared to POCIS, leading to improved analytical detections.

7.2 Challenges and Future Directions

There were a number of challenges encountered throughout this dissertation that serve as logical recommendations for future work to further the development and improve our understanding of the uncertainties inherent with both o-DGT and POCIS techniques. Many of the limitations of this work relate to a lack of complete characterization regarding specific aspects of the o-DGT development. Much of this can be attributed to a lack of time. Over the course of a PhD program, one can simply not cover all possible directions a project of this scope can take. As such, a number of fundamental questions regarding o-DGT development remain. I caution the passive sampling community to not cut short the fundamental development and understanding of this promising new o-DGT technique and learn from the challenges currently facing POCIS end-users. Although POCIS remains an important and useful PSD, I believe many of the uncertainties associated with the technique relate to a lack of fundamental understanding of analyte uptake and a failure to develop standardized approaches to calibrate POCIS and accurately measure sampling rates.

The development of o-DGT began with both agarose and polyacrylamide gels as diffusive membranes. In fact, the initial diffusion coefficient experiments were conducted with polyacrylamide gels. For largely logistical reasons, agarose was chosen as the

ideal gel for full-scale development. The primary reason behind this was that agarose did not swell when soaked in water, meaning the gel dimensions were more consistent and easier to characterize. It was only after many successful deployments in wastewaters and natural waters did the issue of agarose degradation emerge. While the occurrence was rare (≈5% of deployments) and isolated to specific sites it was apparent that polyacrylamide may serve as a more resistant diffusive gel.

The development of an o-DGT variant with a polyacrylamide diffusive gel has since been conducted in our lab, for which I was extensively involved with and co-authored the publication (Stroski et al., 2018). The pore size of polyacrylamide gels are more restricted compared to agarose, consistent with the slightly smaller diffusion coefficients and sampling rates observed with the former. However, a unique aspect of polyacrylamide is that the pore sizes of the gel are tunable based on the amount of cross-linker added. This may provide the opportunity to optimize the pore size to increase diffusivity and thus uptake rates while maintaining sufficient gel strength.

This effort also addressed two areas of o-DGT development not conducted as part of my dissertation research, namely, sorbent type and possible pH effects. The HLB sorbent used in the development of o-DGT was chosen specifically to facilitate comparisons with POCIS. However, Waters OASIS® HLB sorbent is only sold in solid phase extraction products and not in bulk, making it prohibitively expensive for the typical end-user interested in assembling their own samplers. A cheaper and more readily available sorbent analogous to HLB was successfully tested and used as the binding resin.

Additionally, the effect of pH on o-DGT uptake was tested in this study. While the majority of compounds were unaffected by solution pH, certain compounds (e.g., sulfonamide antibiotics) exhibited decreased or in some cases no uptake at a pH above or below their pKa. This was attributed to a reduced binding efficiency and capacity when, for example, the sulfonamides were in their fully deprotonated state. These findings highlight important implications that apply to all polar-PSDs relying on sorptive-type interactions to sequester analytes (e.g., o-DGT, POCIS, Chemcatcher). Under specific pH conditions certain compounds that are present in the environment may not be detected at all, or uptake rates will be significantly decreased *in-situ* leading to uncertainties in calculated concentrations when using a sampling rate determined at a different pH. Compounds most vulnerable to this issue appear to have pKa's within the pH range of typical surface waters. While Stroski et al. (2018) provides an important characterization of this pH issue, further work is required to fully understand the governing sorption mechanisms leading to this reduced uptake, and by extension develop a model to account for these pH effects.

This work also demonstrated that under certain conditions o-DGT uptake is controlled by more than simply diffusion through the diffusive gel. The specific conditions that may result in these scenarios are absolutely crucial to characterize in order to understand the uncertainties and limitations of this and other polar PSDs.

Biofouling and the formation of biofilms on o-DGT during deployments are inevitable. While our *in-situ* field deployments provide indirect evidence that fouling of the outer diffusive gel does not have a significant effect on uptake (e.g., Chapter 3), this remains an environmental condition that has not been systematically characterized.

This could be investigated in a relatively straight forward manner by conducting sampler calibrations with fouled diffusive gels.

The o-DGT uptake model based on the empirical Hayduk-Laudie relationship should be further validated. Although the diffusive hydrogels are comprised of >95% water, there is likely a correction factor required to reconcile hydrogel diffusion with diffusion in water, which the Hayduk-Laudie model was developed for. Additionally, it may be useful to explore more advanced computational modelling approaches to provide more accurate estimates of diffusivities.

The more general theme addressed throughout this dissertation relates to the sources and occurrence of polar organic contaminants in aquatic systems. It is clear that the presence of pharmaceuticals, pesticides, and other consumer and industrial use chemicals in the environment represents a permanent problem, likely only to increase with an increasing global population. Therefore, the role of environmental scientists and engineers relates mostly to improved monitoring, remediation and treatment, and chemical management of these environmental contaminants. The work presented here focuses on improving our ability to accurately and efficiently monitor these chemicals in the environment in order to better understand which chemicals are present and at what levels, representing the cornerstone to effective exposure and risk assessment (e.g., Chapter 3) and ultimately responsible chemical management and policy decisions around chemicals of concern.

Treatment of point-source pollution is another crucial aspect to environmental protection, especially as it relates to wastewaters. Although wastewater treatment approaches are beyond the scope of this dissertation, it is important to understand that

environmental monitoring feeds into regulatory decisions regarding the implementation of or improvements to wastewater treatment systems. Identifying contaminants of concern that may warrant more targeted or advanced treatment requires a considerable amount of supporting evidence, beginning with the accurate and comprehensive spatial and temporal characterization of the contaminant in waste and receiving waters, as demonstrated in Chapters 3 and 4. Overall, the data presented in this dissertation can be utilized precisely for these purposes, namely, to inform exposure and risk assessment and appropriate chemical management of polar organic contaminants in these and other comparable surface waters.

More specifically, this work represents a major contribution to the field of passive sampling and significantly advances our ability to acquire accurate and representative environmental measurements affordably and efficiently. The most powerful and unique aspect of o-DGT is its ability to account for flow-rate and temperature effects on sampler uptake and by extension make simple laboratory measurements and models (e.g., diffusivity) viable predictors of sampler uptake *in-situ*. Already, the o-DGT sampler is being adopted and further developed by the passive sampling community. Trusting that many of the remaining fundamental questions highlighted here are addressed as this technique progresses, it is very likely that o-DGT passive samplers will be widely adopted as a valuable PSD for polar organic contaminants in aquatic systems.

8. REFERENCES

Aboulfadl, K., De Potter, C., Prévost, M., Sauvé, S., **2010**. Time-dependent integrity

    during storage of natural surface water samples for the trace analysis of

    pharmaceutical products, feminizing hormones and pesticides. *Chem. Cent. J.* 4,

    10.

Ahkola, H., Juntunen, J., Laitinen, M., Krogerus, K., Huttula, T., Herve, S., Witick, A.,

    2015. Effect of the orientation and fluid flow on the accumulation of organotin

    compounds to Chemcatcher passive samplers. *Environ. Sci. Process. Impacts* 17,

    813–824.

Alder, A.C., Schaffner, C., Majewsky, M., Klasmeier, J., Fenner, K., **2010**. Fate of beta-

    blocker human pharmaceuticals in surface water: Comparison of measured and

    simulated concentrations in the Glatt Valley Watershed, Switzerland. *Water Res.*

    44, 936–948.

Allan, I.J., Booij, K., Paschke, A., Vrana, B., Mills, G.A., Greenwood, R., **2009**. Field

    performance of seven passive sampling devices for monitoring of hydrophobic

    substances. *Environ. Sci. Technol.* 43, 5383–5390.

Alvarez, D.A., Petty, J.D., Huckins, J.N., Jones-Lepp, T.L., Getting, D.T., Goddard, J.P.,

    Manahan, S.E., **2004**. Development of a Passive, in Situ, Integrative Sampler for

    Hydrophilic Organic Contaminants in Aquatic Environments. *Environ. Toxicol.*

    Chem. 23, 1640.

Anderson, J.C., Carlson, J.C., Low, J.E., Challis, J.K., Wong, C.S., Knapp, C.W.,

    Hanson, M.L., **2013**. Performance of a constructed wetland in Grand Marais,

    Manitoba, Canada: Removal of nutrients, pharmaceuticals, and antibiotic

resistance genes from municipal wastewater. *Chem. Cent. J.* 7.

Anderson, J.C., Dubetz, C., Palace, V.P., **2015a**. Neonicotinoids in the Canadian aquatic environment: A literature review on current use products with a focus on fate, exposure, and biological effects. *Sci. Total Environ.* 505, 409–422.

Anderson, J.C., Joudan, S., Shoichet, E., Cuscito, L.D., Alipio, A.E.C., Donaldson, C.S., Khan, S., Goltz, D.M., Rudy, M.D., Frank, R.A., Knapp, C.W., Hanson, M.L., Wong, C.S., **2015b**. Reducing nutrients, organic micropollutants, antibiotic resistance, and toxicity in rural wastewater effluent with subsurface filtration treatment technology. *Ecol. Eng.* 84, 375–385.

Anderson, P.D., D'Aco, V.J., Shanahan, P., Chapra, S.C., Buzby, M.E., Cunningham, V.L., Duplessie, B.M., Hayes, E.P., Mastrocco, F.J., Parke, N.J., Rader, J.C., Samuelian, J.H., Schwab, B.W., **2004**. Screening Analysis of Human Pharmaceutical Compounds in U.S. Surface Waters. *Environ. Sci. Technol.* 38, 838–849.

Andreozzi, R., Marotta, R., Paxéus, N., **2003**. Pharmaceuticals in STP effluents and their solar photodegradation in aquatic environment. *Chemosphere* 50, 1319–1330.

Andrus, J.M., Winter, D., Scanlan, M., Sullivan, S., Bollman, W., Waggoner, J.B., Hosmer, A.J., Brain, R.A., **2015**. Spatial and temporal variation of algal assemblages in six Midwest agricultural streams having varying levels of atrazine and other physicochemical attributes. *Sci. Total Environ.* 505, 65–89.

Andrus, J.M., Winter, D., Scanlan, M., Sullivan, S., Bollman, W., Waggoner, J.B., Hosmer, A.J., Brain, R.A., **2013**. Seasonal synchronicity of algal assemblages in three Midwestern agricultural streams having varying concentrations of atrazine,

nutrients, and sediment. *Sci. Total Environ.* 458–460, 125–139.

Arditsoglou, A., Voutsa, D., **2008**. Passive sampling of selected endocrine disrupting

compounds using polar organic chemical integrative samplers. *Environ. Pollut.* 156,

316–324.

Arnold, K.E., Brown, A.R., Ankley, G.T., Sumpter, J.P., **2014**. Medicating the

environment: assessing risks of pharmaceuticals to wildlife and ecosystems. *Philos.*

Trans. R. Soc. B Biol. Sci. 369, 20130569–20130569.

Backhaus, T., **2014**. Medicines, shaken and stirred: a critical review on the

ecotoxicology of pharmaceutical mixtures. *Philos. Trans. R. Soc. B Biol. Sci.* 369,

20130585–20130585.

Bade, R., Bijlsma, L., Sancho, J. V., Hernández, F., **2015**. Critical evaluation of a simple

retention time predictor based on LogKow as a complementary tool in the

identification of emerging contaminants in water. *Talanta* 139, 143–149.

Banerjee, K., Utture, S., Dasgupta, S., Kandaswamy, C., Pradhan, S., Kulkarni, S.,

Adsule, P., **2012**. Multiresidue determination of 375 organic contaminants including

pesticides, polychlorinated biphenyls and polyaromatic hydrocarbons in fruits and

vegetables by gas chromatography-triple quadrupole mass spectrometry with

introduction of semi-quantificatio. *J. Chromatogr. A* 1270, 283–295.

Bartelt-Hunt, S.L., Snow, D.D., Damon-Powell, T., Brown, D.L., Prasai, G., Schwarz, M.,

Kolok, A.S., **2011**. Quantitative evaluation of laboratory uptake rates for pesticides,

pharmaceuticals, and steroid hormones using POCIS. *Environ. Toxicol. Chem.* 30,

1412–1420.

Bäuerlein, P.S., Mansell, J.E., Ter Laak, T.L., De Voogt, P., **2012**. Sorption behavior of

charged and neutral polar organic compounds on solid phase extraction materials: Which functional group governs sorption? *Environ. Sci. Technol.* 46, 954–961.

Baz-Lomba, J.A., Harman, C., Reid, M., Thomas, K. V., **2017**. Passive sampling of wastewater as a tool for the long-term monitoring of community exposure: Illicit and prescription drug trends as a proof of concept. *Water Res.* 121, 221–230.

Beek, T. aus der, Weber, F.A., Bergmann, A., Hickmann, S., Ebert, I., Hein, A., Küster, A., **2016**. Pharmaceuticals in the environment-Global occurrences and perspectives. *Environ. Toxicol. Chem.* 35, 823–835.

Belles, A., Alary, C., Aminot, Y., Readman, J.W., Franke, C., **2017**. Calibration and response of an agarose gel based passive sampler to record short pulses of aquatic organic pollutants. *Talanta* 165, 1–9.

Bijlsma, L., Emke, E., Hernández, F., De Voogt, P., **2013**. Performance of the linear ion trap Orbitrap mass analyzer for qualitative and quantitative analysis of drugs of abuse and relevant metabolites in sewage water. *Anal. Chim. Acta* 768, 102–110.

Bodhipaksha, L.C., Sharpless, C.M., Chin, Y.P., Sander, M., Langston, W.K., Mackay, A.A., **2015**. Triplet photochemistry of effluent and natural organic matter in whole water and isolates from effluent-receiving rivers. *Environ. Sci. Technol.* 49, 3453–3463.

Booij, K., Maarsen, N.L., Theeuwen, M., van Bommel, R., **2017**. A method to account for the effect of hydrodynamics on polar organic compound uptake by passive samplers. *Environ. Toxicol. Chem.*

Booij, K., Robinson, C.D., Burgess, R.M., Mayer, P., Roberts, C.A., Ahrens, L., Allan, I.J., Brant, J., Jones, L., Kraus, U.R., Larsen, M.M., Lepom, P., Petersen, J.,

Pröfrock, D., Roose, P., Schäfer, S., Smedes, F., Tixier, C., Vorkamp, K., Whitehouse, P., **2016**. Passive Sampling in Regulatory Chemical Monitoring of Nonpolar Organic Compounds in the Aquatic Environment. *Environ. Sci. Technol.* 50, 3–17.

Booij, K., Vrana, B., Huckins, J.N., **2007**. Chapter 7 Theory, modelling and calibration of passive samplers used in water monitoring, in: Comprehensive Analytical Chemistry. Elsevier, pp. 141–169.

Boreen, A.L., Arnold, W.A., McNeill, K., **2005**. Triplet-sensitized photodegradation of sulfa drugs containing six-membered heterocyclic groups: Identification of an SO2 extrusion photoproduct. *Environ. Sci. Technol.* 39, 3630–3638.

Boreen, A.L., Arnold, W.A., McNeill, K., **2004**. Photochemical fate of sulfa drugs in then aquatic environment: Sulfa drugs containing five-membered heterocyclic groups. *Environ. Sci. Technol.* 38, 3933–3940.

Boreen, A.L., Arnold, W.A., McNeill, K., **2003**. Photodegradation of pharmaceuticals in the aquatic environment: A review. *Aquat. Sci.* 65, 320–341.

Bourne, A., Armstrong, N., Jones, G., **2002**. A preliminary estimate of total nitrogen and total phosphorus loading to streams in Manitoba, Canada. Water Quality Management Section. Manitoba Conservation Report No. 2002-04.

Boxall, A.B.A., Rudd, M.A., Brooks, B.W., Caldwell, D.J., Choi, K., Hickmann, S., Innes, E., Ostapyk, K., Staveley, J.P., Verslycke, T., Ankley, G.T., Beazley, K.F., Belanger, S.E., Berninger, J.P., Carriquiriborde, P., Coors, A., DeLeo, P.C., Dyer, S.D., Ericson, J.F., Gagné, F., Giesy, J.P., Gouin, T., Hallstrom, L., Karlsson, M. V, Larsson, D.G.J., Lazorchak, J.M., Mastrocco, F., McLaughlin, A., McMaster, M.E.,

Meyerhoff, R.D., Moore, R., Parrott, J.L., Snape, J.R., Murray-Smith, R., Servos, M.R., Sibley, P.K., Straub, J.O., Szabo, N.D., Topp, E., Tetreault, G.R., Trudeau, V.L., Van Der Kraak, G., **2012**. Pharmaceuticals and personal care products in the environment: what are the big questions? *Environ. Heal. Perspect.* 120, 1221–1229.

Brodin, T., Piovano, S., Fick, J., Klaminder, J., Heynen, M., Jonsson, M., **2014**. Ecological effects of pharmaceuticals in aquatic systems--impacts through behavioural alterations. *Philos. Trans. R. Soc. B Biol. Sci.* 369, 20130580–20130580.

Brooks, B.W., Chambliss, C.K., Stanley, J.K., Ramirez, A., Banks, K.E., Johnson, R.D., Lewis, R.J., **2005**. Determination of select antidepressants in fish from an effluent-dominated stream 24, 464–469.

Brooks, B.W., Huggett, D.B., Boxall, A.B. a, **2009**. Pharmaceuticals and personal care products: Research needs for the next decade. *Environ. Toxicol. Chem.* 28, 2469–2472.

Brown, A.K., Challis, J.K., Wong, C.S., Hanson, M.L., **2015**. Selective serotonin reuptake inhibitors and β-blocker transformation products may not pose a significant risk of toxicity to aquatic organisms in wastewater effluent-dominated receiving waters. *Integr. Environ. Assess. Manag.* 11, 618–639.

Brown, A.K., Wong, C.S., **2015**. Current trends in environmental analysis of human metabolite conjugates of pharmaceuticals. *Trends Environ. Anal. Chem.* 5, 8–17.

Bu, Q., Wang, D., Liu, X., Wang, Z., **2014**. A high throughout semi-quantification method for screening organic contaminants in river sediments. *J. Environ. Manage.*

143, 135–139.

Byrne-Bailey, K.G., Gaze, W.H., Kay, P., Boxall, A.B.A., Hawkey, P.M., Wellington, E.M.H., **2009**. Prevalence of sulfonamide resistance genes in bacterial isolates from manured agricultural soils and pig slurry in the United Kingdom. *Antimicrob. Agents Chemother.* 53, 696–702.

Caetano, S., Decaestecker, T., Put, R., Daszykowski, M., Van Bocxlaer, J., Vander Heyden, Y., **2005**. Exploring and modelling the responses of electrospray and atmospheric pressure chemical ionization techniques based on molecular descriptors. *Anal. Chim. Acta* 550, 92–106.

Caldwell, D.J., Mastrocco, F., Anderson, P.D., Länge, R., Sumpter, J.P., **2012**. Predicted-no-effect concentrations for the steroid estrogens estrone, 17β-estradiol, estriol, and 17α-ethinylestradiol. *Environ. Toxicol. Chem.* 31, 1396–1406.

Canadian Environmental Quality Guidelines, **2014**. , Canadian Council of Ministers of the Environment. www.ccme.ca. Site accessed January 20, 2018.

Caporaso, J.G., Lauber, C.L., Walters, W.A., Berg-Lyons, D., Lozupone, C.A., Turnbaugh, P.J., Fierer, N., Knight, R., **2011**. Global patterns of 16S rRNA diversity at a depth of millions of sequences per sample. *Proc. Natl. Acad. Sci.* 108, 4516–4522.

Caracciolo, A.B., Topp, E., Grenni, P., **2015**. Pharmaceuticals in the environment: Biodegradation and effects on natural microbial communities. A review. *J. Pharm. Biomed. Anal.* 106, 25–36.

Cardinal, P., Anderson, J.C., Carlson, J.C., Low, J.E., Challis, J.K., Beattie, S.A., Bartel, C.N., Elliott, A.D., Montero, O.F., Lokesh, S., Favreau, A., Kozlova, T.A., Knapp,

C.W., Hanson, M.L., Wong, C.S., **2014**. Macrophytes may not contribute significantly to removal of nutrients, pharmaceuticals, and antibiotic resistance in model surface constructed wetlands. *Sci. Total Environ.* 482–483, 294–304.

Carlson, J.C., Anderson, J.C., Low, J.E., Cardinal, P., MacKenzie, S.D., Beattie, S.A., Challis, J.K., Bennett, R.J., Meronek, S.S., Wilks, R.P.A., Buhay, W.M., Wong, C.S., Hanson, M.L., **2013a**. Presence and hazards of nutrients and emerging organic micropollutants from sewage lagoon discharges into Dead Horse Creek, Manitoba, Canada. *Sci. Total Environ.* 445–446, 64–78.

Carlson, J.C., Challis, J.K., Hanson, M.L., Wong, C.S., **2013b**. Stability of pharmaceuticals and other polar organic compounds stored on polar organic chemical integrative samplers and solid-phase extraction cartridges. *Environ. Toxicol. Chem.* 32, 337–344.

Carson, R., **1962**. Silent Spring. Houghton Mifflin, Boston, MA.

Casas, M.E., Chhetri, R.K., Ooi, G., Hansen, K.M.S., Litty, K., Christensson, M., Kragelund, C., Andersen, H.R., Bester, K., **2015**. Biodegradation of pharmaceuticals in hospital wastewater by staged Moving Bed Biofilm Reactors (MBBR). *Water Res.* 83, 293–302.

Cech, N.B., Krone, J.R., Enke, C.G., **2001**. Predicting electrospray response from chromatographic retention time. *Anal. Chem.* 73, 208–213.

Chalcraft, K.R., Lee, R., Mills, C., Britz-McKibbin, P., **2009**. Virtual Quantifcation of Metabolites by Capillary Electrophoresis-Electrospray Ionization-Mass Spectrometry: Predicting Ionization Ef ciency Without Chemical Standards. *Anal. Chem.* 81, 2506–2515.

Challis, J.K., Carlson, J.C., Friesen, K.J., Hanson, M.L., Wong, C.S., **2013**. Aquatic photochemistry of the sulfonamide antibiotic sulfapyridine. *J. Photochem. Photobiol. A Chem.* 262, 14–21.

Challis, J.K., Hanson, M.L., Friesen, K.J., Wong, C.S., **2014**. A critical assessment of the photodegradation of pharmaceuticals in aquatic environments: defining our current understanding and identifying knowledge gaps. *Environ. Sci. Process. Impacts* 16, 672.

Challis, J.K., Hanson, M.L., Wong, C.S., **2018**. Pharmaceuticals and pesticides archived on polar passive sampling devices can be stable for up to 6 years. *Environ. Toxicol. Chem.* 37, 762–767.

Challis, J.K., Hanson, M.L., Wong, C.S., **2016**. Development and Calibration of an Organic-Diffusive Gradients in Thin Films Aquatic Passive Sampler for a Diverse Suite of Polar Organic Contaminants. *Anal. Chem.* 88, 10583–10591.

Challis, J.K., Hanson, M.L., Wong, C.S., **2016**. Development and Calibration of an Organic-Diffusive Gradients in Thin Films Aquatic Passive Sampler for a Diverse Suite of Polar Organic Contaminants. *Anal. Chem.* 88.

Charriau, A., Lissalde, S., Poulier, G., Mazzella, N., Buzier, R., Guibaud, G., **2016**. Overview of the Chemcatcher® for the passive sampling of various pollutants in aquatic environments Part A: Principles, calibration, preparation and analysis of the sampler. *Talanta* 148, 556–571.

Chaves-Barquero, L.G., Luong, K.H., Mundy, C.J., Knapp, C.W., Hanson, M.L., Wong, C.S., **2016**. The release of wastewater contaminants in the Arctic: A case study from Cambridge Bay, Nunavut, Canada. *Environ. Pollut.* 218, 542–550.

Chen, B., Liang, X., Nie, X., Huang, X., Zou, S., Li, X., **2015**. The role of class I integrons in the dissemination of sulfonamide resistance genes in the Pearl River and Pearl River Estuary, South China. *J. Hazard. Mater.* 282, 61–67.

Chen, C.-E., Jones, K.C., Ying, G.G., Zhang, H., **2014**. Desorption kinetics of sulfonamide and trimethoprim antibiotics in soils assessed with diffusive gradients in thin-films. *Environ. Sci. Technol.* 48, 5530–5536.

Chen, C.-E., Zhang, H., Jones, K.C., **2012**. A novel passive water sampler for in situ sampling of antibiotics. *J. Environ. Monit.* 14, 1523.

Chen, C.-E., Zhang, H., Ying, G.-G., Jones, K.C., **2013**. Use of novel passive water sampling apparatus to quantify antibiotics in wastewater. *Environ. Sci. Technol.* 47, 13587–13593.

Chen, C.-E., Zhang, H., Ying, G.G., Zhou, L.J., Jones, K.C., **2015**. Passive sampling: A cost-effective method for understanding antibiotic fate, behaviour and impact. *Environ. Int.* 85, 284–291.

Chopra, I., Roberts, M., **2001**. Tetracycline Antibiotics: Mode of Action, Applications, Molecular Biology, and Epidemiology of Bacterial Resistance. *Microbiol. Mol. Biol. Rev.* 65, 232–260.

Corcoran, J., Winter, M.J., Tyler, C.R., **2010**. Pharmaceuticals in the aquatic environment: A critical review of the evidence for health effects in fish. *Crit. Rev. Toxicol.* 40, 287–304.

Criquet, J., Dumoulin, D., Howsam, M., Mondamert, L., Goossens, J.F., Prygiel, J., Billon, G., **2017**. Comparison of POCIS passive samplers vs. composite water sampling: A case study. *Sci. Total Environ.* 609, 982–991.

Cunningham, V.L., Perino, C., D'Aco, V.J., Hartmann, A., Bechter, R., **2010**. Human health risk assessment of carbamazepine in surface waters of North America and Europe. *Regul. Toxicol. Pharmacol.* 56, 343–351.

Dalton, R.L., Pick, F.R., Boutin, C., Saleem, A., **2014**. Atrazine contamination at the watershed scale and environmental factors affecting sampling rates of the polar organic chemical integrative sampler (POCIS). *Environ. Pollut.* 189, 134–142.

Daneshvar, A., Svanfelt, J., Kronberg, L., Prévost, M., Weyhenmeyer, G.A., **2010a**. Seasonal variations in the occurrence and fate of basic and neutral pharmaceuticals in a Swedish river-lake system. *Chemosphere* 80, 301–309.

Daneshvar, A., Svanfelt, J., Kronberg, L., Weyhenmeyer, G.A., **2010b**. Winter accumulation of acidic pharmaceuticals in a Swedish river. *Environ. Sci. Pollut. Res.* 17, 908–916.

Daughton, C.G., Ternes, T.A., **1999**. Pharmaceuticals and personal care products in the environment: agents of subtle change? *Environ. Health Perspect.* 107, 907–938.

Davison, W., Zhang, H., **2012**. Progress in understanding the use of diffusive gradients in thin films (DGT) – back to basics. *Environ. Chem.* 9, 1–13.

Davison, W., Zhang, H., **1994**. In situ speciation measurements of trace components in natural waters using thin-film gels. *Nature* 367, 546–548.

Dias, N.C., Poole, C.F., **2002**. Mechanistic study of the sorption properties of OASIS((R)) HLB and its use in solid-phase extraction. *Chromatographia* 56, 269–275.

Drillia, P., Stamatelatou, K., Lyberatos, G., **2005**. Fate and mobility of pharmaceuticals in solid matrices. *Chemosphere* 60, 1034–1044.

Du, B., Haddad, S.P., Luek, A., Scott, W.C., Saari, G.N., Kristofco, L.A., Connors, K.A., Rash, C., Rasmussen, J.B., Chambliss, C.K., Brooks, B.W., **2014**. Bioaccumulation and trophic dilution of human pharmaceuticals across trophic positions of an effluent-dependent wadeable stream. *Philos. Trans. R. Soc. B Biol. Sci.* 369, 20140058–20140058.

Dulin, D., Mill, T., **1982**. Development and Evaluation of Sunlight Actinometers. *Environ. Sci. Technol.* 16, 815–820.

Environment and Climate Change Canada, **2017**. , Federal Environmental Quality Guidelines: Perfluorooctane Sulfonate (PFOS).

Environment Canada, **2011**. State of Lake Winnipeg: 1999-2007. Environment Canada and Manitoba Water Stewardship.

Erickson, B., **2018**. EU to ban neonicotinoid pesticides outdoors. *Chem. Eng. News* 48.

Fairbairn, D.J., Arnold, W.A., Barber, B.L., Kaufenberg, E.F., Koskinen, W.C., Novak, P.J., Rice, P.J., Swackhamer, D.L., **2016**. Contaminants of Emerging Concern: Mass Balance and Comparison of Wastewater Effluent and Upstream Sources in a Mixed-Use Watershed. *Environ. Sci. Technol.* 50, 36–45.

Fan, W., Hamilton, T., Webster-Sesay, S., Nikolich, M.P., Lindler, L.E., **2007**. Multiplex real-time SYBR Green I PCR assay for detection of tetracycline efflux genes of Gram-negative bacteria. *Mol. Cell. Probes* 21, 245–256.

Fauvelle, V., Kaserzon, S.L., Montero, N., Lissalde, S., Allan, I.J., Mills, G., Mazzella, N., Mueller, J.F., Booij, K., **2017**. Dealing with Flow Effects on the Uptake of Polar Compounds by Passive Samplers. *Environ. Sci. Technol.* 51, 2536–2537.

Fauvelle, V., Nhu-Trang, T.T., Feret, T., Madarassou, K., Randon, J., Mazzella, N.,

2015. Evaluation of Titanium Dioxide as a Binding Phase for the Passive Sampling of Glyphosate and Aminomethyl Phosphonic Acid in an Aquatic Environment. *Anal. Chem.* 87, 6004–6009.

Fedorova, G., Golovko, O., Randak, T., Grabic, R., **2014**. Storage effect on the analysis of pharmaceuticals and personal care products in wastewater. *Chemosphere* 111, 55–60.

Fenner, K., Canonica, S., Wackett, L.P., Elsner, M., **2013**. Evaluating pesticide degradation in the environment: Blind spots and emerging opportunities. *Science (80-.).* 341, 752–758.

Fent, K., Weston, A.A., Caminada, D., **2006**. Ecotoxicology of human pharmaceuticals. *Aquat. Toxicol.* 76, 122–159.

Fono, L.J., Kolodziej, E.P., Sedlak, D.L., **2006**. Attenuation of wastewater-derived contaminants in an effluent-dominated river. *Environ. Sci. Technol.* 40, 7257–7262.

Fuller, E.N., Schettler, P.D., Giddings, J.C., **1966**. A new method for prediction of binary gas-phase diffusion coefficients. *Ind. Eng. Chem.* 58, 18–27.

Gabet-Giraud, V., Miège, C., Jacquet, R., Coquery, M., **2014**. Impact of wastewater treatment plants on receiving surface waters and a tentative risk evaluation: The case of estrogens and beta blockers. *Environ. Sci. Pollut. Res.* 21, 1708–1722.

Galloway, T., Handy, R., **2003**. Immunotoxicity of organophosphorous pesticides. *Ecotoxicology* 12, 345–363.

Gatica, J., Kaplan, E., Cytryn, E., **2016**. Antibiotic Resistance Elements in Wastewater Treatment Plants: Scope and Potential Impacts BT - Wastewater Reuse and Current Challenges, in: Fatta-Kassinos, D., Dionysiou, D.D., Kümmerer, K. (Eds.), .

Springer International Publishing, Cham, pp. 129–153.

Ghattas, A.K., Fischer, F., Wick, A., Ternes, T.A., **2017**. Anaerobic biodegradation of (emerging) organic contaminants in the aquatic environment. *Water Res.* 116, 268–295.

Gilbertson, M., Fox, G., Bowerman, W., **1998**. Designing the Environmental Results Workshop: Historical Context, Causality and Candidate Species. *Environ. Monit. Assess.* 53, 17–55.

Gimpel, J., Zhang, H., Hutchinson, W., Davison, W., **2001**. Effect of solution composition, flow and deployment time on the measurement of trace metals by the diffusive gradient in thin films technique. *Anal. Chim. Acta* 448, 93–103.

Golubović, J., Birkemeyer, C., Protić, A., Otašević, B., Zečević, M., **2016**. Structure-response relationship in electrospray ionization-mass spectrometry of sartans by artificial neural networks. *J. Chromatogr. A* 1438, 123–132.

Goolsby, D.A., Thurman, E.M., Pomes, M.L., Meyer, M.T., Battaglin, W.A., **1997**. Herbicides and their metabolites in rainfall: Origin, transport, and deposition patterns across the midwestern and northeastern United States, 1990-1991. *Environ. Sci. Technol.* 31, 1325–1333.

Górecki, T., Namienik, J., **2002**. Passive sampling. *Trends Anal. Chem.* 21, 276–291.

Greskowiak, J., Hamann, E., Burke, V., Massmann, G., **2017**. The uncertainty of biodegradation rate constants of emerging organic compounds in soil and groundwater – A compilation of literature values for 82 substances. *Water Res.* 126, 122–133.

Gross, J.H., **2004**. Mass Spectrometry. Springer International Publishing, Germany.

Guerard, J.J., Miller, P.L., Trouts, T.D., Chin, Y.P., **2009**. The role of fulvic acid composition in the photosensitized degradation of aquatic contaminants. *Aquat. Sci.* 71, 160–169.

Guibal, R., Buzier, R., Charriau, A., Lissalde, S., Guibaud, G., **2017a**. Passive sampling of anionic pesticides using the Diffusive Gradients in Thin films technique (DGT). *Anal. Chim. Acta* 966, 1–10.

Guibal, R., Buzier, R., Charriau, A., Lissalde, S., Guibaud, G., **2017b**. Passive sampling of anionic pesticides using the Diffusive Gradients in Thin films technique (DGT). *Anal. Chim. Acta* 966, 1–10.

Guibal, R., Lissalde, S., Charriau, A., Guibaud, G., **2015a**. Improvement of POCIS ability to quantify pesticides in natural water by reducing polyethylene glycol matrix effects from polyethersulfone membranes. *Talanta* 144, 1316–1323.

Guibal, R., Lissalde, S., Charriau, A., Poulier, G., Mazzella, N., Guibaud, G., **2015b**. Coupling passive sampling and time of flight mass spectrometry for a better estimation of polar pesticide freshwater contamination: Simultaneous target quantification and screening analysis. *J. Chromatogr. A* 1387, 75–85.

Hajj-Mohamad, M., Darwano, H., Duy, S.V., Sauvé, S., Prévost, M., Arp, H.P.H., Dorner, S., **2017**. The distribution dynamics and desorption behaviour of mobile pharmaceuticals and caffeine to combined sewer sediments. *Water Res.* 108, 57–67.

Halling-Sorensen, B., Nielsen, S.N., Lanzky, P.F., Ingerslev, F., Holten Lutzhoft, H.C., Jorgensen, S.E., **1998**. Occurence, fate and effects of pharmaceuticals substance in the environment - A review. *Chemosphere* 36, 357–393.

Harman, C., Allan, I.J., Bauerlein, P.S., **2011**. The PRC and the POCIS.

Harman, C., Allan, I.J., Vermeirssen, E.L.M., **2012**. Calibration and use of the polar organic chemical integrative sampler-a critical review. *Environ. Toxicol. Chem.* 31, 2724–2738.

Hayduk, W., Laudie, H., **1974**. Prediction of diffusion coefficient for non-electrolytes in dilute aqueos solutions. *Am. Inst. Chem. Eng. J.* 20, 611–615.

Heberer, T., **2002**. Occurrence, fate, and removal of pharmaceutical residues in the aquatic environment: a review of recent research data. *Toxicol. Lett.* 131, 5–17.

Hernández, F., Sancho, J. V., Ibáñez, M., Abad, E., Portolés, T., Mattioli, L., **2012**. Current use of high-resolution mass spectrometry in the environmental sciences. *Anal. Bioanal. Chem.* 403, 1251–1264.

Hladik, M., Kolpin, D., **2015**. First national-scale occurrence of neonicotinoid insecticides in streams across the U.S.A. *Environ. Chem.* 12–20.

Hladik, M.L., Corsi, S.R., Kolpin, D.W., Baldwin, A.K., Blackwell, B.R., Cavallin, J.E., **2018**. Year-round presence of neonicotinoid insecticides in tributaries to the Great Lakes, USA. *Environ. Pollut.* 235, 1022–1029.

Hollender, J., Schymanski, E.L., Singer, H., Ferguson, P.L., **2017**. Non-target screening with high resolution mass spectrometry in the environment: Ready to go? *Environ. Sci. Technol.* 51, 11505–11512.

Howard, P.H., Muir, D.C.G., **2011**. Identifying New Persistent and Bioaccumulative Organics Among Chemicals in Commerce II: Pharmaceuticals. *Environ. Sci. Technol.* 45, 6938–6946.

Howard, P.H., Muir, D.C.G., **2010**. Identifying New Persistent and Bioaccumulative

Organics Among Chemicals in Commerce. *Environ. Sci. Technol.* 44, 2277–2285.

Hu, X.C., Andrews, D.Q., Lindstrom, A.B., Bruton, T.A., Schaider, L.A., Grandjean, P., Lohmann, R., Carignan, C.C., Blum, A., Balan, S.A., Higgins, C.P., Sunderland, E.M., **2016**. Detection of Poly- and Perfluoroalkyl Substances (PFASs) in U.S. Drinking Water Linked to Industrial Sites, Military Fire Training Areas, and Wastewater Treatment Plants. *Environ. Sci. Technol. Lett.* 3, 344–350.

Huckins, J.N., Petty, J.D., Lebo, J.A., Almeida, F. V., Booij, K., Alvarez, D.A., Cranor, W.L., Clark, R.C., Mogensen, B.B., **2002**. Development of the permeability/performance reference compound approach for in situ calibration of semipermeable membrane devices. *Environ. Sci. Technol.* 36, 85–91.

Huerta, B., Rodriguez-Mozaz, S., Nannou, C., Nakis, L., Ruhí, A., Acuña, V., Sabater, S., Barcelo, D., **2016**. Determination of a broad spectrum of pharmaceuticals and endocrine disruptors in biofilm from a waste water treatment plant-impacted river. *Sci. Total Environ.* 540, 241–249.

Huffman, B.A., Poltash, M.L., Hughey, C.A., **2012**. Effect of polar protic and polar aprotic solvents on negative-ion electrospray ionization and chromatographic separation of small acidic molecules. *Anal. Chem.* 84, 9942–9950.

Hug, C., Ulrich, N., Schulze, T., Brack, W., Krauss, M., **2014**. Identification of novel micropollutants in wastewater by a combination of suspect and nontarget screening. *Environ. Pollut.* 184, 25–32.

Hughes, S.R., Kay, P., Brown, L.E., **2013**. Global synthesis and critical evaluation of pharmaceutical data sets collected from river systems. *Environ. Sci. Technol.* 47, 661–677.

Huijbers, P.M.C., Blaak, H., De Jong, M.C.M., Graat, E.A.M., Vandenbroucke-Grauls, C.M.J.E., De Roda Husman, A.M., **2015**. Role of the Environment in the Transmission of Antimicrobial Resistance to Humans: A Review. *Environ. Sci. Technol.* 49, 11993–12004.

Islam, F., Wang, J., Farooq, M.A., Khan, M.S.S., Xu, L., Zhu, J., Zhao, M., Muños, S., Li, Q.X., Zhou, W., **2017**. Potential impact of the herbicide 2,4-dichlorophenoxyacetic acid on human and ecosystems. *Environ. Int.* 111, 332–351.

Jacquet, R., Miège, C., Bados, P., Schiavone, S., Coquery, M., **2012**. Evaluating the polar organic chemical integrative sampler for the monitoring of beta-blockers and hormones in wastewater treatment plant effluents and receiving surface waters. *Environ. Toxicol. Chem.* 31, 279–288.

Jasper, J.T., Sedlak, D.L., **2013**. Phototransformation of Wastewater-Derived Trace Organic Contaminants in Open-Water Unit Process Treatment Wetlands. *Environ. Sci. Technol.* 47, 10781–10790.

Jensen, S., Johnels, A.G., Olsson, M., Otterlind, G., **1969**. DDT and PCB in marine animals from Swedish waters. *Nature* 224, 247–250.

Johnson, H.M., Domagalski, J.L., Saleh, D.K., **2011**. Trends in Pesticide Concentrations in Streamsof the Western United States, 1993-2005. *J. Am. Water Resour. Assoc.* 47, 265–286.

Karlaganis, G., Marioni, R., Sieber, I., Weber, A., **2001**. The elaboration of the "Stockholm Convention" on Persistent Organic Pollutants (POPS): A negotiation process fraught with obstacles and opportunities. *Environ. Sci. Pollut. Res.* 8, 216–221.

Kaserzon, S.L., Kennedy, K., Hawker, D.W., Thompson, J., Carter, S., Roach, A.C., Booij, K., Mueller, J.F., **2012**. Development and calibration of a passive sampler for perfluorinated alkyl carboxylates and sulfonates in water. *Environ. Sci. Technol.* 46, 4985–4993.

Kidd, K.A., Blanchfield, P.J., Mills, K.H., Palace, V.P., Evans, R.E., Lazorchak, J.M., Flick, R.W., **2007**. Collapse of a fish population after exposure to a synthetic estrogen. *Proc. Natl. Acad. Sci.* 104, 8897–8901.

Kimiaghalam, N., Goharrokhi, M., Clark, S.P., **2015**. Assessment of Wide River Characteristics Using an Acoustic Doppler Current Profiler. *J. Hydrol. Eng.* 21, 3–7.

Kolpin, D.W., Furlong, E.T., Meyer, M.T., Thurman, E.M., Zaugg, S.D., Barber, L.B., Buxton, H.T., **2002**. Pharmaceuticals, hormones, and other organic wastewater contaminants in U.S. streams, 1999-2000: A national reconnaissance. *Environ. Sci. Technol.* 36, 1202–1211.

Kot-Wasik, A., Zabiegała, B., Urbanowicz, M., Dominiak, E., Wasik, A., Namieśnik, J., **2007**. Advances in passive sampling in environmental studies. *Anal. Chim. Acta* 602, 141–163.

Kruve, A., Kaupmees, K., Liigand, J., Leito, I., **2014**. Negative electrospray ionization via deprotonation: Predicting the ionization efficiency. *Anal. Chem.* 86, 4822–4830.

Kümmerer, K., **2009a**. The presence of pharmaceuticals in the environment due to human use - present knowledge and future challenges. *J. Environ. Manage.* 90, 2354–2366.

Kümmerer, K., **2009b**. Antibiotics in the aquatic environment - A review - Part I. *Chemosphere* 75, 417–434.

Kümmerer, K., **2009c**. Antibiotics in the aquatic environment - A review - Part II. *Chemosphere* 75, 435–441.

Kuster, A., Adler, N., **2014**. Pharmaceuticals in the environment: scientific evidence of risks and its regulation. *Philos. Trans. R. Soc. B Biol. Sci.* 369, 20130587– 20130587.

Lam, M.W., Young, C.J., Brain, R.A., Johnson, D.J., Hanson, M.A., Wilson, C.J., Richards, S.M., Solomon, K.R., Mabury, S.A., **2004**. Aquatic persistence of eight pharmaceuticals in a microcosm study. *Environ. Toxicol. Chem.* 23, 1431–1440.

Laszakovits, J.R., Berg, S.M., Anderson, B.G., O'Brien, J.E., Wammer, K.H., Sharpless, C.M., **2017**. P-Nitroanisole/pyridine and p-Nitroacetophenone/pyridine actinometers revisited: Quantum yield in comparison to ferrioxalate. *Environ. Sci. Technol. Lett.* 4, 11–14.

Lazorko-Connon, S., Achari, G., **2009**. Atrazine: its occurrence and treatment in water. *Environ. Rev.* 17, 199–214.

Le-Minh, N., Khan, S.J., Drewes, J.E., Stuetz, R.M., **2010**. Fate of antibiotics during municipal water recycling treatment processes. *Water Res.* 44, 4295–4323.

Leifer, A., **1988**. The Kinetics of Environmental Aquatic Photochemistry: Theory and Practice, American Chemical Society, USA.

Li, H., Helm, P.A., Metcalfe, C.D., **2010a**. Sampling in the great lakes for pharmaceuticals, personal care products, and endocrine-disrupting substances using the passive polar organic chemical integrative sampler. *Environ. Toxicol. Chem.* 29, 751–762.

Li, H., Helm, P.A., Paterson, G., Metcalfe, C.D., **2011**. The effects of dissolved organic

matter and pH on sampling rates for polar organic chemical integrative samplers (POCIS). *Chemosphere* 83, 271–280.

Li, H., Vermeirssen, E.L.M., Helm, P.A., Metcalfe, C.D., **2010b**. Controlled field evaluation of water flow rate effects on sampling polar organic compounds using polar organic chemical integrative samplers. *Environ. Toxicol. Chem.* 29, 2461–2469.

Li, W., Wang, F., Zhang, W., Evans, D., **2009**. Measurement of stable and radioactive cesium in natural waters by the diffusive gradients in thin films technique with new selective binding phases. *Anal. Chem.* 81, 5889–5895.

Li, X., Zheng, W., Kelly, W.R., **2013**. Occurrence and removal of pharmaceutical and hormone contaminants in rural wastewater treatment lagoons. *Sci. Total Environ.* 445–446, 22–28.

Li, Y.-H., Gregory, S., **1974**. Diffusion of Ions in Sea Water and in Deep Sea Sediments. *Geochim. Cosmochim. Acta, 1974* 38, 703–714.

Li, Z., Kaserzon, S.L., Plassmann, M.M., Sobek, A., Gómez Ramos, M.J., Radke, M., **2017**. A strategic screening approach to identify transformation products of organic micropollutants formed in natural waters. *Environ. Sci. Process. Impacts* 19, 488–498.

Lintelmann, J., Katayama, A., Kurihara, N., Shore, L., Wenzel, A., **2003**. Endocrine disruptors in the environment (IUPAC Technical Report). *Pure Appl. Chem.* 75, 631–681.

Lissalde, S., Charriau, A., Poulier, G., Mazzella, N., Buzier, R., Guibaud, G., **2016**. Overview of the Chemcatcher® for the passive sampling of various pollutants in

aquatic environments Part B: Field handling and environmental applications for the monitoring of pollutants and their biological effects. *Talanta* 148, 572–582.

Liu, H.H., Wong, C.S., Zeng, E.Y., **2013**. Recognizing the limitations of performance reference compound (PRC)-calibration technique in passive water sampling. *Environ. Sci. Technol.* 47, 10104–10105.

Llorca, M., Gros, M., Rodríguez-Mozaz, S., Barceló, D., **2014**. Sample preservation for the analysis of antibiotics in water. *J. Chromatogr. A* 1369, 43–51.

Llorca, M., Lucas, D., Ferrando-Climent, L., Badia-Fabregat, M., Cruz-Morató, C., Barceló, D., Rodríguez-Mozaz, S., **2016**. Suspect screening of emerging pollutants and their major transformation products in wastewaters treated with fungi by liquid chromatography coupled to a high resolution mass spectrometry. *J. Chromatogr. A* 1439, 124–136.

Löffler, D., Römbke, J., Meller, M., Ternes, T.A., **2005**. Environmental fate of pharmaceuticals in water/sediment systems. *Environ. Sci. Technol.* 39, 5209–5218.

Loos, R., Carvalho, R., António, D.C., Comero, S., Locoro, G., Tavazzi, S., Paracchini, B., Ghiani, M., Lettieri, T., Blaha, L., Jarosova, B., Voorspoels, S., Servaes, K., Haglund, P., Fick, J., Lindberg, R.H., Schwesig, D., Gawlik, B.M., **2013**. EU-wide monitoring survey on emerging polar organic contaminants in wastewater treatment plant effluents. *Water Res.* 47, 6475–6487.

Lu, Z., Challis, J.K., Wong, C.S., **2015**. Quantum Yields for Direct Photolysis of Neonicotinoid Insecticides in Water: Implications for Exposure to Nontarget Aquatic Organisms. *Environ. Sci. Technol. Lett.* 2.

Mackay, D., Shiu, W.Y., Ma, K.C., **1997**. Illustrated Handbook of Physical-Chemical

Properties of Environmental Fate for Organic Chemicals. Taylor & Francis.

Macleod, S.L., Mcclure, E.L., Wong, C.S., **2007**. Laboratory Calibration and Field

Deployment of the Polar Organic. *Environ. Toxicol. Chem.* 26, 2517–2529.

MacLeod, S.L., Wong, C.S., **2010**. Loadings, trends, comparisons, and fate of achiral

and chiral pharmaceuticals in wastewaters from urban tertiary and rural aerated

lagoon treatments. *Water Res.* 44, 533–544.

Main, A.R., Headley, J. V., Peru, K.M., Michel, N.L., Cessna, A.J., Morrissey, C.A.,

2014. Widespread use and frequent detection of neonicotinoid insecticides in

wetlands of Canada's prairie pothole region. *PLoS One* 9.

Main, A.R., Michel, N.L., Headley, J. V., Peru, K.M., Morrissey, C.A., **2015**. Ecological

and Landscape Drivers of Neonicotinoid Insecticide Detections and Concentrations

in Canada's Prairie Wetlands. *Environ. Sci. Technol.* 49, 8367–8376.

Manitoba agriculture statistics, **2016**. , https://www.gov.mb.ca/agriculture. Site accessed

February 28, 2018.

Matamoros, V., Arias, C., Brix, H., Bayona, J.M., **2009**. Preliminary screening of small-

scale domestic wastewater treatment systems for removal of pharmaceutical and

personal care products. *Water Res.* 43, 55–62.

Maurer, M., Escher, B.I., Richle, P., Schaffner, C., Alder, A.C., **2007**. Elimination of

beta-blockers in sewage treatment plants. *Water Res.* 41, 1614–1622.

Mayer, P., Tolls, J., Hermens, J., Mackay, D., **2003**. Equilibrium sampling devices.

Environ. Sci. Technol. 37, 184A–191A.

Mazzella, N., Lissalde, S., Moreira, S., Delmas, F., Mazellier, P., Huckins, J.N., **2010**.

Evaluation of the use of performance reference compounds in an oasis-HLB

adsorbent based passive sampler for improving water concentration estimates of polar herbicides in freshwater. *Environ. Sci. Technol.* 44, 1713–1719.

McCluskey, S.M., Knapp, C.W., **2017**. Selection of tetracycline and ampicillin resistance genes during long-term soil-copper exposure, in: Antibiotic Resistance Genes in Natural Environments and Long-Term Effects. Nova Science Publishers Inc., New York, NY, pp. 199–217.

McCullough, G.K., Page, S.J., Hesslein, R.H., Stainton, M.P., Kling, H.J., Salki, A.G., Barber, D.G., **2012**. Hydrological forcing of a recent trophic surge in Lake Winnipeg. *J. Great Lakes Res.* 38, 95–105.

McNeill, K., Canonica, S., **2016**. Triplet state dissolved organic matter in aquatic photochemistry: reaction mechanisms, substrate scope, and photophysical properties. *Environ. Sci. Process. Impacts* 18, 1381–1399.

Messing, P., Farenhorst, A., Waite, D., Sproull, J., **2013**. Influence of usage and chemical-physical properties on the atmospheric transport and deposition of pesticides to agricultural regions of Manitoba, Canada. *Chemosphere* 90, 1997–2003.

Messing, P.G., Farenhorst, A., Waite, D.T., McQueen, D.A.R., Sproull, J.F., Humphries, D.A., Thompson, L.L., **2011**. Predicting wetland contamination from atmospheric deposition measurements of pesticides in the Canadian Prairie Pothole region. *Atmos. Environ.* 45, 7227–7234.

Miège, C., Budzinski, H., Jacquet, R., Soulier, C., Pelte, T., Coquery, M., **2012**. Polar organic chemical integrative sampler (POCIS): application for monitoring organic micropollutants in wastewater effluent and surface water. *J. Environ. Monit.* 14,

626–635.

Miège, C., Choubert, J.M., Ribeiro, L., Eusèbe, M., Coquery, M., **2009**. Fate of pharmaceuticals and personal care products in wastewater treatment plants - Conception of a database and first results. *Environ. Pollut.* 157, 1721–1726.

Miège, C., Mazzella, N., Allan, I., Dulio, V., Smedes, F., Tixier, C., Vermeirssen, E., Brant, J., O'Toole, S., Budzinski, H., Ghestem, J.P., Staub, P.F., Lardy-Fontan, S., Gonzalez, J.L., Coquery, M., Vrana, B., **2015**. Position paper on passive sampling techniques for the monitoring of contaminants in the aquatic environment - Achievements to date and perspectives. *Trends Environ. Anal. Chem.* 8, 20–26.

Miller, P.L., Chin, Y.P., **2005**. Indirect photolysis promoted by natural and engineered wetland water constituents: Processes leading to alachlor degradation. *Environ. Sci. Technol.* 39, 4454–4462.

Miller, S.M., Sweet, C.W., Depinto, J. V., Hornbuckle, K.C., **2000**. Atrazine and nutrients in precipitation: Results from the Lake Michigan mass balance study. *Environ. Sci. Technol.* 34, 55–61.

Miller, T.H., Baz-Lomba, J.A., Harman, C., Reid, M.J., Owen, S.F., Bury, N.R., Thomas, K. V., Barron, L.P., **2016**. The First Attempt at Non-Linear in Silico Prediction of Sampling Rates for Polar Organic Chemical Integrative Samplers (POCIS). *Environ. Sci. Technol.* 50, 7973–7981.

Mills, G.A., Vrana, B., Allan, I., Alvarez, D.A., Huckins, J.N., Greenwood, R., **2007**. Trends in monitoring pharmaceuticals and personal-care products in the aquatic environment by use of passive sampling devices. *Anal. Bioanal. Chem.* 387, 1153–1157.

Moermond, C.T.A., Smit, C.E., **2016**. Derivation of water quality standards for carbamazepine, metoprolol, and metformin and comparison with monitoring data. *Environ. Toxicol. Chem.* 35, 882–888.

Monteiro, S.C., Boxall, A.B.A., **2010**. Occurrence and Fate of Human Pharmaceuticals in the Environment, in: Whitacre, D.M. (Ed.), Reviews of Environmental Contamination and Toxicology. Springer New York, New York, NY, pp. 53–154.

Morin, N., Camilleri, J., Cren-Olivé, C., Coquery, M., Miège, C., **2013**. Determination of uptake kinetics and sampling rates for 56 organic micropollutants using "pharmaceutical" POCIS. *Talanta* 109, 61–73.

Morin, N., Miège, C., Coquery, M., Randon, J., **2012**. Chemical calibration, performance, validation and applications of the polar organic chemical integrative sampler (POCIS) in aquatic environments. *TrAC - Trends Anal. Chem.* 36, 144–175.

Moschet, C., Lew, B.M., Hasenbein, S., Anumol, T., Young, T.M., **2017**. LC- and GC-QTOF-MS as Complementary Tools for a Comprehensive Micropollutant Analysis in Aquatic Systems. *Environ. Sci. Technol.* 51, 1553–1561.

Moschet, C., Wittmer, I., Simovic, J., Junghans, M., Piazzoli, A., Singer, H., Stamm, C., Leu, C., Hollender, J., **2014**. How a complete pesticide screening changes the assessment of surface water quality. *Environ. Sci. Technol.* 48, 5423–5432.

Newton, S., McMahen, R., Stoeckel, J.A., Chislock, M., Lindstrom, A., Strynar, M., **2017**. Novel Polyfluorinated Compounds Identified Using High Resolution Mass Spectrometry Downstream of Manufacturing Facilities near Decatur, Alabama. *Environ. Sci. Technol.* 51, 1544–1552.

Nguyen, T.B., Nizkorodov, S.A., Laskin, A., Laskin, J., **2013**. An approach toward quantification of organic compounds in complex environmental samples using high-resolution electrospray ionization mass spectrometry. *Anal. Methods* 5, 72–80.

Nisbet, I.C.T., **1998**. Trends in concentrations and effects of persistent toxic contaminants in the Great Lakes: Their significance for inferring cause-effect relationships and validating management actions. *Environ. Monit. Assess.*

Novic, A.J., O'Brien, D.S., Kaserzon, S.L., Hawker, D.W., Lewis, S.E., Mueller, J.F., **2017**. Monitoring Herbicide Concentrations and Loads during a Flood Event: A Comparison of Grab Sampling with Passive Sampling. *Environ. Sci. Technol.* 51, 3880–3891.

Nowell, L.H., Moran, P.W., Schmidt, T.S., Norman, J.E., Nakagaki, N., Shoda, M.E., Mahler, B.J., Van Metre, P.C., Stone, W.W., Sandstrom, M.W., Hladik, M.L., **2018**. Complex mixtures of dissolved pesticides show potential aquatic toxicity in a synoptic study of Midwestern U.S. streams. *Sci. Total Environ.* 613–614, 1469–1488.

O'Brien, J.W., Banks, A.P.W., Novic, A.J., Mueller, J.F., Jiang, G., Ort, C., Eaglesham, G., Yuan, Z., Thai, P.K., **2017**. Impact of in-Sewer Degradation of Pharmaceutical and Personal Care Products (PPCPs) Population Markers on a Population Model. *Environ. Sci. Technol.* 51, 3816–3823.

Ort, C., Lawrence, M.G., Rieckermann, J., Joss, A., **2010**. Sampling for Pharmaceuticals and Personal Care Products (PPCPs) and Illicit Drugs in Wastewater Systems : Are Your Conclusions Valid ? A Critical Review Sampling for PPCPs in Wastewater Systems : Comparison of Different Sampling Modes and

Optimization S. *Environ. Sci. Technol.* 44, 6024–6035.

Oss, M., Kruve, A., Herodes, K., Leito, I., **2010**. Electrospray ionization efficiency scale of organic compound. *Anal. Chem.* 82, 2865–2872.

Pal, A., Gin, K.Y.H., Lin, A.Y.C., Reinhard, M., **2010**. Impacts of emerging organic contaminants on freshwater resources: Review of recent occurrences, sources, fate and effects. *Sci. Total Environ.* 408, 6062–6069.

Peak, N., Knapp, C.W., Yang, R.K., Hanfelt, M.M., Smith, M.S., Aga, D.S., Graham, D.W., **2007**. Abundance of six tetracycline resistance genes in wastewater lagoons at cattle feedlots with different antibiotic use strategies. *Environ. Microbiol.* 9, 143–151.

Pei, R., Kim, S.C., Carlson, K.H., Pruden, A., **2006**. Effect of River Landscape on the sediment concentrations of antibiotics and corresponding antibiotic resistance genes (ARG). *Water Res.* 40, 2427–2435.

Pepper, I.L., Brooks, J.P., Gerba, C.P., **2018**. Antibiotic Resistant Bacteria in Municipal Wastes : Is There Reason for Concern ? *Environ. Sci. Technol.* 52, 3949–3959.

Petrie, B., Barden, R., Kasprzyk-Hordern, B., **2014**. A review on emerging contaminants in wastewaters and the environment: Current knowledge, understudied areas and recommendations for future monitoring. *Water Res.* 72, 3–27.

Petrović, M., Hernando, M.D., Díaz-Cruz, M.S., Barceló, D., **2005**. Liquid chromatography-tandem mass spectrometry for the analysis of pharmaceutical residues in environmental samples: A review. *J. Chromatogr. A* 1067, 1–14.

Petty, J.D., Orazio, C.E., Huckins, J.N., Gale, R.W., Lebo, J.A., Meadows, J.C., Echols, K.R., Cranor, W.L., **2000**. Considerations involved with the use of semipermeable

membrane devices for monitoring environmental contaminants. *J. Chromatogr. A* 879, 83–95.

Pickford, D.B., Finnegan, M.C., Baxter, L.R., Böhmer, W., Hanson, M.L., Stegger, P., Hommen, U., Hoekstra, P.F., Hamer, M., **2018**. Response of the Mayfly (Cloeon dipterum) to chronic exposure to thiamethoxam in outdoor mesocosms. *Environ. Toxicol. Chem.* 37, 1040–1050.

Pieke, E.N., Granby, K., Trier, X., Smedsgaard, J., **2017**. A framework to estimate concentrations of potentially unknown substances by semi-quantification in liquid chromatography electrospray ionization mass spectrometry. *Anal. Chim. Acta* 975, 30–41.

Poulier, G., Lissalde, S., Charriau, A., Buzier, R., Delmas, F., Gery, K., Moreira, A., Guibaud, G., Mazzella, N., **2014**. Can POCIS be used in Water Framework Directive (2000/60/EC) monitoring networks? A study focusing on pesticides in a French agricultural watershed. *Sci. Total Environ.* 497–498, 282–292.

Prosser, R.S., Sibley, P.K., **2015**. Human health risk assessment of pharmaceuticals and personal care products in plant tissue due to biosolids and manure amendments, and wastewater irrigation. *Environ. Int.* 75, 223–233.

Raji, M.A., Fryčák, P., Temiyasathit, C., Kim, S.B., Mavromaras, G., Ahn, J. -M., Schug, K.A., **2009**. Using multivariate statistical methods to model the electrospray ionization response of GXG tripeptides based on multiple physicochemical parameters. *Rapid Commun. Mass Spectrom.* 23, 2221–2232.

Rawn, D.F.K., Halldorson, T.H.J., Woychuk, R.N., Muir, D.C.G., **1999**. Pesticides in the Red River and its tributaries in southern Manitoba: 1993-95. *Water Qual. Res. J.*

Canada 34, 183–219.

Reemtsma, T., Berger, U., Arp, H.P.H., Gallard, H., Knepper, T.P., Neumann, M., Quintana, J.B., Voogt, P. De, **2016**. Mind the Gap: Persistent and Mobile Organic Compounds - Water Contaminants That Slip Through. *Environ. Sci. Technol.* 50, 10308–10315.

Reemtsma, T., Weiss, S., Mueller, J., Petrovic, M., González, S., Barcelo, D., Ventura, F., Knepper, T.P., **2006**. Polar pollutants entry into the water cycle by municipal wastewater: A European perspective. *Environ. Sci. Technol.* 40, 5451–5458.

Robles-Molina, J., Lara-Ortega, F.J., Gilbert-López, B., García-Reyes, J.F., Molina-Díaz, A., **2014**. Multi-residue method for the determination of over 400 priority and emerging pollutants in water and wastewater by solid-phase extraction and liquid chromatography-time-of-flight mass spectrometry. *J. Chromatogr. A* 1350, 30–43.

Santos, L.H.M.L.M., Araújo, A.N., Fachini, A., Pena, A., Delerue-Matos, C., Montenegro, M.C.B.S.M., **2010**. Ecotoxicological aspects related to the presence of pharmaceuticals in the aquatic environment. *J. Hazard. Mater.* 175, 45–95.

Sarkar, P.K., Prajapati, P.K., Shukla, V.J., Ravishankar, B., Choudhary, A.K., **2009**. Toxicity and recovery studies of two ayurvedic preparations of iron. *Indian J. Exp. Biol.* 47, 987–992.

Sarmah, A.K., Meyer, M.T., Boxall, A.B.A., **2006**. A global perspective on the use, sales, exposure pathways, occurrence, fate and effects of veterinary antibiotics (VAs) in the environment. *Chemosphere* 65, 725–759.

Sassman, S.A., Lee, L.S., **2005**. Sorption of three tetracyclines by several soils: Assessing the role of pH and cation exchange. *Environ. Sci. Technol.* 39, 7452–

7459.

Scally, S., Davison, W., Zhang, H., **2006**. Diffusion coefficients of metals and metal
complexes in hydrogels used in diffusive gradients in thin films. *Anal. Chim. Acta*
558, 222–229.

Scally, S., Davison, W., Zhang, H., **2003**. In situ measurements of dissociation kinetics
and labilities of metal complexes in solution using DGT. *Environ. Sci. Technol.* 37,
1379–1384.

Schindler, D.W., Hecky, R.E., McCullough, G.K., **2012**. The rapid eutrophication of Lake
Winnipeg: Greening under global change. *J. Great Lakes Res.* 38, 6–13.

Schottler, S.P., Eisenreich, S.J., **1997**. Mass balance model to quantity atrazine
sources, transformation rates, and trends in the Great Lakes. *Environ. Sci. Technol.*
31, 2616–2625.

Schottler, S.P., Eisenrelch, S.J., Capel, P.D., Schottler, S.P., Eisenrelch, S.J., Capel,
P.D., Schottler, S.P., Eisenrelch, S.J., Capel, P.D., **1994**. Atrazine, Alachlor, and
Cyanazine in a Large Agricultural River System. *Environ. Sci. Technol.* 28, 1079–
1089.

Schwarzenbach, R.P., Gschwend, P.M., Imboden, D.M., **2005a**. Sorption II: Partitioning
to Living Media - Bioaccumulation and Baseline Toxicity, in: Environmental Organic
Chemistry, Wiley Online Books. p. 1026.

Schwarzenbach, R.P., Gschwend, P.M., Imboden, D.M., **2005b**. Transport by Random
Motion, in: Environmental Organic Chemistry. p. 1026.

Schwarzenbach, R.P., Gschwend, P.M., Imboden, D.M., **2005c**. Transport by Random
Motion. *Wiley Online Books*, *Environ. Org. Chem.*

Schymanski, E.L., Jeon, J., Gulde, R., Fenner, K., Ruff, M., Singer, H.P., Hollender, J., **2014a**. Identifying small molecules via high resolution mass spectrometry: Communicating confidence. *Environ. Sci. Technol.* 48, 2097–2098.

Schymanski, E.L., Singer, H.P., Longrée, P., Loos, M., Ruff, M., Stravs, M.A., Ripollés Vidal, C., Hollender, J., **2014b**. Strategies to characterize polar organic contamination in wastewater: Exploring the capability of high resolution mass spectrometry. *Environ. Sci. Technol.* 48, 1811–1818.

Scott, B.F., Spencer, C., Lopez, E., Muir, D.C.G., **2009**. Perfluorinated alkyl acid concentrations in Canadian rivers and creeks. *Water Qual. Res. J. Canada* 44, 263–277.

Shaw, M., Eaglesham, G., Mueller, J.F., **2009**. Uptake and release of polar compounds in SDB-RPS Empore™ disks; implications for their use as passive samplers. *Chemosphere* 75, 1–7.

Shaw, M., Mueller, J.F., **2009**. Time integrative passive sampling: How well do chemcatchers integrate fluctuating pollutant concentrations? *Environ. Sci. Technol.* 43, 1443–1448.

Silvani, L., Riccardi, C., Eek, E., Papini, M.P., Morin, N.A.O., Cornelissen, G., Oen, A.M.P., Hale, S.E., **2017**. Monitoring alkylphenols in water using the polar organic chemical integrative sampler (POCIS): Determining sampling rates via the extraction of PES membranes and Oasis beads. *Chemosphere* 184, 1362–1371.

Skoog, D.A., Holler, J.F., Crouch, S.R., **2007**. Principles of Instrumental Analysis. Thompson Brooks/Cole, Kentucky, USA.

Solomon, K., Giesy, J., Jones, P., **2000**. Probabilistic risk assessment of agrochemicals

in the environment. *Crop Prot.* 19, 649–655.

Solomon, K.R., Baker, D.B., Richards, R.P., Dixon, K.R., Klaine, S.J., La Point, T.W., Kendall, R.J., Weisskopf, C.P., Giddings, J.M., Giesy, J.P., Hall, L.W., Williams, W.M., **1996**. Ecological risk assessment of atrazine in North American surface waters. *Environ. Toxicol. Chem.* 15, 31–76.

Solomon, K.R., Williams, W.M., Mackay, D., Purdy, J., Giddings, J.M., Giesy, J.P., **2014**. Properties and Uses of Chlorpyrifos in the United States, in: Giesy JP, Solomon KR, Eds, Ecological Risk Assessment for Chlorpyrifos in Terrestrial and Aquatic Systems in the United States. Reviews of Environmental Contamination and Toxicology, Vol 231. pp. 13–34.

Soulier, C., Coureau, C., Togola, A., **2016**. Environmental forensics in groundwater coupling passive sampling and high resolution mass spectrometry for screening. *Sci. Total Environ.* 563–564, 845–854.

Stephenson, G.R., Solomon, K.R., **2007**. Pesticides and the Environment. Canadian Network of Toxicology Centres Press, Guelph, Ontario.

Stokstad, E., **2013**. Pesticides under fire for risks to pollinators. *Science (80-.).* 340, 674–676.

Stroski, K.M., Challis, J.K., Wong, C.S., **2018**. The influence of pH on sampler uptake for an improved configuration of the organic-diffusive gradients in thin films passive sampler. *Anal. Chim. Acta* 1018, 45–53.

Struger, J., Grabuski, J., Cagampan, S., Sverko, E., McGoldrick, D., Marvin, C.H., **2017**. Factors influencing the occurrence and distribution of neonicotinoid insecticides in surface waters of southern Ontario, Canada. *Chemosphere* 169, 516–523.

Szöcs, E., Brinke, M., Karaoglan, B., Schäfer, R.B., **2017**. Large Scale Risks from
Agricultural Pesticides in Small Streams. *Environ. Sci. Technol.* 51, 7378–7385.

Ternes, T.A., **2001**. Analytical methods for the determination of pharmaceuticals in
aqueous environmental samples. *TrAC - Trends Anal. Chem.* 20, 419–434.

Ternes, T.A., Herrmann, N., Bonerz, M., Knacker, T., Siegrist, H., Joss, A., **2004**. A
rapid method to measure the solid-water distribution coefficient (K d) for
pharmaceuticals and musk fragrances in sewage sludge. *Water Res.* 38, 4075–
4084.

Terzopoulou, E., Voutsa, D., **2016**. Active and passive sampling for the assessment of
hydrophilic organic contaminants in a river basin-ecotoxicological risk assessment.
Environ. Sci. Pollut. Res. 23, 5577–5591.

Tixier, C., Singer, H.P., Oellers, S., Müller, S.R., **2003**. Occurrence and fate of
carbamazepine, clofibric acid, diclofenac, ibuprofen, ketoprofen, and naproxen in
surface waters. *Environ. Sci. Technol.* 37, 1061–1068.

Togola, A., Budzinski, H., **2007**. Development of Polar Organic Compounds Integrative
Sampler (POCIS) for study of pharmaceuticals Study of pharmaceuticals in
aquatic systems. *Anal. Chem.* 79, 6734–6741.

Tolls, J., **2001**. Sorption of veterinary pharmaceuticals in soils: A review. *Environ. Sci.
Technol.* 35, 3397–3406.

Torrents, A., Anderson, B.G., Bilboulian, S., Johnson, W.E., Hapeman, C.J., **1997**.
Atrazine photolysis: Mechanistic investigations of direct and nitrate- mediated
hydroxy radical processes and the influence of dissolved organic carbon from the
Chesapeake Bay. *Environ. Sci. Technol.* 31, 1476–1482.

Trufelli, H., Palma, P., Famiglini, G., Cappiello, A., Geologiche, S., Chimiche, T., Bo, C., Rinascimento, P., **2011**. An overview of matrix effects in liquid chromatography - mass spectrometry. *Mass Spectrom. Rev.* 30, 491–509.

U.S. Environmental Protection Agency, **2017a**. , Aquatic Life Benchmarks for Pesticide Registration. USEPA Office of Pesticide Programs. https://19january2017snapshot.epa.gov/pesticide-science-and-assessing-pesticide-risks/aquatic-life-benchmarks-pesticide-registration_.html. Site Accessed January 28, 2.

U.S. Environmental Protection Agency, **2017b**. , Technical Overview of Ecological Risk Assessment: Risk Characterization. USEPA. https://www.epa.gov/pesticide-scienceand-assessing-pesticide-risks/technical-overview-ecological-risk-assessment-risk. Site accessed January 28, 2018.

Uher, E., Tusseau-Vuillemin, M.-H., Gourlay-France, C., **2013**. DGT measurement in low flow conditions: diffusive boundary layer and lability considerations. *Environ. Sci. Process. Impacts* 15, 1351.

USGS National Water-Quality Assessment Project, **2018**. , https://water.usgs.gov/nawqa/pnsp/usage. Site accessed January 20, 2018.

Van Metre, P.C., Alvarez, D.A., Mahler, B.J., Nowell, L., Sandstrom, M., Moran, P., **2017**. Complex mixtures of Pesticides in Midwest U.S. streams indicated by POCIS time-integrating samplers. *Environ. Pollut.* 220, 431–440.

Vanderford, B.J., Snyder, S.A., **2006**. Analysis of pharmaceuticals in water by isotope dilution liquid chromatography/tandem mass spectrometry. *Environ. Sci. Technol.* 40, 7312–7320.

Vermeirssen, E.L.M., Dietschweiler, C., Escher, B.I., Van Der Voet, J., Hollender, J., **2012**. Transfer kinetics of polar organic compounds over polyethersulfone membranes in the passive samplers pocis and chemcatcher. *Environ. Sci. Technol.* 46, 6759–6766.

Vieno, N.M., Härkki, H., Tuhkanen, T., Kronberg, L., **2007**. Occurrence of pharmaceuticals in river water and their elimination in a pilot-scale drinking water treatment plant. *Environ. Sci. Technol.* 41, 5077–5084.

Vrana, B., Allan, I.J., Greenwood, R., Mills, G.A., Dominiak, E., Svensson, K., Knutsson, J., Morrison, G., **2005**. Passive sampling techniques for monitoring pollutants in water. *TrAC - Trends Anal. Chem.* 24, 845–868.

Wang, D., Singhasemanon, N., Goh, K.S., **2017**. A review of diazinon use, contamination in surface waters, and regulatory actions in California across water years 1992–2014. *Environ. Monit. Assess.* 189.

Wang, Z., Dewitt, J.C., Higgins, C.P., Cousins, I.T., **2017**. A Never-Ending Story of Per- and Polyfluoroalkyl Substances (PFASs)? *Environ. Sci. Technol.* 51, 2508–2518.

Warnken, K.W., Zhang, H., Davison, W., **2006**. Accuracy of the diffusive gradients in thin-films technique: Diffusive boundary layer and effective sampling area considerations. *Anal. Chem.* 78, 3780–3787.

Wenk, J., Eustis, S.N., McNeill, K., Canonica, S., **2013**. Quenching of Excited Triplet States by Dissolved Natural Organic Matter. *Environ. Sci. Technol.* 47, 12802–12810.

Wenk, J., von Gunten, U., Canonica, S., **2011**. Effect of Dissolved Organic Matter on the Transformation of Contaminants Induced by Excited Triplet States and the

Hydroxyl Radical. *Environ. Sci. Technol.* 45, 1334–1340.

Westerhoff, P., Yoon, Y., Snyder, S., Wert, E., **2005**. Fate of endocrine-disruptor, pharmaceutical, and personal care product chemicals during simulated drinking water treatment processes. *Environ. Sci. Technol.* 39, 6649–6663.

Wilson, J., **2012**. Agricultural Pesticide Use Trends in Manitoba and 2,4-D Fate in Soil. Doctoral Thesis. University of Manitoba.

Wode, F., van Baar, P., Dünnbier, U., Hecht, F., Taute, T., Jekel, M., Reemtsma, T., **2015**. Search for over 2000 current and legacy micropollutants on a wastewater infiltration site with a UPLC-high resolution MS target screening method. *Water Res.* 69, 274–283.

Writer, J.H., Barber, L.B., Ryan, J.N., Bradley, P.M., **2011**. Biodegradation and attenuation of steroidal hormones and alkylphenols by stream biofilms and sediments. *Environ. Sci. Technol.* 45, 4370–4376.

Xu, W. hai, Zhang, G., Zou, S. chun, Li, X. dong, Liu, Y. chun, **2007**. Determination of selected antibiotics in the Victoria Harbour and the Pearl River, South China using high-performance liquid chromatography-electrospray ionization tandem mass spectrometry. *Environ. Pollut.* 145, 672–679.

Yamamoto, H., Nakamura, Y., Moriguchi, S., Nakamura, Y., Honda, Y., Tamura, I., Hirata, Y., Hayashi, A., Sekizawa, J., **2009**. Persistence and partitioning of eight selected pharmaceuticals in the aquatic environment: Laboratory photolysis, biodegradation, and sorption experiments. *Water Res.* 43, 351–362.

Yang, J.F., Ying, G.G., Zhao, J.L., Tao, R., Su, H.C., Chen, F., **2010**. Simultaneous determination of four classes of antibiotics in sediments of the Pearl Rivers using

RRLC-MS/MS. *Sci. Total Environ.* 408, 3424–3432.

Yang, X., Flowers, R.C., Weinberg, H.S., Singer, P.C., **2011**. Occurrence and removal of pharmaceuticals and personal care products (PPCPs) in an advanced wastewater reclamation plant. *Water Res.* 45, 5218–5228.

Yargeau, V., Taylor, B., Li, H., Rodayan, A., Metcalfe, C.D., **2014**. Analysis of drugs of abuse in wastewater from two Canadian cities. *Sci. Total Environ.* 487, 722–730.

Yates, A.G., Culp, J.M., Chambers, P.A., **2012**. Estimating nutrient production from human activities in subcatchments of the Red River, Manitoba. *J. Great Lakes Res.* 38, 106–114.

Yu, K., Delaune, R.D., Tao, R., Beine, R.L., **2008**. Nonpoint source of nutrients and herbicides associated with sugarcane production and its impact on Louisiana coastal water quality. *J. Environ. Qual.* 37, 2275–83.

Yu, Y., Huang, Q., Wang, Z., Zhang, K., Tang, C., Cui, J., Feng, J., Peng, X., **2011**. Occurrence and behavior of pharmaceuticals, steroid hormones, and endocrine-disrupting personal care products in wastewater and the recipient river water of the Pearl River Delta, South China. *J. Environ. Monit.* 13, 871.

Zabiegała, B., Kot-Wasik, A., Urbanowicz, M., Namieśnik, J., **2010**. Passive sampling as a tool for obtaining reliable analytical information in environmental quality monitoring. *Anal. Bioanal. Chem.* 396, 273–296.

Zhang, H., Davison, W., **1999**. Diffusional characteristics of hydrogels used in DGT and DET techniques. *Anal. Chim. Acta* 398, 329–340.

Zhang, H., Davison, W., **1995**. Performance Characteristics of Diffusion Gradients in Thin Films for the in Situ Measurement of Trace Metals in Aqueous Solution. *Anal.*

Chem 67, 3391–3400.

Zhang, Z., Hibberd, A., Zhou, J.L., **2008**. Analysis of emerging contaminants in sewage effluent and river water: Comparison between spot and passive sampling. *Anal. Chim. Acta* 607, 37–44.

Zheng, J.L., Guan, D.X., Luo, J., Zhang, H., Davison, W., Cui, X.Y., Wang, L.H., Ma, L.Q., **2015**. Activated charcoal based diffusive gradients in thin films for in situ monitoring of bisphenols in waters. *Anal. Chem.* 87, 801–807.

Zhou, J., Broodbank, N., **2013**. Sediment-water interactions of pharmaceutical residues in the river environment. *Water Res.* 48, 61–70.

Zhou, L.J., Ying, G.G., Liu, S., Zhao, J.L., Chen, F., Zhang, R.Q., Peng, F.Q., Zhang, Q.Q., **2012**. Simultaneous determination of human and veterinary antibiotics in various environmental matrices by rapid resolution liquid chromatography-electrospray ionization tandem mass spectrometry. *J. Chromatogr. A* 1244, 123–138.

Zou, H., Radke, M., Kierkegaard, A., Macleod, M., McLachlan, M.S., **2015**. Using chemical benchmarking to determine the persistence of chemicals in a swedish lake. *Environ. Sci. Technol.* 49, 1646–1653.

9. APPENDICES

- Appendix A – Additional information for Chapter 2

- Appendix B – Additional information for Chapter 3

- Appendix C – Additional information for Chapter 4

9.1 APPENDIX A: ADDITIONAL INFORMATION FOR CHAPTER 2

INPUTS, SOURCE APPORTIONMENT, AND TRANSBOUNDARY TRANSPORT OF

PESTICIDES AND OTHER POLAR ORGANIC CONTAMINANTS ALONG THE

LOWER RED RIVER, MANITOBA, CANADA

SUMMARY

This document contains additional details of analytical methods and procedures and the

raw Red River contaminant data in the form of tables and figures.

METHODS AND MATERIALS

Chemicals and Reagents

The complete list of 23 positive mode pharmaceutical and pesticide targets and the matched isotopically labelled internal standards or surrogates (in brackets) are listed below: Atenolol[a] (-d$_7$)[b]; Atrazine[c] (-d$_5$)[b]; Carbamazepine[c] (-d$_{10}$)[b]; Chlorpyrifos[a] (-d$_{10}$)[d]; Clarithromycin[a] (Josamycin)[c]; Clothianidin[e] (-d$_3$)[e]; Diazinon[a] (-d$_{10}$)[b]; Enrofloxacin[a] (-d$_5$)[b]; Erythromycin[a] (Josamycin); Fluoxetine[a] (-d$_6$)[f]; Imidacloprid[g] (-d$_4$)[b]; Metoprolol[a] (-d$_7$)[b]; Paroxetine[h] (fluoxetine-d$_6$); Propranolol[a] (-d$_7$)[b]; Roxithromycin[a] (Josamycin); Sulfadimethoxine (-d$_6$)[d]; Sulfamethazine[a] (-^{13}C$_6$)[f]; Sulfamethoxazole[a] (-d$_4$)[d]; Sulfapyridine[h] (-d$_4$)[h]; Sulfisoxazole[a] (sulfamethoxazole-d$_4$); Sulfachloropyridazine[a] (sulfamethazine-^{13}C$_6$); Thiamethoxam[e] (-d$_3$)[e]; Trimethoprim[a] (-d$_3$)[b]. All target chemicals were of >98% purity except for ERY, which was 95% pure. Stable isotope standards were all of >99% isotopic purity. Target analytes were obtained from (a) Sigma-Aldrich (Oakville, ON); (b) C/D/N Isotopes Inc. (Pointe-Claire, QC); (c) MP Biomedicals (Montreal, QC); (d) ICN Biomedicals (Irvine, CA); (e) Syngenta Canada Inc. (Guelph, ON); (f) Cambridge Isotopes (Andover, MA); (g) EQ Laboratories Inc. (Atlanta, GA); (h) Toronto Research Chemicals (Toronto, ON).

The complete list of nine negative mode PFAS targets, abbreviations, and matched isotopically labelled internal standards or surrogates are listed below.
Native: perfluoro-*n*-pentanoic acid (PFPeA), perfluoro-*n*-hexanoic acid (PFHxA), perfluoro-*n*-heptanoic acid (PFHpA), perfluoro-*n*-octanoic acid (PFOA), perfluoro-*n*-nonanoic acid (PFNA), perfluoro-*n*-decanoic acid (PFDA), perfluoro-*n*undecanoic acid (PFUnDA), sodium perfluoro-1 hexanesulfonate (PFHxS), sodium perfluoro-1 -

octanesulfonate (PFOS). **Isotopic internal standards:** perfluoro-*n*-[1,2-^{13}C$_2$]hexanoic acid (PFHxA-^{13}C$_2$), perfluoro-*n*-[1,2,3,4-^{13}C$_4$]octanoic acid (PFOA-^{13}C$_4$), perfluoro-*n*-[1,2,3,4,5-^{13}C$_5$] nonanoic acid (PFNA-^{13}C$_5$), perfluoro-*n*-[1,2-^{13}C$_2$]decanoic acid (PFDA-^{13}C$_2$), perfluoro-*n*-[1,2-^{13}C$_2$]undecanoic acid (PFUnDA-^{13}C$_2$), sodium perfluoro-1-hexane[^{18}O$_2$]sulfonate (PFHxS-^{18}O$_2$), sodium perfluoro-1- [1,2,3,4-^{13}C$_4$]octanesulfonate (PFOS-^{13}C$_4$).

HPLC grade methanol and acetonitrile from Fischer Scientific (Ottawa, ON) and 18.2 MΩ-cm Milli-Q water (EMD Milli-Pore Synergy® system, Etobicoke, ON), were used for LC solvents, analytical standards, and sample extractions. Optima LC/MS grade formic acid (Fischer Scientific, Ottawa, ON) and ammonium acetate (Sigma-Aldrich, St. Louis, MO) were used as LC solvent additives for positive and negative mode methods, respectively.

Instrumental analysis

Batch analyses of samples sets were conducted by running 14 calibration standards (ranging of 0.01 – 750 µg/L) along with the samples. Blanks were run between triplicate sets of samples and single calibration standards (10, 25, or 50 µg/L) were run every 15 samples as a QA/QC protocol (concentration to be within 20% of target). Linearity (r^2) of calibration standards was ≥0.98 over all analyses and all 34 analytes. Method detection limits were determined using an extracted POCIS blank. The sample was measured seven subsequent times by LC-MS/MS. Slopes taken from five 13-point calibration curves were averaged and used in the LOD calculations (Table A1 and A2).

Pharmaceutical and pesticide method. Positive mode gradient elution method used a flow rate 0.45 mL/min and column temperature of 42 °C. Positive mode solvents were 95% H2O: 5% MeOH (A) and 100% MeOH (B) buffered with 0.05% formic acid. Separation was accomplished with a gradient run starting at 6% B for 1 min, ramping linearly to 50% B until 2.8 min and held at 50:50 to 3.5 min. Solvent B was again increased linearly from 50% to 95% over a 3 min period and then held at 95% B for 1 min. The column was re-conditioned to initial conditions for 4 min (6% B from 7.5 to 11.5 min). Analytes were quantified in positive electrospray ionization mode using dynamic multiple reaction monitoring (MRM) (Table A1). The source temperature was 300°C, gas flow 10.5 L/min, nebulizer pressure 50 psi, and capillary voltage 4000 V. Standards ranging from 0.01-500 µg/L were used as an external calibration and analytes were quantified using isotope dilution.

Table A1. m/z transition, fragmentor voltage (Frag), collision energy (CE), and limits of detection (LOD) details for the MS/MS positive mode MRM method for 23 pharmaceuticals and pesticides.

Compound Name	Precursor Ion	Product Ion	Frag (V)	CE (V)	LOD (ng/L)
Atenolol (Q)	267.2	190.2	135	16	0.29
Atenolol (q)	267.2	145.2	135	16	0.29
Atenolol-d7 (IS)	274.2	145.1	135	24	0.29
Atrazine (Q)	216.1	174.1	130	16	1.3
Atrazine (q)	216.1	146.2	130	20	1.3
Atrazine-d$_5$ (IS)	221.1	179.1	130	16	1.3
Carbamazepine (Q)	237.1	194.2	145	18	1.7
Carbamazepine (q)	237.1	179.2	145	36	1.7
Carbamazepine-d$_{10}$ (IS)	247.1	204.2	145	36	1.7
Chlorpyrifos (Q)	352.2	200.1	105	15	2.0
Chlorpyrifos (q)	352.2	124.9	105	15	2.0
Chlorpyrifos-d$_{10}$ (IS)	362.0	201.0	105	15	2.0
Clarithromycin (Q)	748.5	158.1	165	11	0.60
Clothianidin (Q)	250.0	169.0	106	8	0.69
Clothianidin (q)	250.0	132.0	106	12	0.69
Clothianidin-d$_3$ (IS)	253.0	132.0	111	12	0.69
Diazinon (Q)	305.2	169.2	132	19	4.5
Diazinon (q)	305.2	153.2	132	19	4.5

Compound Name	Precursor Ion	Product Ion	Frag (V)	CE (V)	LOD (ng/L)
Diazinon-d_{10} (IS)	315.2	170.1	132	20	4.5
Enrofloxacin (Q)	360.1	342.1	140	18	15
Enrofloxacin (q)	360.1	316.2	140	14	15
Enrofloxacin-d_5 (IS)	365.1	347.1	140	19	15
Erythromycin (Q)	734.5	158.0	155	33	0.18
Fluoxetine (Q)	310.3	148.1	92	5	1.7
Fluoxetine-d_6 (IS)	316.2	154.2	90	4	1.7
Imidacloprid (Q)	256.2	209.0	95	12	1.0
Imidacloprid (q)	256.2	175.2	95	17	1.0
Imidacloprid-d_4 (IS)	259.7	212.7	95	17	1.0
Josamycin (IS)	828.0	174.3	80	35	3.4
Metoprolol (Q)	268.2	191.1	133	15	3.4
Metoprolol (q)	268.2	133.1	133	17	3.4
Metoprolol-d_7 (IS)	275.1	123.1	125	19	3.4
Paroxetine (Q)	330.2	192.2	145	16	1.3
Propranolol (Q)	260.1	183.1	130	14	1.2
Propranolol (q)	260.1	155.1	130	23	1.2
Propranolol-d_7 (IS)	267.2	189.1	130	16	1.2
Roxithromycin (Q)	837.5	158.0	180	30	0.44
Sulfadimethoxine (Q)	311.1	156.0	125	17	1.6
Sulfadimethoxine (q)	311.1	245.0	125	15	1.6
Sulfadimethoxine-d_6 (IS)	317.1	162.1	125	19	1.6
Sulfamethazine (Q)	279.1	186.1	120	13	0.25
Sulfamethazine (q)	279.1	156.1	120	14	0.25
Sulfamethazine-$^{13}C_6$ (IS)	285.1	186.1	120	14	0.25
Sulfamethoxazole (Q)	254.0	156.1	110	11	20
Sulfamethoxazole (q)	254.0	108.1	110	22	20
Sulfamethoxazole-d_4 (IS)	258.0	160.0	110	13	20
Sulfapyridine (Q)	250.1	156.1	110	12	0.57
Sulfapyridine (q)	250.1	184.1	110	13	0.57
Sulfapyridine-d_4 (IS)	254.1	160.1	110	12	0.57
Sulfisoxazole (Q)	268.1	156.1	105	8	0.24
Sulfisoxazole (q)	268.1	113.1	105	12	0.24
Sulfachloropyridazine (Q)	285.1	156.1	105	10	13
Sulfachloropyridazine (q)	285.1	108.2	105	20	13
Thiamethoxam (Q)	292.0	211.0	111	8	0.85
Thiamethoxam (q)	292.0	181.0	111	20	0.85
Thiamethoxam-d_3 (IS)	295.0	184.0	111	20	0.85
Trimethoprim (Q)	291.1	230.1	150	21	3.6
Trimethoprim (q)	291.1	261.1	150	20	3.6
Trimethoprim-d_3 (IS)	294.1	230.1	150	22	3.6

Q = quantifier ion; q = qualifier ion; IS = internal standard

PFAS method. Concentrations of 9 PFASs were determined using LC-MS/MS. LC mobile phases contained 95% H2O: 5% MeOH (A) and 90% acetonitrile: 10% H_2O (B), each containing 2 mM ammonium acetate (Sigma-Aldrich, St. Louis, MO). Separation was accomplished with a gradient run starting at 85:15 A:B for 1.40 minutes, increasing solvent B linearly to 67% B until 5.00 minutes. Solvent B was held at 67% until 5.60 minutes and then ramped to 90% B from 5.61-7.60 minutes. The column was reconditioned to starting conditions, 85:15 A:B for 3 minutes before the start of the next run. The guard and analytical column setup was the same one used for the pharmaceutical and pesticide method. The column temperature and flow rate were 40°C and 0.5 mL/min respectively. An Agilent Eclipse Plus C_{18} column ($4.6 \times 30mm \times 3.5\mu m$ particle size) (Agilent Technologies, Mississauga, ON) was attached to solvent pump A and used as a PFAS trap. Analytes were quantified in negative electrospray ionization mode using dynamic multiple reaction monitoring (MRM) (Table A2). The source temperature was 300°C, gas flow 10.5 L/min, nebulizer pressure 50 psi, and capillary voltage 4000 V. Standards ranging from 0.01-100 $\mu g/L$ were used as an external calibration and analytes were quantified using isotope dilution.

Table A2. m/z transition, fragmentor voltage (Frag), collision energy (CE), and limits of detection (LOD) details for the MS/MS negative mode MRM method for nine PFAS.

Compound Name	Precursor Ion	Product Ion	Frag (V)	CE (V)	LOD (ng/L)
PFDA (Q)	513.0	468.9	-104	8	0.3
PFDA (q)	513.0	269.0	-104	13	0.3
PFDA $^{13}C_2$ (IS)	515.0	469.9	-104	8	0.1
PFHpA (Q)	362.9	319.0	-66	4	0.1
PFHpA (q)	362.9	169.0	-66	13	0.1
PFHxS (Q)	398.9	80.0	-166	48	0.1
PFHxS (q)	398.9	99.0	-166	40	0.1
PFHxS $^{18}O_2$ (IS)	402.9	84.0	-166	48	0.1
PFHxA (Q)	313.0	269.0	-53	0	0.6
PFHxA (q)	313.0	119.0	-53	16	0.6
PFHxA $^{13}C_2$ (IS)	315.0	270.0	-53	0	0.1
PFNA (Q)	463.0	418.9	-78	8	0.3
PFNA (q)	463.0	168.9	-78	20	0.3
PFNA $^{13}C_5$ (IS)	468.0	422.9	-78	8	0.1
PFOS (Q)	498.9	99.0	-198	46	0.1
PFOS (q)	498.9	80.0	-198	66	0.1
PFOS $^{13}C_4$ (IS)	502.9	99.0	-198	46	0.1
PFOA (Q)	413.0	368.9	-72	16	0.2
PFOA (q)	413.0	168.9	-72	4	0.2
PFOA $^{13}C_4$ (IS)	417.0	371.9	-72	4	0.1
PFPeA (Q)	263.0	219.0	-52	0	0.8
PFUnDA (Q)	563.0	519.0	-87	8	0.8
PFUnDA (Q)	563.0	269.0	-87	16	0.6
PFUnDA $^{13}C_2$ (IS)	565.0	520.0	-87	16	0.1

Q = quantifier ion; q = qualifier ion; IS = internal standard

Antibiotic resistance genes. PCR conditions involved the mixture of Primer Design qPCR Mastermix with SYBR-green (2×), primers (100-300 nM each), molecular water and diluted DNA template (2µL) to create 20µL reactions. Samples were thermally cycled at 10min at 95°C, then 40 cycles of: 94°C (30 sec), annealing temperatures (55-60°C, as according to previously published assays), and elongation at 72°C for 30 sec, at which SYBR-green fluorescence was detected. Post-analytical temperature melt-curve analysis were conducted from 72°C to 97°C at 0.1°C intervals.

RESULTS

Chemical Concentrations

Table A3: POCIS sampling rates used for the TWA concentration calculations of each measured analyte. Individual sampling rates and their respective references are shown for each compound. In the case where multiple sampling rate values were reported in the literature and it was not evident which value should be chosen, the average sampling rates was used.

Thiamethoxam	Clothianidin	Imidacloprid	Atrazine	Metoprolol	Propranolol
0.25 (ref. 1)	0.22 (ref. 1)	0.18 (ref. 1)	0.228 (ref. 2)	0.156 (ref. 6)	0.271 (ref. 6)
			0.239 (ref. 3)	0.309 (ref. 6)	0.646 (ref. 6)
0.25	**0.22**	**0.18**	0.091 (ref. 4)	0.321 (ref. 7)	0.478 (ref. 7)
			0.19	**0.26**	**0.47**

Carbamazepine	Clarithromycin	Sulfamethoxazole	Sulfapyridine	Trimethoprim
0.288 (ref. 5)	0.091 (ref. 8)	0.21 (ref. 9)	0.201 (ref. 6)	0.215 (ref. 6)
0.235 (ref. 6)	0.668 (ref. 8)	0.118 (ref. 5)	0.319 (ref. 6)	0.411 (ref. 6)
0.397 (ref. 6)		0.202 (ref. 6)	0.041 (ref. 8)	0.209 (ref. 7)
0.354 (ref. 7)	**0.38**	0.348 (ref. 6)	0.051 (ref. 8)	0.090 (ref. 8)
0.112 (ref. 8)				0.360 (ref. 8)
0.348 (ref. 8)		**0.22**	**0.15**	
0.28				**0.26**

PFDA	PFNA	PFHxA	PFHpA	PFOA	PFOS
0.19 (ref. 10)	0.23 (ref. 10)	0.29 (ref. 10)	0.32 (ref. 10)	0.16 (ref. 10)	0.19 (ref. 10)

1. Ahrens, L.; Daneshvar, A.; Lau, A.E.; Kreuger, J. *J. Chromatogr. A* **2015,** 1405, 1–11.

2. Lissalde, S.; Mazzella, N.; Fauvelle, V.; Delmas, F.; Mazellier, P.; Legube, B. *J Chrom A* **2011**, *1218*, 1492-1502.
3. Mazzella, N.; Dubernet, J.-F.; Delmas, F. *J Chrom A* **2007**, *1154*, 42-51.
4. Mazzella, N.; Lissalde, S.; Moreira, S.; Delmas, F.; Mazellier, P.; Huckins, J. N. *Environ. Sci. Technol.* **2010**, *44*, 1713-1719.
5. Bartelt-Hunt, S. L.; Snow, D. D.; Damon-Powell, T.; Brown, D. L.; Prasai, G.; Schwarz, M.; Kolok, A. S. *Environ. Toxicol. Chem.* **2011**, *30*, 1412-1420.
6. Li, H.; Helm, P. A.; Metcalfe, C. D. *Environ. Toxicol. Chem.* **2010**, *29*, 751-762.
7. Li, H.; Helm, P. A.; Paterson, G.; Metcalfe, C. D. *Chemosphere* **2011**, *83*, 271-280.
8. Macleod, S. L.; McClure, E. L.; Wong, C. S. *Environ. Toxicol. Chem.* **2007**, *26*, 2517-2529.
9. Bartelt-Hunt, S. L.; Snow, D. D.; Damon, T.; Shockley, J.; Hoagland, K. *Environ. Poll* **2009**, *157*, 786-791.
10. Kaserzon, S.L.; Kennedy, K.; Hawker, D.W.; Thompson, J.; Carter, S.; Roach, A.C.; Booij, K.; Mueller, J.F. *Environ. Sci. Technol.* **2012,** 46, 4985–4993.

Table A4a-e: Analyte concentrations measured by POCIS in the Red River (EM, NB, NE, SK, BP) and Assiniboine River (HD). Sampling sites are ordered (left to right) to reflect the Red River flow direction (south to north); EM→NB→NE→SK→BP. HD is on the Assiniboine River and a tributary to the Red River. Mass on sampler is used to calculate the time weighted average (TWA) concentration based on deployment time (days, d) and sampling rate (R_S, L/d), both provided in table. Reported in bold is the mean and standard deviation (SD) of triplicate TWA measurements. The date listed represents the start of the deployment period. The start of the subsequent deployment represents the end of the previous. Total deployment time in days (d) provided in brackets.

Table A4a: Atrazine

Atrazine POCIS Year	Deployment date (days)	Emerson (EM) (R_S=0.19 L/d) Mass (ng)	TWA (ng/L)	SD	St. Norbert (NB) (R_S=0.19 L/d) Mass (ng)	TWA (ng/L)	SD	North End (NE) (R_S=0.19 L/d) Mass (ng)	TWA (ng/L)	SD	Selkirk (SK) (R_S=0.19 L/d) Mass (ng)	TWA (ng/L)	SD	Breezy Point (BP) (R_S=0.19 L/d) Mass (ng)	TWA (ng/L)	SD	Headingley (HD) (R_S=0.19 L/d) Mass (ng)	TWA (ng/L)	SD
2014 POCIS	May 28 (13 d)	50.0			N/A			34.6			N/A			N/A			N/A		
		64.9	24.3	3.5	N/A	--	--	40.1	14.6	1.4	N/A	--	--	N/A	--	--	N/A	--	--
		65.0			N/A			33.7			N/A			N/A			N/A		
	Jun 10 (28 d) (42 d)*	N/A			1217			N/A			1073			N/A			17.1		
		N/A	--	--	2681	313	150	N/A	--	--	734.6	178	34.9	N/A	--	--	19.8	2.6	1.6
		N/A			3597			N/A			1036			N/A			3.8		
	Jul 8 (14 d) (59 d)*	N/A			1033			477.2			374.7			377.9			15.2		
		N/A	357	--	809.0	356	45.3	156.5	122	60.5	466.7	147	26.6	273.5	116	22.3	3.2	5.4	4.0
		4005			998.4			338.6			327.9			276.6			24.6		
	Jul 22 (7 d)	221.9			140.5			86.4			148.6			75.6			10.7		
		262.4	185	16.1	76.5	96.2	34.8	116.3	87.6	22.8	123.7	94.2	17.0	46.1	44.0	11.5	3.6	5.9	2.8
		254.4			166.6			147.0			103.5			53.8			9.3		
	Jul 29 (14 d)	159.2			155.5			68.1			88.8			75.2			25.8		
		173.2	58.8	6.9	141.0	45.2	18.5	90.9	30.5	4.4	98.4	31.2	7.1	12.1	14.6	12.3	29.8	10.2	0.9
		137.0			63.9			84.7			61.8			29.2			25.5		
	Aug 12 (14 d)	168.1			13.6			42.5			47.2			33.7			15.9		
		99.0	51.0	13.0	124.7	24.2	21.1	47.7	15.5	2.7	50.2	16.4	3.3	33.0	13.5	1.7	12.4	4.6	1.4
		139.6			54.9			33.5			33.7			41.2			8.7		
	Aug 26 (14 d)	56.3			119.4			13.8			48.0			22.4			8.1		
		132.8	35.2	14.4	97.0	37.9	6.4	3.6	2.7	2.2	45.6	16.3	2.3	26.8	10.0	1.5	10.0	3.2	0.5
		91.5			85.9			3.9			36.6			30.6			7.3		
	Sept 9 (14 d)	92.8			40.8			23.2			52.7			17.6			4.1		
		91.4	35.4	1.4	73.8	20.2	6.6	36.4	12.4	3.2	65.9	23.7	3.4	31.2	11.0	4.1	9.2	2.8	1.1
		98.4			46.9			39.2			70.2			39.0			9.1		
	Sept 23 (14 d)	65.5			8.6			14.4			19.5			27.7			0.62		
		59.0	22.6	1.8	26.8	7.7	3.8	17.8	6.0	0.6	31.7	9.6	3.2	8.7	7.9	4.0	1.7	0.6	0.4
		56.2			25.8			15.7			N/A			26.3			2.7		
	Oct 7 (14 d)	41.0			51.3			2.0			5.1			7.0			3.0		
		37.1	13.3	2.4	8.5	11.1	8.0	3.7	1.2	0.4	4.6	1.8	0.1	9.4	3.1	0.5	1.9	1.0	0.2
		28.5			28.6			4.0			4.5			8.5			2.9		
	Oct 21 (7 d)	25.7			7.2			1.3			12.5			N/A			3.0		
		20.3	18.8	3.3	6.7	4.1	1.9	7.0	3.5	2.2	11.8	8.9	0.4	N/A	--	--	3.4	2.4	0.1
		29.0			2.6			5.7			11.5			N/A			3.2		

256

		Site 1			Site 2			Site 3			Site 4			Site 5			Site 6		
2015 POCIS	Apr 29 (14 d)	28.4			18.6			9.8			6.7			N/A			6.2		
		31.2	11.2	0.7	28.1	9.5	2.1	8.7	3.5	0.3	8.7	3.4	1.0	N/A	--	--	4.7	1.9	0.4
		N/A			28.9			N/A			12.0			N/A			4.2		
	May 13 (14 d)	431.3			49.9			8.3			7.9			13.0			5.6		
		254.2	108	49.4	82.0	28.8	9.2	6.8	3.4	1.0	9.1	2.3	1.5	36.3	8.5	4.6	5.0	2.1	0.2
		174.7			97.8			11.8			1.5			18.7			6.0		
	May 27 (13 d)	242.0			126.6			82.0			226.5			235.8			6.0		
		316.3	113	21.3	222.8	70.7	27.6	104.4	37.0	4.7	195.6	86.9	6.8	235.5	87.2	14.3	7.1	2.7	0.2
		N/A			N/A			88.0			221.9			174.6			6.8		
	Jun 9 (14 d)	474.1			267.9			65.8			461.1			665.2			27.5		
		441.3	240	118	613.5	149	70.9	209.1	64.0	34.3	369.7	156	24.3	742.1	238	48.8	21.5	8.2	2.0
		998.8			309.3			235.6			N/A			488.7			16.7		
	Jun 23 (14 d)	986.6			312.7			207.7			887.2			599.7			20.7		
		1392.8	520	147	309.9	119	2.7	403.0	93.0	52.7	204.1	193	130	692.5	228	31.0	23.5	7.2	2.0
		1770.1			323.3			131.3			450.2			528.0			13.4		
	Jul 7 (14 d)	552.6			140.6			119.8			187.3			489.0			6.4		
		609.0	161	99.3	199.4	76.9	25.0	154.9	46.0	11.8	371.4	119	41.8	463.4	181	6.0	9.2	3.5	1.2
		125.7			273.4			92.5			387.2			492.3			12.7		
	Jul 21 (14 d)	227.9			109.6			28.6			157.4			143.6			9.5		
		260.1	99.7	15.1	145.8	48.0	9.6	47.6	14.0	3.6	192.4	67.6	7.3	100.0	56.0	19.5	7.8	3.6	0.7
		307.5			N/A			35.6			189.9			203.2			11.6		
	Aug 4 (14 d)	223.6			57.8			91.9			108.4			126.1			5.2		
		49.0	46.8	33.7	66.1	26.8	6.2	119.9	38.9	5.5	103.9	38.1	3.3	125.1	48.7	2.6	5.8	2.4	0.6
		100.9			89.7			98.5			91.5			137.7			8.1		
	Aug 18 (15 d)	84.6			48.9			27.9			66.4			59.0			4.7		
		58.6	27.7	5.1	31.2	17.8	5.7	33.0	12.2	1.6	56.3	23.2	1.9	57.8	22.2	0.5	3.2	1.4	0.3
		77.5			61.7			36.1			62.7			60.2			3.2		
	Sept 2 (14 d)	33.6			12.9			15.0			20.1			28.8			4.8		
		31.3	12.6	0.8	16.0	5.1	0.8	14.8	5.4	0.3	25.0	8.5	1.3	24.5	10.0	0.8	6.1	1.8	0.5
		35.6			11.8			13.4			N/A			26.4			3.7		
	Sept 16 (21 d)	80.0			47.1			16.6			N/A			17.1			4.9		
		114.9	23.8	4.5	93.5	17.5	5.8	17.4	4.2	0.2	N/A	--	--	19.8	4.5	0.4	4.9	1.1	0.2
		89.9			69.1			16.0			N/A			16.8			3.3		
	Oct 7 (21 d)	42.7			42.1			6.1			N/A			13.9			2.1		
		28.8	8.5	1.9	25.1	7.9	2.3	8.1	1.8	0.4	N/A	--	--	16.8	3.8	0.4	2.1	0.7	0.3
		30.2			27.4			N/A			N/A			15.3			4.2		

N/A = Sampler at that site and time could not be analyzed (e.g., lost to flooding, damaged in field, stolen, vandalized, etc.). ND = Not detected. *Deployed for >21d due to flooding; may be outside of linear uptake regime

*Note: POCIS samplers deployed on May 28, 2014 at St. Norbert, Selkirk, Breezy Point, and Headingley and on June 10, 2014 at Emerson, North End, and Breezy Point were inaccessible due to high water levels. Samplers deployed on October 21, 2014 at Breezy Point were destroyed as low waters left them out of water for an unknown period of time. POCIS samplers deployed on April 29, 2015 at Breezy Point and on September 16 and October 7, 2015 at Selkirk were lost due to vandalism.

Table A4b: Thiamethoxam

Thiamethoxam POCIS		Emerson (EM) (R_S=0.25 L/d)			St. Norbert (NB) (R_S=0.25 L/d)			North End (NE) (R_S=0.25 L/d)			Selkirk (SK) (R_S=0.25 L/d)			Breezy Point (BP) (R_S=0.25 L/d)			Headingley (HD) (R_S=0.25 L/d)		
Year	Deployment date (days)	Mass (ng)	TWA (ng/L)	SD	Mass (ng)	TWA (ng/L)	SD	Mass (ng)	TWA (ng/L)	SD	Mass (ng)	TWA (ng/L)	SD	Mass (ng)	TWA (ng/L)	SD	Mass (ng)	TWA (ng/L)	SD
2014 POCIS	May 28 (13 d)	5.6			N/A			6.2			N/A			N/A			N/A		
		5.8	1.9	0.3	N/A	--	--	6.5	2.0	0.1	N/A	--	--	N/A	--	--	N/A	--	--
		7.3			N/A			6.8			N/A			N/A			N/A		
	Jun 10 (28 d) (42 d)*	N/A			120.7			N/A			157.5			N/A			11.3		
		N/A	--	--	155.2	15.7	4.8	N/A	--	--	140.5	20.8	1.4	N/A	--	--	29.5	1.9	2.1
		N/A			219.6			N/A			139.5			N/A			ND		
	Jul 8 (14 d) (59 d)*	N/A			98.5			122.8			79.4			94.4			105.7		
		N/A	7.3	--	78.8	26.9	4.0	46.8	23.5	10.9	107.4	24.8	5.1	75.0	23.3	3.2	28.9	28.9	20.0
		107.7			105.6			76.7			74.1			75.2			168.4		
	Jul 22 (7 d)	21.2			8.0			16.8			36.2			20.3			23.8		
		27.2	14.3	1.9	5.9	6.1	3.6	30.2	15.6	5.3	32.4	19.6	1.1	14.1	9.7	1.8	14.1	11.6	3.1
		26.8			17.9			34.6			34.4			16.7			22.9		
	Jul 29 (14 d)	13.5			10.8			22.1			35.1			27.1			40.4		
		24.5	9.7	7.5	16.6	3.2	1.5	24.2	7.4	1.4	31.2	8.1	2.5	6.0	4.3	3.1	34.8	10.5	0.9
		63.4			5.9			31.6			18.3			12.0			35.5		
	Aug 12 (14 d)	ND			9.0			20.0			19.7			10.7			11.0		
		16.0	3.7	1.2	6.7	2.0	0.5	13.9	5.1	1.0	14.7	5.4	1.1	11.4	3.0	0.3	8.1	4.9	3.9
		9.9			5.5			19.9			22.1			9.4			32.8		
	Aug 26 (14 d)	6.8			12.4			6.2			17.4			8.8			9.2		
		13.5	2.5	1.2	12.2	3.4	0.1	7.4	1.7	0.4	20.5	4.9	1.0	6.6	2.7	0.9	25.4	4.4	2.5
		6.1			11.6			4.4			13.4			12.9			11.6		
	Sept 9 (14 d)	12.8			5.1			9.0			21.2			6.6			8.2		
		7.2	2.5	1.0	7.0	1.5	0.5	11.1	2.9	0.3	16.8	5.5	0.6	9.2	2.8	1.0	20.9	4.5	1.9
		6.4			3.2			10.5			19.8			13.6			17.9		
	Sept 23 (14 d)	1.5			1.7			7.1			9.9			11.0			1.5		
		2.2	0.59	0.1	1.8	0.58	0.1	8.4	2.2	0.2	10.5	2.9	0.1	6.3	2.6	0.7	4.0	0.80	0.4
		2.5			2.6			7.5			N/A			10.3			2.9		
	Oct 7 (14 d)	2.6			0.9			0.9			1.4			1.7			3.9		
		0.6	0.39	0.3	1.1	0.49	0.4	1.1	0.40	0.2	2.0	0.48	0.1	1.8	0.54	0.1	1.9	0.80	0.3
		0.8			3.2			2.2			1.5			2.1			2.6		
	Oct 21 (7 d)	0.8			0.5			2.1			2.8			N/A			3.9		
		1.2	0.51	0.2	0.4	0.29	0.1	1.0	0.89	0.3	2.1	1.5	0.2	N/A	--	--	4.7	2.2	0.5
		0.7			0.6			1.6			2.7			N/A			2.9		

258

Table A4b continued: Thiamethoxam

	Date	S1			S2			S3			S4			S5			S6		
2015 POCIS	Apr 29 (14 d)	ND			ND			8.0			ND			N/A			ND		
		ND	ND		17.9	4.2	1.2	6.0	2.0	0.4	7.8	2.7	0.7	N/A	--	--	6.9	1.5	1.3
		N/A			11.8			N/A			11.2			N/A			8.6		
	May 13 (14 d)	109.7			22.0			ND			6.7			13.9			9.3		
		36.8	16.4	13.1	31.5	7.8	1.4	4.6	1.0	0.9	4.9	1.6	0.4	38.8	6.1	4.3	7.8	2.7	0.5
		25.3			28.7			6.2			ND			11.6			11.0		
	May 27 (13 d)	17.9			17.9			7.9			20.3			27.7			4.4		
		20.9	6.0	0.7	23.0	6.3	1.1	8.9	2.8	0.4	20.8	6.6	0.5	22.1	7.0	1.4	4.3	2.8	2.6
		N/A			N/A			10.2			23.2			18.6			18.9		
	Jun 9 (14 d)	16.5			20.4			3.6			23.2			51.7			11.3		
		14.1	5.4	1.7	30.9	6.1	2.6	9.8	2.8	1.8	16.7	5.7	1.3	60.2	14.1	3.5	5.3	2.0	1.0
		25.7			13.1			16.1			N/A			36.2			4.7		
	Jun 23 (14 d)	8.9			7.4			2.6			19.2			14.2			13.7		
		17.0	4.0	1.2	7.0	2.1	0.1	10.5	2.1	1.2	8.9	3.8	1.5	16.4	4.2	0.4	14.7	3.7	0.7
		15.7			7.2			9.3			11.3			13.5			10.0		
	Jul 7 (14 d)	23.2			6.1			7.5			8.0			21.9			3.2		
		28.4	5.4	3.4	9.0	2.5	0.7	3.8	1.5	0.6	14.0	3.8	1.4	19.8	6.1	0.4	2.0	0.70	0.2
		5.4			10.7			4.8			17.6			22.1			2.2		
	Jul 21 (14 d)	24.2			20.1			4.8			23.5			24.6			2.6		
		19.2	6.3	0.7	20.4	5.8	0.1	5.6	1.6	0.2	28.6	7.7	0.8	17.6	6.5	1.3	1.8	0.8	0.3
		22.3			N/A			6.1			28.4			26.3			4.2		
	Aug 4 (14 d)	9.4			5.7			18.0			20.2			25.3			13.2		
		3.5	1.6	0.9	6.0	1.9	0.4	19.5	5.5	0.3	14.9	4.6	1.0	20.0	6.5	0.8	20.3	6.7	3.5
		4.2			8.4			19.8			13.3			23.3			37.2		
	Aug 18 (15 d)	11.2			4.2			7.7			18.2			18.9			6.2		
		6.3	3.0	1.1	3.1	1.4	0.6	9.2	2.5	0.3	17.9	5.1	0.1	14.9	4.8	0.6	8.0	2.0	0.3
		14.0			7.3			9.7			17.5			17.0			7.1		
	Sept 2 (14 d)	9.7			9.8			13.1			22.0			25.1			8.0		
		9.5	2.6	0.2	10.5	3.0	0.2	13.3	3.6	0.3	18.3	5.8	0.7	18.7	6.2	0.9	7.7	2.1	0.2
		8.3			11.4			11.3			N/A			21.2			6.7		
	Sept 16 (21 d)	4.3			7.0			101.6			N/A			33.3			4.7		
		4.1	0.73	0.1	12.3	1.9	0.5	109.1	21.9	3.2	N/A	--	--	44.7	7.3	1.1	4.7	0.77	0.2
		3.1			10.2			133.7			N/A			36.8			2.7		
	Oct 7 (21 d)	1.2			2.2			2.1			N/A			4.3			1.8		
		1.0	0.21	0.02	1.5	0.33	0.1	4.0	0.58	0.3	N/A	--	--	2.8	0.67	0.1	1.0	0.33	0.1
		1.1			1.4			N/A			N/A			3.4			2.3		

N/A = Sampler at that site and time could not be analyzed (e.g., lost to flooding, damaged in field, stolen, vandalized, etc.). ND = Not detected. *Deployed for >21d due to flooding; may be outside of linear uptake regime

*Note: POCIS samplers deployed on May 28, 2014 at St. Norbert, Selkirk, Breezy Point, and Headingley and on June 10, 2014 at Emerson, North End, and Breezy Point were inaccessible due to high water levels. Samplers deployed on October 21, 2014 at Breezy Point were destroyed as low waters left them out of water for an unknown period of time. POCIS samplers deployed on April 29, 2015 at Breezy Point and on September 16 and October 7, 2015 at Selkirk were lost due to vandalism.

Table A4c: Clothianidin

Clothianidin POCIS		Emerson (EM) (Rs=0.22 L/d)			St. Norbert (NB) (Rs=0.22 L/d)			North End (NE) (Rs=0.22 L/d)			Selkirk (SK) (Rs=0.22 L/d)			Breezy Point (BP) (Rs=0.22 L/d)			Headingley (HD) (Rs=0.22 L/d)		
Year	Deployment date (days)	Mass (ng)	TWA (ng/L)	SD	Mass (ng)	TWA (ng/L)	SD	Mass (ng)	TWA (ng/L)	SD	Mass (ng)	TWA (ng/L)	SD	Mass (ng)	TWA (ng/L)	SD	Mass (ng)	TWA (ng/L)	SD
2014 POCIS	May 28 (13 d)	10.2			N/A			7.0			N/A			N/A			N/A		
		10.9	3.7	0.1	N/A	--	--	8.2	2.9	0.5	N/A	--	--	N/A	--	--	N/A	--	--
		10.8			N/A			9.8			N/A			N/A			N/A		
	Jun 10 (28 d) (42 d)*	N/A			112.1			N/A			160.9			N/A			10.5		
		N/A	--	--	189.5	20.2	7.9	N/A	--	--	104.9	21.5	4.5	N/A	--	--	25.3	2.4	1.5
		N/A			257.8			N/A			132.3			N/A			8.9		
	Jul 8 (14 d) (59 d)*	N/A			101.8			87.2			62.6			68.4			67.6		
		N/A	17.3	--	68.0	28.8	5.9	38.8	20.7	7.9	83.1	22.5	3.9	60.0	20.1	1.9	19.4	21.5	15.0
		224.9			96.4			65.3			62.0			57.3			111.7		
	Jul 22 (7 d)	45.6			17.8			16.4			33.2			18.9			23.4		
		57.2	31.7	4.8	16.7	12.8	2.9	27.9	18.7	8.4	31.9	18.9	4.0	11.5	8.7	3.1	6.9	9.8	5.3
		43.7			24.8			42.0			22.0			9.9			14.8		
	Jul 29 (14 d)	13.1			16.8			18.3			32.0			26.9			22.5		
		15.0	4.5	0.3	19.6	4.6	2.3	23.9	7.8	1.9	30.2	8.8	2.2	6.7	5.0	3.4	31.2	8.2	1.7
		13.7			6.3			30.3			19.6			12.6			22.3		
	Aug 12 (14 d)	8.7			2.9			10.0			14.7			9.5			11.4		
		5.9	2.3	0.5	4.7	1.2	0.3	11.7	3.4	0.3	10.3	3.5	1.2	10.3	3.3	0.1	9.1	2.9	0.8
		8.1			3.5			9.8			7.5			10.2			6.7		
	Aug 26 (14 d)	10.6			28.2			6.0			18.4			10.2			9.9		
		32.6	6.1	3.9	18.3	8.0	1.8	4.1	1.5	0.4	19.4	5.6	0.9	9.7	3.3	0.1	14.2	3.6	0.9
		13.2			27.1			4.0			14.3			10.2			8.9		
	Sept 9 (14 d)	13.8			9.4			8.9			18.0			6.8			7.0		
		16.6	5.1	0.5	11.5	2.8	1.1	12.6	3.9	1.0	20.8	6.8	1.0	12.3	4.0	1.9	21.0	5.0	2.4
		16.3			5.0			14.8			23.9			18.3			18.4		
	Sept 23 (14 d)	3.8			2.7			7.0			9.4			13.4			1.2		
		3.7	1.4	0.3	3.0	1.2	0.5	10.6	2.8	0.6	15.2	4.0	1.3	5.4	3.8	1.9	2.3	0.69	0.3
		5.4			5.4			8.4			N/A			16.7			2.8		
	Oct 7 (14 d)	1.7			1.2			0.58			1.8			2.3			3.6		
		0.79	0.46	0.2	1.3	0.41	0.03	0.89	0.31	0.1	2.3	0.67	0.1	3.0	0.80	0.1	2.9	1.2	0.2
		1.8			1.2			1.4			2.0			2.1			4.2		
	Oct 21 (7 d)	0.68			0.76			0.91			3.0			N/A			5.0		
		1.2	0.76	0.3	0.80	0.34	0.3	1.6	0.83	0.2	2.9	1.9	0.04	N/A	--	--	5.4	3.1	0.4
		1.6			ND			1.3			2.9			N/A			4.1		

260

Table A4c continued: Clothianidin

	Date																		
2015 POCIS	Apr 29 (14 d)	7.0			5.9			7.6			5.5			N/A			12.3		
		7.6	2.4	0.1	9.9	2.4	0.7	5.2	2.1	0.6	6.6	2.5	0.9	N/A	--	--	8.2	3.2	0.7
		N/A			6.5			N/A			10.8			N/A			8.9		
	May 13 (14 d)	72.6			32.8			6.9			8.6			16.9			8.9		
		90.7	23.1	6.6	40.5	11.8	1.3	4.2	2.8	1.7	8.3	2.0	1.3	47.1	8.6	5.8	7.5	2.9	0.5
		50.3			35.4			14.5			1.7			15.3			10.4		
	May 27 (13 d)	28.4			24.8			9.9			30.2			35.0			5.3		
		33.3	10.8	1.2	32.8	10.1	2.0	13.9	4.4	0.8	27.4	10.4	0.7	27.8	10.3	1.7	7.8	2.8	1.0
		N/A			N/A			13.8			31.2			25.6			11.0		
	Jun 9 (14 d)	18.7			20.4			5.8			27.4			57.3			13.1		
		16.3	7.5	3.1	37.2	8.6	3.0	21.9	5.4	3.1	25.4	8.6	0.5	60.3	16.9	3.9	6.6	3.1	1.1
		33.8			21.5			22.3			N/A			38.1			8.6		
	Jun 23 (14 d)	13.6			8.7			9.2			23.9			17.3			14.4		
		26.8	7.6	2.8	8.9	2.7	0.2	11.4	3.2	0.5	9.8	5.1	2.4	20.0	5.7	0.8	17.1	4.6	1.1
		29.5			7.7			8.8			13.4			15.1			10.6		
	Jul 7 (14 d)	46.6			6.5			7.4			16.4			30.9			4.5		
		54.7	11.8	8.1	9.2	3.0	0.9	8.6	2.3	0.5	20.9	7.3	2.2	29.9	9.4	0.8	3.7	1.7	0.7
		8.2			11.8			5.5			29.9			26.5			7.5		
	Jul 21 (14 d)	33.0			23.5			4.8			27.7			31.7			5.8		
		30.1	10.6	0.8	21.3	7.3	0.5	6.3	2.0	0.4	35.5	11.7	2.8	20.3	9.8	3.0	3.9	1.8	0.6
		34.9			N/A			7.1			44.7			38.8			7.3		
	Aug 4 (14 d)	21.0			5.9			23.6			24.3			30.0			14.0		
		15.7	5.8	0.9	8.3	2.9	1.0	27.0	8.0	0.7	20.9	7.1	0.7	25.2	9.1	0.8	20.8	7.5	3.4
		16.7			12.2			23.0			20.2			28.9			34.7		
	Aug 18 (15 d)	18.6			5.2			10.5			27.2			30.8			9.3		
		8.8	5.7	2.7	5.0	2.5	1.5	12.7	4.3	1.0	24.8	8.7	0.6	25.8	8.8	1.0	7.7	2.6	0.4
		25.4			13.2			16.3			28.6			24.9			7.0		
	Sept 2 (14 d)	23.1			17.0			23.5			36.8			43.7			9.5		
		20.5	6.9	0.5	19.0	5.7	0.4	22.4	6.8	1.1	41.1	12.6	1.0	34.6	12.7	1.5	9.1	2.9	0.2
		20.2			16.8			17.0			N/A			39.0			8.2		
	Sept 16 (21 d)	8.0			13.9			11.2			N/A			21.0			5.8		
		10.9	1.8	0.5	23.4	4.0	1.0	10.5	2.2	0.2	N/A	--	--	20.1	4.7	0.5	6.2	1.2	0.1
		6.0			17.5			9.4			N/A			24.1			5.2		
	Oct 7 (21 d)	2.6			3.6			1.7			N/A			2.6			1.5		
		2.2	0.47	0.1	2.2	0.63	0.2	1.7	0.37	0.01	N/A	--	--	3.5	0.65	0.1	1.7	0.46	0.2
		1.7			3.0			N/A			N/A			2.9			3.2		

N/A = Sampler at that site and time could not be analyzed (e.g., lost to flooding, damaged in field, stolen, vandalized, etc.). ND = Not detected. *Deployed for >21d due to flooding; may be outside of linear uptake regime

*Note: POCIS samplers deployed on May 28, 2014 at St. Norbert, Selkirk, Breezy Point, and Headingley and on June 10, 2014 at Emerson, North End, and Breezy Point were inaccessible due to high water levels. Samplers deployed on October 21, 2014 at Breezy Point were destroyed as low waters left them out of water for an unknown period of time. POCIS samplers deployed on April 29, 2015 at Breezy Point and on September 16 and October 7, 2015 at Selkirk were lost due to vandalism.

Table A4d: Imidacloprid

Imidacloprid POCIS		Emerson (EM) (R_S=0.18 L/d)			St. Norbert (NB) (R_S=0.18 L/d)			North End (NE) (R_S=0.18 L/d)			Selkirk (SK) (R_S=0.18 L/d)			Breezy Point (BP) (R_S=0.18 L/d)			Headingley (HD) (R_S=0.18 L/d)		
Year	Deployment date (days)	Mass (ng)	TWA (ng/L)	SD	Mass (ng)	TWA (ng/L)	SD	Mass (ng)	TWA (ng/L)	SD	Mass (ng)	TWA (ng/L)	SD	Mass (ng)	TWA (ng/L)	SD	Mass (ng)	TWA (ng/L)	SD
2014 POCIS	May 28 (13 d)	4.7			N/A			3.7			N/A			N/A			N/A		
		4.5	2.0	0.2	N/A	--	--	3.4	1.3	0.3	N/A	--	--	N/A	--	--	N/A	--	--
		5.3			N/A			2.2			N/A			N/A			N/A		
	Jun 10 (28 d) (42 d)*	N/A			36.8			N/A			46.4			N/A			1.9		
		N/A	--	--	72.9	9.0	3.9	N/A	--	--	38.5	8.5	0.8	N/A	--	--	3.0	0.4	0.2
		N/A			95.3			N/A			43.0			N/A			0.5		
	Jul 8 (14 d) (59 d)*	N/A			27.5			22.3			11.6			15.2			7.5		
		N/A	2.1	--	23.2	10.4	1.1	7.8	5.8	2.9	15.3	5.1	0.8	11.2	5.0	0.9	2.8	2.7	1.5
		22.1			28.2			13.6			11.7			11.4			10.1		
	Jul 22 (7 d)	15.4			5.6			4.2			7.9			3.5			3.3		
		18.8	14.1	1.6	1.5	4.1	2.8	6.4	5.0	1.6	7.3	5.5	1.1	1.9	2.2	0.7	1.0	1.8	0.9
		18.9			8.4			8.3			5.4			3.0			2.5		
	Jul 29 (14 d)	10.5			11.2			7.6			10.4			8.8			3.6		
		7.4	3.1	1.0	14.5	3.8	2.3	8.8	3.5	0.5	10.7	3.4	1.3	1.6	1.9	1.5	4.0	1.4	0.1
		5.4			3.4			9.9			4.9			4.3			3.3		
	Aug 12 (14 d)	4.1			0.9			2.1			2.2			1.5			2.1		
		2.7	1.2	0.3	2.6	0.6	0.4	2.0	0.8	0.0	2.1	0.8	0.1	1.6	0.7	0.1	1.1	1.0	0.6
		2.5			1.4			2.0			1.8			2.0			4.1		
	Aug 26 (14 d)	2.8			6.4			1.6			3.7			1.9			0.7		
		10.0	2.1	1.6	6.3	2.2	0.5	1.1	0.4	0.3	6.8	1.9	0.7	3.1	1.0	0.3	4.0	0.9	0.7
		3.2			4.3			0.3			3.8			ND			1.8		
	Sept 9 (14 d)	4.0			0.8			1.9			11.7			1.2			1.3		
		4.9	1.9	0.3	6.5	1.1	1.3	2.2	1.2	0.6	12.9	4.8	0.3	3.0	2.3	2.6	10.0	2.8	2.0
		5.6			1.0			4.7			11.7			13.3			10.1		
	Sept 23 (14 d)	2.5			ND			3.7			N/A			4.9			1.5		
		1.1	1.6	1.5	0.9	0.78	0.6	7.1	2.1	0.7	8.3	4.5	1.7	3.2	1.6	0.3	2.7	0.8	0.2
		8.3			3.0			5.2			14.5			4.2			2.2		
	Oct 7 (14 d)	2.7			1.7			1.3			1.4			2.1			ND		
		2.1	0.9	0.1	1.7	0.7	0.02	1.6	0.6	0.1	ND	0.6	--	1.9	0.8	0.03	ND	ND	
		2.1			1.6			1.4			ND			2.1			ND		
	Oct 21 (7 d)	ND			ND			ND			ND			N/A			ND		
		ND	ND		ND	ND		ND	ND		ND	ND		N/A	--	--	ND	ND	
		ND			ND			ND			ND			N/A			ND		

262

Table A4d continued: Imidacloprid

2015 POCIS	**Apr 29 (14 d)**	1.3			1.5			1.1			0.89			N/A			4.6		
		1.3	0.52	0.01	2.3	0.72	0.2	0.79	0.38	0.1	1.8	0.53	0.2	N/A	--	--	1.5	0.94	0.8
		N/A			1.7			N/A			1.4			N/A			1.0		
	May 13 (14 d)	54.2			7.4			1.1			1.7			2.7			1.0		
		18.7	11.3	8.9	8.6	3.34	0.4	1.4	0.78	0.49	1.6	0.48	0.3	9.0	2.0	1.4	1.5	0.50	0.1
		12.8			9.2			3.4			0.32			3.2			1.3		
	May 27 (13 d)	8.7			5.2			3.0			8.3			9.7			1.1		
		10.3	4.1	0.5	8.4	2.9	0.9	5.2	1.7	0.5	8.2	3.7	0.3	9.2	3.6	0.7	1.1	0.54	0.1
		N/A			N/A			3.5			9.5			6.7			1.5		
	Jun 9 (14 d)	10.4			7.8			3.8			15.4			25.5			5.3		
		8.6	5.1	2.4	19.4	5.4	2.3	9.7	3.3	1.6	13.5	5.7	0.5	30.3	10.0	2.1	2.3	1.3	0.7
		19.9			13.5			11.4			N/A			19.7			2.1		
	Jun 23 (14 d)	6.9			4.1			4.0			7.5			5.5			2.7		
		9.7	3.8	1.0	3.3	1.60	0.3	5.2	1.7	0.3	2.3	1.9	1.0	6.7	2.4	0.3	4.5	1.3	0.4
		12.1			4.7			3.4			4.4			5.7			2.7		
	Jul 7 (14 d)	18.7			1.7			2.4			5.4			9.4			1.2		
		18.5	6.5	1.5	2.2	1.1	0.5	2.3	0.87	0.1	7.0	2.8	0.6	8.2	3.6	0.3	1.7	0.60	0.1
		12.2			4.0			1.9			8.4			9.6			1.7		
	Jul 21 (14 d)	15.6			7.1			2.2			10.1			10.3			1.6		
		15.9	6.8	0.9	8.1	3.0	0.3	2.3	1.0	0.2	13.5	5.0	0.8	6.1	4.1	1.7	1.1	0.61	0.2
		19.8			N/A			2.9			14.0			14.8			1.9		
	Aug 4 (14 d)	8.8			3.0			5.5			6.2			9.5			2.1		
		2.4	1.86	1.4	2.8	1.26	0.2	7.4	2.4	0.4	6.5	2.5	0.1	7.1	3.0	0.7	2.3	1.1	0.4
		2.9			3.7			5.4			6.2			6.2			4.0		
	Aug 18 (15 d)	7.6			3.3			4.5			10.8			6.3			ND		
		3.8	2.9	1.3	2.9	1.4	0.4	6.2	2.3	0.4	10.2	4.3	0.2	6.4	2.8	0.5	ND	ND	
		10.2			4.7			6.5			11.3			8.5			ND		
	Sept 2 (14 d)	10.5			4.9			7.2			9.2			13.9			ND		
		8.9	3.8	0.3	5.9	2.2	0.2	8.3	2.9	0.3	10.8	4.0	0.4	12.3	5.0	0.4	1.2	0.39	0.3
		9.4			5.7			6.6			N/A			11.7			1.7		
	Sept 16 (21 d)	3.9			3.0			2.3			N/A			4.0			0.85		
		5.4	1.2	0.2	7.6	1.4	0.6	4.0	0.86	0.2	N/A	--	--	5.1	1.2	0.2	1.1	0.22	0.08
		3.9			4.7			3.4			N/A			4.2			0.52		
	Oct 7 (21 d)	1.6			2.8			0.74			N/A			1.0			ND		
		1.8	0.38	0.1	0.90	0.45	0.3	1.3	0.27	0.1	N/A	--	--	1.0	0.25	0.03	ND	ND	
		1.0			1.5			N/A			N/A			0.85			ND		

N/A = Sampler at that site and time could not be analyzed (e.g., lost to flooding, damaged in field, stolen, vandalized, etc.). ND = Not detected. *Deployed for >21d due to flooding; may be outside of linear uptake regime*

*Note: POCIS samplers deployed on May 28, 2014 at St. Norbert, Selkirk, Breezy Point, and Headingley and on June 10, 2014 at Emerson, North End, and Breezy Point were inaccessible due to high water levels. Samplers deployed on October 21, 2014 at Breezy Point were destroyed as low waters left them out of water for an unknown period of time. POCIS samplers deployed on April 29, 2015 at Breezy Point and on September 16 and October 7, 2015 at Selkirk were lost due to vandalism.

Table A4e: Carbamazepine

Carbamazepine POCIS		Emerson (EM) (Rs=0.28 L/d)			St. Norbert (NB) (Rs=0.28 L/d)			North End (NE) (Rs=0.28 L/d)			Selkirk (SK) (Rs=0.28 L/d)			Breezy Point (BP) (Rs=0.28 L/d)			Headingley (HD) (Rs=0.28 L/d)		
Year	Deployment date (days)	Mass (ng)	TWA (ng/L)	SD	Mass (ng)	TWA (ng/L)	SD	Mass (ng)	TWA (ng/L)	SD	Mass (ng)	TWA (ng/L)	SD	Mass (ng)	TWA (ng/L)	SD	Mass (ng)	TWA (ng/L)	SD
2014 POCIS	May 28 (13 d)	2.6			N/A			16.7			N/A			N/A			N/A		
		2.5	0.59	0.2	N/A	--	--	18.1	5.7	1.6	N/A	--	--	N/A	--	--	N/A	--	--
		1.4			N/A			27.3			N/A			N/A			N/A		
	Jun 10 (28 d) (42 d)*	N/A			5.4			N/A			14.6			N/A			7.7		
		N/A	--	--	9.1	0.73	0.3	N/A	--	--	17.6	2.1	0.2	N/A	--	--	5.0	0.62	0.4
		N/A			11.3			N/A			17.2			N/A			1.9		
	Jul 8 (14 d) (59 d)*	N/A			4.6			33.1			5.3			6.7			2.7		
		N/A	1.0	--	3.7	1.1	0.1	16.5	6.6	2.2	7.5	1.6	0.3	6.2	1.4	0.4	0.68	0.73	0.6
		17.0			4.2			27.8			5.9			4.0			5.2		
	Jul 22 (7 d)	5.9			2.4			17.7			8.6			5.2			3.0		
		4.9	2.6	0.3	2.1	1.2	0.1	22.9	11.8	2.9	7.3	3.9	0.4	3.3	2.0	0.6	1.0	1.1	0.5
		4.6			2.4			28.9			7.1			3.1			2.5		
	Jul 29 (14 d)	2.8			3.4			25.1			9.7			7.6			2.4		
		3.6	0.76	0.1	2.9	0.67	0.2	34.4	7.8	1.2	8.8	2.0	0.7	0.78	0.90	0.9	3.0	0.73	0.1
		2.5			1.5			32.0			4.9			2.1			3.1		
	Aug 12 (14 d)	6.5			0.68			29.8			10.9			7.3			2.9		
		4.1	1.4	0.3	5.9	0.78	0.7	31.4	7.2	1.1	10.4	2.4	0.6	7.6	2.0	0.1	2.8	0.62	0.2
		5.5			2.6			23.4			6.8			8.3			1.7		
	Aug 26 (14 d)	1.3			4.1			13.8			10.1			3.7			1.7		
		4.2	0.60	0.4	3.3	0.75	0.4	2.5	1.6	1.7	10.1	2.3	0.5	3.7	1.0	0.1	3.6	0.58	0.3
		1.5			1.4			2.0			6.5			4.7			1.5		
	Sept 9 (14 d)	4.2			2.1			35.9			13.9			5.5			3.6		
		4.0	1.1	0.2	4.2	0.73	0.3	58.5	13.3	3.6	17.2	4.2	0.6	9.2	2.1	0.6	9.4	1.9	0.9
		5.1			2.2			61.8			18.2			10.1			9.4		
	Sept 23 (14 d)	8.3			0.55			43.5			14.9			18.4			0.74		
		7.6	2.0	0.1	2.8	0.49	0.3	60.3	13.8	2.3	22.0	4.7	1.3	5.9	3.6	1.8	1.5	0.36	0.2
		7.8			2.4			57.9			N/A			18.1			2.0		
	Oct 7 (14 d)	7.5			2.3			9.9			2.1			6.8			3.7		
		5.8	1.5	0.4	1.2	0.69	0.4	22.9	5.0	2.2	3.4	0.76	0.2	8.6	2.0	0.2	2.2	0.77	0.2
		4.3			4.7			26.2			3.3			7.9			3.1		
	Oct 21 (7 d)	5.0			1.3			6.9			11.9			N/A			6.6		
		4.0	2.4	0.4	1.1	0.46	0.3	28.6	9.9	5.7	10.6	5.7	0.4	N/A	--	--	8.0	3.6	0.4
		5.4			0.31			23.0			10.9			N/A			6.5		

Table A4e continued: Carbamazepine

2015 POCIS	Apr 29 (14 d)	8.3 9.8 N/A	2.3	0.3	5.1 9.4 8.7	2.0	0.6	44.9 41.1 N/A	11.0	0.7	9.3 10.4 13.9	2.9	0.6	N/A N/A N/A	--	--	7.5 5.1 4.8	1.5	0.4
	May 13 (14 d)	15.6 5.8 3.8	2.1	1.6	3.6 3.4 3.8	0.92	0.1	12.7 22.3 24.9	5.1	1.6	5.7 7.2 2.6	1.3	0.6	8.3 11.4 6.9	2.3	0.6	5.8 4.6 6.1	1.4	0.2
	May 27 (13 d)	1.3 1.4 N/A	0.4	0.03	0.86 1.5 N/A	0.32	0.1	7.3 11.8 9.3	2.6	0.6	7.8 6.1 7.8	2.0	0.3	8.4 8.8 6.4	2.2	0.3	4.9 5.8 7.3	1.6	0.3
	Jun 9 (14 d)	1.8 2.0 3.6	0.64	0.3	1.6 2.3 1.1	0.43	0.1	4.1 11.9 11.8	2.4	1.1	6.7 5.9 N/A	1.6	0.2	13.1 13.6 10.1	3.1	0.5	7.6 5.2 4.1	1.4	0.5
	Jun 23 (14 d)	2.9 5.1 6.0	1.2	0.4	1.8 2.0 1.9	0.49	0.02	16.0 27.3 9.4	4.5	2.3	18.2 5.4 9.1	2.8	1.7	14.1 14.9 12.0	3.5	0.4	10.2 10.5 5.9	2.3	0.7
	Jul 7 (14 d)	4.3 3.8 1.1	0.78	0.4	1.0 1.1 1.3	0.29	0.04	5.5 6.1 4.5	1.4	0.2	5.7 9.1 10.4	2.1	0.6	13.7 12.5 12.9	3.3	0.1	5.6 7.2 12.0	2.1	0.8
	Jul 21 (14 d)	4.5 4.9 5.5	1.3	0.1	2.1 2.7 N/A	0.61	0.1	6.5 11.3 8.1	2.2	0.6	14.5 16.6 16.5	4.1	0.3	12.8 8.0 17.7	3.3	1.2	7.6 6.6 11.2	2.2	0.6
	Aug 4 (14 d)	6.9 1.0 3.0	0.93	0.8	1.3 1.5 1.9	0.40	0.1	36.3 46.0 37.8	10.2	1.3	20.0 17.9 16.5	4.6	0.4	26.5 23.4 25.9	6.4	0.4	10.7 12.1 21.1	3.7	1.4
	Aug 18 (15 d)	6.3 4.2 5.9	1.4	0.3	3.1 2.1 4.0	0.78	0.2	19.3 23.4 24.6	5.7	0.7	27.1 23.4 25.8	6.5	0.5	23.2 21.4 24.0	5.8	0.3	15.4 10.2 10.6	3.1	0.7
	Sept 2 (14 d)	4.1 3.7 4.0	1.0	0.1	1.5 1.5 1.3	0.37	0.02	22.0 21.5 18.2	5.2	0.5	14.1 16.6 N/A	3.9	0.4	18.8 15.6 17.0	4.4	0.4	15.7 21.4 13.9	4.3	1.0
	Sept 16 (21 d)	11.3 17.5 12.4	2.3	0.6	6.5 13.2 9.9	1.7	0.6	66.5 68.5 64.4	11.3	0.3	N/A N/A N/A	--	--	19.5 21.8 19.3	3.4	0.2	17.0 17.8 13.9	2.8	0.3
	Oct 7 (21 d)	9.3 6.5 6.7	1.3	0.3	9.5 5.5 6.3	1.2	0.4	28.9 41.4 N/A	6.0	1.5	N/A N/A N/A	--	--	18.5 21.4 20.2	3.4	0.1	8.2 8.4 17.5	1.9	0.9

N/A = Sampler at that site and time could not be analyzed (e.g., lost to flooding, damaged in field, stolen, vandalized, etc.). ND = Not detected. *Deployed for >21d due to flooding; may be outside of linear uptake regime

*Note: POCIS samplers deployed on May 28, 2014 at St. Norbert, Selkirk, Breezy Point, and Headingley and on June 10, 2014 at Emerson, North End, and Breezy Point were inaccessible due to high water levels. Samplers deployed on October 21, 2014 at Breezy Point were destroyed as low waters left them out of water for an unknown period of time. POCIS samplers deployed on April 29, 2015 at Breezy Point and on September 16 and October 7, 2015 at Selkirk were lost due to vandalism.

Table A5: North End pharmaceutical data. Analyte concentrations measured by POCIS in the Red River at the North End site. Mass on sampler is used to calculate the time weighted average (TWA) concentration based on deployment time (days, d) and sampling rate (RS, L/d), both provided in table. Reported in bold is the mean and standard deviation (SD) of triplicate TWA measurements. The date listed represents the start of the deployment period. The start of the subsequent deployment represents the end of the previous. Total deployment time in days (d) is provided in brackets.

Compound		Clarithromycin (Rs = 0.38 L/d)			Metoprolol (Rs = 0.26 L/d)			Propranolol (Rs = 0.47 L/d)			Sulfamethoxazole (Rs = 0.22 L/d)			Sulfapyridine (Rs = 0.15 L/d)			Trimethoprim (Rs = 0.26 L/d)		
Year	Deployment date (days)	Mass (ng)	TWA (ng/L)	SD	Mass (ng)	TWA (ng/L)	SD	Mass (ng)	TWA (ng/L)	SD	Mass (ng)	TWA (ng/L)	SD	Mass (ng)	TWA (ng/L)	SD	Mass (ng)	TWA (ng/L)	SD
2014 POCIS	May 28 (13 d)	2.0			8.7			ND			4.5			12.5			5.1		
		1.9	0.4	0.01	10.8	2.9	0.3	ND	**ND**		5.1	2.3	1.1	13.7	12.3	9.7	5.7	1.6	0.1
		1.9			9.8			ND			10.3			45.8			5.6		
	Jun 10 (28 d)	N/A			N/A			N/A			N/A			N/A			N/A		
		N/A	--	--	N/A	--	--	N/A	--	--	N/A	--	--	N/A	--	--	N/A	--	--
		N/A			N/A			N/A			N/A			N/A			N/A		
	Jul 8 (14 d)	2.0			27.4			ND			19.5			22.8			14.5		
		2.6	0.4	0.1	13.3	5.9	2.0	ND	**ND**		5.5	3.7	2.4	9.3	7.5	3.2	5.8	2.9	1.2
		1.8			24.6			ND			8.8			15.3			11.3		
	Jul 22 (7 d)	ND			16.3			1.2			5.2			8.1			7.0		
		ND	**ND**		20.2	11.6	3.0	1.4	0.5	0.2	10.1	5.6	2.0	14.4	12.6	4.4	11.0	5.6	1.6
		ND			27.2			2.2			10.8			17.0			12.7		
	Jul 29 (14 d)	1.6			19.2			1.4			6.2			10.9			9.7		
		1.8	0.4	0.1	22.9	6.4	1.2	1.6	0.3	0.05	8.6	2.7	0.7	15.5	7.1	1.8	13.9	3.5	0.7
		2.9			28.2			2.0			10.2			18.5			14.2		
	Aug 12 (14 d)	3.1			31.5			3.8			11.2			14.1			13.3		
		3.8	2.0	2.3	34.3	8.5	1.0	3.8	0.5	0.1	10.1	3.2	0.5	12.7	6.4	0.4	14.8	3.5	0.7
		24.8			27.3			2.8			7.9			13.6			9.9		
	Aug 26 (14 d)	65.6			22.7			1.2			5.3			11.9			8.1		
		59.4	16.7	8.6	12.2	4.4	1.6	0.7	0.1	0.1	4.9	1.6	0.1	7.1	3.9	1.6	2.4	1.2	0.9
		141			13.0			0.3			2.7			5.5			2.7		
	Sept 9 (14 d)	10.1			26.1			3.4			16.7			20.3			15.6		
		2.9	1.1	0.7	35.2	10.0	3.2	4.6	0.7	0.2	26.6	7.6	1.9	32.7	13.8	3.6	26.5	6.6	2.1
		5.4			49.3			5.6			26.7			33.9			30.4		
	Sept 23 (14 d)	3.0			23.5			2.9			16.4			24.6			18.3		
		4.4	1.1	0.8	31.7	8.8	2.5	3.8	0.6	0.1	18.1	6.5	1.6	38.2	15.4	3.4	23.8	6.4	1.3
		10.9			42.1			4.5			25.6			34.5			27.7		
	Oct 7 (14 d)	107			16.7			1.4			2.7			264			6.1		
		232	34.2	12.4	27.4	6.2	1.5	2.4	0.3	0.1	5.4	1.5	0.6	582	250	113	11.1	2.6	0.8
		207			24.1			2.8			6.0			727			11.7		
	Oct 21 (7 d)	ND			16.3			0.6			1.5			7.0			4.6		
		7.1	2.2	0.6	12.0	7.1	1.6	1.3	0.3	0.1	8.4	4.1	2.7	14.9	11.7	4.3	8.0	3.8	1.1
		4.8			10.7			1.1			9.0			14.9			8.2		

Table A5 continued: North End pharmaceutical data

2015 POCIS	Apr 29 (14 d)	8.0			42.4			3.5			27.4			19.2			ND	
		ND	1.5	0.0	45.6	12.0	0.6	3.6	0.5	0.02	12.7	6.5	3.4	19.9	9.3	0.2	ND	ND
		N/A			N/A			N/A			N/A			N/A			N/A	
	May 13 (14 d)	26.9			18.1			1.4			7.7			8.3			ND	
		36.1	5.9	1.2	24.9	8.4	4.4	1.8	0.3	0.1	8.8	4.9	3.9	15.1	6.1	1.9	ND	ND
		ND			49.0			3.0			29.0			15.2			ND	
	May 27 (13 d)	6.5			10.4			1.0			2.7			3.1			ND	
		7.0	1.4	0.1	12.3	5.0	3.0	1.1	0.2	0.03	9.2	1.9	1.2	5.9	2.4	0.8	ND	ND
		7.6			28.9			1.3			4.3			5.0			ND	
	Jun 9 (14 d)	55.0			5.4			0.5			1.2			1.5			ND	
		75.8	12.3	2.8	9.8	2.3	0.7	0.9	0.1	0.04	9.1	1.7	1.3	6.8	2.3	1.4	ND	ND
		ND			10.0			0.9			5.6			6.0			ND	
	Jun 23 (14 d)	ND			14.4			1.6			5.8			23.8			ND	
		104	19.5	0.1	26.5	4.7	2.3	2.6	0.3	0.1	11.8	2.5	1.1	11.9	6.4	4.6	ND	ND
		105			10.6			1.1			5.9			4.8			ND	
	Jul 7 (14 d)	867			8.0			0.5			11.6			3.7			ND	
		913	167	6.1	7.0	2.2	0.3	0.5	0.1	0.01	2.5	1.7	1.8	2.5	1.4	0.3	ND	ND
		ND			9.0			0.4			1.9			2.7			ND	
	Jul 21 (14 d)	83.9			15.7			1.1			2.7			4.2			ND	
		44.3	10.2	4.9	11.4	3.9	0.7	1.2	0.2	0.01	6.8	1.5	1.0	4.7	2.3	0.3	ND	ND
		34.2			16.1			1.3			ND			5.4			ND	
	Aug 4 (14 d)	3.0			32.9			3.0			10.6			17.8			ND	
		4.1	0.8	0.2	42.8	10.1	1.4	3.4	0.5	0.03	10.5	3.4	0.1	21.3	9.2	0.9	ND	ND
		5.1			35.3			3.0			10.0			18.8			ND	
	Aug 18 (15 d)	2.4			16.7			1.5			7.4			11.9			ND	
		2.0	0.5	0.2	19.5	5.3	0.7	1.7	0.2	0.02	14.6	3.5	1.2	13.5	5.7	0.7	ND	ND
		4.1			21.6			1.6			10.2			10.6			ND	
	Sept 2 (14 d)	6.8			21.6			1.7			7.1			10.1			ND	
		1.8	0.8	0.5	20.0	5.8	0.3	1.8	0.3	0.01	7.8	2.3	0.3	9.1	4.2	0.7	ND	ND
		4.3			22.0			1.7			6.0			7.3			ND	
	Sept 16 (21 d)	17.0			60.6			6.0			37.8			29.6			ND	
		18.5	2.2	0.1	61.2	10.7	0.6	5.7	0.6	0.02	15.0	5.1	2.7	30.2	9.9	0.7	ND	ND
		16.2			55.5			5.5			18.2			33.5			ND	
	Oct 7 (21 d)	4.1			23.2			1.8			10.3			15.8			ND	
		7.6	0.7	0.3	32.4	5.1	1.2	2.8	0.2	0.1	17.8	3.0	1.1	25.6	6.6	2.2	ND	ND
		N/A			N/A			N/A			N/A			N/A			N/A	

N/A = Sampler at that site and time could not be analyzed (e.g., lost to flooding, damaged in field, stolen, vandalized, etc.). ND = Not detected.

267

Table A6a-h: PFAS concentrations measured by POCIS in the Red River and Assiniboine River (HD). Sampling sites are ordered (left to right) to reflect Red River flow (south to north); EM→NB→NE→SK→BP. HD on the Assiniboine River is a tributary to the Red River. Mass on sampler is used to calculate the time weighted average (TWA) concentration based on deployment time (days, d) and sampling rate (R_S, L/d), both provided in table. Reported in bold is the mean and standard deviation (SD) of triplicate TWA measurements. The date listed represents the start of the deployment period. The start of the subsequent deployment represents the end of the previous. Total deployment time in days (d) is provided in brackets.

Table A6a: PFDA

PFDA R_s = 0.19 L/d		Emerson (EM)			St. Norbert (NB)			North End (NE)			Selkirk (SK)			Breezy Point (BP)			Headingley (HD)		
Year	Deployment date (days)	Mass (ng)	TWA (ng/L)	SD	Mass (ng)	TWA (ng/L)	SD	Mass (ng)	TWA (ng/L)	SD	Mass (ng)	TWA (ng/L)	SD	Mass (ng)	TWA (ng/L)	SD	Mass (ng)	TWA (ng/L)	SD
2014 POCIS	Jul 22 (7 d)	ND			ND			0.22			0.26			0.22			0.10		
		0.17	0.13	--	ND	0.19	--	0.21	0.19	0.05	0.25	0.19	0.01	0.19	0.15	0.02	0.00	0.07	--
		ND			0.25			0.34			0.23			0.18			0.00		
	Jul 29 (14 d)	0.28			0.48			0.40			5.20			0.65			0.50		
		0.89	0.22	0.11	0.41	0.17	0.02	0.52	0.17	0.03	3.99	1.73	0.32	0.38	0.19	0.05	0.28	0.14	0.04
		0.55			NA			NA			NA			0.46			0.35		
	Aug 12 (14 d)	0.20			0.23			1.00			0.17			0.25			0.25		
		0.25	0.09	0.01	0.23	0.09	0.01	0.36	0.21	0.14	0.20	0.07	0.01	0.18	0.09	0.02	0.17	0.07	0.02
		0.23			NA			0.31			0.20			0.28			0.18		
	Aug 26 (14 d)	0.20			0.25			0.28			0.28			0.19			0.14		
		0.21	0.08	0.01	0.30	0.09	0.02	0.33	0.10	0.02	0.33	0.11	0.01	0.16	0.06	0.01	0.20	0.07	0.02
		0.20			0.19			0.21			0.29			0.15			0.21		
	Sept 9 (14 d)	0.10			0.17			0.27			0.13			0.13			0.24		
		0.12	0.04	0.01	0.12	0.05	0.01	0.21	0.10	0.03	0.14	0.05	0.01	0.00	0.07	0.02	0.11	0.06	0.03
		NA			0.12			0.30			0.12			0.22			0.11		

N/A = Sampler at that site and time could not be analyzed (e.g., lost to flooding, damaged in field, stolen, vandalized, etc.). ND = Not detected.

Table A6b: PFHpA

PFHpA R_s = 0.32 L/d		Emerson (EM)			St. Norbert (NB)			North End (NE)			Selkirk (SK)			Breezy Point (BP)			Headingley (HD)		
Year	Deployment date (days)	Mass (ng)	TWA (ng/L)	SD	Mass (ng)	TWA (ng/L)	SD	Mass (ng)	TWA (ng/L)	SD	Mass (ng)	TWA (ng/L)	SD	Mass (ng)	TWA (ng/L)	SD	Mass (ng)	TWA (ng/L)	SD
2014 POCIS	Jul 22 (7 d)	3.04			1.79			4.12			3.26			1.93			2.60		
		2.94	1.23	0.18	2.19	0.81	0.17	3.17	1.56	0.25	4.28	1.51	0.38	2.75	1.04	0.18	3.73	1.40	0.25
		2.31			1.44			3.17			2.58			2.29			3.11		
	Jul 29 (14 d)	5.91			1.49			1.49			11.29			0.17			1.82		
		4.43	1.00	0.31	2.50	0.45	0.16	2.85	0.48	0.21	11.75	2.57	0.07	0.85	0.22	0.20	1.40	0.40	0.09
		3.14			NA			NA			NA			1.91			2.19		
	Aug 12 (14 d)	1.18			0.86			0.78			1.06			0.87			1.36		
		1.62	0.32	0.05	0.73	0.18	0.02	0.87	0.17	0.03	1.20	0.27	0.03	0.91	0.21	0.01	1.19	0.23	0.09
		1.52			NA			0.61			1.34			0.98			0.60		
	Aug 26 (14 d)	1.44			1.76			0.67			1.94			1.16			2.44		
		3.05	0.50	0.18	1.77	0.43	0.05	1.25	0.18	0.09	2.81	0.60	0.15	1.04	0.26	0.03	2.16	0.56	0.09
		2.24			2.18			0.52			3.25			1.34			2.97		
	Sept 9 (14 d)	1.59			0.40			0.77			2.59			1.22			0.44		
		1.27	0.32	0.05	1.35	0.20	0.11	1.70	0.25	0.12	2.18	0.55	0.06	0.00	0.26	0.02	2.44	0.30	0.23
		NA			0.90			0.85			2.63			1.12			1.19		

N/A = Sampler at that site and time could not be analyzed (e.g., lost to flooding, damaged in field, stolen, vandalized, etc.). ND = Not detected.

Table A6c: PFHxA

PFHxA R_s = 0.29 L/d		Emerson (EM)			St. Norbert (NB)			North End (NE)			Selkirk (SK)			Breezy Point (BP)			Headingley (HD)		
Year	Deployment date (days)	Mass (ng)	TWA (ng/L)	SD	Mass (ng)	TWA (ng/L)	SD	Mass (ng)	TWA (ng/L)	SD	Mass (ng)	TWA (ng/L)	SD	Mass (ng)	TWA (ng/L)	SD	Mass (ng)	TWA (ng/L)	SD
2014 POCIS	Jul 22 (7 d)	3.88			1.79			3.92			3.39			1.81			1.69		
		3.11	1.65	0.23	3.05	1.07	0.37	3.76	1.94	0.10	4.39	1.70	0.45	2.35	1.07	0.16	2.91	1.13	0.30
		3.05			1.68			4.15			2.58			2.37			2.27		
	Jul 29 (14 d)	14.25			4.03			3.44			1.75			0.56			2.64		
		8.93	2.48	0.92	6.78	*1.33*	*0.48*	6.21	1.19	0.48	1.98	0.46	0.04	1.76	0.53	0.45	1.96	0.64	0.15
		7.04			NA			NA			NA			4.18			3.17		
	Aug 12 (14 d)	2.07			1.80			2.78			1.40			1.50			1.84		
		2.58	0.59	0.07	1.23	0.37	0.10	2.00	0.52	0.16	1.69	0.44	0.11	1.60	0.40	0.03	1.76	0.35	0.16
		2.49			NA			1.51			2.27			1.73			0.66		
	Aug 26 (14 d)	1.30			1.43			0.99			1.73			0.60			2.15		
		2.74	0.49	0.18	1.74	0.39	0.04	ND	0.24	--	2.97	0.63	0.18	0.49	0.13	0.02	1.69	0.48	0.06
		1.86			1.63			ND			3.04			0.44			2.04		
	Sept 9 (14 d)	2.17			0.48			1.70			2.74			1.64			0.46		
		1.04	0.4	0.2	2.02	0.32	0.19	3.32	0.52	0.26	2.45	0.66	0.05	1.49	0.47	0.09	2.72	0.37	0.28
		NA			1.40			1.37			2.80			2.14			1.32		

N/A = Sampler at that site and time could not be analyzed (e.g., lost to flooding, damaged in field, stolen, vandalized, etc.). ND = Not detected.

Table A6d: PFNA

PFNA R_s = 0.23 L/d		Emerson (EM)			St. Norbert (NB)			North End (NE)			Selkirk (SK)			Breezy Point (BP)			Headingley (HD)		
Year	Deployment date (days)	Mass (ng)	TWA (ng/L)	SD	Mass (ng)	TWA (ng/L)	SD	Mass (ng)	TWA (ng/L)	SD	Mass (ng)	TWA (ng/L)	SD	Mass (ng)	TWA (ng/L)	SD	Mass (ng)	TWA (ng/L)	SD
2014 POCIS	Jul 22 (7 d)	1.17			0.58			1.19			1.10			1.11			0.72		
		1.09	0.63	0.13	1.04	0.58	0.19	1.27	0.73	0.06	1.31	0.69	0.12	1.16	0.63	0.13	1.35	0.63	0.20
		0.77			1.16			1.08			0.93			0.77			0.95		
	Jul 29 (14 d)	3.52			2.03			1.21			14.07			1.12			1.04		
		2.77	0.86	0.23	2.31	0.67	0.06	2.00	0.50	0.17	17.87	4.96	0.83	1.00	0.35	0.04	0.98	0.37	0.11
		2.02			NA			NA			NA			1.25			1.60		
	Aug 12 (14 d)	0.83			0.83			1.69			0.83			0.82			0.95		
		1.05	0.30	0.04	1.01	0.29	0.04	0.82	0.36	0.14	0.82	0.27	0.02	0.62	0.23	0.03	0.74	0.25	0.04
		1.02			NA			1.02			0.96			0.81			0.73		
	Aug 26 (14 d)	0.63			1.00			0.57			0.76			0.45			0.92		
		1.24	0.27	0.10	1.36	0.35	0.07	0.72	0.19	0.03	1.25	0.34	0.09	0.46	0.14	0.01	0.61	0.25	0.05
		0.73			0.98			0.50			1.23			0.42			0.88		
	Sept 9 (14 d)	0.59			0.75			0.89			0.76			0.39			1.14		
		0.60	0.18	0.01	0.60	0.19	0.04	0.87	0.28	0.02	0.87	0.27	0.03	0.00	0.19	0.10	0.69	0.24	0.10
		NA			0.48			0.97			0.95			0.83			0.51		

N/A = Sampler at that site and time could not be analyzed (e.g., lost to flooding, damaged in field, stolen, vandalized, etc.). ND = Not detected.

Table A6e: PFOA

PFOA R_s = 0.16 L/d

Year	Deployment date (days)	Emerson (EM) Mass (ng)	TWA (ng/L)	SD	St. Norbert (NB) Mass (ng)	TWA (ng/L)	SD	North End (NE) Mass (ng)	TWA (ng/L)	SD	Selkirk (SK) Mass (ng)	TWA (ng/L)	SD	Breezy Point (BP) Mass (ng)	TWA (ng/L)	SD	Headingley (HD) Mass (ng)	TWA (ng/L)	SD
2014 POCIS	Jul 22 (7 d)	2.36			1.08			2.58			2.18			1.33			1.30		
		2.31	1.92	0.28	2.13	1.31	0.52	2.42	2.26	0.09	2.63	1.98	0.35	1.58	1.26	0.13	2.29	1.64	0.45
		1.80			1.19			2.60			1.86			1.32			1.94		
	Jul 29 (14 d)	7.15			2.84			2.47			2.45			1.13			2.49		
		6.14	2.60	0.68	3.86	1.49	0.32	4.22	1.49	0.55	2.20	1.04	0.08	1.57	0.83	0.40	1.90	1.13	0.29
		4.17			NA			NA			NA			2.85			3.18		
	Aug 12 (14 d)	1.68			1.26			2.03			1.53			1.26			1.96		
		2.55	0.94	0.20	1.17	0.54	0.03	1.64	0.73	0.18	1.72	0.78	0.10	1.22	0.59	0.07	1.72	0.67	0.27
		2.08			NA			1.22			1.99			1.51			0.83		
	Aug 26 (14 d)	1.23			1.46			0.50			1.71			0.86			1.96		
		2.75	0.88	0.34	1.83	0.75	0.09	1.11	0.30	0.17	2.66	1.09	0.29	0.89	0.39	0.01	1.89	0.93	0.12
		1.91			1.76			0.38			2.94			0.86			2.39		
	Sept 9 (14 d)	1.35			0.68			0.99			1.77			0.93			0.85		
		1.10	0.55	0.08	1.22	0.41	0.12	2.07	0.59	0.29	1.93	0.82	0.03	0.00	0.47	0.08	1.73	0.53	0.21
		NA			0.87			0.92			1.84			1.17			1.02		

N/A = Sampler at that site and time could not be analyzed (e.g., lost to flooding, damaged in field, stolen, vandalized, etc.). ND = Not detected.

Table A6f: PFOS

PFOS R_s = 0.36 L/d

Year	Deployment date (days)	Emerson (EM) Mass (ng)	TWA (ng/L)	SD	St. Norbert (NB) Mass (ng)	TWA (ng/L)	SD	North End (NE) Mass (ng)	TWA (ng/L)	SD	Selkirk (SK) Mass (ng)	TWA (ng/L)	SD	Breezy Point (BP) Mass (ng)	TWA (ng/L)	SD	Headingley (HD) Mass (ng)	TWA (ng/L)	SD
2014 POCIS	Jul 22 (7 d)	4.89			1.93			3.79			2.22			2.79			0.84		
		4.71	1.70	0.36	4.09	1.44	0.60	3.82	1.59	0.13	3.40	1.07	0.25	3.19	1.10	0.17	0.86	0.35	0.03
		3.22			4.85			4.38			2.49			2.35			0.96		
	Jul 29 (14 d)	53.95			39.26			10.72			0.10			6.96			1.60		
		43.25	8.47	2.29	45.13	8.37	0.82	17.75	2.82	0.99	0.14	0.02	0.01	6.71	1.59	0.41	1.31	0.35	0.11
		30.90			NA			NA			NA			10.40			2.39		
	Aug 12 (14 d)	6.18			8.81			13.51			4.39			4.95			1.55		
		7.97	1.43	0.18	9.71	1.84	0.13	5.62	1.65	0.89	4.26	0.88	0.04	3.63	0.92	0.18	1.22	0.27	0.04
		7.51			NA			5.89			4.65			5.37			1.24		
	Aug 26 (14 d)	2.68			7.87			2.23			2.92			1.30			1.77		
		6.04	0.90	0.34	6.92	1.32	0.28	2.79	0.46	0.08	4.90	0.94	0.34	1.22	0.27	0.03	1.82	0.44	0.15
		4.95			5.12			1.96			6.37			1.50			3.13		
	Sept 9 (14 d)	2.58			2.97			2.80			1.17			1.02			1.11		
		1.75	0.43	0.12	1.64	0.41	0.16	1.95	0.47	0.08	1.53	0.28	0.05	0.00	0.29	0.12	0.58	0.15	0.06
		NA			1.56			2.33			1.60			1.87			0.52		

N/A = Sampler at that site and time could not be analyzed (e.g., lost to flooding, damaged in field, stolen, vandalized, etc.). ND = Not detected.

Table A6g: PFHxS

PFHxS R_s = N/A*		Emerson (EM)			St. Norbert (NB)			North End (NE)			Selkirk (SK)			Breezy Point (BP)			Headingley (HD)		
Year	Deployment date (days)	Mass (ng)	Mass/d (ng/d)	SD	Mass (ng)	Mass/d (ng/d)	SD	Mass (ng)	Mass/d (ng/d)	SD	Mass (ng)	Mass/d (ng/d)	SD	Mass (ng)	Mass/d (ng/d)	SD	Mass (ng)	Mass/d (ng/d)	SD
2014 POCIS	Jul 22 (7 d)	4.46			1.57			3.26			2.72			1.20			1.36		
		4.04	0.56	0.08	4.37	0.37	0.22	3.11	0.48	0.04	3.60	0.40	0.11	2.35	0.26	0.08	2.23	0.26	0.06
		3.35			1.76			3.67			2.10			1.93			1.94		
	Jul 29 (14 d)	32.01			11.27			7.79			3.82			0.79			3.27		
		25.07	1.81	0.46	18.84	1.08	0.38	11.70	0.70	0.20	4.07	0.28	0.01	4.27	0.31	0.26	2.73	0.26	0.08
		19.05			NA			NA			NA			7.98			4.96		
	Aug 12 (14 d)	3.25			2.60			1.88			2.56			2.01			2.80		
		4.07	0.27	0.03	1.83	0.16	0.04	2.37	0.13	0.04	2.59	0.20	0.02	1.92	0.15	0.01	2.37	0.14	0.08
		3.90			NA			1.18			3.12			2.22			0.59		
	Aug 26 (14 d)	2.65			1.65			0.45			2.56			1.15			4.14		
		6.63	0.31	0.15	2.41	0.16	0.04	1.54	0.05	0.05	4.31	0.31	0.12	1.55	0.10	0.02	3.35	0.28	0.04
		3.90			2.63			0.25			5.97			1.64			4.37		
	Sept 9 (14 d)	3.01			0.35			0.77			1.86			0.94			0.09		
		1.50	0.16	0.08	2.02	0.09	0.06	1.42	0.07	0.03	2.53	0.15	0.02	0.00	0.08	0.02	2.01	0.07	0.07
		NA			1.56			0.65			2.06			1.27			0.99		

N/A = Sampler at that site and time could not be analyzed (e.g., lost to flooding, damaged in field, stolen, vandalized, etc.). ND = Not detected. *No R_s value exists in the literature for this analyte, therefore data is presented as mass on POCIS per day

Table A6h: PFPeA

PFPeA R_s = N/A*		Emerson (EM)			St. Norbert (NB)			North End (NE)			Selkirk (SK)			Breezy Point (BP)			Headingley (HD)		
Year	Deployment date (days)	Mass (ng)	Mass/d (ng/d)	SD	Mass (ng)	Mass/d (ng/d)	SD	Mass (ng)	Mass/d (ng/d)	SD	Mass (ng)	Mass/d (ng/d)	SD	Mass (ng)	Mass/d (ng/d)	SD	Mass (ng)	Mass/d (ng/d)	SD
2014 POCIS	Jul 22 (7 d)	ND			ND			ND			ND			ND			ND		
		ND	ND		ND	ND		ND	ND		ND	ND		ND	ND		ND	ND	
		ND			ND			ND			ND			ND			ND		
	Jul 29 (14 d)	6.12			1.78			1.74			ND			0.34			1.13		
		3.98	0.31	0.12	2.84	0.17	0.05	3.03	0.17	0.07	ND	ND		1.05	0.08	0.06	0.96	0.10	0.04
		2.89			NA			NA			ND			2.10			2.00		
	Aug 12 (14 d)	1.76			1.28			1.41			1.43			1.30			1.51		
		2.08	0.14	0.02	1.46	0.10	0.01	1.06	0.08	0.02	1.26	0.10	0.01	1.47	0.10	0.01	1.18	0.08	0.03
		2.18			NA			0.89			1.59			1.22			0.73		
	Aug 26 (14 d)	1.17			1.58			1.41			1.52			ND			ND		
		2.00	0.12	0.03	2.15	0.12	0.03	ND	0.10	--	2.32	0.09	0.08	ND	ND		ND	ND	
		1.97			1.39			ND			0.00			ND			ND		
	Sept 9 (14 d)	1.61			0.51			1.22			1.89			NA			0.00		
		2.85	0.16	0.06	1.51	0.07	0.04	2.92	0.13	0.07	2.28	0.13	0.03	1.04	0.13	0.08	1.31	0.06	0.05
		NA			1.08			1.23			1.48			2.54			1.01		

N/A = Sampler at that site and time could not be analyzed (e.g., lost to flooding, damaged in field, stolen, vandalized, etc.). ND = Not detected. *No R_s value exists in the literature for this analyte, therefore data is presented as mass on POCIS per day
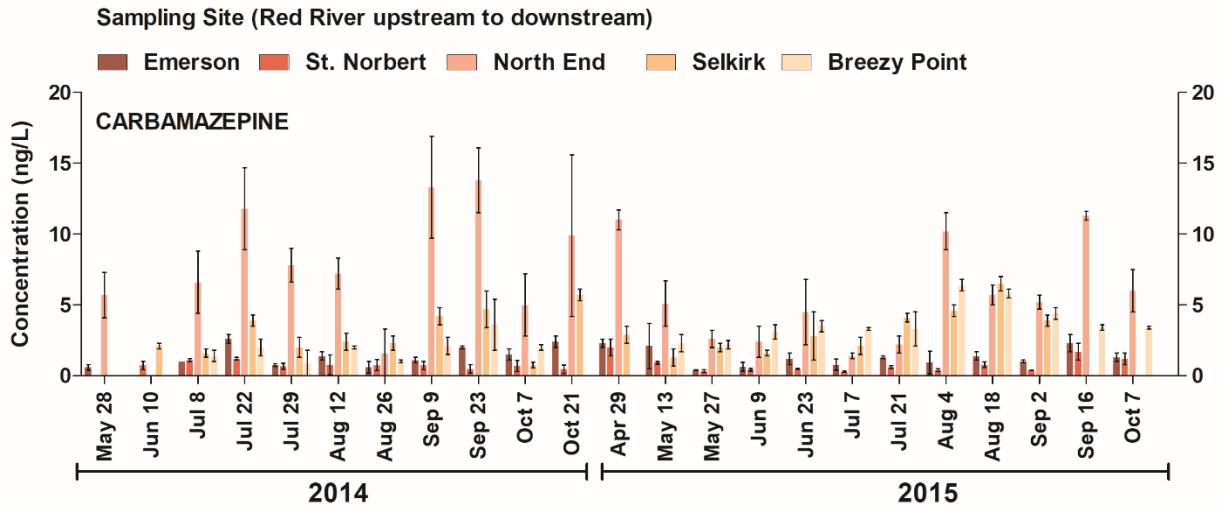
Figure A1: Time weighted average concentrations of carbamazepine detected over the two-year study as measured using POCIS. Bars represent the mean and standard deviation (SD) of triplicate measurements. Bar colour corresponds to sampling site in direction of flow (Emerson, St. Norbert, North End, Selkirk, Breezy Point). Headingley on the Assiniboine River is not shown.
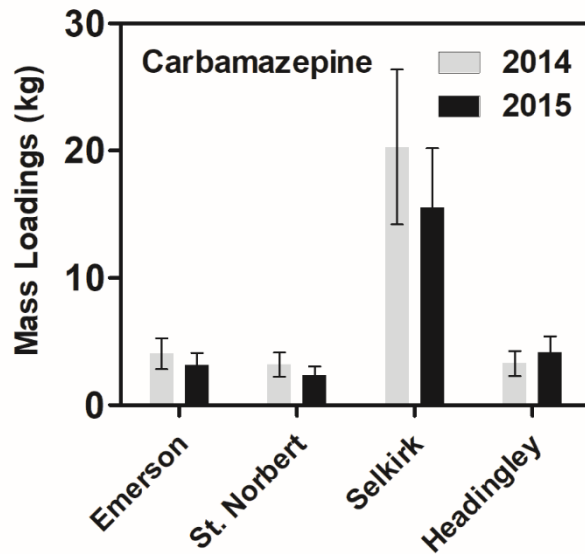
Figure A2: Mass loadings over the duration of each sampling season of carbamazepine along the Red River from south to north (flow direction) at Emerson, St. Norbert, and Selkirk and on the Assiniboine River at Headingley. Each bar in the plot represents 11 samples in 2014 and 12 samples in 2015. Error bars represent 30% relative standard deviation, estimated based on the uncertainty observed for replicate POCIS measurements.

272
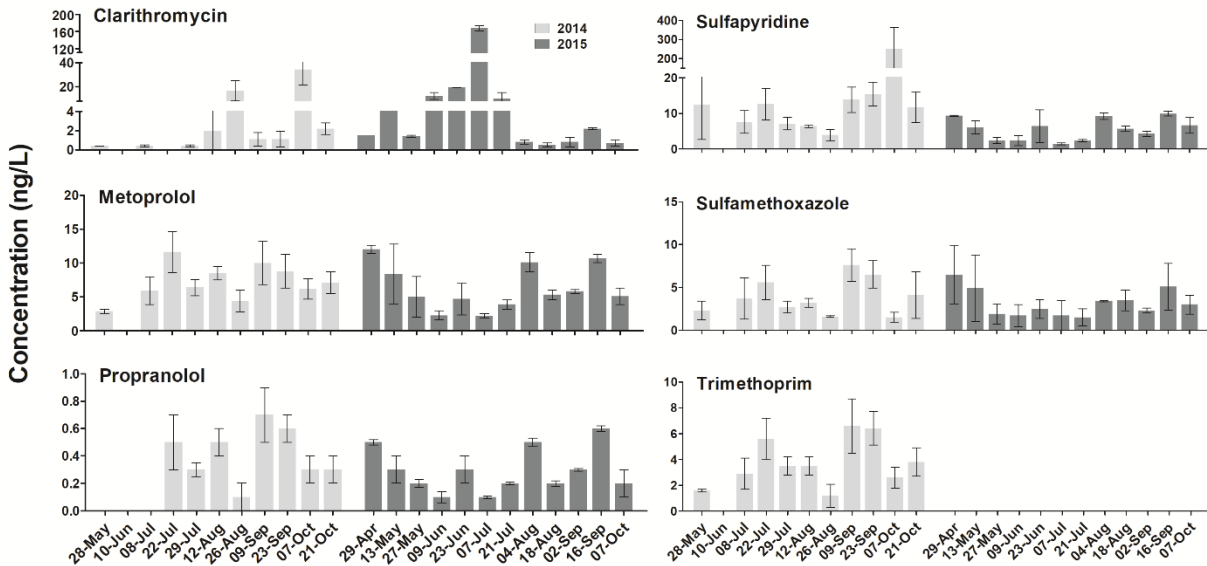
Figure A3: Concentrations of six pharmaceuticals at the North End Red River site as measured by POCIS. Left to right on each plot is spring to fall samples in 2014 (light gray bars) and 2015 (dark gray bars). Each bar represents the mean and standard deviation (error bars) of triplicate POCIS. Trimethoprim was not detected in any samples in 2015.

Table A7: Per capita loadings (µg/person/d) of pharmaceuticals into the Red River from the North End WWTP estimated based on measured concentrations at the North End site (Table A5). Comparisons with two other studies also provided.

Per capita loadings (µg/person/d)	CBZ	CLA	MET	PRO	SMX	SPY	TRI
Red River (this work)	128	33	132	7	68	150	76
Dead Horse Creek[a] (ref. 1)	203	NR	33	NR	160	NR	24
Gold Bar[b] (ref. 2)	≈60	≈65	≈20	≈2	NR	NR	≈10
Capital Region[c] (ref. 2)	≈75	≈115	≈20	≈4	NR	NR	≈15

NR – not reported. a – population = 18,000. b – population = 750,000. c – population = 250,000. Values from MacLeod and Wong, 2010 were interpolated from graph, thus approximate (≈).

1. Carlson, J.C., Anderson, J.C., Low, J.E., Cardinal, P., MacKenzie, S.D., Beattie, S.A., Challis, J.K., Bennett, R.J., Meronek, S.S., Wilks, R.P.A., Buhay, W.M., Wong, C.S., Hanson, M.L. *Sci. Total Environ.* **2013a,** 445-446, 64-78.
2. MacLeod, S.L., Wong, C.S. *Water Res.* **2010,** 44, 533–544.

Pesticide Exposure Distributions

Table A8: Linear regression statistics for the exposure distributions in Figure 2.5, Chapter 2.

Compound	River	Slope	Intercept	r^2	n
Thiamethoxam	Red	1.99	-1.01	0.97	105 (1<LOD)
	Assiniboine	1.89	-0.73	0.97	22
Clothianidin	Red	2.06	-1.33	0.97	105
	Assiniboine	2.34	-1.09	0.95	22
Imidacloprid	Red	2.34	-0.65	0.98	105 (6<LOD)
	Assiniboine	2.58	0.41	0.98	22 (5<LOD)
Atrazine	Red	1.60	-2.28	0.99	105
	Assiniboine	2.70	-1.14	0.99	22

LOD – Limit of detection.

Antibiotic Resistance Genes

Table A9: Levels of total bacteria (16S-rRNA genes), tetracycline- and sulfonaminde-resistance genes (sum of measured genes of each class) at sites along the Red River (n = 11). Values (genes/mL) were log-transformed before statistical calculations.

Location	Total bacteria *Log*(16SrRNA)	Tetracycline resistance *Log [$\sum(tet)$]*	Sulfonamide resistance *Log[$\sum(sul)$]*
Emerson	5.95 (0.06)	2.04 (0.28)	3.75 (0.10)
St. Norbert	5.90 (0.08)	2.31 (0.16)	3.79 (0.78)
North End	6.22 (0.11)	1.97 (0.40)	3.69 (0.14)
Selkirk	5.96 (0.09)	2.44 (0.28)	2.80 (0.44)
Breezy Point	6.00 (0.05)	2.19 (0.41)	3.61 (0.07)
Headingly	6.07 (0.07)	2.54 (0.16)	3.45 (0.12)

Table A10: Frequency of gene determinants at each site along the river.

Gene	Emerson (n=11)	St. Norbert (n = 11)	North End (n = 11)	Selkirk (n = 11)	Breezy Point (n = 10)	Headingly (n = 10)
*tet*A	27%	9%	18%	18%	10%	20%
*tet*B	45%	64%	18%	45%	70%	60%
*tet*C	55%	55%	27%	64%	50%	60%
*tet*D	9%	9%	18%	27%	30%	0%
*tet*E	0%	0%	18%	9%	10%	10%
*tet*G	0%	0%	9%	0%	0%	0%
*tet*K	9%	9%	18%	27%	20%	20%
*tet*L	0%	9%	9%	0%	0%	10%
*tet*M	0%	0%	9%	9%	20%	20%
*tet*O / *tet*Q / *tet*X	0%	0%	0%	0%	0%	0%
*tet*S	18%	18%	18%	9%	0%	30%
*Sul*1	91%	100%	82%	82%	100%	80%
*Sul*2	91%	91%	82%	73%	100%	90%
*Sul*3	100%	91%	55%	55%	70%	100%
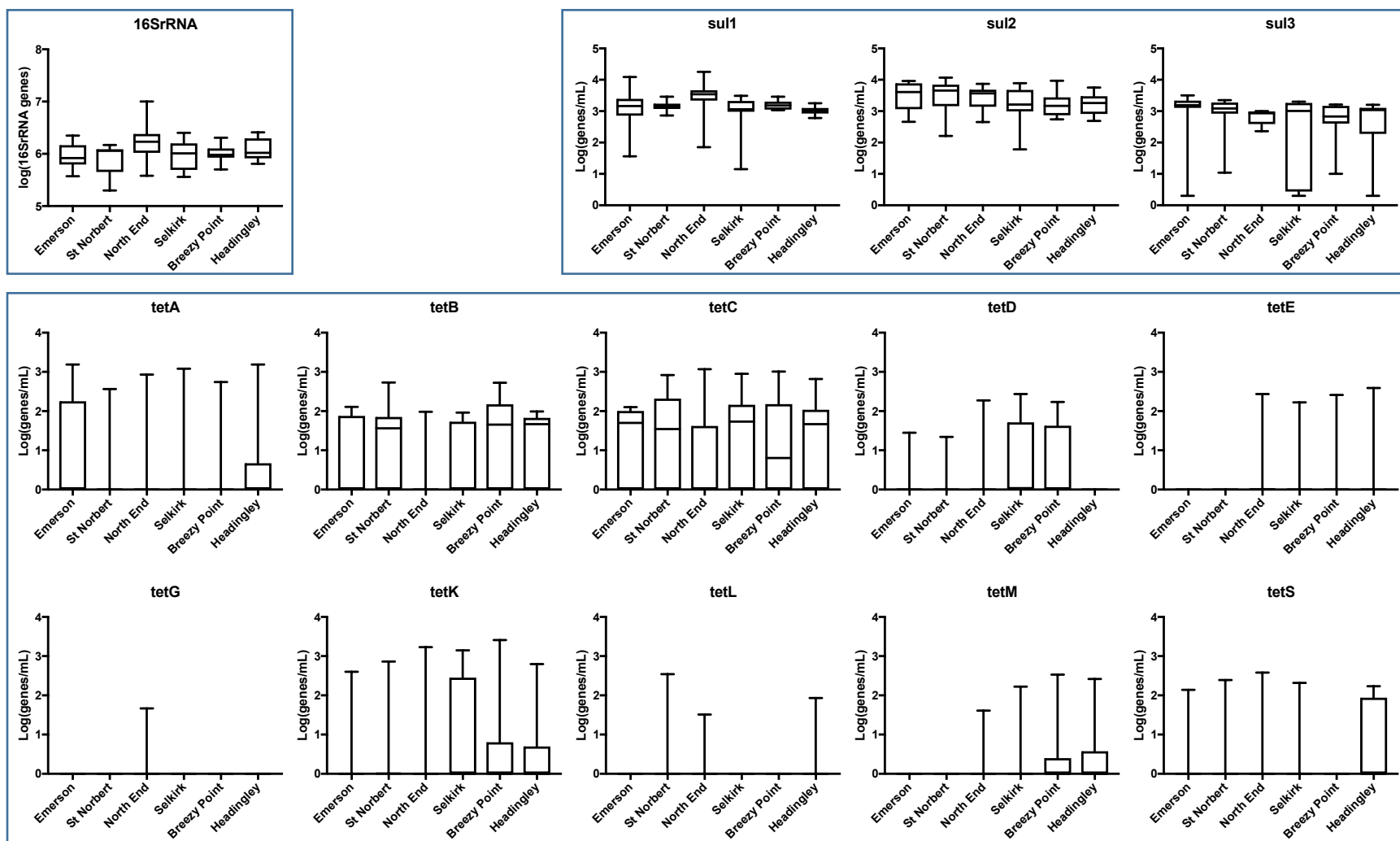
Figure A4: Gene abundances normalized to volume (genes/mL) and log transformed for each gene-determinant measured in this work. Left to right along the x-axis corresponds to flow direction in the Red River (Emerson, St. Norbert, North End, Selkirk, Breezy Point). Assiniboine River (Headingley) on the right.

9.2 APPENDIX B: ADDITIONAL INFORMATION FOR CHAPTER 3

DEVELOPMENT AND CALIBRATION OF AN ORGANIC-DIFFUSIVE GRADIENTS IN THIN FILMS AQUATIC PASSIVE SAMPLER FOR A DIVERSE SUITE OF POLAR ORGANIC CONTAMINANTS

SUMMARY

The following includes further experimental details and procedures for the various o-DGT experiments (sampler optimization, diffusion, calibration, field validation). Additional results (tables and graphs) for the diffusion and calibration studies and the sampling rate modelling is also provided for all 34 analytes.

METHODS AND MATERIALS

Chemicals and Reagents

HPLC grade methanol from Fischer Scientific (Ottawa, ON) and 18.2 MΩ-cm Milli-Q water (EMD Milli-Pore Synergy® system, Etobicoke, ON), were used for LC solvents, analytical standards, and sample extractions. Optima LC/MS grade formic acid was purchased from Fischer Scientific as an LC solvent additive. Agarose and potassium nitrate (>99% purity) from Sigma-Aldrich, were used for making gels and adjusting ionic strength, respectively.

Instrumental analysis

Batch analyses of samples sets were conducted by running 13 calibration standards (ranging of 0.01 – 500 µg/L) along with the samples. Blanks were run between triplicate sets of samples and single calibration standards (10, 25, or 50 µg/L) were run every 15 samples as a QA/QC protocol (concentration to be within 20% of target). Linearity (r^2) of calibration standards was ≥0.98 over all analyses and all 34 analytes.

LC Parameters.

Table B1. Negative and positive mode gradient elution methods. A flow rate 0.45 mL/min and column temperature of 42 °C was used for both methods. Negative mode solvents were unbuffered 95% H_2O: 5% MeOH (A) and 100% MeOH (B). Positive mode solvents contained 0.05% formic acid.

Negative mode		Positive mode	
Time (min)	%B	Time (min)	%B
0.00	6.0	0.00	6.0
0.50	6.0	1.00	6.0
6.00	95.0	2.80	50.0
7.00	95.0	3.50	50.0
7.01	6.0	6.50	95.0
11.00	6.0	7.50	95.0
		7.51	6.0
		11.50	6.0
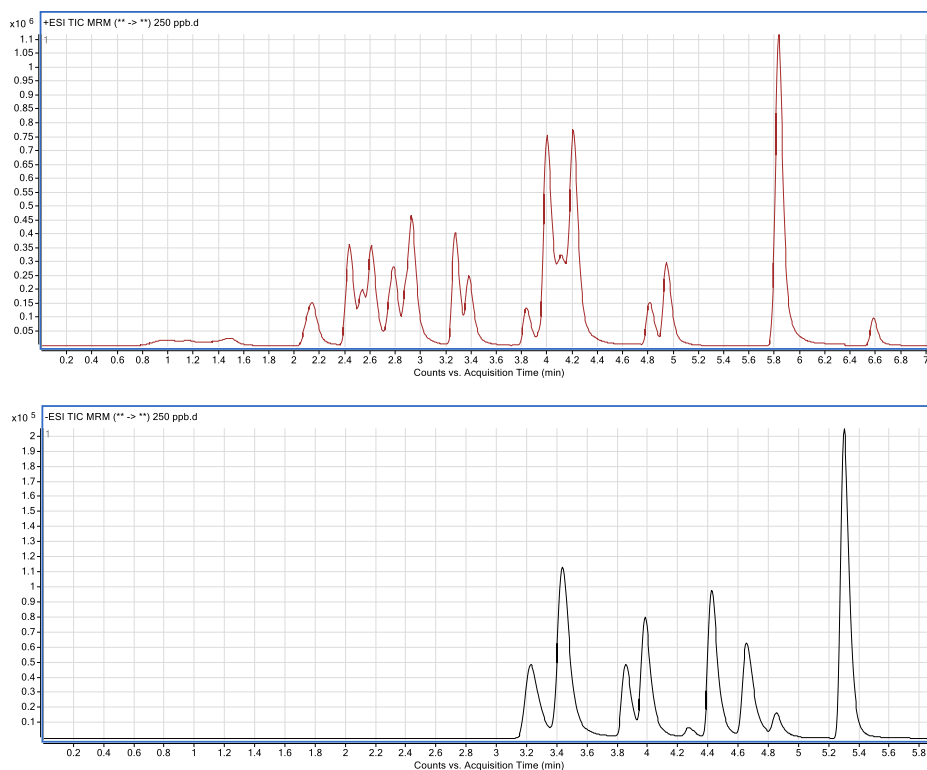
Figure B1: Chromatograms for positive mode (top) and negative mode (bottom).

MS/MS Parameters.

Table B2a. Source parameters for positive and negative mode MS/MS methods.

Gas Temp (°C)	300	Nebulizer (psi)	50
Gas Flow (L/min)	10.5	Capillary (V)	4000

Table B2b. m/z transition, fragmentor voltage (Frag), collision energy (CE), and retention time details for the MS/MS positive mode dynamic MRM method.

Compound Name	Precursor Ion	Product Ion	Frag (V)	CE (V)	Ret Time (min)
Atenolol (Q)	267.2	190.2	135	16	1.49
Atenolol (q)	267.2	145.2	135	16	1.49
Atenolol-d7 (IS)	274.2	145.1	135	24	1.69
Atrazine (Q)	216.1	174.1	130	16	4.20
Atrazine (q)	216.1	146.2	130	20	4.23
Atrazine-d5 (IS)	221.1	179.1	130	16	4.23
Carbamazepine (Q)	237.1	194.2	145	18	4.00
Carbamazepine (q)	237.1	179.2	145	36	4.00
Carbamazepine-d10 (IS)	247.1	204.2	145	36	4.00
Chlorpyrifos (Q)	352.2	200.1	105	15	6.55
Chlorpyrifos (q)	352.2	124.9	105	15	6.55
Chlorpyrifos-d10 (IS)	362.0	201.0	105	15	6.59

Compound Name	Precursor Ion	Product Ion	Frag (V)	CE (V)	Ret Time (min)
Clarithromycin (Q)	748.5	158.1	165	11	4.79
Clothianidin (Q)	250.0	169.0	106	8	2.88
Clothianidin (q)	250.0	132.0	106	12	2.88
Clothianidin-d3 (IS)	253.0	132.0	111	12	2.88
Diazinon (Q)	305.2	169.2	132	19	5.83
Diazinon (q)	305.2	153.2	132	19	5.83
Diazinon-d10 (IS)	315.2	170.1	132	20	5.83
Enrofloxacin (Q)	360.1	342.1	140	18	2.77
Enrofloxacin (q)	360.1	316.2	140	14	2.77
Enrofloxacin-d5 (IS)	365.1	347.1	140	19	2.77
Erythromycin (Q)	734.5	158.0	155	33	4.09
Fluoxetine (Q)	310.3	148.1	92	5	4.23
Fluoxetine-d6 (IS)	316.2	154.2	90	4	4.23
Imidacloprid (Q)	256.2	209.0	95	12	2.63
Imidacloprid (q)	256.2	175.2	95	17	2.63
Imidacloprid-d4 (IS)	259.7	212.7	95	17	2.63
Josamycin (IS)	828.0	174.3	80	35	4.85
Metoprolol (Q)	268.2	191.1	133	15	2.89
Metoprolol (q)	268.2	133.1	133	17	2.89
Metoprolol-d7 (IS)	275.1	123.1	125	19	2.89
Paroxetine (Q)	330.2	192.2	145	16	3.81
Propranolol (Q)	260.1	183.1	130	14	3.37
Propranolol (q)	260.1	155.1	130	23	3.37
Propranolol-d7 (IS)	267.2	189.1	130	16	3.37
Roxithromycin (Q)	837.5	158.0	180	30	4.93
Sulfadimethoxine (Q)	311.1	156.0	125	17	3.27
Sulfadimethoxine (q)	311.1	245.0	125	15	3.27
Sulfadimethoxine-d6 (IS)	317.1	162.1	125	19	3.27
Sulfamethazine (Q)	279.1	186.1	120	13	2.61
Sulfamethazine (q)	279.1	156.1	120	14	2.61
Sulfamethazine-13C6 (IS)	285.1	186.1	120	14	2.61
Sulfamethoxazole (Q)	254.0	156.1	110	11	2.79
Sulfamethoxazole (q)	254.0	108.1	110	22	2.79
Sulfamethoxazole-d4 (IS)	258.0	160.0	110	13	2.79
Sulfapyridine (Q)	250.1	156.1	110	12	2.13
Sulfapyridine (q)	250.1	184.1	110	13	2.13
Sulfapyridine-d4 (IS)	254.1	160.1	110	12	2.13
Sulfisoxazole (Q)	268.1	156.1	105	8	2.93
Sulfisoxazole (q)	268.1	113.1	105	12	2.93
Sulfachloropyridazine (Q)	285.1	156.1	105	10	2.76
Sulfachloropyridazine (q)	285.1	108.2	105	20	2.76
Thiamethoxam (Q)	292.0	211.0	111	8	2.54
Thiamethoxam (q)	292.0	181.0	111	20	2.54
Thiamethoxam-d3 (IS)	295.0	184.0	111	20	2.54
Trimethoprim (Q)	291.1	230.1	150	21	2.43
Trimethoprim (q)	291.1	261.1	150	20	2.43
Trimethoprim-d3 (IS)	294.1	230.1	150	22	2.43

Q = quantifier ion; q = qualifier ion; IS = internal standard

Table B2c. m/z transition, fragmentor voltage (Frag), collision energy (CE), and retention time details for the MS/MS negative mode dynamic MRM method.

Compound Name	Precursor Ion	Product Ion	Frag (V)	CE (V)	Ret Time (min)
17β-estradiol (Q)	271.0	145.0	195	40	4.28
17 β-estradiol-d4 (IS)	275.0	147.1	195	39	4.28
17α-ethynylestradiol (Q)	295.0	145.0	176	40	4.31
17α-ethynylestradiol-d4 (IS)	299.0	147.0	176	40	4.31
2,4-D (Q)	219.0	161.0	75	5	3.21
2,4-D (q)	219.0	124.9	75	24	3.21
2,4-D-13C6 (IS)	225.0	167.0	75	5	3.21
Clofibric Acid (Q)	213.1	127.0	82	8	3.43
Clofibric Acid-d4 (IS)	217.1	131.0	82	8	3.43
Diclofenac (Q)	294.0	250.0	85	5	4.64
Diclofenac-d4 (IS)	298.0	254.0	85	5	4.64
Estrone (Q)	269.0	145.0	176	38	4.27
Estrone-d4 (IS)	273.1	147.1	180	36	4.27
Fenoprofen (Q)	241.1	197.0	70	0	4.42
Fenoprofen (q)	241.1	93.0	70	24	4.42
Gemfibrozil (Q)	249.1	121.0	90	4	5.30
Gemfibrozil-d6 (IS)	255.1	121.0	90	4	5.30
Ibuprofen (Q)	205.0	161.0	70	2	4.85
Ibuprofen-d3 (IS)	208.0	164.0	70	2	4.85
Ketoprofen (Q)	253.0	209.0	70	1	3.85
Ketoprofen-d4 (IS)	257.0	213.0	70	1	3.85
Naproxen (Q)	229.0	170.0	72	11	3.98
Naproxen (q)	229.0	185.0	72	1	3.98
Naproxen-d3 (IS)	232.0	173.0	72	11	3.98

Q = quantifier ion; q = qualifier ion; IS = internal standard

Detection Limits

Method detection limits were determined using an o-DGT lab blank, extracted and processed as detailed in the main text. The sample was measured seven subsequent times by LC-MS/MS. Slopes taken from five 13-point calibration curves were averaged and used in the LOD and LOQ calculations (equations shown in Table B3). Averages of the five slopes for all 34 analytes varied on average by 12% (RSD), and maximally by 60%.

Table B3: Method detection limits for all 34 analytes in ng/L.

Compound Name	LOD*	LOQ**	Compound Name	LOD	LOQ
Atenolol	0.29	0.96	Gemfibrozil	27	91
Atrazine	1.3	4.4	Ibuprofen	76	250
Carbamazepine	1.7	5.7	Imidacloprid	1.0	3.4
Chlorpyrifos	2.0	6.8	Ketoprofen	56	190
Clarithromycin	0.60	2.0	Metoprolol	3.4	11
Clofibric Acid	4.2	14	Naproxen	35	120
Clothianidin	0.69	2.3	Paroxetine	1.3	4.2
Diazinon	4.5	15	Propranolol	1.2	4.0
2,4-D	4.1	14	Roxithromycin	0.44	1.5
Diclofenac	11	37	Sulfachloropyridazine	13	43
Enrofloxacin	15	48	Sulfadimethoxine	1.6	5.2
Erythromycin	0.18	0.61	Sulfamethazine	0.25	0.83
17β-estradiol	140	470	Sulfamethoxazole	20	66
Estrone	3.4	11	Sulfapyridine	0.57	1.9
17α-ethynylestradiol	1100	3700	Sulfisoxazole	0.24	0.78
Fenoprofen	63	210	Thiamethoxam	0.85	2.8
Fluoxetine	1.7	5.7	Trimethoprim	3.6	12

*Limit of detection (LOD) = $(X_{BLK} + 3\sigma_{BLK})$/slope; **Limit of quantitation (LOQ) = $(X_{BLK} + 10\sigma_{BLK})$/slope

RESULTS

Experimental details

Casting binding gels. Setting the binding gels was conducted with the cast laying horizontally to ensure the binding resin would settle to one face of the gel (Figure B2).

Figure B2: Gel casting system (left), casted binding gel sheet (middle), and individually cut binding gel discs (right).

Sorption tests. Sorption to all parts of the o-DGT sampler and testing equipment was investigated through simple exposure experiments at various points during sampler development. The diffusive gels, plastic o-DGT holder, and acrylic plastic (diffusion cell material) were exposed to the 34-analyte mixture for a designated period of time, extracted, and analyzed. No sorption of the 34 analytes to the plastic o-DGT holders, diffusive gels, or diffusion cell plastic was observed. Sorption to the polyethersulfone (PES) membrane was investigated as part of the full o-DGT calibration study as noted below and shown in Figure B3.

o-DGT extraction efficiency. Four o-DGT samplers were exposed for three days in a static 3L pre-mixed tank (unstirred) containing 25 ng/mL of the 34-analyte mixture and 5 mM KNO_3. Samplers were retrieved and extracted exactly as described above, with the addition of a fourth extraction to assess efficiency. The 'three-times' extracted binding gel was re-spiked with 50 ng of IS and a fourth methanol rinse was conducted, transferred into a separate test tube, and processed alongside the initial extract. The mass of analyte remaining on the binding gel after the first three extractions (i.e., the mass in the fourth fraction) was used to determine recoveries. All 34 analytes showed extraction efficiencies >95%, with exception of the single compound enrofloxacin (74%).

Table B4. Percent recoveries (± % error) for the 34 target analytes.

Compound Name	% Recovery	Compound Name	% Recovery
Atenolol	98.8 ± 5.4	Gemfibrozil	99.2 ± 3.3
Atrazine	99.6 ± 6.0	Ibuprofen	99.6 ± 5.7
Carbamazepine	99.6 ± 4.8	Imidacloprid	99.6 ± 5.2
Chlorpyrifos	99.3 ± 5.0	Ketoprofen	99.1 ± 4.2
Clarithromycin	98.8 ± 4.0	Metoprolol	99.0 ± 7.9
Clofibric Acid	99.7 ± 6.1	Naproxen	99.6 ± 6.0
Clothianidin	99.6 ± 5.4	Paroxetine	97.7 ± 1.9
Diazinon	99.4 ± 4.8	Propranolol	98.8 ± 5.1
2,4-D	99.7 ± 5.9	Roxithromycin	98.6 ± 3.9
Diclofenac	99.6 ± 7.4	Sulfachloropyridazine	99.6 ± 5.7
Enrofloxacin	74.1 ± 8.6	Sulfadimethoxine	99.6 ± 6.2
Erythromycin	98.9 ± 4.2	Sulfamethazine	99.6 ± 6.1
17β-estradiol	95.4 ± 1.6	Sulfamethoxazole	99.7 ± 6.6
Estrone	99.3 ± 2.0	Sulfapyridine	99.6 ± 6.8
17α-ethynylestradiol	99.9 ± 14.7	Sulfisoxazole	99.7 ± 7.6
Fenoprofen	99.4 ± 4.5	Thiamethoxam	99.5 ± 5.6
Fluoxetine	98.7 ± 5.8	Trimethoprim	99.4 ± 6.6

Sampler optimization

Binding gels. The mass of sorbent used per binding gel was optimized to ensure a sufficient binding capacity over a typical sampler deployment period (3-4 weeks). A simple exposure experiment demonstrated that 25 mg of HLB per binding gel disc was the optimal configuration. o-DGT with 10, 25, and 50 mg HLB binding gels were exposed to the 34-analyte mixture over 27 days, and sampled periodically to obtain a time-series (data not shown). The upper limit of sorbent was largely fixed by the ability of agarose to set and hold the sorbent in place. Above a binding gel density of 50 mg/disc (making the binding gel mixture ≈15% sorbent) the gel casting became increasingly difficult and inconsistent (e.g., air bubble intrusion, patchy sorbent distribution, etc.). Both the 25 and 50 mg binding gels produced linear uptake plots with similar slopes over the 27 d, suggesting that the former had sufficient binding capacity.

Polyethersulfone (PES) membrane. o-DGT with and without the PES membrane were exposed for eight days in the full-scale calibration experiment. Each layer of the o-DGT was extracted separately; the diffusive and binding gels from the standard o-DGT and the diffusive gels, binding gels, and PES membrane from the o-DGT with PES.
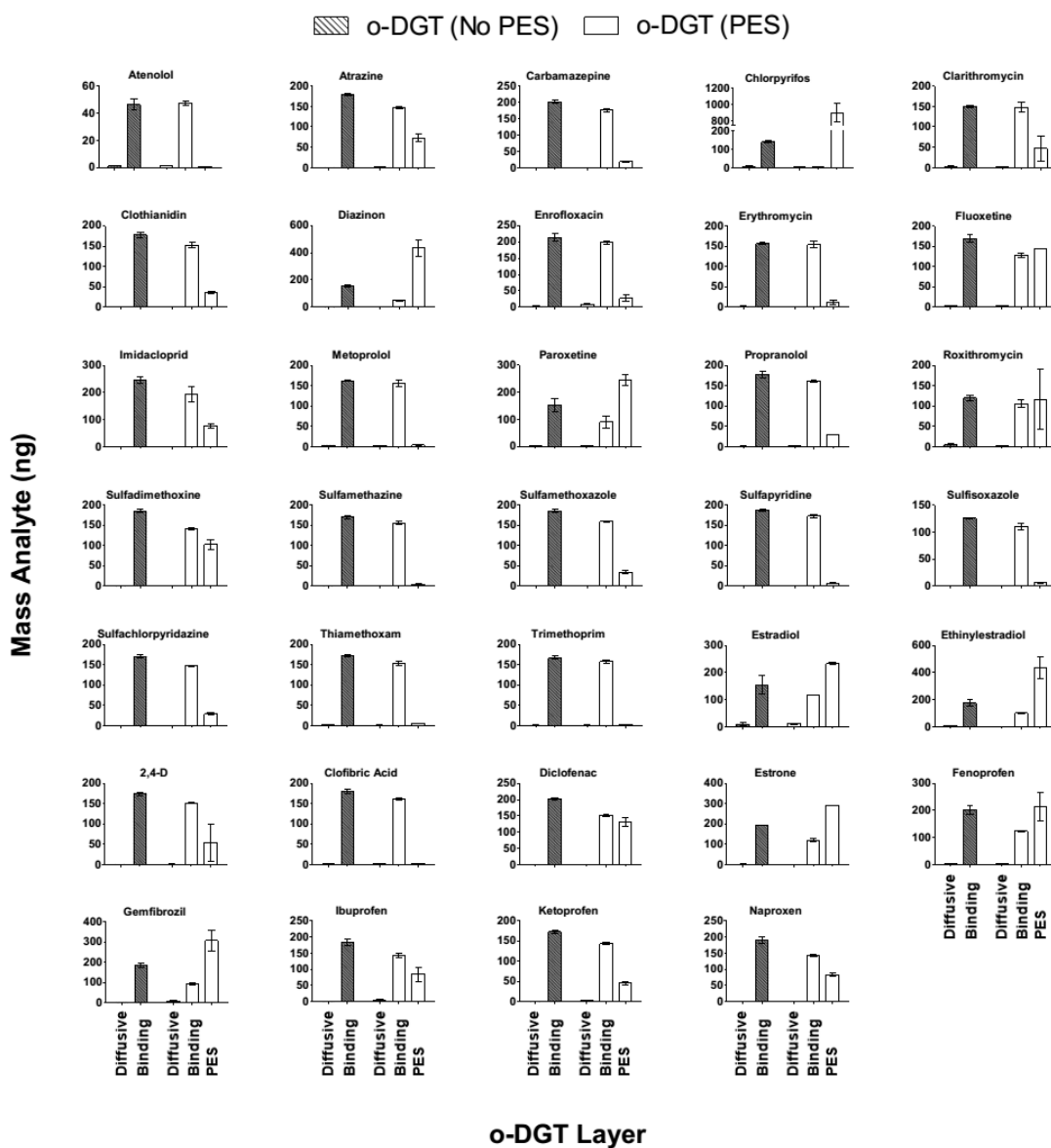
Figure B3: Mass of analyte in each o-DGT layer after exposure to all 34 compounds. Hashed bars represent the standard o-DGT (no PES) and the white bars represent o-DGT with the PES membrane. Error bars are standard deviations of duplicate samples.

Diffusion coefficients

Each cell (made of ¼" clear acrylic) held ca. 2 L and had a 2.5 cm^2 circular connecting window. A 0.75 mm diffusive gel was placed on the window between the two cells and gently sealed together with clamps. To each cell, 1 L of 5 mM KNO_3 was added, followed by a spike of the 34-analyte mixture into the source compartment (200 ng/mL) and corresponding methanol spike (solvent carrier) into the receiving compartment to give 2% (v/v) methanol. The cells were stirred gently on stir-plates. The 5 and 13°C experiments were conducted in a temperature controlled walk-in refrigerator, while the 23°C experiment was done at room temperature in our laboratory. Triplicate samples (195 µL) were taken from the receiving cell at ten time intervals spread over the experiments' duration (9 to 25 d, depending on the temperature) while the source cell was sampled five times at every second time interval. Samples were micro-pipetted directly into LC vials and spiked with 5 ng of IS before analysis via LC-MS/MS.
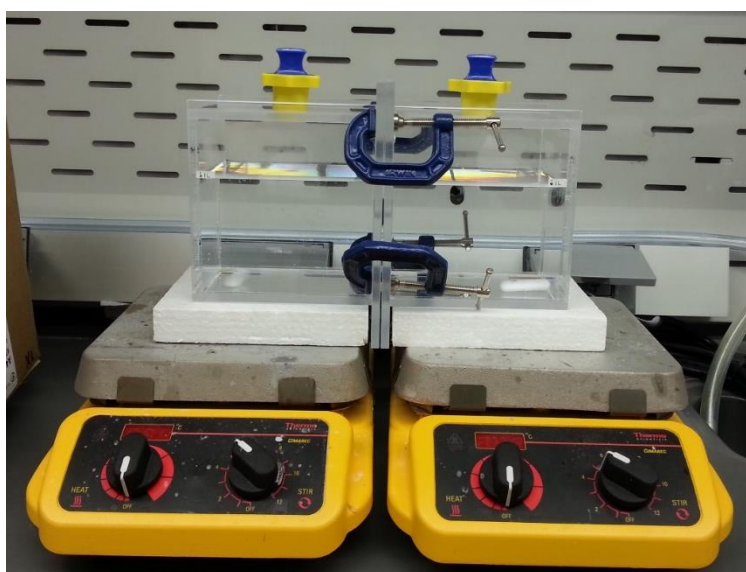
Figure B4: Diffusion cell.

Table B5. Measured diffusion coefficient data at three temperatures (T) with linear regression parameters of the D-T empirical relationships for each analyte.

Compound	D (×10^{-6} cm^2/s) [a]			Linear Regression [b]		
	5°C	13°C	23°C	Slope (×10^{-7})	y-int. (×10^{-6})	r^2
Atenolol	1.51 ± 0.089	2.00 ± 0.082	3.65 ± 0.15	1.23 ± 0.29	0.694 ± 0.45	0.948
Atrazine	1.86 ± 0.075	2.53 ± 0.10	3.53 ± 0.14	0.947± 0.040	1.34 ± 0.062	0.998
Carbamazepine	2.11 ± 0.096	2.76 ± 0.14	4.74 ± 0.25	1.52 ± 0.33	1.12 ± 0.51	0.955
Chlorpyrifos	1.50 ± 0.065	1.81 ± 0.10	3.24 ± 0.16	1.01 ± 0.30	0.799 ± 0.46	0.920
Clarithromycin	1.18 ± 0.073	1.36 ± 0.068	3.13 ± 0.14	1.14 ± 0.44	0.322 ± 0.67	0.873
Clofibric acid	1.88 ± 0.084	2.33 ± 0.10	4.05 ± 0.17	1.26 ± 0.32	1.03 ± 0.50	0.938
Clothianidin	1.85 ± 0.082	2.60 ± 0.16	4.00 ± 0.30	1.23 ± 0.12	1.13 ± 0.19	0.991
Diazinon	1.62 ± 0.077	2.01 ± 0.091	3.60 ± 0.19	1.15 ± 0.31	0.838 ± 0.49	0.930
2,4-D	1.96 ± 0.10	2.64 ± 0.11	4.52 ± 0.21	1.47 ± 0.29	1.02 ± 0.44	0.964
Diclofenac	1.98 ± 0.11	2.89 ± 0.12	4.20 ± 0.24	1.27 ± 0.042	1.29 ± 0.066	0.999
Erythromycin	1.09 ± 0.12	1.34 ± 0.099	1.67*	0.333	0.909	--
17β-Estradiol	1.71 ± 0.13	2.25 ± 0.36	2.96*	0.708	1.33	--
Estrone	1.63 ± 0.16	2.50 ± 0.13	3.63 ± 0.46	1.14 ± 0.014	1.02 ± 0.021	0.999
17α-ethynylestradiol	1.83 ± 0.19	2.41 ± 0.25	3.15*	0.745	1.44	--
Fenoprofen	1.78 ± 0.10	2.60 ± 0.17	3.91 ± 0.92	1.22 ± 0.073	1.09 ± 0.11	0.996
Fluoxetine	1.71 ± 0.091	2.22 ± 0.11	4.15 ± 0.24	1.41 ± 0.36	0.750 ± 0.56	0.938
Gemfibrozil	1.50 ± 0.086	2.11 ± 0.085	3.39 ± 0.15	1.09 ± 0.14	0.843 ± 0.21	0.984
Ibuprofen	1.81 ± 0.14	2.60 ± 0.20	3.85 ± 0.45	1.16 ± 0.069	1.16 ± 0.11	0.997
Imidacloprid	2.13 ± 0.13	2.48 ± 0.14	4.35 ± 0.48	1.29 ± 0.41	1.22 ± 0.63	0.909
Ketoprofen	1.51 ± 0.11	2.38 ± 0.11	3.13 ± 0.30	0.912 ± 0.11	1.09 ± 0.17	0.986
Metoprolol	1.59 ± 0.067	2.05 ± 0.093	4.15 ± 0.40	1.48 ± 0.43	0.564 ± 0.66	0.923
Naproxen	1.78 ± 0.094	2.43 ± 0.13	4.14 ± 0.28	1.36 ± 0.25	0.915 ± 0.38	0.968
Paroxetine	1.96 ± 0.12	2.15 ± 0.11	4.36 ± 0.19	1.40 ± 0.56	0.895 ± 0.86	0.864
Propranolol	1.79 ± 0.086	2.30 ± 0.14	4.22 ± 0.28	1.41 ± 0.36	0.840 ± 0.56	0.938
Roxithromycin	1.02 ± 0.060	1.20 ± 0.085	2.30 ± 0.12	0.740 ± 0.25	0.488 ± 0.39	0.900
Sulfachlorpyridazine	1.87 ± 0.090	2.99 ± 0.14	4.64 ± 0.20	1.58 ± 0.059	1.00 ± 0.092	0.999
Sulfadimethoxine	1.84 ± 0.078	2.46 ± 0.11	3.61 ± 0.16	1.01 ± 0.10	1.24 ± 0.15	0.991
Sulfamethazine	1.88 ± 0.075	2.50 ± 0.11	3.83 ± 0.16	1.12 ± 0.15	1.20 ± 0.24	0.982
Sulfamethoxazole	2.04 ± 0.085	2.54 ± 0.11	4.40 ± 0.29	1.36 ± 0.34	1.12 ± 0.53	0.940
Sulfapyridine	2.07 ± 0.083	2.71 ± 0.11	3.97 ± 0.17	1.09 ± 0.12	1.43 ± 0.19	0.987
Sulfisoxazole	1.49 ± 0.074	1.84 ± 0.11	3.47 ± 0.27	1.15 ± 0.34	0.695 ± 0.52	0.920
Thiamethoxam	1.96 ± 0.11	2.79 ± 0.18	3.95 ± 0.22	1.14 ± 0.029	1.34 ± 0.046	0.999
Trimethoprim	1.77 ± 0.076	2.41 ± 0.11	3.81 ± 0.23	1.17 ± 0.17	1.06 ± 0.26	0.979

-- Data not applicable due to poor linearity in the diffusion rate plots (analyte mass versus time). [a] Errors determined through error propagation based on Equation 3.3 (Chapter 3). [b] Errors represent standard deviations about the regression line. * Estimated based on two-point regression.
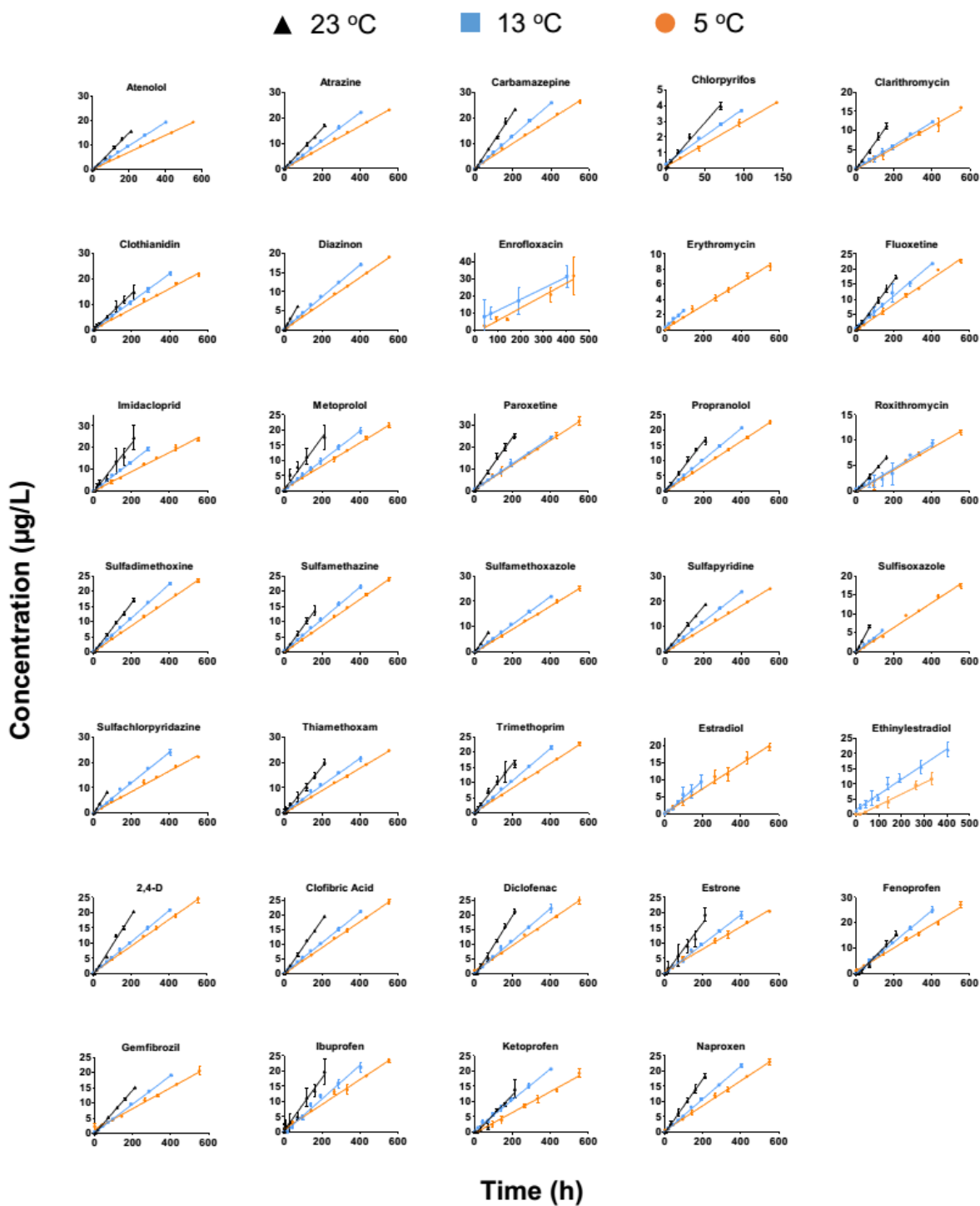
Figure B5: Concentration in the receiving cell for all 34 analytes at 5, 13, and 23ºC. All diffusion experiments had a minimum of 5 time points, representing the mean of triplicate measurements ± standard deviation (error bars). Least-squares linear regressions (solid lines) of each time-series provided the slope (diffusion rate constant) which was used to calculate diffusion coefficients according to Equation 3.3.

Table B6: Comparing measured and predicted diffusion coefficients at 5 and 13°C. Predicted D were based on measured D at 23°C using Equation 3.5.

Compound	D (×10⁻⁶ cm²/s) at 5 °C			D (×10⁻⁶ cm²/s) at 13 °C		
	Measured	Rel. error	Predicted	Measured	Rel. error	Predicted
Atenolol	1.5	30%	2.0	2.0	28%	2.6
Atrazine	1.9	2%	1.9	2.5	2%	2.5
Carbamazepine	2.1	21%	2.6	2.8	21%	3.3
Chlorpyrifos	1.5	16%	1.8	1.8	26%	2.3
Clarithromycin	1.2	44%	1.7	1.4	62%	2.2
Clofibric acid	1.9	16%	2.2	2.3	23%	2.9
Clothianidin	1.8	17%	2.2	2.6	8%	2.8
Diazinon	1.6	20%	1.9	2.0	26%	2.5
2,4-D	2.0	24%	2.4	2.6	21%	3.2
Diclofenac	2.0	15%	2.3	2.9	3%	3.0
Erythromycin*	1.1	20%	0.9	1.3	14%	1.2
17β-Estradiol*	1.7	7%	1.6	2.3	8%	2.1
Estrone	1.6	21%	2.0	2.5	2%	2.6
17α-ethynylestradiol*	1.8	8%	1.7	2.4	8%	2.2
Fenoprofen	1.8	19%	2.1	2.6	6%	2.8
Fluoxetine	1.7	31%	2.2	2.2	32%	2.9
Gemfibrozil	1.5	22%	1.8	2.1	13%	2.4
Ibuprofen	1.8	15%	2.1	2.6	4%	2.7
Imidacloprid	2.1	10%	2.3	2.5	24%	3.1
Ketoprofen	1.5	12%	1.7	2.4	7%	2.2
Metoprolol	1.6	40%	2.2	2.1	42%	2.9
Naproxen	1.8	26%	2.2	2.4	20%	2.9
Paroxetine	2.0	20%	2.4	2.2	43%	3.1
Propranolol	1.8	27%	2.3	2.3	29%	3.0
Roxithromycin	1.0	21%	1.2	1.2	35%	1.6
Sulfachlorpyridazine	1.9	34%	2.5	3.0	9%	3.3
Sulfadimethoxine	1.8	6%	1.9	2.5	3%	2.5
Sulfamethazine	1.9	10%	2.1	2.5	8%	2.7
Sulfamethoxazole	2.0	16%	2.4	2.5	22%	3.1
Sulfapyridine	2.1	3%	2.1	2.7	3%	2.8
Sulfisoxazole	1.5	25%	1.9	1.8	33%	2.4
Thiamethoxam	2.0	9%	2.1	2.8	0%	2.8
Trimethoprim	1.8	16%	2.1	2.4	12%	2.7
Average		**19%**			**18%**	

*Predicted D for ERY, E2, EE2 based on 23°C D-value calculated from two-point regression (Table B5)
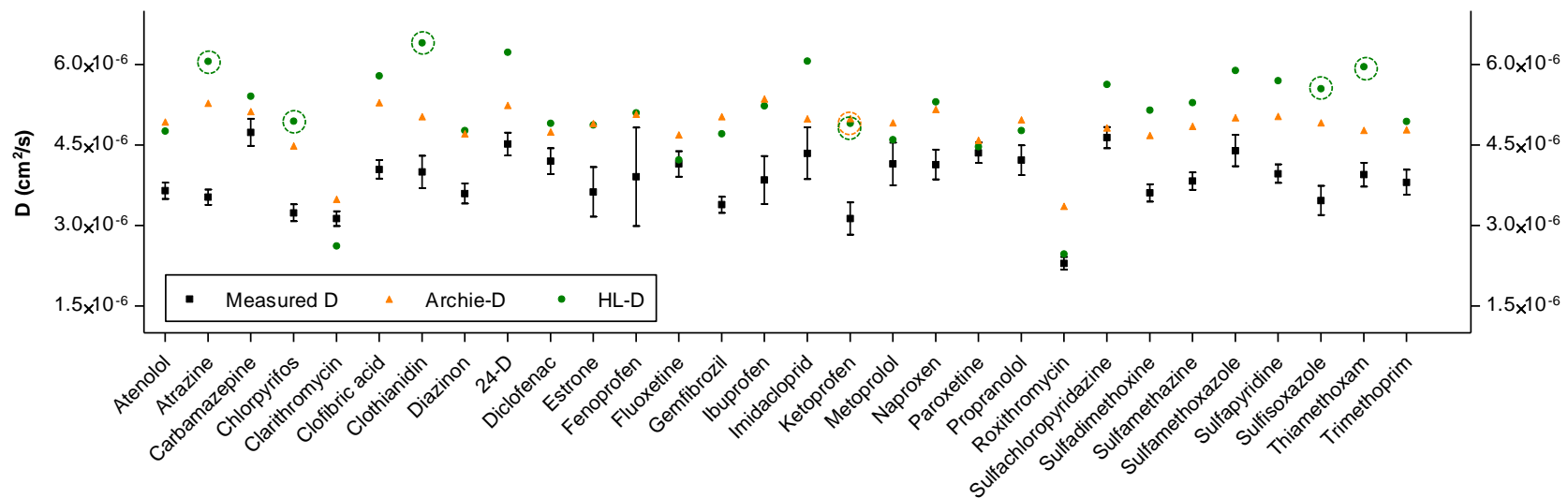
Figure B6: Experimentally measured D (23ºC) compared to empirically modelled D using Archie's law equation and the Hayduk-Laudie (HL) equation. Circled data points indicate relative errors of >50% compared to measured D. Error bars for measured D represent standard deviation of mean.

o-DGT Calibration

Laboratory-based sampler calibration was conducted to measure the uptake

dependence on time, and determine the capacity of the sampler throughout its

linear/kinetic uptake regime. Samplers were exposed in a 40 L round glass tank

containing 25 L of 5 mM KNO_3 (deionized water) and spiked with the 34-analyte mixture

at a nominal concentration of 2 ng/mL (nominal). To produce a flowing system, the

samplers were suspended on metal arms from a motorized variable-speed carousel and

rotated through the water at a linear velocity of ca. 2.4 cm/s (Figure B7).

Figure B7: Experimental setup for the calibration of o-DGT. Negative and positive controls (left), treatment tank (right).

Water pH was constant around 5.5 and temperature ranged from 25°C at initial

renewal (temperature of tap water), dropping to 21°C over the course of 6-8 h, where it

remained stable until the next renewal period. Evaporation from the 40 L tank was

measured to be maximally 450 mL over 48 h, representing <2% of the renewal volume.

Appropriate positive and negative controls were run concurrently in 5 L glass tanks. The

negative control contained standard o-DGT exposed to 3 L of 5mM KNO_3 in un-spiked DI water. The o-DGT and water served as laboratory blanks at each sampling point. The positive control was spiked at the same target concentration as the exposure tank (2 ng/mL) and renewed once per week (3 L), with evaporation being monitored during each week (100-110 mL/day of evaporation). Triplicate water samples (195 µL) were taken three times per week. The entire experiment was conducted in a ventilated bench which was covered by black-out curtains to minimize photolysis.

To ensure water concentrations were constant over the 25 days, complete tank renewals were conducted every 24 h for the first nine days of the experiment, switching to 48 h renewals for the remainder. Target water concentrations were confirmed with triplicate water samples (195 µL) at the beginning and end of each renewal. Additionally, single 20 mL water samples were taken at each sampling point and pre-concentrated by SPE for analytes with detection limits close to 2 ng/mL. o-DGT extracts, water samples, and SPE samples were processed accordingly, described in detail previously. Water concentrations were kept constant over the duration of the calibration experiment, as seen below in Figure B8. While there were a few instances of concentration spikes, the largest of which was or enrofloxacin at ≈ 4 µg/L on the first sampling, these fluctuations were ironed out given the frequent renewal periods and were unlikely to have had any observable effect on the overall uptake kinetics of the exposed o-DGT.

The experimental setup for the o-DGT calibration can be seen in Figure B7. The negative control (5 mM KNO_3) contained o-DGT and served as a source of blank water samples and o-DGT extraction blanks, both of which were clean (e.g., no detected

analytes at their LOD) over the course of the experiment. The positive control was used to monitor water evaporation and account for all analyte losses not a result of o-DGT uptake. Given the frequent renewals and consistent exposure concentrations achieved (Figure B8), no corrections were needed. The small errors (SD of duplicate o-DGT) in Figure 3.1 and Figure B9 suggests the experimental setup was appropriate and that o-DGT uptake was highly reproducible.

The β-blocker ATE was the single analyte in this study that demonstrated poor uptake in o-DGT (Figure B9). ATE was linear (r^2=0.90) through 12 d of exposure, however the total accumulated mass was only 57 ng. The very low capacity for ATE was in contrast to our preliminary binding gel tests that showed a much greater capacity (data not shown). The reason for this inconsistency in the ATE data set is not known at this time.
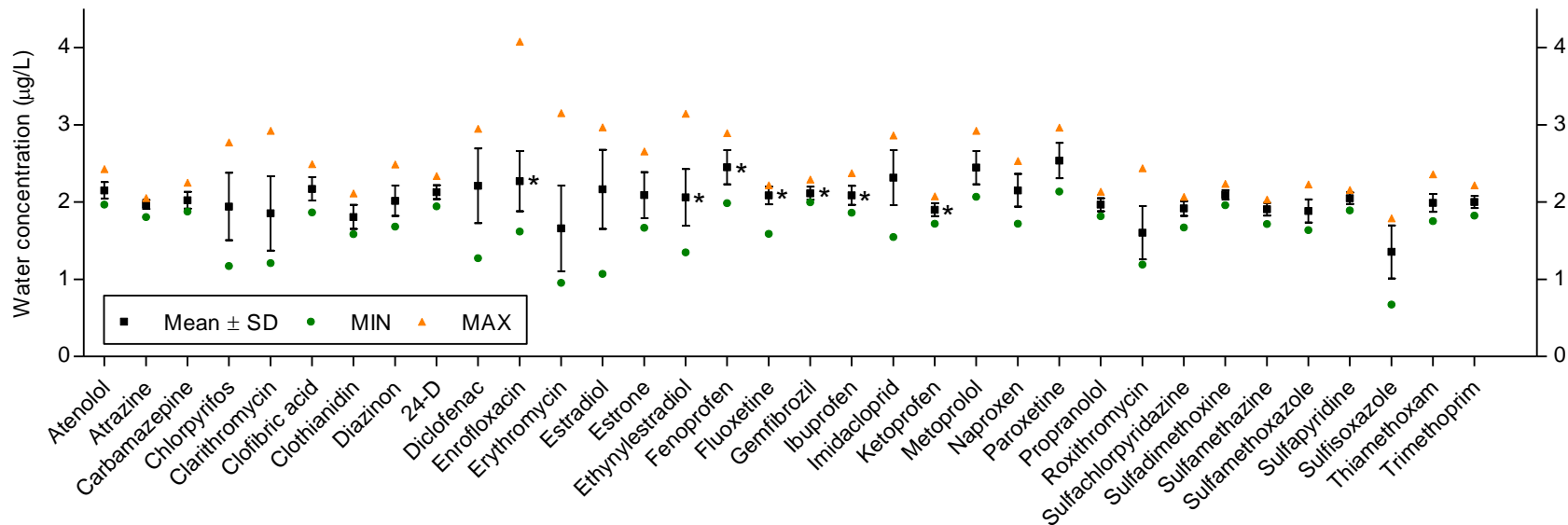
*Figure B8: Water concentrations (μg/L) of all 34 analytes over the 25 d calibration experiment. Water was renewed every 1-2 days. *Asterisked data points represent those compounds requiring pre-concentration by SPE. All others were direct-inject samples. Square data points and error bars represent mean and standard deviation of 32 sampling points (triplicates for direct-inject, singles for SPE) over the 25 day experiment. The minimum (green circles) and maximum (orange triangles) concentrations measured over the 32 sampling points are also shown.*

Table B7. Sampling rates (R_s – mL/d) for each analyte determined experimentally (23ºC) through sampler calibration and compared to calculated R_s based on measured D (23ºC) and modelled D using Archie's Law (Equation 3.7). Equation 3.8 and 3.9 (Chapter 3) were used to determine E-R_s and D-R_s, respectively. D-R_s and M-R_s errors are calculated relative to E-R_s. Averages, standard deviations, and ranges are provided for each column.

Compound	Diffusion (D)		Experimental (E)	Model (M)	
	D-R_s (mL/d)	Rel. error	E-R_s (mL/d)	Rel. error	M-R_s (mL/d)
Atenolol	12.0 ± 0.6	--	--	--	16.2
Atrazine	11.6 ± 0.6	17%	**14.0 ± 0.4**	24%	17.3
Carbamazepine	15.6 ± 0.9	7%	**14.6 ± 0.8**	15%	16.8
Chlorpyrifos	10.7 ± 0.6	25%	**14.2 ± 3.3**	4%	14.7
Clarithromycin	10.3 ± 0.5	14%	**11.9 ± 3.1**	4%	11.5
Clofibric Acid	13.3 ± 0.7	15%	**11.5 ± 0.8**	51%	17.4
Clothianidin	13.1 ± 1.1	3%	**12.7 ± 1.1**	30%	16.5
Diazinon	11.8 ± 0.7	9%	**13.1 ± 1.3**	18%	15.5
2,4-D	14.8 ± 0.8	36%	**10.9 ± 0.5**	58%	17.2
Diclofenac	13.8 ± 0.9	42%	**9.7 ± 2.1**	61%	15.6
Enrofloxacin	9.7*	34%	**14.7 ± 2.6**	1%	14.6
Erythromycin	5.5 ± 3.0	61%	**13.9 ± 4.7**	17%	11.5
17β-estradiol	9.7 ± 3.0	32%	**14.2 ± 3.5**	13%	16.1
Estrone	11.9 ± 1.6	15%	**14.1 ± 2.0**	14%	16.1
17α-ethynylestradiol	10.3 ± 3.0	3%	**10.6 ± 2.0**	47%	15.6
Fenoprofen	12.8 ± 3.0	7%	**12.0 ± 1.1**	39%	16.7
Fluoxetine	13.6 ± 0.9	25%	**10.9 ± 0.6**	41%	15.4
Gemfibrozil	11.1 ± 0.6	10%	**12.3 ± 0.5**	34%	16.5
Ibuprofen	12.6 ± 1.5	0%	**12.6 ± 0.8**	40%	17.6
Imidacloprid	14.3 ± 1.6	11%	**16.1 ± 2.6**	2%	16.4
Ketoprofen	10.3 ± 1.0	21%	**13.0 ± 0.6**	26%	16.4
Metoprolol	13.6 ± 1.4	55%	**8.8 ± 0.8**	84%	16.2
Naproxen	13.6 ± 1.0	6%	**12.8 ± 1.3**	33%	17.0
Paroxetine	14.3 ± 0.7	54%	**9.3 ± 0.9**	62%	15.1
Propranolol	13.9 ± 1.0	5%	**13.2 ± 0.6**	24%	16.3
Roxithromycin	7.6 ± 0.4	26%	**10.2 ± 2.2**	9%	11.0
Sulfachloropyridazine	15.2 ± 0.8	16%	**13.1 ± 0.7**	21%	15.8
Sulfadimethoxine	11.8 ± 0.6	8%	**12.9 ± 0.4**	19%	15.4
Sulfamethazine	12.6 ± 0.6	6%	**11.9 ± 0.6**	34%	15.9
Sulfamethoxazole	14.4 ± 1.0	6%	**15.3 ± 1.3**	8%	16.4
Sulfapyridine	13.0 ± 0.7	13%	**11.5 ± 0.4**	43%	16.5
Sulfisoxazole	11.4 ± 0.9	11%	**12.8 ± 3.3**	26%	16.2
Thiamethoxam	13.0 ± 0.8	27%	**10.2 ± 0.6**	53%	15.7
Trimethoprim	12.5 ± 0.8	8%	**11.5 ± 0.5**	36%	15.7
MEAN	12.2	19%	**12.4**	30%	15.7
STD. DEV.	2.2	16%	**1.8**	20%	1.6
MINIMUM	5.5	0%	**8.8**	1%	11.0
MAXIMUM	15.6	61%	**16.1**	84%	17.6

*D used to determine D-R_s for enrofloxacin was borrowed from Chen et al. (2013)

Boundary Layer

Only those compounds that produced linear (r^2 values > 0.9) DBL plots (1/M vs.

Δg) and had positive y-intercepts were considered in the δ calculations (n=29). This

excluded five compounds in the flowing (atenolol, clarithromycin, erythromycin, 17α-

ethynylestradiol, roxithromycin) and static (atenolol, clarithromycin, erythromycin, 17β-

estradiol, roxithromycin) experiments.

Table B8: Boundary layer measurements for all analytes in flowing and static conditions. DBL thickness (δ) determined from a plot of reciprocal mass (accumulated in o-DGT) as a function of diffusive gel thickness (Δg) (see Figure 3.3). The slope and y-intercept are used to calculate δ. The linearity (r^2) of each plot is provided.

Compound	Flowing (≈ 2.4 cm/s) DBL			Static DBL		
	δ (cm)	Error	r^2	δ (cm)	Error	r^2
Atrazine	0.017	0.0030	0.999	0.076	0.008	0.992
Carbamazepine	0.024	0.0044	0.999	0.082	0.008	0.992
Chlorpyrifos	0.034	0.0122	0.989	0.041	0.005	0.995
Clofibric Acid	0.023	0.0091	0.994	0.087	0.009	0.992
Clothianidin	0.019	0.0026	1.000	0.117	0.021	0.965
Diazinon	0.023	0.0004	1.000	0.069	0.007	0.994
2,4-D	0.045	0.0047	0.999	0.101	0.009	0.992
Diclofenac	0.026	0.0034	0.999	0.133	0.012	0.989
Enrofloxacin	0.023	0.0059	0.997	0.045	0.006	0.994
17β-estradiol*	0.034	0.0056	0.998	---		
Estrone	0.050	0.0146	0.986	0.104	0.018	0.970
17α-ethynylestradiol*	---			0.075	0.026	0.921
Fenoprofen	0.0094	0.0047	0.998	0.066	0.012	0.982
Fluoxetine	0.0092	0.0012	1.000	0.064	0.012	0.981
Gemfibrozil	0.016	0.0051	0.998	0.074	0.010	0.987
Ibuprofen	0.006	0.0084	0.994	0.076	0.018	0.960
Imidacloprid	0.003	0.0289	0.939	0.088	0.015	0.977
Ketoprofen	0.023	0.0026	0.999	0.073	0.008	0.991
Metoprolol	0.021	0.0011	1.000	0.064	0.004	0.997
Naproxen	0.008	0.0058	0.997	0.068	0.008	0.992
Paroxetine	0.039	0.0055	0.998	0.060	0.003	0.998
Propranolol	0.022	0.0031	0.999	0.077	0.013	0.979
Sulfachloropyridazine	0.021	0.0059	0.997	0.087	0.011	0.987
Sulfadimethoxine	0.022	0.0043	0.999	0.072	0.009	0.990
Sulfamethazine	0.020	0.0038	0.999	0.074	0.008	0.991
Sulfamethoxazole	0.019	0.0029	0.999	0.075	0.008	0.993
Sulfapyridine	0.025	0.0062	0.997	0.093	0.011	0.987
Sulfisoxazole	0.010	0.0054	0.998	0.075	0.000	1.000
Thiamethoxam	0.029	0.0025	1.000	0.091	0.012	0.984
Trimethoprim	0.019	0.0036	0.999	0.066	0.027	0.906
MEDIAN	**0.022**			**0.075**		
STD. DEV.	**0.011**			**0.019**		
REL. STD. DEV.	**50%**			**24%**		
MINIMUM	**0.003**			**0.041**		
MAXIMUM	**0.050**			**0.133**		
MEAN	**0.022**			**0.078**		

*Data omitted due to poor linearity in the 1/M vs. Δg plots

Field evaluation

      This specific site was used as part of a larger, on-going study into the occurrence of wastewater contaminants in the community of Norway House Cree Nation (NHCN, 53° 59' 26" N, 97° 46' 25" W). The limited infrastructure in the community means that only one quarter ($\approx$300) of the homes have piped-in sewage services. The remaining 900 homes rely on septic tank trucks to deliver waste to the treatment plant. The residence time of the waste in septic tanks is largely unknown, and could potentially be impacting the profile and levels of contaminants eventually entering the lagoon/ treatment plant system.

      The community has three staging lagoons (1°→2°→3°) that undergo aeration and then enter (from the 3° lagoon) into a full scale wastewater treatment system. The effluent is released into Little Playgreen Lake, which sits at the confluence of Lake Winnipeg and the Nelson River. Comparisons between o-DGT, POCIS, and grab samples occurred at the tertiary lagoon, final effluent, and upstream sites. Sampling rates for POCIS were obtained from the peer-reviewed literature. Where multiple sampling rate measurements existed for a single compound, the average of the reported values were taken and used in the TWA water concentration calculations. This was done to avoid undue bias from any single study as a result of differing conditions (e.g., flow-rate, temperature, pH discrepancies) between our field site and those used in the sampler calibrations.

Table B9: POCIS sampling rates used (in bold) to calculate TWA water concentrations in NHCN. Individual sampling rates and their respective references are shown for each compound. Bolded values represent the mean of the individual sampling rate values.

Atrazine	Carbamazepine	Sulfamethoxazole	Trimethoprim	Sulfapyridine	Clarithromycin
0.228 (ref. 4)	0.288 (ref. 7)	0.21 (ref. 11)	0.215 (ref. 8)	0.201 (ref. 8)	0.091 (ref. 10)
0.239 (ref. 5)	0.235 (ref. 8)	0.118 (ref. 7)	0.411 (ref. 8)	0.319 (ref. 8)	0.668 (ref. 10)
0.091 (ref. 6)	0.397 (ref. 8)	0.202 (ref. 8)	0.209 (ref. 9)	0.041 (ref. 10)	
	0.354 (ref. 9)	0.348 (ref. 8)	0.09 (ref. 10)	0.051 (ref. 10)	**0.38**
0.19	0.112 (ref. 10)		0.36 (ref. 10)		
	0.348 (ref. 10)	**0.22**		**0.15**	
	0.28		**0.26**		

1. Zhang, H.; Davison, W. *Anal. Chim. Acta* **1999**, *398*, 329-340.
2. Carlson, J. C.; Anderson, J. C.; Low, J. E.; Cardinal, P.; MacKenzie, S. D.; Beattie, S. A.; Challis, J. K.; Bennett, R. J.; Meronek, S. S.; Wilks, R. P. A.; Buhay, W. M.; Wong, C. S.; Hanson, M. L. *Sci. Total Environ.* **2013b**, *445*, 64-78
3. Chen, C.-E.; Zhang, H.; Ying, G.-G.; Jones, K. C. *Environ. Sci. Technol.* **2013**, *47*, 13587-13593.
4. Lissalde, S.; Mazzella, N.; Fauvelle, V.; Delmas, F.; Mazellier, P.; Legube, B. *J. Chrom. A* **2011**, *1218*, 1492-1502.
5. Mazzella, N.; Dubernet, J.-F.; Delmas, F. *J. Chrom. A* **2007**, *1154*, 42-51.
6. Mazzella, N.; Lissalde, S.; Moreira, S.; Delmas, F.; Mazellier, P.; Huckins, J. N. *Environ. Sci. Technol.* **2010**, *44*, 1713-1719.
7. Bartelt-Hunt, S. L.; Snow, D. D.; Damon-Powell, T.; Brown, D. L.; Prasai, G.; Schwarz, M.; Kolok, A. S. *Environ. Toxicol. Chem.* **2011**, *30*, 1412-1420.
8. Li, H.; Helm, P. A.; Metcalfe, C. D. *Environ. Toxicol. Chem.* **2010**, *29*, 751-762.
9. Li, H.; Helm, P. A.; Paterson, G.; Metcalfe, C. D. *Chemosphere* **2011**, *83*, 271-280.
10. Macleod, S. L.; McClure, E. L.; Wong, C. S. *Environ. Toxicol. Chem.* **2007**, *26*, 2517-2529.
11. Bartelt-Hunt, S. L.; Snow, D. D.; Damon, T.; Shockley, J.; Hoagland, K. *Environ. Poll.* **2009**, *157*, 786-791.

Figure B9: Biofilm formation on the outer diffusive gel after 21 days of deployment in the final effluent site at the NHCN wastewater treatment plant. Photo A depicts a retrieved o-DGT on site and photo B shows an opened up sampler to be extracted (left; binding gel and right; outer diffusive gel). There is a visual biofilm layer that has formed on the diffusive gel (right). Photo C is a retrieved POCIS triplicate retrieved from the final effluent site, also showing significant bio-fouling.
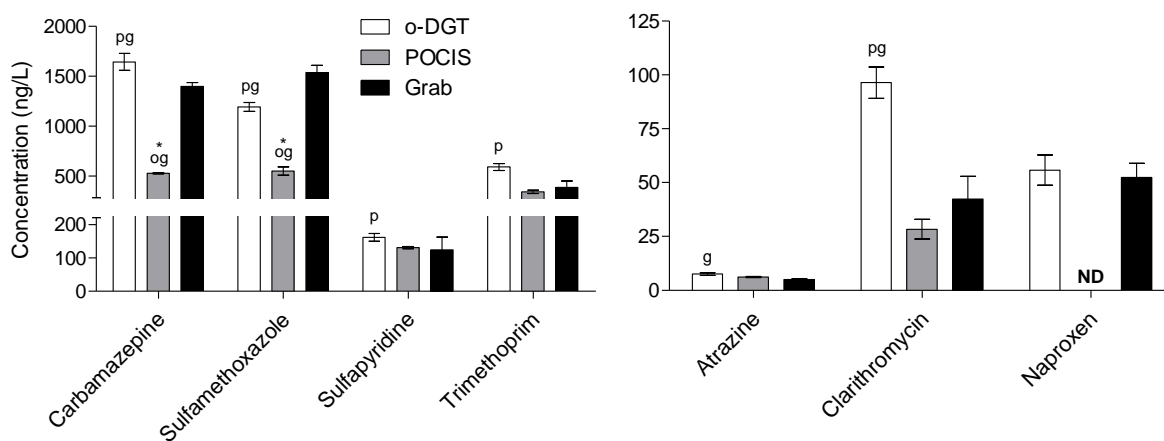
Figure B10: Concentration data as measured by o-DGT, POCIS, and grab samples at the tertiary lagoon site (influent) of a wastewater treatment plant in the northern Manitoban community of Norway House Cree Nation, Canada. Plots are split by high and low concentration compounds based on the y-axis scales. Bars represent the mean ± SD of triplicate o-DGT samples, triplicate POCIS samples, and two sets (n=2) of triplicate grab samples taken on deployment and 21 days later upon retrieval. Statistical differences between sampling techniques were tested using a one-way ANOVA with a Tukey post-hoc test at 95% confidence ($\alpha = 0.05$). Letters above the bars represent statistical difference from o-DGT (o), POCIS (p), and grab (g) samples. ND = not detected. *POCIS extracts for carbamazepine and sulfamethoxazole were outside of the calibration range.

Table B10: Boundary layer measurement conducted in-situ at the NHCN final effluent wastewater treatment plant site. Approximate flow velocity at this site was 6.8 cm/s. DBL thickness (δ) determined from a plot of reciprocal mass (accumulated in o-DGT) as a function of diffusive gel thickness (Δg) (see Figure B11). The slope and y-intercept are used to calculate δ. The linearity (r²) of each plot is provided.

Compound	Final Effluent DBL		
	δ (cm)	Error	r²
Atrazine	0.049	0.048	0.870
Carbamazepine	0.043	0.035	0.923
Gemfibrozil	0.040	0.028	0.948
Naproxen	0.029	0.027	0.950
Sulfamethoxazole	0.128	0.071	0.852
Sulfapyridine	0.108	0.034	0.955
Trimethoprim	0.038	0.024	0.961
MEDIAN	**0.043**		
STD. DEV.	**0.039**		
REL. STD. DEV.	**63%**		
MINIMUM	**0.029**		
MAXIMUM	**0.128**		
MEAN	**0.062**		
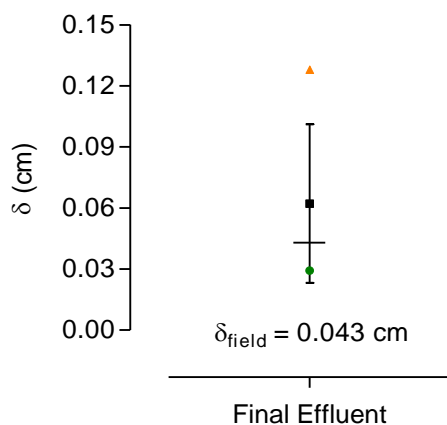
Figure B11: Diffusive boundary layer thickness (δ) determined using Equation 3.4 based on a plot of reciprocal mass (accumulated in o-DGT) as a function of diffusive gel thickness (Δg). The slope and y-intercept are used to calculate δ. Seven of the eight detected analytes in the final effluent site were used to obtain the median δ (horizontal line). The horizontal lines, black squares and errors bars represent the median, mean, and standard deviation of the estimated δ, respectively. The green circle is the measured minimum and orange triangle the measured maximum for the seven detected analytes used in the determination.

9.3 APPENDIX C: ADDITIONAL INFORMATION FOR CHAPTER 4

FIELD EVALUATION AND IN-SITU STRESS-TESTING OF THE ORGANIC-DIFFUSIVE GRADIENTS IN THIN-FILMS PASSIVE SAMPLER

SUMMARY

This document contains additional details of sampling locations and raw contaminant concentration data for all samples in the form of tables and figures.

MATERIALS AND METHODS

Sampling Locations

Red River. Sampling sites (Figure C1) on the Red River and its tributaries are as follows. Emerson is a border town and therefore integrates all net inputs coming directly from the United States. The St. Norbert site is south of the city perimeter, upstream of the South End sewage treatment plant and immediately downstream to the St. Norbert floodway diversion. The North End site is downstream of the North End Wastewater Treatment plant (WWTP) and processes approximately 70% ($\approx$ 404,000 people) of Winnipeg's wastewater. Breezy Point is upstream of Lake Winnipeg, removed from known point and non-point sources of pollution and thus should represent near-final inputs into Lake Winnipeg from the Red River. The Assiniboine River at Headingley is a tributary to the Red River and integrates inputs from western Manitoba and eastern Saskatchewan. Dead Horse Creek (DHC) is a small creek flowing between the two southern Manitoba towns of Morden and Winkler (combined population $\approx$ 18,000), receiving intense agricultural inputs and lagoon treated wastewater. Samplers were deployed on the east bank at Emerson and St. Norbert, the west bank at North End and Breezy Point, and the south bank at Headingley. At DHC cages were hung from a bridge in the middle of the creek.

Table C1: Sampling locations and dates for the Red River in 2016.

Site	Coordinates	Sampling device	Deploy/retrieve dates
Emerson (EM)	N 49.008442 W 97.215310	o-DGT & POCIS	April 15 (14 d) April 29 (19 d)
St. Norbert (NB)	N 49.754725 W 97.137746	o-DGT	May 18 (14 d)
North End (NE)	N 49.951508 W 97.097491	o-DGT	June 1 (21 d) June 22 (14 d)
Selkirk (SK)	N 50.142747 W 96.864826	o-DGT	July 6 (13 d)
Breezy Point (BP)	N 50.278267 W 96.851626	o-DGT	July 19 (21 d) August 9 (21 d)
Headingley (HD)	N 49.868906 W 97.409807	o-DGT	August 30 (21 d) September 20 (21 d)
Dead Horse Creek (DHC)	N 49.250556 W 97.549722	o-DGT & POCIS (grab samples Aug. 9-30)	October 11 (final retrieval)
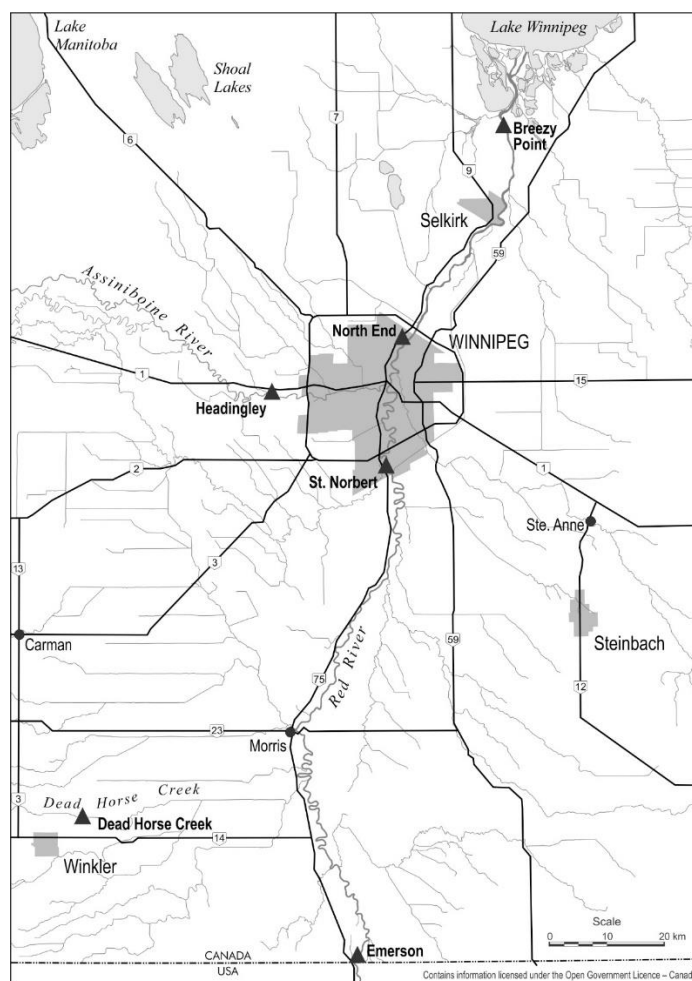
Figure C1: Sampling sites on the Red River at Emerson, St. Norbert, North End, and Breezy Point, on the Assiniboine River at Headingley, and in Dead Horse Creek.

303

Lake Winnipeg. Samplers were deployed from three weather buoys located in the south basin, narrows, and north basin, as part of the Lake-wide surveys conducted on the *MV Namao* (Figure 4.1). There is no data for the south basin in 2014 as the POCIS samplers were destroyed during deployment.

Table C2: Sampling locations and dates for Lake Winnipeg over three years from 2014-16.

Site	Coordinates	Sampling device	Year	Deploy/retrieve dates
South Basin	N 50.8000 W 96.7330	POCIS	2014	POCIS destroyed
		POCIS	2015	August 6 – September 2 (27 d)
		o-DGT	2016	June 2 – July 19 (48 d)
Narrows	N 51.8667 W 96.9666	POCIS	2014	July 23 – September 19 (58 d)
		POCIS	2015	June 10 – July 22 (41 d)
		o-DGT	2016	June 9 – July 21 (43 d)
North Basin	N 53.3833 W 98.4833	POCIS	2014	August 1 – September 21 (51 d)
		POCIS	2015	June 13 – July 24 (41 d)
		o-DGT	2016	June 15 – July 24 (40 d)

Little Playgreen Lake. The WWTP uses three aerated lagoons followed by a full-scale treatment plant equipped with chemical addition, sand and carbon filtration and UV-treatment. Sampling was conducted in the summer of 2014 with POCIS, the summer of 2015 with o-DGT, POCIS, and grab samples, and in the winter of 2016 with o-DGT. Sampling locations and dates in Table C3 and Figure C2. For the winter deployments an auger was used to drill holes in the ice. The o-DGT cages equipped with temperature loggers were hung down through the ice with stainless steel cable approximately five feet below the water surface.

Table C3: Sampling locations and dates for Norway House Cree Nation, Manitoba over three years from 2014-16.

Site	Coordinates	Sampling device	Year	Deploy/retrieve dates
Influent (to WWTP)	Tertiary lagoon	POCIS	2014 (summer)	August 6 – August 27 (21 d)
		o-DGT/POCIS	2015 (summer)	July 3 – July 24 (21 d)
		o-DGT	2016 (winter)	March 4 – March 19 (15 d)
Final effluent	WWTP	POCIS	2014 (summer)	August 6 – August 27 (21 d)
		o-DGT/POCIS	2015 (summer)	July 3 – July 24 (21 d)
		o-DGT	2016 (winter)	March 4 – March 19 (15 d)
Upstream	N 53.9730 W 97.7946	POCIS	2014 (summer)	August 6 – August 27 (21 d)
		o-DGT/POCIS	2015 (summer)	July 3 – July 24 (21 d)
		o-DGT	2016 (winter)	March 4 – March 19 (15 d)
Downstream (summer)	N 53.9960 W 97.7920	POCIS	2014 (summer)	August 6 – August 27 (21 d)
		POCIS	2015 (summer)	July 3 – July 24 (21 d)
Downstream (Winter)	N 53.9835 W 97.7851	o-DGT	2016 (winter)	March 4 – March 19 (15 d)
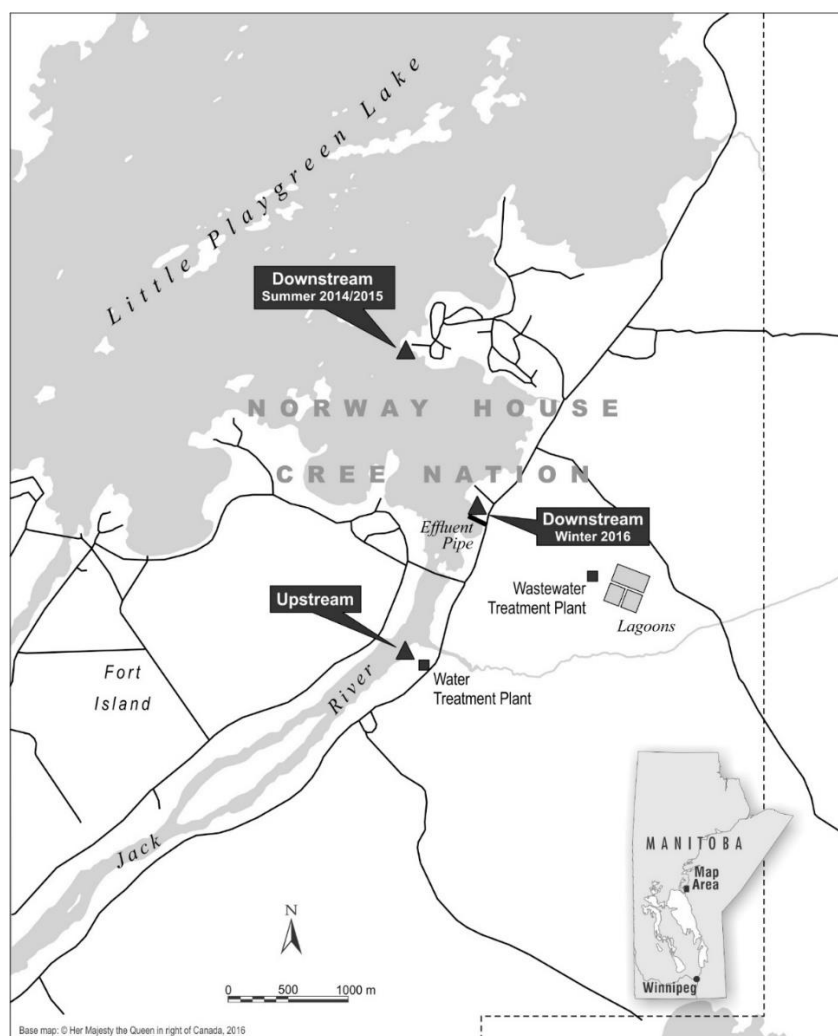
Figure C2: Sampling sites in the wastewater treatment plant and along the Nelson River flow path in Little Playgreen Lake, Norway House Cree Nation, Manitoba, Canada.

305

RESULTS

POCIS Sampling Rates.

Table C4: POCIS sampling rates used for the TWA concentration calculations of each measured analyte. Individual sampling rates and their respective references are shown for each compound. In the case where multiple sampling rate values were reported in the literature and it was not evident which value should be chosen, the average sampling rates was used.

Thiamethoxam	Clothianidin	Imidacloprid	Atrazine	Metoprolol	Propranolol
0.25 (ref. 1)	0.22 (ref. 1)	0.18 (ref. 1)	0.228 (ref. 2)	0.156 (ref. 6)	0.271 (ref. 6)
0.25	**0.22**	**0.18**	0.239 (ref. 3)	0.309 (ref. 6)	0.646 (ref. 6)
			0.091 (ref. 4)	0.321 (ref. 7)	0.478 (ref. 7)
			0.19	**0.26**	**0.47**

Carbamazepine	Clarithromycin	Sulfamethoxazole	Sulfapyridine	Trimethoprim
0.288 (ref. 5)	0.091 (ref. 8)	0.21 (ref. 9)	0.201 (ref. 6)	0.215 (ref. 6)
0.235 (ref. 6)	0.668 (ref. 8)	0.118 (ref. 5)	0.319 (ref. 6)	0.411 (ref. 6)
0.397 (ref. 6)	**0.38**	0.202 (ref. 6)	0.041 (ref. 8)	0.209 (ref. 7)
0.354 (ref. 7)		0.348 (ref. 6)	0.051 (ref. 8)	0.090 (ref. 8)
0.112 (ref. 8)		**0.22**	**0.15**	0.360 (ref. 8)
0.348 (ref. 8)				**0.26**
0.28				

1. Ahrens, L.; Daneshvar, A.; Lau, A.E.; Kreuger, J. *J. Chromatogr. A* **2015,** 1405, 1–11.

2. Lissalde, S.; Mazzella, N.; Fauvelle, V.; Delmas, F.; Mazellier, P.; Legube, B. *J Chrom A* **2011**, *1218*, 1492-1502.
3. Mazzella, N.; Dubernet, J.-F.; Delmas, F. *J Chrom A* **2007**, *1154*, 42-51.
4. Mazzella, N.; Lissalde, S.; Moreira, S.; Delmas, F.; Mazellier, P.; Huckins, J. N. *Environ. Sci. Technol.* **2010**, *44*, 1713-1719.
5. Bartelt-Hunt, S. L.; Snow, D. D.; Damon-Powell, T.; Brown, D. L.; Prasai, G.; Schwarz, M.; Kolok, A. S. *Environ. Toxicol. Chem.* **2011**, *30*, 1412-1420.
6. Li, H.; Helm, P. A.; Metcalfe, C. D. *Environ. Toxicol. Chem.* **2010**, *29*, 751-762.
7. Li, H.; Helm, P. A.; Paterson, G.; Metcalfe, C. D. *Chemosphere* **2011**, *83*, 271-280.
8. Macleod, S. L.; McClure, E. L.; Wong, C. S. *Environ. Toxicol. Chem.* **2007**, *26*, 2517-2529.
9. Bartelt-Hunt, S. L.; Snow, D. D.; Damon, T.; Shockley, J.; Hoagland, K. *Environ. Poll* **2009**, *157*, 786-791.

Red River Concentration Data.

Table C5a-f: Chemical concentrations measured by o-DGT in 2016 in the Red River (EM, NB, NE, BP), Assiniboine River (HD), and Dead Horse Creek (DHC). Sampling sites are ordered (left to right) to reflect the Red River flow direction (south to north); EM→NB→CP→BP. HD is a site on the Assiniboine River and DHC is a small creek, both tributaries to the Red River. Mass on sampler is used to calculate the time weighted average (TWA) concentration based on deployment time (days, d) and sampling rate (RS, L/d). Reported in bold is the mean and standard deviation (SD) of triplicate TWA measurements. The date listed represents the start of the deployment period. The start of the subsequent deployment represents the end of the previous. Total deployment time in days (d) is provided in brackets. Temperature-specific sampling rates for o-DGT, calculated according to Table B5, are reported in the table as averages (Ave R_S) over the entire deployment season.

Table C5a: Atrazine

Year	Deployment date (days)	Emerson (EM) (Ave R_S=0.009 L/d) Mass (ng)	TWA (ng/L)	SD	St. Norbert (NB) (Ave R_S=0.009 L/d) Mass (ng)	TWA (ng/L)	SD	North End (NE) (Ave R_S=0.009 L/d) Mass (ng)	TWA (ng/L)	SD	Breezy Point (BP) (Ave R_S=0.008 L/d) Mass (ng)	TWA (ng/L)	SD	Headingley (HD) (Ave R_S=0.009 L/d) Mass (ng)	TWA (ng/L)	SD	Dead Horse Creek (DHC) (Ave R_S=0.008 L/d) Mass (ng)	TWA (ng/L)	SD
2016	Apr 15 (14 d)	3.1			3.3			2.6			1.6			2.7			2.5		
		3.5	**39.7**	**2.5**	3.4	**39.3**	**3.6**	2.5	**30.7**	**0.7**	2.8	**28.8**	**7.8**	5.1	**36.2**	**25.2**	4.3	**47.3**	**14.0**
		3.4			2.8			2.5			2.6			1.0			4.6		
	Apr 29 (19 d)	7.2			8.0			2.3			3.1			0.27			7.6		
		3.0	**36.4**	**21.3**	3.1	**30.7**	**25.2**	1.9	**15.3**	**1.6**	3.6	**19.4**	**8.9**	0.36	**2.1**	**0.4**	6.9	**45.9**	**11.8**
		N/A			1.4			2.2			1.3			0.24			4.5		
	May 18 (14 d)	10.3			4.7			2.4			N/A			0.41			4.8		
		10.5	**87.4**	**2.3**	6.0	**51.8**	**11.9**	4.2	**23.1**	**12.4**	N/A	**N/A**		0.71	**5.5**	**1.7**	4.3	**42.1**	**7.5**
		10.8			7.5			1.4			N/A			0.79			6.1		
	Jun 1 (21 d)	2.6			6.1			N/A			N/A			0.54			164.0		
		5.1	**18.5**	**7.4**	9.5	**33.9**	**14.9**	N/A	**N/A**		N/A	**N/A**		0.76	**3.1**	**0.8**	214.4	**1249.5**	**458.0**
		2.7			3.8			N/A			N/A			0.47			333.3		
	Jun 22 (14 d)	31.5			47.1			13.8			29.5			5.2			61.2		
		56.8	**288.3**	**119.4**	41.1	**331.4**	**22.9**	22.2	**140.3**	**50.8**	31.5	**210.6**	**36.3**	4.4	**35.9**	**4.3**	121.2	**761.8**	**253.4**
		27.3			43.8			N/A			22.4			N/A			115.1		
	Jul 6 (13 d)	13.9			15.6			0.72			2.7			2.4			31.6		
		27.9	**228.3**	**120.6**	16.0	**131.4**	**8.9**	3.7	**41.6**	**16.0**	4.8	**25.3**	**12.2**	1.9	**16.5**	**2.3**	40.8	**316.4**	**53.2**
		44.1			17.7			6.5			1.9			2.0			44.3		
	Jul 19 (21 d)	32.1			37.4			27.9			N/A			1.1			17.9		
		61.0	**213.4**	**68.8**	40.5	**188.8**	**11.3**	17.9	**197.8**	**61.4**	N/A	**N/A**		0.89	**5.3**	**1.3**	17.6	**74.8**	**18.5**
		42.8			42.1			27.1			N/A			1.4			11.1		
	Aug 9 (21 d)	17.3			11.9			7.2			N/A			0.30			2.1		
		24.7	**97.6**	**19.1**	10.3	**61.5**	**13.9**	8.2	**57.2**	**5.1**	N/A	**N/A**		0.95	**3.0**	**1.6**	4.9	**21.4**	**9.6**
		18.7			15.9			8.5			N/A			0.56			5.7		
	Aug 30 (21 d)	14.8			10.9			10.5			10.5			0.35			57.5		
		14.1	**78.5**	**2.9**	8.9	**54.7**	**5.8**	11.0	**86.6**	**2.9**	10.8	**84.2**	**1.7**	0.37	**1.9**	**0.2**	52.8	**314.4**	**18.9**
		N/A			10.5			N/A			N/A			0.32			N/A		
	Sept 20 (21 d)	24.5			2.1			N/A			N/A			0.53			2.5		
		28.5	**167.5**	**17.7**	1.8	**11.1**	**2.3**	N/A	**N/A**		N/A	**N/A**		0.34	**2.9**	**0.6**	2.7	**17.5**	**1.4**
		N/A			1.4			N/A			N/A			0.45			N/A		

N/A = Sampler at that site and time could not be analyzed (e.g., muddied surface, lost to flooding, damaged in field, stolen, vandalized, etc.). ND = Not detected.

Table C5b: Thiamethoxam

Thiamethoxam o-DGT		Emerson (EM) (Ave Rs=0.01 L/d)			St. Norbert (NB) (Ave Rs=0.01 L/d)			North End (NE) (Ave Rs=0.009 L/d)			Breezy Point (BP) (Ave Rs=0.009 L/d)			Headingley (HD) (Ave Rs=0.009 L/d)			Dead Horse Creek (DHC) (Ave Rs=0.009 L/d)		
Year	Deployment date (days)	Mass (ng)	TWA (ng/L)	SD	Mass (ng)	TWA (ng/L)	SD	Mass (ng)	TWA (ng/L)	SD	Mass (ng)	TWA (ng/L)	SD	Mass (ng)	TWA (ng/L)	SD	Mass (ng)	TWA (ng/L)	SD
2016	Apr 15 (14 d)	1.3			2.2			2.0			1.3			1.2			25.5		
		1.5	16.1	1.1	2.0	22.8	2.0	1.9	23.2	1.8	2.0	20.0	4.2	1.8	19.5	5.0	44.0	471.3	158.4
		1.5			1.8			2.2			1.9			2.0			52.1		
	Apr 29 (19 d)	1.6			1.6			1.2			1.5			0.86			50.7		
		0.84	8.1	3.7	0.83	6.4	4.2	1.1	7.8	0.4	1.4	8.1	2.2	1.3	6.9	1.7	45.5	286.6	56.2
		N/A			0.41			1.2			0.85			0.94			34.1		
	May 18 (14 d)	6.6			1.1			2.3			N/A			1.1			26.3		
		5.5	45.9	4.6	3.4	22.7	12.9	3.2	16.3	8.9	N/A	N/A		1.8	12.3	3.3	25.7	205.7	20.8
		6.4			4.4			0.88			N/A			1.9			30.8		
	Jun 1 (21 d)	1.0			9.1			N/A			N/A			2.0			40.7		
		3.5	11.0	6.0	9.2	40.7	3.6	N/A	N/A		N/A	N/A		1.9	9.1	0.3	79.8	352.3	150.1
		2.4			7.8			N/A			N/A			1.9			103.8		
	Jun 22 (14 d)	5.9			8.1			5.5			6.9			2.4			17.3		
		6.1	15.3	1.6	7.4	53.2	3.0	2.5	26.9	14.2	7.8	48.8	3.6	2.4	15.8	0.1	35.1	197.6	68.4
		5.5			8.3			N/A			7.0			N/A			34.1		
	Jul 6 (13 d)	3.1			1.9			0.69			2.1			3.7			16.7		
		1.4	22.4	12.1	1.6	11.5	1.7	0.59	5.0	0.8	2.6	14.0	5.7	1.8	19.0	6.9	20.3	143.4	20.9
		4.9			1.4			0.81			1.1			2.6			22.4		
	Jul 19 (21 d)	5.6			7.1			4.6			N/A			1.7			25.1		
		9.1	30.4	7.2	7.7	30.8	1.2	3.3	31.8	5.9	N/A	N/A		1.6	7.7	1.4	24.5	95.9	17.6
		7.1			7.3			4.5			N/A			2.3			17.7		
	Aug 9 (21 d)	3.2			3.3			2.5			N/A			0.54			3.8		
		3.3	13.3	1.2	2.9	13.8	1.2	3.0	17.9	1.6	N/A	N/A		1.1	3.4	1.1	7.0	27.6	9.5
		2.8			3.4			2.9			N/A			0.72			7.8		
	Aug 30 (21 d)	4.9			3.0			2.9			4.4			0.32			10.7		
		4.5	22.7	1.4	3.2	14.6	1.3	3.1	21.6	1.4	3.2	26.8	5.7	0.23	1.2	0.4	10.3	53.7	1.2
		N/A			2.7			N/A			N/A			0.17			N/A		
	Sept 20 (21 d)	3.5			1.2			N/A			N/A			0.31			5.3		
		3.9	21.3	1.9	1.1	6.4	0.5	N/A	N/A		N/A	N/A		0.26	1.6	0.2	6.6	36.3	5.5
		N/A			1.0			N/A			N/A			0.25			N/A		

N/A = Sampler at that site and time could not be analyzed (e.g., muddied surface, lost to flooding, damaged in field, stolen, vandalized, etc.). ND = Not detected.

Table C5c: Clothianidin

Clothianidin o-DGT		Emerson (EM) (Ave R_s=0.01 L/d)			St. Norbert (NB) (Ave R_s=0.009 L/d)			North End (NE) (Ave R_s=0.009 L/d)			Breezy Point (BP) (Ave R_s=0.009 L/d)			Headingley (HD) (Ave R_s=0.009 L/d)			Dead Horse Creek (DHC) (Ave R_s=0.009 L/d)		
Year	Deployment date (days)	Mass (ng)	TWA (ng/L)	SD	Mass (ng)	TWA (ng/L)	SD	Mass (ng)	TWA (ng/L)	SD	Mass (ng)	TWA (ng/L)	SD	Mass (ng)	TWA (ng/L)	SD	Mass (ng)	TWA (ng/L)	SD
201	Apr 15 (14 d)	1.4			1.8			1.6			1.3			1.0			4.2		
		1.4	16.9	0.3	1.7	21.9	0.9	1.6	21.4	3.2	2.0	20.8	4.5	1.2	14.6	2.3	6.8	79.3	25.2
		1.5			1.9			2.0			1.8			1.4			8.2		
	Apr 29 (19 d)	1.9			1.6			0.22			1.0			0.20			11.7		
		1.0	9.8	4.5	0.20	4.7	5.6	0.64	3.5	1.8	0.25	3.4	3.2	1.1	4.2	2.9	10.1	66.2	14.7
		N/A			0.20			0.69			0.21			0.58			7.4		
	May 18 (14 d)	8.7			1.4			2.6			N/A			0.81			5.5		
		8.6	62.9	3.9	4.0	29.4	17.9	3.5	18.1	11.0	N/A	N/A		1.5	10.1	3.3	4.8	44.4	10.3
		7.8			6.0			0.79			N/A			1.5			7.4		
	Jun 1 (21 d)	1.1			7.0			N/A			N/A			1.2			12.1		
		4.0	12.1	6.8	6.7	28.1	7.2	N/A	N/A		N/A	N/A		1.3	5.9	0.3	19.0	91.8	35.4
		2.5			4.2			N/A			N/A			1.2			27.1		
	Jun 22 (14 d)	7.2			9.6			5.3			6.5			2.0			10.2		
		7.6	47.4	3.6	8.8	60.1	4.1	2.6	26.7	13.0	7.7	48.3	3.8	2.0	13.2	0.04	24.3	127.1	50.6
		6.5			8.4			N/A			7.2			N/A			20.9		
	Jul 6 (13 d)	1.2			1.4			0.4			1.3			2.6			19.8		
		1.5	22.0	21.9	1.0	9.0	1.5	0.5	3.2	0.5	1.7	8.3	4.3	1.1	13.2	5.3	24.9	169.9	17.9
		6.7			1.4			ND			0.5			2.0			25.5		
	Jul 19 (21 d)	8.0			10.2			3.7			N/A			1.1			20.5		
		13.9	46.7	12.6	10.5	43.4	0.9	2.5	27.9	8.1	N/A	N/A		0.85	4.5	1.0	20.3	76.6	17.9
		11.8			10.6			4.6			N/A			1.3			13.1		
	Aug 9 (21 d)	4.1			5.7			5.0			N/A			0.67			3.8		
		5.3	19.8	2.7	5.5	24.6	0.8	5.2	31.5	1.6	N/A	N/A		1.2	3.8	1.3	6.7	33.1	4.2
		4.5			5.9			4.7			N/A			0.74			8.1		
	Aug 30 (21 d)	9.8			5.7			6.1			9.1			0.39			11.3		
		8.8	45.8	3.5	5.5	27.0	1.0	6.8	46.9	3.5	6.1	54.3	15.1	0.42	1.6	0.7	10.3	56.0	3.5
		N/A			5.3			N/A			N/A			0.18			N/A		
	Sept 20 (21 d)	4.9			1.6			N/A			N/A			0.51			5.9		
		4.3	26.9	2.3	1.3	8.3	0.7	N/A	N/A		N/A	N/A		0.19	1.8	1.1	6.0	37.8	0.3
		N/A			1.3			N/A			N/A			0.20			N/A		

N/A = Sampler at that site and time could not be analyzed (e.g., muddied surface, lost to flooding, damaged in field, stolen, vandalized, etc.). ND = Not detected.

309

Table C5d: Imidacloprid

Imidicloprid o-DGT		Emerson (EM) (Ave R_s=0.01 L/d)			St. Norbert (NB) (Ave R_s=0.01 L/d)			North End (NE) (Ave R_s=0.01 L/d)			Breezy Point (BP) (Ave R_s=0.01 L/d)			Headingley (HD) (Ave R_s=0.01 L/d)			Dead Horse Creek (DHC) (Ave R_s=0.01 L/d)		
Year	Deployment date (days)	Mass (ng)	TWA (ng/L)	SD	Mass (ng)	TWA (ng/L)	SD	Mass (ng)	TWA (ng/L)	SD	Mass (ng)	TWA (ng/L)	SD	Mass (ng)	TWA (ng/L)	SD	Mass (ng)	TWA (ng/L)	SD
201	Apr 15 (14 d)	0.46			0.52			0.21			ND			0.03			0.10		
		0.79	6.5	2.0	0.46	5.7	0.4	ND	1.0	1.2	ND	3.6	--	0.33	2.3	1.7	0.30	3.2	2.0
		0.50			0.50			0.06			0.32			0.22			0.43		
	Apr 29 (19 d)	ND			ND			ND			ND			ND			ND		
		ND	ND		ND	ND		ND	ND		ND	ND		ND	ND		ND	ND	
		N/A			ND			ND			ND			ND			ND		
	May 18 (14 d)	2.7			0.25			0.90			N/A			0.07			0.44		
		3.3	22.3	2.6	1.5	9.1	6.4	1.3	5.6	4.8	N/A	N/A		0.04	0.76	0.6	0.29	2.5	0.5
		3.3			1.9			0.05			N/A			0.19			0.33		
	Jun 1 (21 d)	0.63			3.2			N/A			N/A			0.36			0.93		
		1.5	5.1	2.0	2.8	11.4	3.4	N/A	N/A		N/A	N/A		0.35	1.4	0.4	1.4	6.2	2.1
		1.3			1.7			N/A			N/A			0.21			1.9		
	Jun 22 (14 d)	3.4			4.2			2.9			2.6			0.57			1.4		
		4.1	20.3	5.9	3.4	23.8	2.6	0.91	12.2	9.0	3.2	18.7	1.9	0.62	3.7	0.2	2.6	13.9	4.2
		2.2			3.6			N/A			3.0			N/A			2.4		
	Jul 6 (13 d)	0.22			0.19			0.1			0.14			1.1			1.0		
		0.27	4.9	5.7	ND	0.72	0.8	0.04	0.4	0.2	0.11	0.87	0.1	0.46	5.0	2.0	1.3	9.2	2.2
		1.7			0.03			ND			0.13			0.74			1.7		
	Jul 19 (21 d)	1.5			2.2			0.37			N/A			0.1			4.1		
		2.5	7.5	2.1	2.5	10.7	2.5	0.41	3.0	0.4	N/A	N/A		0.2	1.0	0.6	4.1	14.9	2.9
		1.7			3.4			0.48			N/A			0.4			2.8		
	Aug 9 (21 d)	2.6			2.3			1.7			N/A			0.3			0.7		
		2.7	10.2	1.0	2.0	9.4	1.2	2.2	12.0	1.6	N/A	N/A		0.2	1.0	0.2	1.4	6.8	1.1
		2.3			2.6			2.1			N/A			0.3			1.8		
	Aug 30 (21 d)	4.3			2.3			2.1			3.0			0.3			2.2		
		3.8	19.0	1.6	2.0	9.2	1.4	2.3	15.0	1.0	2.2	17.6	3.5	0.4	1.7	0.1	2.0	10.2	0.6
		N/A			1.7			N/A			N/A			0.4			N/A		
	Sept 20 (21 d)	1.4			0.7			N/A			N/A			0.3			0.8		
		1.9	7.5	3.4	0.6	3.7	0.3	N/A	N/A		N/A	N/A		0.3	2.1	0.3	1.4	5.9	2.1
		N/A			0.7			N/A			N/A			0.4			N/A		

N/A = Sampler at that site and time could not be analyzed (e.g., muddied surface, lost to flooding, damaged in field, stolen, vandalized, etc.). ND = Not detected.

Table C5e: 2,4-D

2,4-D o-DGT		Emerson (EM) (Ave R_s=0.01 L/d)			St. Norbert (NB) (Ave R_s=0.01 L/d)			North End (NE) (Ave R_s=0.01 L/d)			Breezy Point (BP) (Ave R_s=0.01 L/d)			Headingley (HD) (Ave R_s=0.01 L/d)			Dead Horse Creek (DHC) (Ave R_s=0.01 L/d)		
Year	Deployment date (days)	Mass (ng)	TWA (ng/L)	SD	Mass (ng)	TWA (ng/L)	SD	Mass (ng)	TWA (ng/L)	SD	Mass (ng)	TWA (ng/L)	SD	Mass (ng)	TWA (ng/L)	SD	Mass (ng)	TWA (ng/L)	SD
2016	Apr 15 (14 d)	3.3			3.8			17.4			3.5			1.6			2.5		
		3.6	39.6	1.9	3.7	41.9	4.0	15.3	197.7	15.0	5.0	53.5	11.3	2.5	27.3	7.5	3.6	39.8	8.8
		3.7			3.2			17.7			5.2			2.9			3.9		
	Apr 29 (19 d)	5.1			4.6			5.1			3.5			1.40			0.7		
		5.3	32.4	1.0	3.6	21.2	9.6	3.8	28.1	4.1	3.6	18.8	6.3	1.78	9.6	1.5	1.1	5.4	1.2
		N/A			1.7			4.4			1.8			1.36			0.8		
	May 18 (14 d)	9.0			2.3			8.0			N/A			1.04			1.0		
		10.1	66.0	3.8	5.1	33.4	16.3	6.3	44.2	13.5	N/A	N/A		0.82	6.7	0.8	1.3	7.9	0.9
		9.8			6.8			4.2			N/A			0.95			1.2		
	Jun 1 (21 d)	1.4			9.0			N/A			N/A			ND			25.8		
		2.7	10.2	3.8	9.8	35.9	7.1	N/A	N/A		N/A	N/A		ND	ND		25.5	122.3	21.2
		3.0			6.6			N/A			N/A			ND			34.3		
	Jun 22 (14 d)	6.3			6.2			9.1			5.8			ND			2.5		
		5.7	37.5	3.0	3.9	34.0	9.2	2.3	34.0	28.4	7.4	39.3	5.3	ND	ND		2.4	17.8	4.8
		6.7			6.7			N/A			6.1			N/A			3.8		
	Jul 6 (13 d)	2.2			3.1			1.90			4.3			ND			1.9		
		4.7	36.9	27.1	3.1	18.5	1.8	6.1	40.8	1.1	5.4	30.9	3.8	ND	ND		2.6	15.6	2.9
		10.5			2.6			6.4			4.6			ND			2.7		
	Jul 19 (21 d)	7.5			5.2			4.3			N/A			ND			2.5		
		11.1	37.2	8.2	4.5	18.0	1.4	5.4	49.7	4.9	N/A	N/A		ND	ND		3.1	10.3	1.3
		11.4			4.8			4.6			N/A			ND			2.5		
	Aug 9 (21 d)	8.6			8.9			8.8			N/A			ND			ND		
		9.8	34.3	3.0	7.3	33.2	4.4	8.5	45.7	6.5	N/A	N/A		ND	ND		ND	ND	
		8.3			9.5			6.7			N/A			ND			ND		
	Aug 30 (21 d)	17.3			11.8			10.9			11.8			ND			12.1		
		14.7	71.4	8.2	12.4	51.0	5.1	9.8	68.0	4.7	10.5	71.9	6.2	ND	ND		12.5	58.3	1.2
		N/A			10.2			N/A			N/A			ND			N/A		
	Sept 20 (21 d)	11.5			5.2			N/A			N/A			1.11			2.9		
		12.8	66.0	5.1	5.1	25.0	4.9	N/A	N/A		N/A	N/A		0.55	4.6	1.6	3.2	18.2	1.2
		N/A			3.6			N/A			N/A			0.78			N/A		

N/A = Sampler at that site and time could not be analyzed (e.g., muddied surface, lost to flooding, damaged in field, stolen, vandalized, etc.). ND = Not detected.

Table C5f: Carbamazepine

Carbamazepine o-DGT Year	Deployment date (days)	Emerson (EM) (Ave Rs=0.011 L/d) Mass (ng)	TWA (ng/L)	SD	St. Norbert (NB) (Ave Rs=0.011 L/d) Mass (ng)	TWA (ng/L)	SD	North End (NE) (Ave Rs=0.011 L/d) Mass (ng)	TWA (ng/L)	SD	Breezy Point (BP) (Ave Rs=0.011 L/d) Mass (ng)	TWA (ng/L)	SD	Headingley (HD) (Ave Rs=0.011 L/d) Mass (ng)	TWA (ng/L)	SD	Dead Horse Creek (DHC) (Ave Rs=0.011 L/d) Mass (ng)	TWA (ng/L)	SD
2016	Apr 15 (14 d)	0.26			0.13			1.9			0.38			0.26			0.26		
		0.31	3.0	0.3	0.11	1.5	0.2	1.5	21.0	4.1	0.65	5.8	1.5	0.45	4.3	1.3	0.30	3.2	0.3
		0.27			0.15			2.3			0.55			0.46			0.29		
	Apr 29 (19 d)	0.55			0.53			3.5			1.1			0.25			0.79		
		0.34	2.6	0.9	0.28	2.0	1.1	2.5	17.6	2.9	1.2	5.6	2.5	0.35	1.7	0.4	0.67	3.8	1.1
		N/A			0.16			2.8			0.45			0.25			0.44		
	May 18 (14 d)	0.52			0.34			1.9			N/A			1.1			1.1		
		0.47	3.3	0.2	0.32	2.5	0.4	3.2	14.4	6.6	N/A	N/A		0.82	6.4	1.2	1.2	7.8	0.7
		0.53			0.43			1.3			N/A			0.85			1.3		
	Jun 1 (21 d)	0.026			0.11			N/A			N/A			0.45			0.29		
		0.12	0.31	0.2	0.10	0.41	0.04	N/A	N/A		N/A	N/A		0.55	2.1	0.2	0.58	2.2	0.9
		0.081			0.09			N/A			N/A			0.50			0.73		
	Jun 22 (14 d)	0.70			0.32			0.61			0.83			1.0			0.23		
		0.59	3.0	1.3	0.29	1.7	0.2	0.16	2.2	1.7	0.82	4.2	0.9	1.0	5.6	0.03	0.34	1.8	0.4
		0.27			0.27			N/A			0.54			N/A			0.36		
	Jul 6 (13 d)	0.13			0.020			0.40			0.50			2.0			0.32		
		0.30	1.5	0.6	0.30	1.1	0.9	0.33	3.2	1.6	0.63	3.5	0.5	1.2	0.39	0.1	0.48	0.16	0.08
		0.30			0.20			0.69			ND			1.1			0.91		
	Jul 19 (21 d)	0.13			0.33			0.90			N/A			0.38			0.86		
		0.62	1.3	0.9	0.27	1.0	0.2	0.73	5.5	0.7	N/A	N/A		0.32	1.4	0.4	0.84	2.7	0.7
		0.31			0.24			0.90			N/A			0.52			0.50		
	Aug 9 (21 d)	0.51			0.39			1.0			N/A			0.53			15.4		
		0.64	2.1	0.2	0.35	1.5	0.3	1.3	6.8	1.1	N/A	N/A		1.7	3.9	2.2	17.8	68.1	8.8
		0.57			0.49			1.4			N/A			0.93			20.0		
	Aug 30 (21 d)	0.54			0.37			2.0			2.0			0.66			2.6		
		0.46	2.1	0.3	0.34	1.5	0.1	2.1	13.1	0.4	1.9	12.0	0.6	0.81	3.0	0.5	2.3	11.1	0.7
		N/A			0.36			N/A			N/A			0.57			N/A		
	Sept 20 (21 d)	0.42			0.073			N/A			N/A			1.4			8.0		
		0.44	2.2	0.1	0.10	0.42	0.1	N/A	N/A		N/A	N/A		1.0	6.7	1.1	10.0	50.4	7.8
		N/A			0.067			N/A			N/A			1.3			N/A		

N/A = Sampler at that site and time could not be analyzed (e.g., muddied surface, lost to flooding, damaged in field, stolen, vandalized, etc.). ND = Not detected.

312

Table C6: North End pharmaceutical data. Analyte concentrations measured by o-DGT in the Red River at the North End site. Mass on sampler is used to calculate the time weighted average (TWA) concentration based on deployment time (days, d) and sampling rate (R$_S$, L/d), both provided in table. Reported in bold is the mean and standard deviation (SD) of triplicate TWA measurements. The date listed represents the start of the deployment period. The start of the subsequent deployment represents the end of the previous. Total deployment time in days (d) is provided in brackets. Temperature-specific sampling rates for o-DGT, calculated according to Table B5, are reported in the table as averages (Ave R$_S$) over the entire deployment season.

Compound		Sulfamethoxazole (Ave R$_S$ = 0.01 L/d)			Sulfapyridine (Ave R$_S$ = 0.009 L/d)			Metoprolol (Ave R$_S$ = 0.009 L/d)			Trimethoprim (Ave R$_S$ = 0.01 L/d)			Naproxen (Ave R$_S$ = 0.009 L/d)			Diclofenac (Ave R$_S$ = 0.01 L/d)		
Year	Deployment date (days)	Mass (ng)	TWA (ng/L)	SD	Mass (ng)	TWA (ng/L)	SD	Mass (ng)	TWA (ng/L)	SD	Mass (ng)	TWA (ng/L)	SD	Mass (ng)	TWA (ng/L)	SD	Mass (ng)	TWA (ng/L)	SD
2016 o-DGT	Apr 15 (14 d)	2.3	**28.8**	**6.9**	1.8	**19.4**	**3.5**	1.6	**26.7**	**2.5**	1.1	**13.6**	**2.6**	11.2	**141.5**	**31.1**	2.4	**36.4**	**16.9**
		1.9			1.4			1.9			0.8			8.4			2.4		
		3.1			2.0			1.9			1.2			13.2			5.0		
	Apr 29 (19 d)	2.3	**13.1**	**2.3**	ND	**ND**		3.3	**22.0**	**2.2**	2.0	**19.9**	**6.6**	10.7	**66.3**	**8.4**	6.9	**36.4**	**6.4**
		1.6			ND			2.7			3.8			8.3			5.1		
		2.2			ND			3.0			3.7			9.9			5.3		
	May 18 (14 d)	1.5	**10.3**	**1.2**	1.7	**12.1**	**4.5**	1.6	**15.0**	**10.5**	1.1	**6.3**	**2.6**	3.4	**28.3**	**14.9**	1.5	**12.4**	**11.8**
		1.5			2.1			3.2			1.2			5.7			3.4		
		1.2			0.95			0.70			0.49			1.9			0.16		
	Jun 1 (21 d)	N/A	**N/A**		N/A	**N/A**		N/A	**N/A**		N/A	**N/A**		N/A	**N/A**		N/A	**N/A**	
		N/A			N/A			N/A			N/A			N/A			N/A		
		N/A			N/A			N/A			N/A			N/A			N/A		
	Jun 22 (14 d)	0.79	**5.2**	**0.3**	0.45	**3.0**	**0.1**	1.0	**5.5**	**1.6**	0.82	**5.3**	**1.0**	2.0	**14.5**	**1.4**	ND	**ND**	
		0.80			0.40			0.60			1.0			2.2			ND		
		N/A			N/A			N/A			N/A			N/A			N/A		
	Jul 6 (13 d)	0.51	**4.2**	**0.8**	ND	**ND**		0.09	**0.81**	**0.4**	1.5	**10.3**	**1.5**	1.7	**10.9**	**1.2**	0.64	**5.4**	**1.2**
		0.61			ND			0.17			1.6			1.4			0.73		
		0.73			ND			0.07			2.0			ND			1.0		
	Jul 19 (21 d)	0.83	**6.1**	**1.1**	ND	**ND**		ND	**ND**		ND	**ND**		ND	**ND**		ND	**ND**	
		1.2			ND			ND			ND			ND			ND		
		0.87			ND			ND			ND			ND			ND		
	Aug 9 (21 d)	0.47	**3.0**	**0.4**	1.2	**9.2**	**1.2**	1.1	**7.2**	**0.8**	0.80	**4.1**	**0.2**	1.4	**8.9**	**0.8**	0.49	**3.3**	**1.2**
		0.59			1.4			1.0			0.76			1.3			0.40		
		0.48			N/A			1.3			0.82			1.6			0.78		
	Aug 30 (21 d)	1.2	**6.7**	**1.9**	1.3	**9.3**	**0.4**	1.0	**10.2**	**4.2**	1.2	**5.9**	**2.1**	0.73	**5.5**	**0.4**	0.88	**3.9**	**3.0**
		0.79			1.3			1.8			0.72			0.80			0.26		
		N/A			N/A			N/A			N/A			N/A			N/A		

N/A = Sampler at that site and time could not be analyzed (e.g., lost to flooding, damaged in field, stolen, vandalized, etc.). ND = Not detected.

Table C7a-e: Atrazine

Table C7a-e: Chemical concentrations measured by o-DGT and POCIS in 2016 in the Red River at Emerson (EM) and in Dead Horse Creek (DHC). Both types of samplers were deployed simultaneously at each time point. Mass on sampler is used to calculate the time weighted average (TWA) concentration based on deployment time (days, d) and sampling rate (R_S, L/d). Reported in bold is the mean and standard deviation (SD) of triplicate TWA measurements. The date listed represents the start of the deployment period. The start of the subsequent deployment represents the end of the previous. Total deployment time in days (d) is provided in brackets. References for POCIS sampling rates are provided in Table A3. Temperature-specific sampling rates for o-DGT, calculated from Table B5, are reported in the table as averages (Ave R_S) over the entire deployment season.

Table C7a: Atrazine

Atrazine		Emerson (EM)						Dead Horse Creek (DHC)					
		o-DGT (Ave R_S=0.009 L/d)			POCIS (R_S=0.19 L/d)			o-DGT (Ave R_S=0.008 L/d)			POCIS (R_S=0.19 L/d)		
Year	Deployment date (days)	Mass (ng)	TWA (ng/L)	SD	Mass (ng)	TWA (ng/L)	SD	Mass (ng)	TWA (ng/L)	SD	Mass (ng)	TWA (ng/L)	SD
2016 o-DGT & POCIS	Apr 15 (14 d)	3.1			28.3			2.5			53.2		
		3.5	**39.7**	**2.5**	34.7	**11.8**	**1.7**	4.3	**47.3**	**14.0**	50.1	**18.0**	**2.5**
		3.4			N/A			4.6			40.2		
	Apr 29 (19 d)	7.2			155.5			7.6			123.7		
		3.0	**36.4**	**21.3**	34.1	**25.2**	**16.9**	6.9	**45.9**	**11.8**	93.4	**31.4**	**4.8**
		N/A			83.3			4.5			123.2		
	May 18 (14 d)	10.3			220.9			4.8			85.1		
		10.5	**87.4**	**2.3**	225.0	**80.7**	**5.5**	4.3	**42.1**	**7.5**	72.0	**30.1**	**2.7**
		10.8			197.9			6.1			83.2		
	Jun 1 (21 d)	2.6			14.5			164.0			3254.1		
		5.1	**18.5**	**7.4**	N/A	**3.6**	--	214.4	**1250**	**458**	3699.3	**1012**	**250**
		2.7			N/A			333.3			5162.6		
	Jun 22 (14 d)	31.5			594.9			61.2			1392.7		
		56.8	**288.3**	**119.4**	746.7	**245.2**	**31.0**	121.2	**761.8**	**253.4**	1288.2	**518.5**	**32.0**
		27.3			615.4			115.1			1456.7		
	Jul 6 (13 d)	13.9			497.8			31.6			448.2		
		27.9	**228.3**	**120.6**	485.6	**223.2**	**42.0**	40.8	**316.4**	**53.2**	411.6	**181.0**	**14.1**
		44.1			670.9			44.3			481.1		
	Jul 19 (21 d)	32.1			1009.4			17.9			194.6		
		61.0	**213.4**	**68.8**	1385.2	**323.1**	**61.7**	17.6	**74.8**	**18.5**	205.4	**53.3**	**5.7**
		42.8			1472.9			11.1			237.9		
	Aug 9 (21 d)	17.3			314.6			2.1			94.1		
		24.7	**97.6**	**19.1**	290.5	**64.9**	**19.1**	4.9	**21.4**	**9.6**	82.6	**22.1**	**2.0**
		18.7			171.9			5.7			N/A		

N/A = Sampler at that site and time could not be analyzed (e.g., muddied surface, lost to flooding, damaged in field, stolen, vandalized, etc.). ND = Not detected. Level of significance based on a two-way ANOVA and Bonferroni post-hoc test: *P<0.05, **P<0.01, ***P<0.001

Table C7b: Thiamethoxam

Thiamethoxam		Emerson (EM)						Dead Horse Creek (DHC)					
		o-DGT (Ave R_s=0.01 L/d)			POCIS (R_s=0.25 L/d)			o-DGT (Ave R_s=0.009 L/d)			POCIS (R_s=0.25 L/d)		
Year	Deployment date (days)	Mass (ng)	TWA (ng/L)	SD	Mass (ng)	TWA (ng/L)	SD	Mass (ng)	TWA (ng/L)	SD	Mass (ng)	TWA (ng/L)	SD
2016 o-DGT & POCIS	Apr 15 (14 d)	1.3			9.0			25.5			317.9		
		1.5	16.1	1.1	30.3	5.6	4.3	44.0	471.3	158.4	305.2	87.0***	4.0
		1.5			N/A			52.1			290.0		
	Apr 29 (19 d)	1.6			16.3			50.7			533.9		
		0.84	8.1	3.7	6.7	2.2	1.1	45.5	286.6	56.2	423.0	105.2**	14.0
		N/A			8.1			34.1			541.9		
	May 18 (14 d)	6.6			39.3			26.3			273.7		
		5.5	45.9	4.6	47.2	12.3***	1.1	25.7	205.7	20.8	275.0	79.4	1.7
		6.4			42.6			30.8			284.6		
	Jun 1 (21 d)	1.0			7.2			40.7			967.6		
		3.5	11.0	6.0	N/A	1.4	--	79.8	352.3	150.1	1026.0	191.1*	6.0
		2.4			N/A			103.8			1016.5		
	Jun 22 (14 d)	5.9			59.3			17.3			263.7		
		6.1	38.9	2.2	53.8	15.3***	1.6	35.1	197.6	68.4	224.3	69.7	5.6
		5.5			47.9			34.1			243.7		
	Jul 6 (13 d)	3.1			11.9			16.7			174.3		
		1.4	22.4	12.1	21.6	8.7*	6.4	20.3	143.4	20.9	161.6	56.1	7.9
		4.9			51.5			22.4			211.1		
	Jul 19 (21 d)	5.6			94.7			25.1			227.6		
		9.1	30.4	7.2	117.0	21.3	2.9	24.5	95.9	17.6	200.0	42.9	4.7
		7.1			123.1			17.7			248.8		
	Aug 9 (21 d)	3.2			26.8			3.8			76.3		
		3.3	13.3	1.2	23.3	4.1	1.2	7.0	27.6	9.5	80.0	14.9	0.5
		2.8			14.5			7.8			N/A		

N/A = Sampler at that site and time could not be analyzed (e.g., muddied surface, lost to flooding, damaged in field, stolen, vandalized, etc.). ND = Not detected. Level of significance based on a two-way ANOVA and Bonferroni post-hoc test: *P<0.05, **P<0.01, ***P<0.001

Table C7c: Clothianidin

Clothianidin		Emerson (EM)						Dead Horse Creek (DHC)					
		o-DGT (Ave R_s=0.01 L/d)			POCIS (R_s=0.25 L/d)			o-DGT (Ave R_s=0.009 L/d)			POCIS (R_s=0.25 L/d)		
Year	Deployment date (days)	Mass (ng)	TWA (ng/L)	SD	Mass (ng)	TWA (ng/L)	SD	Mass (ng)	TWA (ng/L)	SD	Mass (ng)	TWA (ng/L)	SD
2016 o-DGT & POCIS	Apr 15 (14 d)	1.4			5.8			4.2			74.2		
		1.4	16.9	0.3	8.5	2.3	0.6	6.8	79.3	25.2	73.3	21.8**	3.7
		1.5			N/A			8.2			53.9		
	Apr 29 (19 d)	1.9			27.0			11.7			165.9		
		1.0	9.8	4.5	7.0	3.5	2.6	10.1	66.2	14.7	108.2	33.6	7.1
		N/A			9.5			7.4			147.7		
	May 18 (14 d)	8.7			90.3			5.5			68.5		
		8.6	62.9	3.9	102.4	30.7***	2.2	4.8	44.4	10.3	62.0	21.9	1.6
		7.8			90.8			7.4			71.7		
	Jun 1 (21 d)	1.1			9.6			12.1			270.3		
		4.0	12.1	6.8	N/A	2.1	--	19.0	91.8	35.4	303.3	65.6	7.0
		2.5			N/A			27.1			335.1		
	Jun 22 (14 d)	7.2			112.9			10.2			170.3		
		7.6	47.4	3.6	90.4	30.3	5.9	24.3	127.1	50.6	169.9	57.0***	3.0
		6.5			76.6			20.9			186.2		
	Jul 6 (13 d)	1.2			19.2			19.8			270.3		
		1.5	9.4	1.4	39.7	15.7	10.1	24.9	169.9	22.7	198.0	88.3***	16.8
		ND			76.1			25.5			289.0		
	Jul 19 (21 d)	8.0			204.1			20.5			200.1		
		13.9	46.7	12.6	219.4	49.6	6.7	20.3	76.6	17.9	192.6	45.8	5.8
		11.8			263.4			13.1			242.6		
	Aug 9 (21 d)	4.1			57.2			3.8			97.1		
		5.3	19.8	2.7	55.0	10.3	3.3	6.7	33.1	4.2	94.5	20.7	0.4
		4.5			30.0			8.1			N/A		

N/A = Sampler at that site and time could not be analyzed (e.g., muddied surface, lost to flooding, damaged in field, stolen, vandalized, etc.). ND = Not detected. Level of significance based on a two-way ANOVA and Bonferroni post-hoc test: *P<0.05, **P<0.01, ***P<0.001

Table C7d: Imidacloprid

Imidicloprid		Emerson (EM)						Dead Horse Creek (DHC)					
		o-DGT (Ave R_s=0.01 L/d)			POCIS (R_s=0.25 L/d)			o-DGT (Ave R_s=0.009 L/d)			POCIS (R_s=0.25 L/d)		
Year	Deployment date (days)	Mass (ng)	TWA (ng/L)	SD	Mass (ng)	TWA (ng/L)	SD	Mass (ng)	TWA (ng/L)	SD	Mass (ng)	TWA (ng/L)	SD
2016 o-DGT & POCIS	Apr 15 (14 d)	0.46	6.5	2.0	3.2	1.3	0.02	0.10	3.2	2.0	2.2	0.86	0.10
		0.79			3.2			0.30			2.4		
		0.50			N/A			0.43			1.9		
	Apr 29 (19 d)	ND	--	--	ND	--	--	ND	--	--	ND	--	--
		ND			ND			ND			ND		
		N/A			ND			ND			ND		
	May 18 (14 d)	2.7	22.3	2.6	38.0	12.5*	2.5	0.44	2.5	0.5	3.2	1.3	0.03
		3.3			30.6			0.29			3.1		
		3.3			25.6			0.33			3.2		
	Jun 1 (21 d)	0.63	5.1	2.0	3.8	1.0	--	0.93	6.2	2.1	16.1	4.8	0.7
		1.5			N/A			1.4			16.9		
		1.3			N/A			1.9			21.2		
	Jun 22 (14 d)	3.4	20.3	5.9	43.1	15.6	1.7	1.4	13.9	4.2	15.3	6.0***	0.5
		4.1			40.4			2.6			14.0		
		2.2			34.7			2.4			16.2		
	Jul 6 (13 d)	0.22	4.9	5.7	9.1	9.5	6.4	1.0	9.2	2.2	17.4	7.5	0.9
		0.27			19.0			1.3			15.5		
		1.7			38.6			1.7			19.6		
	Jul 19 (21 d)	1.5	7.5	2.1	68.5	21.3***	4.4	4.1	14.9	2.9	26.1	7.3***	1.0
		2.5			73.8			4.1			24.9		
		1.7			99.5			2.8			31.9		
	Aug 9 (21 d)	2.6	10.2	1.0	33.0	7.5	2.1	0.7	6.8	1.1	16.3	5.1	1.1
		2.7			32.8			1.4			22.0		
		2.3			19.2			1.8			N/A		

N/A = Sampler at that site and time could not be analyzed (e.g., muddied surface, lost to flooding, damaged in field, stolen, vandalized, etc.). ND = Not detected. Level of significance based on a two-way ANOVA and Bonferroni post-hoc test: *P<0.05, **P<0.01, ***P<0.001

Table C7e: Carbamazepine

Carbamazepine		Emerson (EM)						Dead Horse Creek (DHC)					
		o-DGT (Ave R_s=0.01 L/d)			POCIS (R_s=0.25 L/d)			o-DGT (Ave R_s=0.009 L/d)			POCIS (R_s=0.25 L/d)		
Year	Deployment date (days)	Mass (ng)	TWA (ng/L)	SD	Mass (ng)	TWA (ng/L)	SD	Mass (ng)	TWA (ng/L)	SD	Mass (ng)	TWA (ng/L)	SD
2016 o-DGT & POCIS	Apr 15 (14 d)	0.26	3.0	0.3	2.9	0.90	0.2	0.26	3.2	0.3	7.7	1.6	0.5
		0.31			4.0			0.30			7.4		
		0.27			N/A			0.29			4.2		
	Apr 29 (19 d)	0.55	2.6	0.9	12.7	1.6	0.7	0.79	3.8	1.1	12.6	2.1	0.4
		0.34			5.2			0.67			8.6		
		N/A			7.9			0.44			11.8		
	May 18 (14 d)	0.52	3.3	0.2	12.2	3.1	0.2	1.1	7.8	0.7	18.9	4.5	0.4
		0.47			13.3			1.2			16.2		
		0.53			11.6			1.3			17.7		
	Jun 1 (21 d)	0.026	0.31	0.2	1.0	0.16	--	0.29	2.2	0.9	10.2	2.1	0.5
		0.12			N/A			0.58			11.8		
		0.081			N/A			0.73			15.7		
	Jun 22 (14 d)	0.70	3.0	1.3	6.2	3.0	2.2	0.23	1.8	0.4	39.6	1.1	0.04
		0.59			7.5			0.34			4.3		
		0.27			21.8			0.36			4.6		
	Jul 6 (13 d)	0.13	1.5	0.6	3.0	1.3	0.6	0.32	0.16	0.08	4.2	1.1	0.1
		0.30			4.0			0.48			3.7		
		0.30			6.9			0.91			4.6		
	Jul 19 (21 d)	0.13	1.3	0.9	5.5	1.2	0.2	0.86	2.7	0.7	9.3	1.5	0.1
		0.62			6.9			0.84			8.2		
		0.31			8.0			0.50			9.8		
	Aug 9 (21 d)	0.51	2.1	0.2	7.7	1.0	0.4	15.4	68.1	8.8	272.8	46.4***	0.04
		0.64			7.2			17.8			272.5		
		0.57			3.6			20.0			N/A		

N/A = Sampler at that site and time could not be analyzed (e.g., muddied surface, lost to flooding, damaged in field, stolen, vandalized, etc.). ND = Not detected. Level of significance based on a two-way ANOVA and Bonferroni post-hoc test: *P<0.05, **P<0.01, ***P<0.001
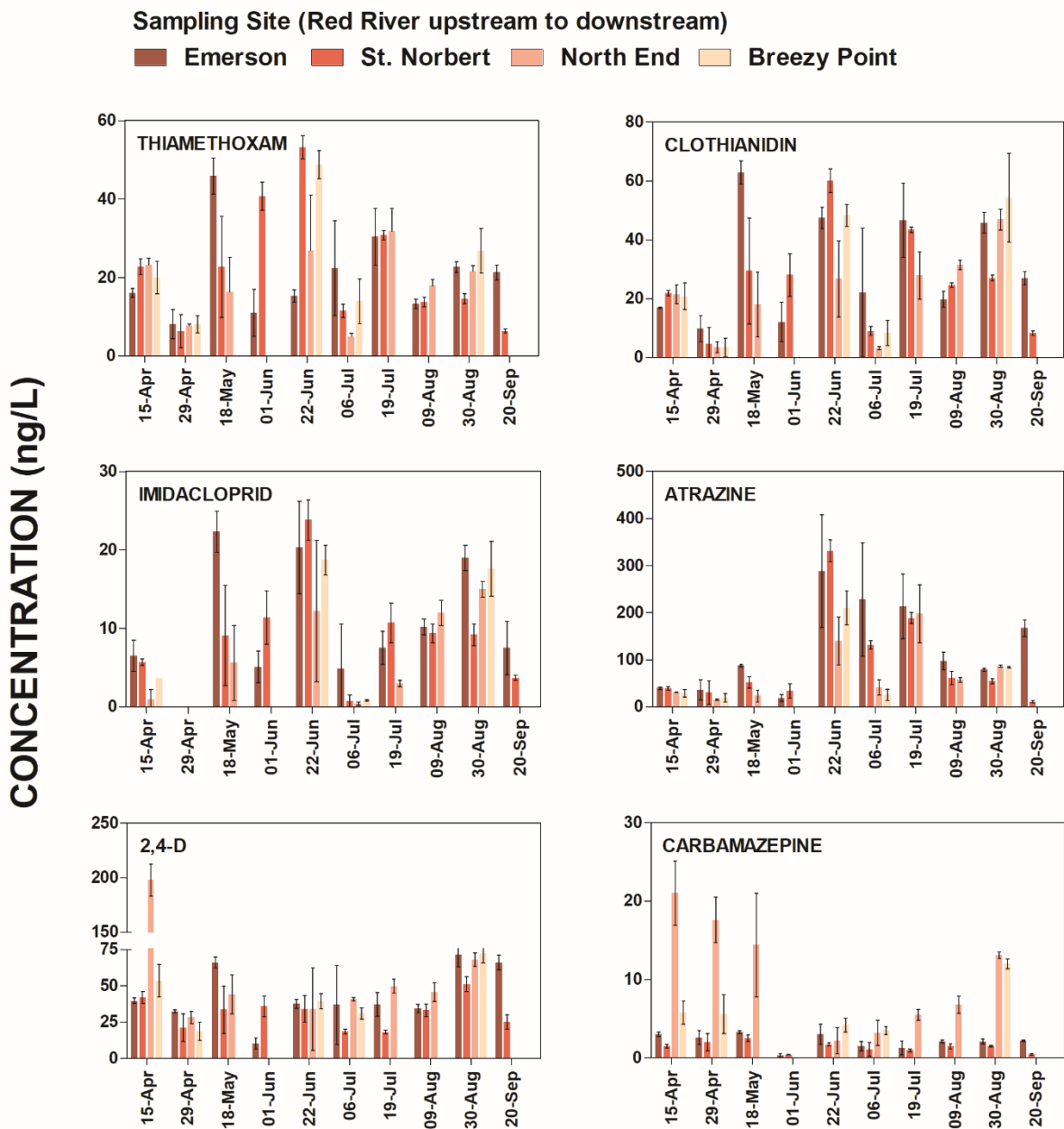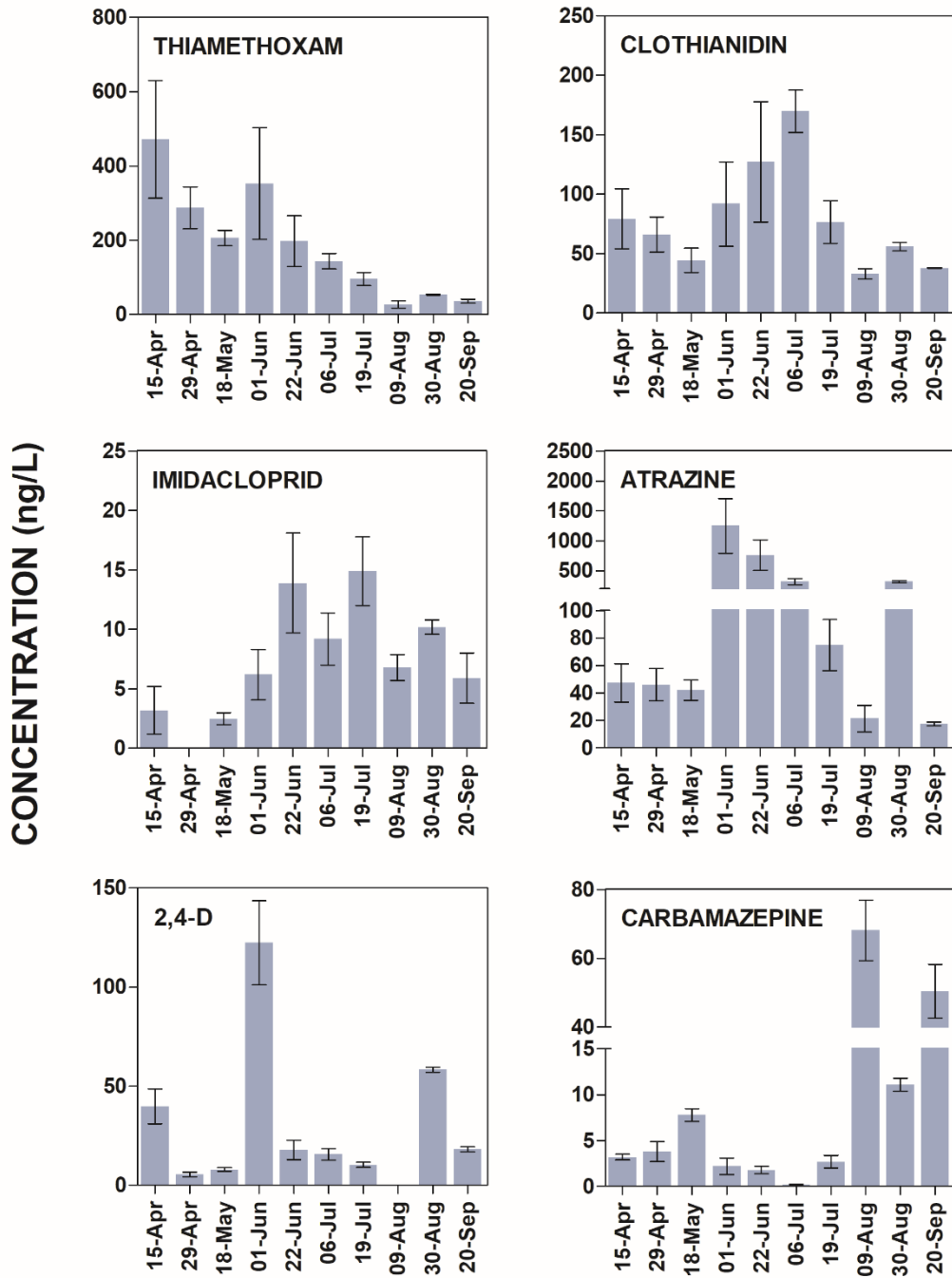
Figure C3: Time weighted average o-DGT concentrations of thiamethoxam, clothianidin, imidacloprid, atrazine, 2,4-D, and carbamazepine detected over the 2016 sampling season in the Red River. Bars represent the mean and standard deviation (SD) of triplicate measurements. Bar colour corresponds to sampling site in direction of flow (Emerson, St. Norbert, North End, Breezy Point). Assiniboine River and DHC data are shown in separate graphs. Absence of a bar indicates either no detection (ND) or that the samplers were destroyed (NA). Details in Table C5.

317

ASSINIBOINE RIVER AT HEADINGLEY
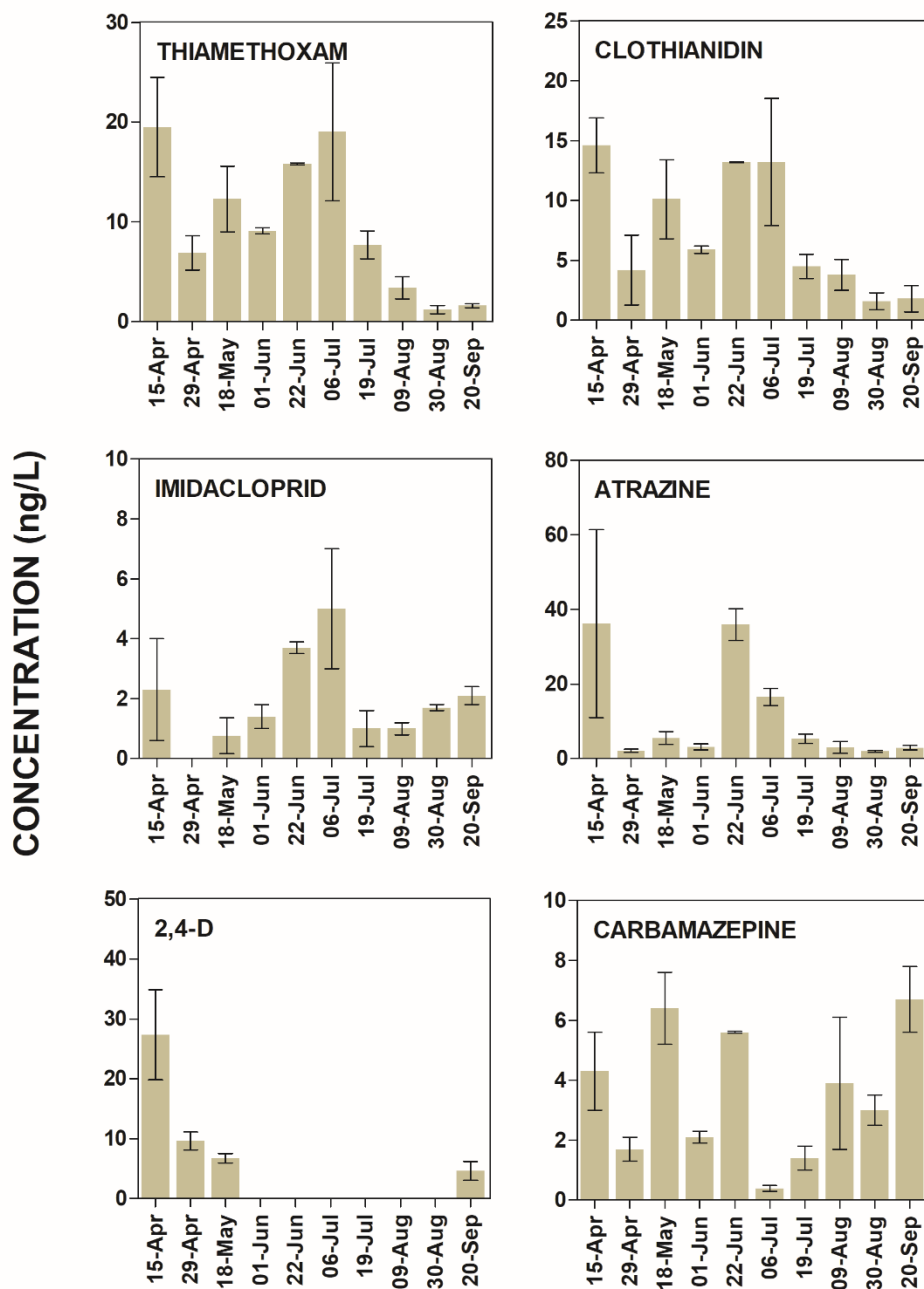
Figure C4: Time weighted average o-DGT concentrations of thiamethoxam, clothianidin, imidacloprid, atrazine, 2,4-D, and carbamazepine detected over the 2016 sampling season in the Assiniboine River. Bars represent the mean and standard deviation (SD) of triplicate measurements. Absence of a bar indicates either no detection (ND) or that the samplers were destroyed (NA). Details in Table C5.

318

# DEAD HORSE CREEK

Figure C5: Time weighted average o-DGT concentrations of thiamethoxam, clothianidin, imidacloprid, atrazine, 2,4-D, and carbamazepine detected over the 2016 sampling season in DHC. Bars represent the mean and standard deviation (SD) of triplicate measurements. Absence of a bar indicates either no detection (ND) or that samplers were destroyed (NA). Details in Table C5.
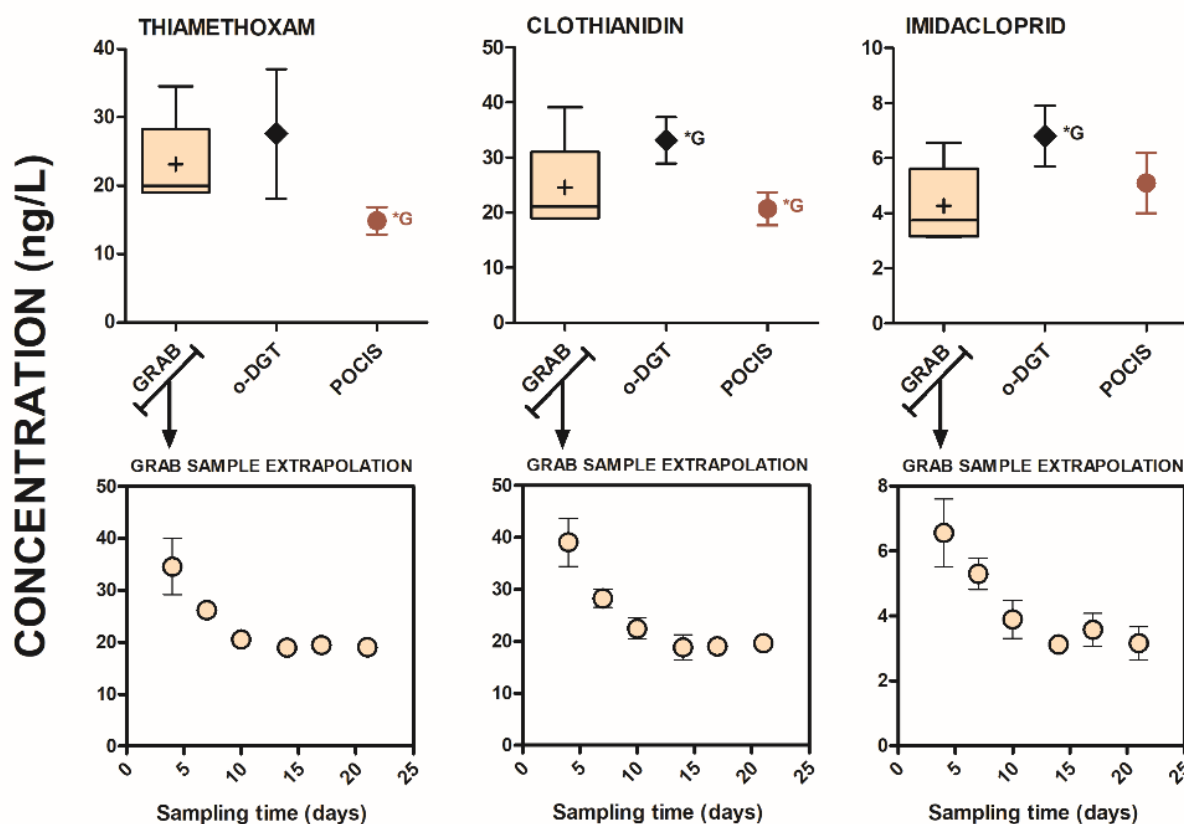
Figure C6: Water concentrations measured by o-DGT, POCIS, and grab sampling in DHC over 21 days from August 9-30, 2016. Six grab samples in triplicate were taken over the 21-d period. Box and whisker plots (top panel) of the six triplicate sets of grab samples represent: minimum and maximum, lower and upper quartile, median and mean (+). Extrapolation of the box and whisker plot in the bottom panel show the mean and standard deviation of each triplicate set of grab samples taken at 4, 7, 10, 14, 17, and 21 days (in cases where error bars aren't showing they are smaller than the data point). Mean and standard deviation represent the triplicate o-DGT and POCIS data. Thiamethoxam, clothianidin, and imidacloprid only have a single reported sampling rate value in the literature (Table C4), hence the single POCIS data point. Statistical significance (P<0.05) denoted by (*) based on a one-way ANOVA and Tukey's post-hoc test. The letter G (grab) beside a data point indicates that data point is statistically different from the grab sample mean.
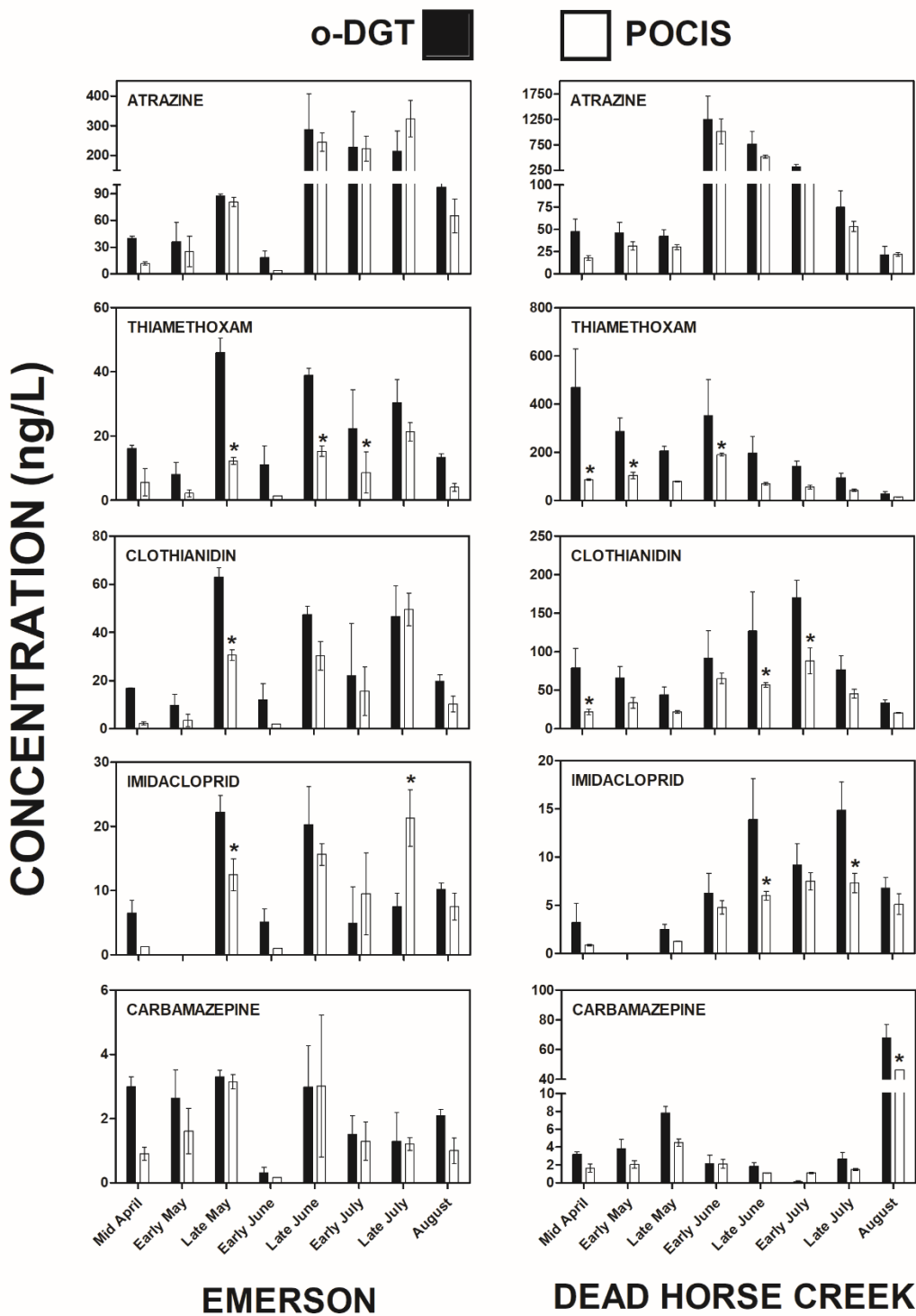
Figure C7: TWA concentrations of co-deployed o-DGT and POCIS samplers at Emerson and DHC over the 2016 sampling season. Bars represent the mean and standard deviation (error bars) of triplicate samples. Statistical difference between paired observations (P<0.05) denoted by (*), determined by two-way ANOVA and Bonferroni post-hoc test.
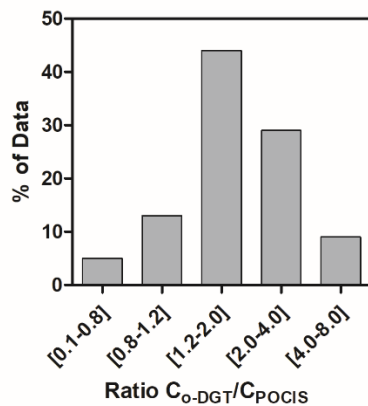
Figure C8: Percentage of data from Table C7 (N=80 paired o-DGT/POCIS measurements) falling in the designated ratio intervals. Only 9% of the measurements (N=7) were underestimated by o-DGT compared to POCIS (e.g., Co-DGT/CPOCIS<1).

Sampler Extractions.
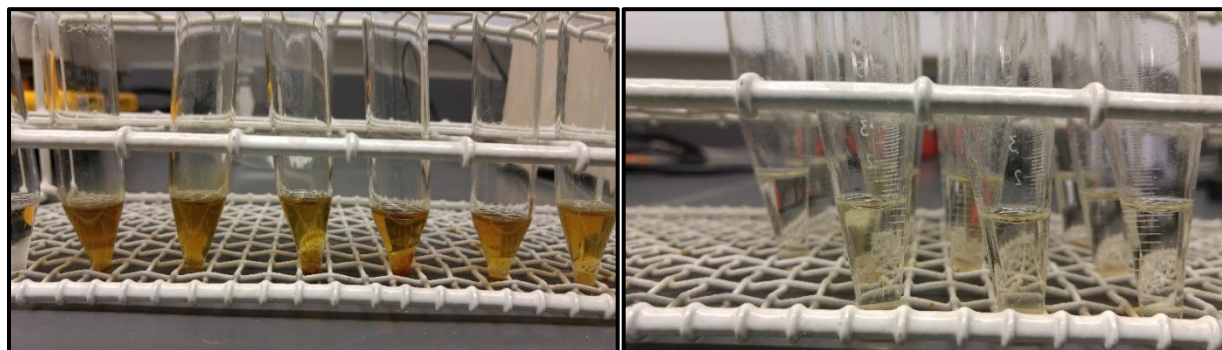
Figure C9: Sample extracts from POCIS (left) and o-DGT (right) from the August 9-30, 2016 Red River deployment. Images are of final reconstituted extracts in 1 mL 50:50 H2O:MeOH prior to syringe filtering.

Sampler Variability.

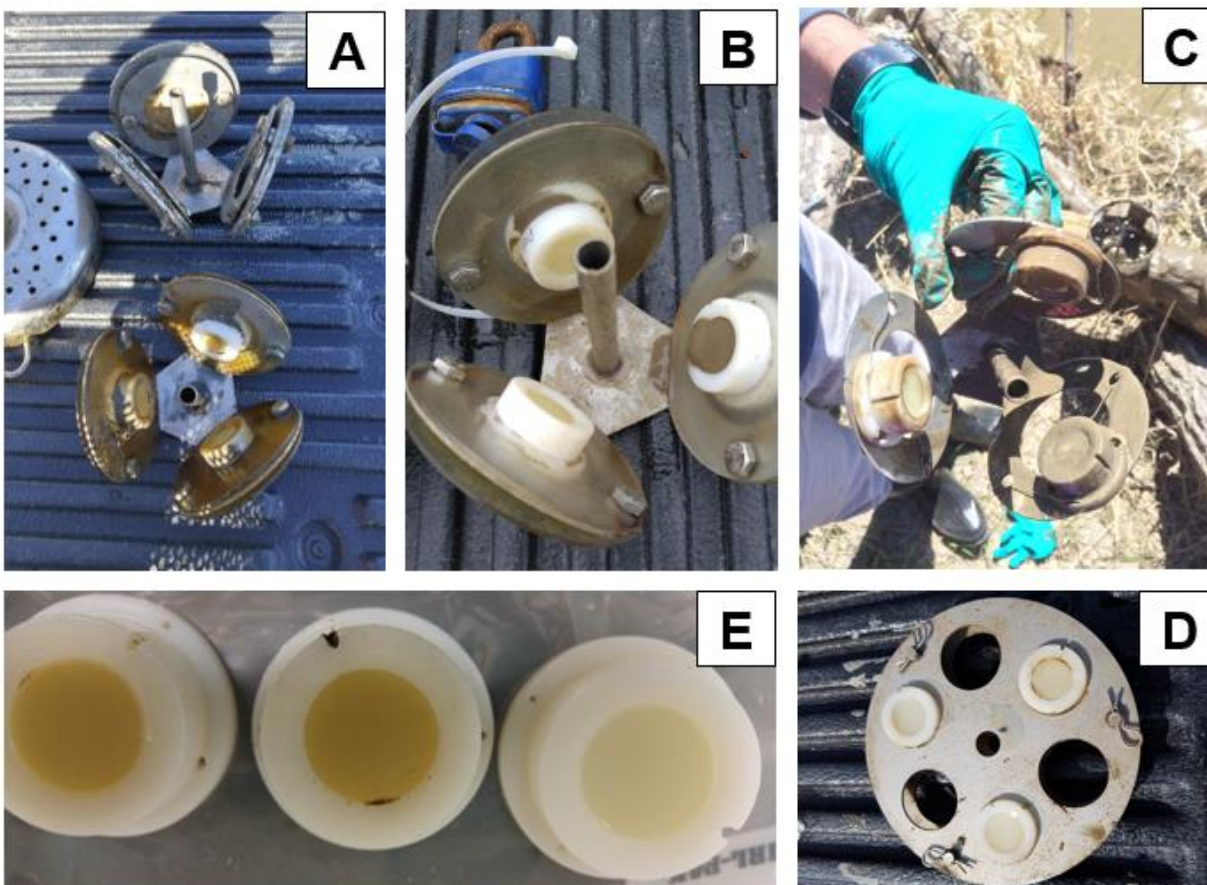

Figure C10: Deployment issues with o-DGT leading to sampler variability. Spindle used to deploy POCIS and o-DGT (A). Retrieved o-DGT with one (B) and two (C) surfaces covered. The sediment covered surface in (B) is the 'clean' o-DGT (right) in (D). The new design for deploying o-DGT horizontally in a single plane, facing down toward the bottom of the water column (E).

Figure C10 depicts the issue encountered with o-DGT when deployed using the typical POCIS 'spindle'. On a number of occasions we would retrieve the sampler cage to find one (Figure C10B) or two (Figure C10C) o-DGT covered in sediment and particulate that had settled preferentially on those surfaces during the deployment. Given how the spindle is designed, one or two o-DGT will always be facing the direction of flow, while the other one or two will be facing away from the flow. Typically, only one of three samplers would be covered, as in Figure C10B. In the cases where the surface

of the o-DGT was fully covered, those samples measured low, leading to greater

variability in triplicate measurements. In certain cases, the single low value was omitted

(e.g., August 30, 2016 at Emerson, Table C5). In other cases all three values were kept

(e.g., June 22, 2015 at DHC, Table C5). Regardless, the observation of a single low

value in a triplicate set consistently matched the field observation of a fully or partially

covered o-DGT surface. This was further observed during extraction of the samplers in

the lab. Figure C10D shows two 'fouled' samplers (darker gels) and one 'clean' sampler.

The 'clean' sampler corresponds to the sediment covered o-DGT surface in Figure

C10D. The discoloration of the gels indicated clearance of water through the sampler,

likely from dissolved organic matter in the surface waters. A 'clean' sampler in these

systems generally indicated that it had not been sampling the water. To test this

potential source of o-DGT variability samplers were deployed in DHC using the typical

POCIS spindle and our newly developed horizontal spindle (Figure C10E). Samplers

were deployed for 17 days in September 2017. The results of this comparison are

shown in Table C8.

Table C8: Comparison of o-DGT using two different deployment configurations. Triplicate o-DGT deployed horizontally using the new horizontal spindle were compared to deployments with the triangle spindle, originally designed for use with POCIS. Data presented in this table are mass of analyte/o-DGT (ng), not water concentrations.

o-DGT	Atrazine			Thiamethoxam			Chlorpyriofs			Carbamazepine			AVERAGE %RSD
	Mass (ng)	AVE	SD	Mass (ng)	AVE	SD	Mass (ng)	AVE	SD	Mass (ng)	AVE	SD	
Horizontal spindle	8.3	8.2	0.3	0.43	0.55	0.11	8.5	8.8	1.2	14.6	15.1	1.0	**Horizontal spindle**
	8.3			0.66			7.8			16.3			
	7.9			0.58			10.1			14.5			
	% RSD	3		% RSD	20		% RSD	13		% RSD	7		**11%**
Triangle spindle	8.4	7.6	1.1	0.49	0.33	0.14	5.7	10.8	4.4	18.6	15.8	7.5	**Triangle spindle**
	8.0			0.27			13.8			21.5			
	6.3			0.23			12.9			7.2			
	% RSD	15		% RSD	42		% RSD	41		% RSD	48		**36%**

Lake Winnipeg Concentration Data.
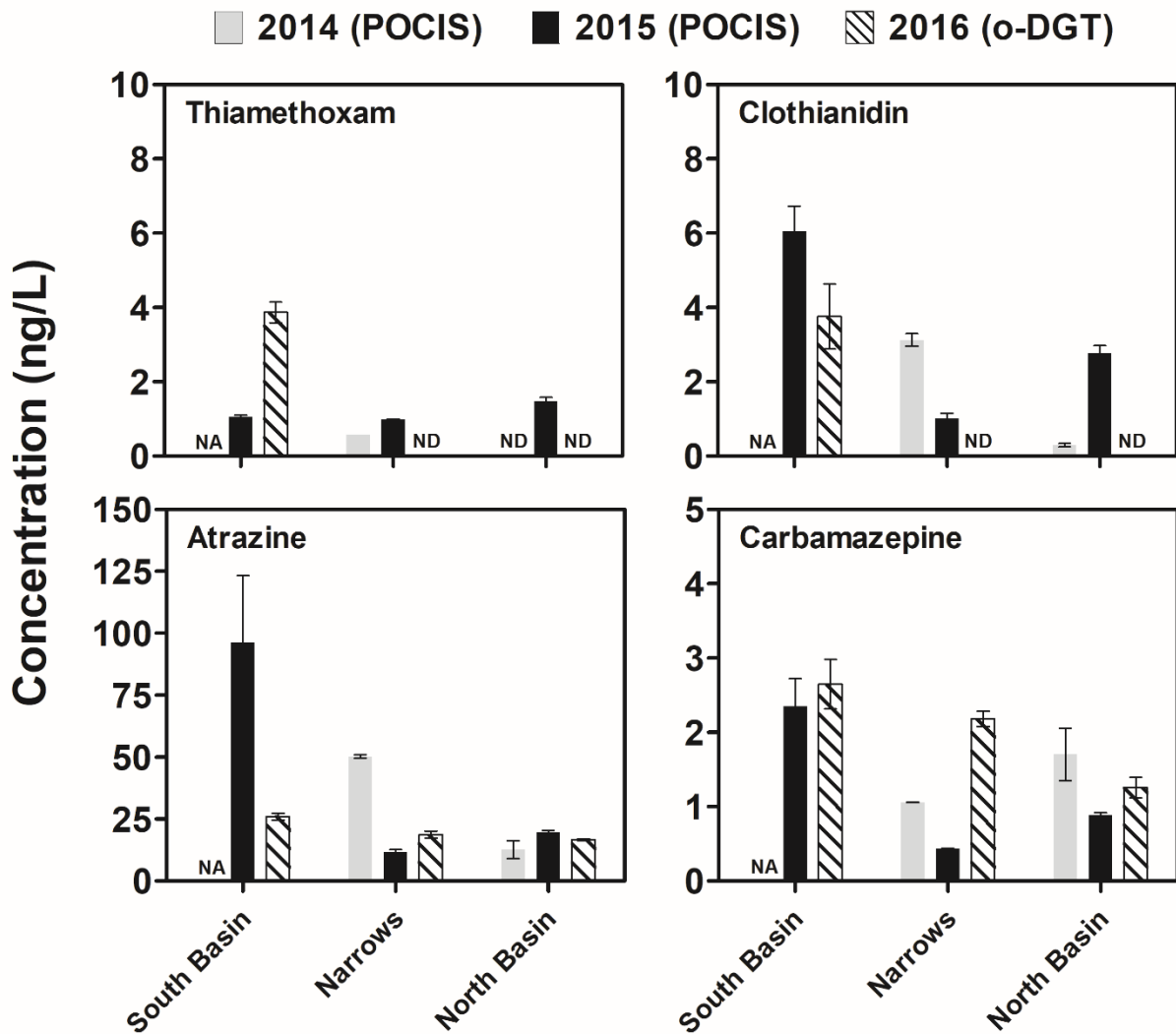
Figure C11: Concentrations of the four detected target analytes in Lake Winnipeg by POCIS (2014-15) and o-DGT (2016). POCIS samplers in 2014 in the south basin were destroyed (NA – not applicable). ND – non detect. Thiamethoxam and clothianidin were not detected by o-DGT in 2016 at the narrows and north basin sites. This may be due to annual variation in use and/or concentrations below detection limits as opposed to an o-DGT specific issue, especially as POCIS also failed to detect thiamethoxam in 2014 at the north basin site.

Nelson River Concentration Data.

Table C9: Analyte concentrations measured by POCIS in 2014 and 2015 and o-DGT in 2015 and 2016. Mass on sampler is used to calculate the time weighted average (TWA) concentration based on deployment time (days, d) and sampling rate (R_S, L/d). Reported in bold is the mean and standard deviation (SD) of triplicate TWA measurements. POCIS R_S in Table C4. Temperature-specific sampling rates for o-DGT, calculated according Table B5. Downstream o-DGT samples in 2015 not taken. N/A = no sample (e.g., lost to flooding, damaged in field, stolen, vandalized). ND = not detected.

Compound	Year (Ave R_S) (deployment time)	Upstream Mass (ng)	Upstream TWA (ng/L)	Upstream SD	Influent Mass (ng)	Influent TWA (ng/L)	Influent SD	Effluent Mass (ng)	Effluent TWA (ng/L)	Effluent SD	Downstream Mass (ng)	Downstream TWA (ng/L)	Downstream SD
Carbamazepine	2014 POCIS (0.28 L/d) (21d)	ND ND ND	ND		3410 2332 1044	389.8	204	1576 1711 1020	247.4	63.1	ND ND ND	ND	
	2015 POCIS (0.28 L/d) (21d)	ND ND ND	ND		3084 3051 3023	526.1	5.2	2331 2373 N/A	405.3	5.2	ND ND ND	ND	
	2015 o-DGT (0.011 L/d) (21d)	ND ND ND	ND		327.1 348.0 314.1	1310	73	329.9 299.0 330.3	1350	70			
	2016 o-DGT (0.003 L/d) (14d)	ND ND ND	ND		111.9 108.0 133.9	2740	324	122.7 140.3 132.6	2770	150	ND ND ND	ND	
Sulfamethoxazole	2014 POCIS (0.22 L/d) (21d)	ND ND ND	ND		397.2 1302 931.0	190.2	98.7	1018 1070 481.5	185.8	70.7	ND ND ND	ND	
	2015 POCIS (0.22 L/d) (21d)	ND ND ND	ND		2758 2396 2439	549.1	42.9	1873 1916 N/A	410.9	6.7	ND ND ND	ND	
	2015 o-DGT (0.011 L/d) (21d)	ND ND ND	ND		214.6 230.2 218.2	980	36	194.7 191.7 196.4	860	11			
	2016 o-DGT (0.003 L/d) (14d)	ND ND ND	ND		311.9 300.3 314.4	7180	175	341.3 293.8 303.9	7070	580	ND ND ND	ND	
Sulfapyridine	2014 POCIS (0.15 L/d) (21d)	ND ND ND	ND		142.5 62.6 48.2	26.3	16	34.4 34.5 15.1	8.7	3.5	ND ND ND	ND	
	2015 POCIS (0.15 L/d) (21d)	ND ND ND	ND		431.4 409.2 417.5	130.5	3.5	281.8 306.3 N/A	91.5	5.4	ND ND ND	ND	
	2015 o-DGT (0.010 L/d) (21d)	ND ND ND	ND		27.1 30.2 26.4	130	10	27.2 26.5 28.0	130	3.5			
	2016 o-DGT (0.004 L/d) (14d)	ND ND ND	ND		181.7 159.5 195.3	3280	330	177.9 196.0 199.2	3330	270	ND ND ND	ND	

Compound	Sampler												
Trimethoprim	2014 POCIS (0.26 L/d) (21d)	ND			396.6			937.6			ND		
		ND	ND		1320	135.4	95	1092	154.7	59	ND	ND	
		ND			475.6			475.0			ND		
	2015 POCIS (0.26 L/d) (21d)	ND			1936			1538			ND		
		ND	ND		1814	340.5	16	1565	287.5	4	ND	ND	
		ND			1763			N/A			ND		
	2015 o-DGT (0.012 L/d) (21d)	ND			99.4			89.8					
		ND	ND		100.4	387	22	87.6	364	16			
		ND			90.3			95.5					
	2016 o-DGT (0.001 L/d) (14d)	ND			158.4			167.8			ND		
		ND	ND		127.5	7650	1050	181.0	7190	2	ND	ND	
		ND			166.7			167.7			ND		
Clarithromycin	2014 POCIS (0.38 L/d) (21d)	ND			60.1			76.0			ND		
		ND	ND		178.1	15.0	10	84.1	8.3	3.2	ND	ND	
		ND			ND			36.9			ND		
	2015 POCIS (0.38 L/d) (21d)	ND			256.1			240.0			ND		
		ND	ND		235.5	28.3	4.6	238.8	30.1	0.1	ND	ND	
		ND			185.1			N/A			ND		
	2015 o-DGT (0.007 L/d) (21d)	ND			13.1			7.4					
		ND	ND		12.4	80.1	6	9.9	60.3	11			
		ND			11.2			10.7					
	2016 o-DGT (0.001 L/d) (14d)	ND			55.0			53.4			ND		
		ND	ND		55.9	4430	70	106.7	4150	780	ND	ND	
		ND			56.8			69.7			ND		
Atrazine	2014 POCIS (0.19 L/d) (21d)	22.9			2.4			10.8			30.1		
		10.3	5.0	2.1	15.1	1.9	1.6	13.6	2.5	1.0	19.3	5.6	1.6
		27.0			5.6			5.7			18.7		
	2015 POCIS (0.19 L/d) (21d)	34.3			24.7			22.7			16.4		
		13.9	5.3	2.8	25.9	6.2	0.2	25.8	6.0	0.5	17.9	3.8	0.7
		16.4			24.3			N/A			12.1		
	2015 o-DGT (0.009 L/d) (21d)	1.6			1.1			1.2					
		1.5	7.3	1.3	1.3	6.2	0.5	1.1	6.2	0.4			
		1.1			1.1			1.2					
	2016 o-DGT (0.004 L/d) (14d)	ND			ND			ND			ND		
		ND	ND		ND	ND	ND	ND	ND	ND	ND	ND	
		ND			ND			ND			ND		
Naproxen	2015 o-DGT (0.010 L/d) (21d)	ND			11.2			10.5					
		ND	ND		9.1	45.4	5.7	7.7	43.6	6.9			
		ND			9.1			9.8					
	2016 o-DGT (0.003 L/d) (14d)	ND			1303			1381			0.73		
		ND	ND		1134	36400	3950	1378	37500	1420	0.53	19.0	3.4
		ND			1410			1457			0.74		
Metoprolol	2016 o-DGT (0.002 L/d) (14d)	ND			28.9			30.1			ND		
		ND	ND		22.4	1230	180	30.1	1210	3	ND	ND	
		ND			29.4			30.0			ND		
Diclofenac	2016 o-DGT (0.004 L/d) (14d)	ND			31.3			34.0			ND		
		ND	ND		27.6	623	59	35.1	676	27	ND	ND	
		ND			33.3			36.0			ND		
Ibuprofen	2016 o-DGT (0.003 L/d) (14d)	ND			20.7			23.7			ND		
		ND	ND		22.3	494	26	22.3	531	32	ND	ND	
		ND			22.9			25.8			ND		

Contaminant Trends.
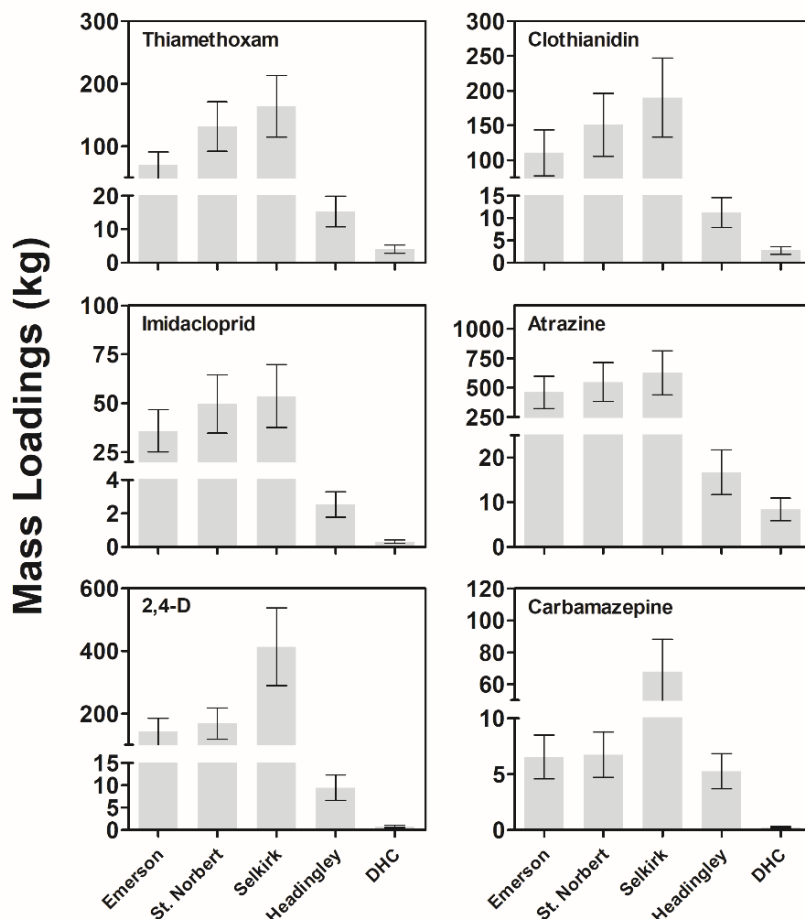
Figure C12: Mass loadings of each detected compound in the Red River, Assiniboine River at Headingley, and Dead Horse Creek (DHC) in 2016 measured by o-DGT. Each bar represents total loadings over the sampling period April to October.

Mass loading calculations. Chemical fluxes (kg/d) were calculated at sites that had Environment Canada gauging stations (Emerson, St. Norbert, Headingley, and DHC). Daily discharge volumes were obtained from Environment Canada Water Level and Flow website (https://wateroffice.ec.gc.ca/). The calculation of flux and mass loading data assumed homogenous concentrations at the cross-sectional area of the river where the gauging stations/passive samplers were located. Loadings were

calculated based on the TWA water concentration over each deployment period and the daily discharge volume over that same period. Loadings were summed over the sampling season to get a total. Selkirk was not a sampling location for this study, but represented the nearest discharge gauging station between the North End site and Breezy Point site. The loadings data for Selkirk extrapolated water concentrations by taking the average of the two bordering sites (North End and Breezy Point).

Table C10: Parameters used for predicting concentrations of atrazine in Lake Winnipeg based on measured inputs from the Red River. Lake Winnipeg was split into two compartments, the south basin and north basin which are connected by the narrows.

South Basin →		North Basin →		Nelson River	
Volume (m^3)	5.16x10^{10}	Volume (m^3)	2.32x10^{11}	Volume (m^3)	2.76x10^9
Residence time (yr)	1.3	Residence time (yr)	3.5	Residence time (yr)	0.04
Flushing rate (yr^{-1})	0.77	Flushing rate (yr^{-1})	0.29	Flushing rate (yr^{-1})	25
Outflow (m^3/yr)	3.97x10^{10}	Outflow (m^3/yr)	6.74x10^{10}	Outflow (m^3/yr)	6.9x10^{10}
Annual influx (kg)* (Red River)	868	Annual influx (kg) (South basin)	668	Annual influx (kg) (North basin)	194
Concentration (ng/L) Model (measured)	22 (41)	Concentration (ng/L) Model (measured)	10 (16)	Concentration (ng/L) Model (measured)	2.8 (3.3)

Calculations: flushing rate = 1/residence time; outflow = volume·flushing rate; concentration = influx/outflow; annual influx (south basin) = annual influx (Red River)·flushing rate (south basin); annual influx (north basin) = annual influx (south basin)·flushing rate (north basin)
*Annual flux from Red River was calculated using the 2016 Selkirk flux, and 2014 and 2015 Selkirk flux data from Chapter 2. Annual flux was calculated as July 2014 to June 2015 (1113 kg) and July 2015 to June 2016 (622 kg). The two annual influx values were averaged to give 868 kg.

Table C11: Parameters used for predicting concentrations of carbamazepine in Lake Winnipeg based on measured inputs from the Red River. Lake Winnipeg was split into two compartments, the south basin and north basin which are connected by the narrows.

South Basin →		North Basin →		Nelson River	
Volume (m^3)	5.16x10^{10}	Volume (m^3)	2.32x10^{11}	Volume (m^3)	2.76x10^9
Residence time (yr)	1.3	Residence time (yr)	3.5	Residence time (yr)	0.04
Flushing rate (yr^{-1})	0.77	Flushing rate (yr^{-1})	0.29	Flushing rate (yr^{-1})	25
Outflow (m^3/yr)	3.97x10^{10}	Outflow (m^3/yr)	6.74x10^{10}	Outflow (m^3/yr)	6.9x10^{10}
Annual influx (kg)* (Red River)	48	Annual influx (kg) (South basin)	37	Annual influx (kg) (North basin)	11
Concentration (ng/L) Model (measured)	1.2 (1.7)	Concentration (ng/L) Model (measured)	0.55 (1.3)	Concentration (ng/L) Model (measured)	0.15 (ND)

Calculations: flushing rate = 1/residence time; outflow = volume·flushing rate; concentration = influx/outflow; annual influx (south basin) = annual influx (Red River)·flushing rate (south basin); annual influx (north basin) = annual influx (south basin)·flushing rate (north basin)
*Annual flux from Red River was calculated using the 2016 Selkirk flux, and 2014 and 2015 Selkirk flux data from Chapter 2. Annual flux was calculated as July 2014 to June 2015 (35 kg) and July 2015 to June 2016 (62 kg). The two annual influx values were averaged to give 48 kg.